# GPNMB: EXPLORING A NOVEL TARGET FOR THERAPY IN HODGKIN LYMPHOMA

**by**

**DR NAVTA MASAND**


A thesis submitted to the

University of Birmingham

for the degree of

DOCTOR IN PHILOSOPHY

Institute of Cancer and Genomic Sciences

College of Medical and Dental Sciences

University of Birmingham

March 2021

# Abstract

Glycoprotein non-metastatic melanoma protein B (GPNMB) is a transmembrane protein highly expressed in multiple tumours, including classical Hodgkin lymphoma (cHL); a tumour in which the malignant Hodgkin and Reed-Sternberg (HRS) cells rely on the tumour microenvironment (TME) to survive and evade detection by the host immune system. In this study, I explore the contribution of GPNMB to immune evasion of cHL as a novel therapeutic target.

I have shown that GPNMB is highly expressed in tumour-associated macrophages (TAM) in cHL tissues but expression is highly variable. In vitro differentiation of macrophages (from $CD14^+$ monocytes) was shown to be associated with an increase in GPNMB expression, including the generation of a soluble form of GPNMB (sGPNMB). sGPNMB partially inhibited T-cell activation and T-cell recognition of Epstein-Barr virus (EBV)-specific epitopes in cHL cell lines. Preliminary experiments indicated that the inhibition of T cell activation by GPNMB could be overcome with GPNMB neutralising antibodies.

This work provides evidence in support of the hypothesis that GPNMB can mediate an immune checkpoint that inhibits anti-tumour cytotoxic T-lymphocytes (CTL). It provides a basis for further investigations designed to explore the therapeutic potential of targeting GPNMB in cHL.

# Acknowledgements

Firstly, I am extremely grateful to Birmingham Children's Hospital Research Foundation and Children's Cancer and Leukaemia Group/ The Little Princess Trust for funding this project and allowing me this opportunity.

Next, thank you to Professor Paul Murray for his guidance, support, invaluable experience and belief in my abilities and for pushing me, especially in these last few months. I'm also very sorry for spilling coffee all over you!

Professor Pamela Kearns has been my academic and clinical mentor, supervisor and friend since I started my training in Paediatrics and has supported and nurtured me in both my clinical and academic career. Thank you for your continued encouragement, insight and unwavering support.

My thanks also go to Dr Graham Taylor, who is incredibly knowledgeable and experienced in his field and helped bring my work to a higher level.

I had the great pleasure of working in the Murray/Kearns/Taylor groups and have worked alongside some great scientists and friends- Dr Eszter Nagy, Dr Lauren Lupino, Dr Martina Vockerodt, Dr Sandra Davies, Dr Kate Vrzalikova, Dr Maha Ibrahim, Dr Robert Hollows, and Dr Xiaohong Lu.

Special thanks go to Dr Tracey Adams Perry for all her help, guidance and company in the lab during our long experiments. Also to Tracey Haigh for all her help with the T-cell clone experiments and to Dr Matthew Pugh for his assistance with pathology. Thank you to Dr David Burns for collecting the clinical data for our cohort of HL patients and to Dr Wenbin Wei for his re-analysis of gene expression data. Dr Elena Syrimi has been a good friend and colleague during my clinical and academic training.

Finally, thank you to my friends and family. My parents have always encouraged me to reach my potential- you are my inspiration and I would not have been able to make it this far without you. I am lucky to have had my good friends Nasreen and Liam in my 'bubble' during the last 2 lockdowns and they have been incredibly supportive, and to my cat Stan for his company during long writing sessions.

# Table of Contents

# List of Figures

page(s)

# List of Tables

page(s)

# List of abbreviations

| | |
|---|---|
| ABVD | adriamycin (doxorubicin), bleomycin, vincristine and dacarbazine |
| ADC | antibody-drug conjugate |
| ASCT | autologous stem-cell transplantation |
| BCR | B cell receptor |
| BEACOPP | bleomycin, etoposide, doxorubicin, cyclophosphamide, vincristine, procarbazine, prednisolone |
| BSA | bovine serum albumin |
| CCL5 | C-C motif chemokine ligand 5 |
| cHL | classical Hodgkin Lymphoma |
| CM | conditioned media |
| CNS | central nervous system |
| COPDAC | cyclophosphamide, vincristine, prednisolone, dacarbazine |
| CTL | cytotoxic T-lymphocyte |
| DC-HIL | dendritic cell-associated, heparan sulphate proteoglycan-dependent integrin ligand |
| DLBCL | diffuse large B-cell lymphoma |
| DMSO | dimethyl sulfoxide |
| DTH | delayed type hypersensitivity |
| EBER | EBV-encoded RNAs |
| EBNA | Epstein-Barr nuclear antigen |
| EBV | Epstein-Barr virus |
| ECD | extracellular domain |
| EF | extrafollicular |
| ELISA | enzyme-linked immunosorbent assay |
| EMP | erythro-myeloid progenitor |
| EOT | end of treatment |
| EV | empty vector |
| FBS | foetal bovine serum |
| GC | germinal centre |
| GM-CFU | granulocyte/macrophage colony forming unit |

| | |
|---|---|
| GM-CSF | granulocyte-macrophage colony-stimulating factor |
| GPNMB | glycoprotein non-metastatic melanoma protein B |
| HBRC | human biomaterial resource centre |
| hemITAM | half immunoreceptor tyrosine-based activation motif |
| HGFIN | hematopoietic growth factor inducible, neurokinin-1 type |
| HL | Hodgkin lymphoma |
| HPF | high-power fields |
| HRS | Hodgkin and Reed-Sternberg |
| HSC | haematopoietic stem cells |
| IC | immune complex |
| ICAM-1 | intercellular adhesion molecule 1 |
| IFNγ | interferon Gamma |
| Ig | immunoglobulin |
| IHC | immunohistochemistry |
| IL-1R | IL-1 receptor |
| IU | international units |
| LCL | lymphoblastoid cell line |
| LDCHL | lymphocyte-depleted classical Hodgkin lymphoma |
| LMP1/2 | latent membrane protein 1 or 2 |
| LP | lymphocyte predominant |
| LRCHL | lymphocyte-rich classical Hodgkin lymphoma |
| LPS | lipopolysaccharide |
| M1 | GM-CSF polarised macrophages |
| M2 | M-CSF polarised macrophages |
| MCCHL | mixed cellularity classical HL |
| M-CFU | macrophage colony-forming unit |
| M-CSF | macrophage colony-stimulating factor |
| MIF | macrophage inhibitory factor |
| MLA | monkey leukocyte antigen |
| MMAE | monomethyl auristatin E |
| MOI | multiplicity of infection |
| MVA | modified vaccinia Ankara |

| | |
|---|---|
| MVD | micro-vessel density |
| NK | natural killer cell |
| NLPHL | nodular lymphocyte predominant Hodgkin lymphoma |
| NSCHL | nodular sclerosis classical Hodgkin lymphoma |
| OEPA | vincristine, etoposide, prednisolone, adriamycin (doxorubicin) |
| ORR | overall response rate |
| OS | overall survival |
| PBS | phosphate buffered saline |
| PBMCs | peripheral blood mononuclear cells |
| PCR | polymerase chain reaction |
| PD | progressive disease |
| PD-1 | programmed cell death protein-1 |
| PFS | progression-free survival |
| PHA | phytohaemagglutinin |
| PKD | polycystic kidney disease |
| QE | Queen Elizabeth Hospital |
| qPCR | quantitative real-time PCR |
| rGPNMB | recombinant GPNMB |
| RMA | robust multi-array analysis |
| RNI | reactive nitrogen intermediate |
| ROI | reactive oxygen intermediate |
| RPKM | reads per kilobase per million reads placed |
| sGPNMB | soluble GPNMB |
| SNV | singe nucleotide variant |
| TAM | tumour-associated macrophage |
| TLR | toll-like receptor |
| TMA | tissue microarray |
| TME | tumour microenvironment |
| TRM | tissue-resident macrophage |
| TNF | tumour necrosis factor |
| USA | United States of America |
| VEGF | vascular endothelial growth factor |

# CHAPTER 1

## INTRODUCTION

# Chapter 1 Introduction

## 1.1 Hodgkin Lymphoma

Hodgkin lymphoma (HL) is characterised by malignant Hodgkin and Reed-Sternberg (HRS) cells and a prominent tumour microenvironment which is believed to contribute to HRS growth and protect them from a host immune response which includes cytotoxic T cells. Approximately 40% of all patients with HL carry the oncogenic Epstein-Barr virus (EBV) in HRS cells [reviewed in (Kuppers, 2009)]. Whilst the majority of patients with HL are cured using conventional cytotoxic chemotherapies there is little prospect of further improvement in outcomes without innovation in the therapeutic approaches, as further chemotherapy intensification is limited by the current treatment-related toxicities. Outcomes are particularly poor in older patients (5-year survival 34-48% in patients >74 years) and in those who relapse or have refractory disease (Statistics, 2016). Moreover, survivors of HL experience significant long-term effects of therapy, including reduced fertility, and an increased risk of cardiac deficiency and second malignancies (Goodman et al., 2008). Therefore, new agents that target molecular abnormalities in these lymphomas are required. The goal is to integrate less toxic, but equally effective, targeted therapies into front-line treatment protocols for all patients.

## 1.2 Types of HL

There are 2 main types of HL: classical HL (cHL) and nodular lymphocyte predominant HL (NLPHL). Classical HL makes up approximately 95% of all HL, and NLPHL only 5% of cases in Europe and the United States of America (USA) (Smith et al., 2018). HRS cells are the tumour cells in cHL, and those in NLPHL are called lymphocyte predominant (LP) cells. cHL can be further subdivided in to 4 groups: mixed cellularity classical HL (MCCHL), nodular sclerosis

classical HL (NSCHL), lymphocyte-rich classical HL (LRCHL) and lymphocyte-depleted classical HL (LDCHL). Of these, NSCHL is the most common type of classical HL (70% of cases in Europe and USA), and LDCHL the rarest (<1% cases) (Smith et al., 2018).

Histologically, NSCHL shows a 'nodular' pattern of a sclerotic nodal capsule surrounded by fibrous bands of collagen, often with areas of necrosis. They are usually EBV-negative. NSCHL usually occurs in teenagers and young adults, and disease is often in the mediastinum (Jaffe et al., 2018, Smith et al., 2018).

In MCCHL, there are no fibrous collagen bands or sclerotic nodal capsule as in NSCHL; instead, there is a diffuse infiltrate (with obliteration of lymph node architecture). It often presents at a more advanced stage than NSCHL; is more likely to be EBV-positive; usually seen in young children and older adults; and more likely in HIV-positive patients (Jaffe et al., 2018, Smith et al., 2018).

LRCHL can look very similar to NLPHL morphologically, although immunophenotypically and genetically look like other classical HLs. It is mostly nodular but can be diffuse, and the background is mostly lymphocytes (with almost absent neutrophils and eosinophils). Patients are usually older adults and tend to have localised disease (Jaffe et al., 2018, Smith et al., 2018).

LDCHL contains a diffuse fibrotic and necrotic infiltrate and a relatively high number of HRS cells compared to lymphocytes. Occasionally the HRS cells appear anaplastic or pleomorphic, giving them a 'sarcomatous' appearance. The majority are EBV positive and histologically can look like B- or T-cell lymphomas but immunophenotype is characteristic of

classical HL. It is common in older adults, HIV-positive patients and usually presents with more advanced stage disease (Jaffe et al., 2018, Smith et al., 2018)

### 1.2.1 Origin of HRS and LP tumour cells

Although both cHL and NLPHL have only a small number of malignant cells surrounded by a background of inflammatory cells, they are different in several ways, including: immunophenotype, morphology, makeup of the microenvironment and clinical features (Ansell, 2015, Weniger and Küppers, 2021). LP cells express markers typical of B cells, e.g CD19, CD20 and CD79 on the surface; transcription factors such as BOB1 and PAX5; germinal centre (GC) B cell markers e.g BCL6 and activation-induced cytidine deaminase; and are typically $CD45^{+}$, $CD30^{-}$ and $CD15^{-}$ (Weniger and Küppers, 2021, Küppers, 2018, Jaffe et al., 2018). HRS cells in cHL are usually CD30+, CD45-, CD15+/-, CD20-, CD79-; they show downregulation of B cell transcription factors, e.g. BOB1; upregulation of transcription factors which in turn suppress B cell gene expression, e.g. STAT5, NOTCH1, ID2; some of these are markers of different cell lineages, e.g. T cell genes, myeloid genes, dendritic cell genes and natural killer cell genes (Jaffe et al., 2018, Küppers, 2018, Weniger and Küppers, 2021).

The immunophenotype of LP cells suggests they originate from B cells, but the immunophenotype of HRS cells is unusual in that it does not match that of any 'normal' immune cells. Therefore, it was only through genetic analysis of micro-dissected HRS that their origin was also confirmed to be from B-cells (Küppers, 2018). HRS cells carry gene rearrangements and somatic mutations of immunoglobulin (Ig) heavy and light chain V genes which are very specific to GC-B cells (as somatic hypermutation occurs during B-cell differentiation in the GC of secondary lymphoid organs) (Martin et al., 2015). The normal

process of somatic hypermutation itself is no longer happening in HRS cells, and in approximately 25% of cHL cases, these Ig V gene mutations are pathological; B cells normally carrying these types of mutations would undergo apoptosis, suggesting HRS cells are derived from pre-apoptotic B cells which have undergone a transforming event to escape apoptosis (Kanzler et al., 1996, Küppers, 2018). Table 1.1 compares the features of HRS cells and LP cells (Küppers, 2018).

### 1.2.2 Genetic alterations and deregulated signalling pathways in HL

Table 1.2 provides a summary of the most common genetic lesions in HRS and LP cells, discussed further below (Weniger and Küppers, 2021).

As mentioned, HRS cells derive from pre-apoptotic B cells which undergo transforming events to escape apoptosis. HRS cells contain multiple genomic aberrations which affect several pathways or cellular functions, namely: deregulation of the NF-κB and JAK/STAT signalling pathways; immune evasion; infection with EBV; affecting cytokinesis/DNA/RNA/nuclear function (Brune et al., 2021).

The NF-κB pathway is constitutively activated in HRS cells, by either the classical or alterative pathways (Küppers, 2018). Two of the most frequent mutations to genes in the NF-κB pathway are gains or amplifications of *REL* (encoding an NF-κB factor) and inactivation of *TNFAIP3* (a negative regulator of NF-κB) but pathological mutations that can disrupt this pathway include inactivation of NFKBIA and NFKBIE (also inhibitors of the pathway) (Table 1.2) (Weniger and Küppers, 2021, Brune et al., 2021, Wienand et al., 2019). In total, approximately 50% of classical HL cases contain mutations in this pathway, but it should be noted that these mutations are more common in $EBV^-$ HL cases, as $EBV^+$ cases have another mechanism for

activating this pathway (see section 1.4) (Küppers, 2018). LP cells are not infected by EBV and although some of them contain mutations in REL, there must be other mechanisms causing activation of the NF-κB pathway (Küppers, 2018).

The JAK/STAT pathway (involved in cytokine signalling) is also constitutively activated in HRS and LP cells. As seen in Table 1.2, *JAK2*, *PD-L1*, *PD-L2* and *JMJD2C* are all located at chromosome 9p24 very near each other, therefore are usually seen to be amplified or gained together (Weniger and Küppers, 2021). *PD-L1* and *PD-L2* are involved in the immune evasion of HL by host cells (see section 1.6). *SOCS1* is an inhibitor of the JAK/STAT pathway and is inactivated in about 40% of HL and NLPHL cases (Weniger and Küppers, 2021).

Mutations are frequently seen in the PI3K/AKT/mTOR pathway (up to 45% of classical HL cases), which functions to regulate the cell cycle. Aberrations in this pathway lead to uninhibited proliferation and reduced apoptosis. For example, pathological mutations in *GNA13* (which helps to control proliferation of GC B cells) leads to increased survival of pre-apoptotic GC B cells (Brune et al., 2021, Wienand et al., 2019).

HRS cells are bi- or multi-nucleated cells- this is caused by incomplete or impaired cytokinesis through mutations of *GNA13*, *CDH1* and *DNAH12*. These genes are involved in microtubule dynamics during cytokinesis or DNA-binding, and genetic alterations cause impairments of these processes (Brune et al., 2021).

| Feature | Hodgkin and Reed-Sternberg cells | Lymphocyte Predominant cells |
|---|---|---|
| Somatically mutated Ig V genes | Yes | Yes |
| Crippling Ig V gene mutations | Yes (~25% cases) | No |
| Ongoing somatic hypermutation | No | Yes (moderate) |
| Presumed cellular origin | Pre-apoptotic GC-B cells | Positively selected, mutating GC-B cells |
| B cell receptor expression | No | Yes |
| Expression of B cell transcription factors (e.g., OCT2, BOB1, PAX5) | Rarely +/- at low levels | Yes |
| Expression of GC B cell markers (e.g., BCL6, GCET, AID, HGAL) | No/ rarely | Yes |
| Expression of B cell surface markers (e.g., CD19 and CD20) | No/ rarely | Yes |
| Expression of molecules involved in antigen-presentation and interaction with T-helper cells (e.g., CD40, CD80, CD86, MHC Class II) | Yes | Yes |
| Expression of non-B cell markers (NOTCH1, CCL17, ID2, GATA3, CSFR1) | Yes | No |
| EBV infection of tumour cells | Yes (30-40%) | No |

**Table 1.1. Comparing features of Hodgkin and Reed-Sternberg cells and lymphocyte predominant lymphoma cells** (modified from (Küppers, 2018))

| Gene | | Pathway/ Main Function | Type of genetic mutation | Frequency (%) |
|---|---|---|---|---|
| HRS cells | *NFKBIA* | NF-κB pathway | SNVs, indels | 10-20 |
| | *NFKBIE* | | SNVs, indels | 10 |
| | *TNFAIP3* | | SNVs, indels | 40 |
| | *REL* | | Gains/amplifications | 50 |
| | *MAP3K14* | | Gains/amplifications | 25 |
| | *BCL3* | | Gains, translocations | 20 |
| | *JAK2** | JAK/STAT pathway | Gains/amplifications | 30 |
| | *SOCS1* | | SNVs, indels | 40 |
| | *STAT6* | | SNVs, gains | 30 |
| | *PTPN1* | | SNVs, indels | 20 |
| | *CSF2RB* | | SNVs | 20 |
| | *ITPKB* | PI3K/AKT pathway | SNVs | 15 |
| | *GNA13* | | SNVs | 20 |
| | *B2M* | Immune evasion | SNVs, indels | 30 |
| | *MHC2TA* | | SNVs, translocations | 15 |
| | *PD-L1** | | Gains/amplifications | 30 |
| | *PD-L2** | | Gains/amplifications | 30 |
| | *XPO1* | Nuclear RNA/ protein export | SNVs, gains | 20 |
| | *ARID1A* | Chromatin remodelling | SNVs, indels | 25 |
| | *JMJD2C** | Epigenetic regulator | Translocations | 30 |
| LP cells | *BCL6* | Transcription factor | SNVs, indels | 35 |
| | *SOCS1* | JAK/STAT pathway | SNVs | 40 |
| | *SGK1* | | SNVs | 50 |
| | *JUNB* | Transcription factor | SNVs | 50 |
| | *DUSP2* | | SNVs | 50 |
| | *REL* | NF-κB pathway | Gains | 40 |

**Table 1.2 Genetic mutations in HRS and LP cells** (modified from (Weniger and Küppers, 2021)). SNV- single nucleotide variants. *JAK2, PD-L1, PD-L2 and JMJD2C- closely located on chromosome 9p24, therefore are usually co-amplified/ gained together.

## 1.3 Tumour Microenvironment in cHL

Malignant HRS cells only make up approximately 1% of cells in cHL tumours (Kuppers, 2009). The majority of cells in cHL tumours are inflammatory/immune cells including T-cells, B-cells, macrophages, mast cells, plasma cells and eosinophils (Kuppers, 2009, Aldinucci et al., 2010, Scott and Steidl, 2014). The presence of these cells and cytokines/ chemokines secreted by HRS cells themselves aid proliferation of HRS cells and maintenance of the immunosuppressive tumour microenvironment, e.g. IL-10, CCL4, and CCL22 (Aldinucci et al., 2010). As part of the immunosuppressive microenvironment, M2 macrophages, T-helper (Th2) and regulatory T cells are present, but M1 macrophages, CD8+ CTLs and natural killer (NK) cells are generally lacking (Aldinucci et al., 2010, Nagpal et al., 2020). Tumour associated macrophages in cHL are discussed in detail in 1.6, but have been shown to promote an anti-inflammatory response, angiogenesis and metastasis (Nagpal et al., 2020). A recent study explored the immune landscape of cHL using transcriptomics and immunohistochemistry (IHC) and found cHL samples to be significantly enriched $CD4^+$ and $CD8^+$ T-cells compared to diffuse large B-cell lymphoma (DLBCL) (Péricart et al., 2018). Using IHC and immunofluorescence, the cHL immune cell infiltrate contains 60% $CD3^+$ T-cells (35% of total cells $CD4^+$, 25% of total cells $CD8^+$) and 13% $CD68^+$ macrophages (Péricart et al., 2018). In EBV-positive cHL, CTL responses are known to be suppressed through immune checkpoints (see 1.6). The distribution of inhibitory immune checkpoints in cHL was also investigated; a mean of 16% cells were PD-1+; 29% of total cells were PD-L1+, 11% were TIM-3+ (Péricart et al., 2018). The overexpression of immune checkpoints and high numbers of T-cells in cHL suggest it is a tumour that can modulate an immune response, especially in conjunction with immunotherapy (Péricart et al., 2018).

## 1.4 Epstein-Barr Virus (EBV)

Epstein-Barr virus (EBV) is a herpesvirus that was first discovered in 1964 when Burkitt lymphoma tumour cells were being studied by electron microscopy. From here, it was subsequently discovered that EBV could transform B-cells in cell culture into lymphoblastoid cell lines (LCLs) (Young et al., 2016). Primary EBV causes infectious mononucleosis, X-linked lymphoproliferative disease or chronic active EBV; EBV also plays an aetiological role in the development of multiple cancers, including B cell lymphomas (Burkitt lymphoma, HL, diffuse large B cell lymphoma and post-transplant lymphoproliferative disease), gastric carcinoma, nasopharyngeal carcinoma and a T-cell/natural killer cell lymphoma (Taylor et al., 2015). Once infected with EBV, it persists in asymptomatic individuals in up to 95% of the world's population (Young et al., 2016). Three latency gene expression patterns are known about, through which EBV infection occurs. Latency III (also called the 'growth programme') occurs in LCLs, acute infection or in immunodeficiency, where unrestricted expression of all latent genes; six Epstein-Barr nuclear antigens (EBNAs 1, 2, 3A, 3B, 3C, and EBNA leader protein), latent membrane proteins (LMP1, LMP2A, and LMP2B), microRNAs and EBV-encoded small RNAs (EBER1 and EBER2) which are non-coding (Young et al., 2016). In latency II, EBNA1, LMP1 and LMP2a are expressed. In latency I, only EBNA1 is expressed (Küppers, 2018). Latency 0 is the pattern seen in EBV-infected resting memory B cells where latent viral proteins are not expressed, i.e. latent infection (Young et al., 2016, Dojcinov et al., 2018). In latency 0, only non-coding EBERs are expressed. Whilst EBV-associated epithelial cancers express the latency II pattern, the B cell lymphomas can express any of latency I-III patterns (Young et al., 2016).

### 1.4.1 EBV in cHL

As mentioned, approximately 40% of cHL cases are $EBV^+$ in the West; this is as high as 90% in paediatric HL in Central and South America (Küppers, 2018). In cHL, HRS cells exhibit latency II pattern; EBNA1 is necessary for replication of EBV genomes in episomes; oncogenic LMP1 mainly functions to activate the NF-κB pathway which is constitutively activated in cHL by imitating a CD40 receptor; LMP2a, which contains a motif similar to that of a B cell receptor (BCR), acts to weaken BCR signalling and rescue GC B cells from apoptosis where they have lost BCR-expression due to crippling Ig V gene mutations (see sections 1.2.1 and 1.2.2) (Küppers, 2018).

## 1.5 Current treatment for cHL

First-line treatment for HL usually involves a combination of chemotherapy and/or radiotherapy depending on stage of disease at presentation. Examples of combination chemotherapy regimens include ABVD (Adriamycin (Doxorubicin), bleomycin, vincristine and dacarbazine), OEPA (vincristine, etoposide, prednisolone, adriamycin), BEACOPP (bleomycin, etoposide, doxorubicin, cyclophosphamide, vincristine, procarbazine, prednisolone) or COPDAC (cyclophosphamide, vincristine, prednisolone, dacarbazine) used in different combinations/doses for adults and paediatric patients.

Extended-field radiation therapy was previously used as standard; it was found in a randomised clinical trial that subtotal nodal radiation +/- ABVD had worse overall survival compared to ABVD alone and death from non-HL causes in early-stage disease (Meyer et al., 2012). Thus, most patients with early disease are treated with chemotherapy and involved-

field radiation to restricted sites. Patients with advanced- stage cHL tend to be treated with chemotherapy alone (Ansell, 2015).

Those with refractory disease or who relapse usually go on to have high-dose chemotherapy and autologous stem-cell transplantation (ASCT), but for those who relapse following ASCT prognosis is extremely poor (approximately 50% survival) (Statistics, 2015). Brentuximab vedotin is a monoclonal antibody-drug conjugate against CD30 (expressed by HRS cells), currently only licensed for use in those who relapse following ASCT but has shown positive results in this group (Younes et al., 2010, Arai et al., 2013, Moskowitz et al., 2015). Although therapies targeting the immune checkpoint Programmed cell death protein-1 (PD-1) pathway using drugs such as nivolumab have shown promise in the treatment of refractory/relapsed HL, not all patients respond to these drugs (Ansell et al., 2015, Kasamon et al., 2017, Bond and Alinari, 2017). Furthermore, studies from other cancers, such as melanoma, suggest that combination therapies employing the simultaneous blockade of two or more different immune checkpoints are likely to be more effective [reviewed in (Marquez-Rodas et al., 2015)].

## 1.6 Tumour- Associated Macrophages (TAM)

### 1.6.1 Macrophage Ontogeny

Macrophages have previously been described as being derived from common myeloid precursor cells which originate from haematopoietic stem cells (HSC) (Mosser and Edwards, 2008). The 'mononuclear phagocyte system,' described by van Furth *et al*. (1972) grouped cells together based on similar 'morphology, function, origin and kinetics' and on that basis, promonocytes, their bone marrow precursors, circulating monocytes and tissue macrophages

were included in this system, whereby circulating monocytes migrate to tissues and differentiate into tissue-specific macrophages, e.g. osteoclasts (bone) or histiocytes (connective tissue) and depending on the stimuli received could become activated in different ways (Mosser and Edwards, 2008, van Furth et al., 1972). Tissue-resident macrophages (TRMs) include alveolar macrophages in the lung, brain microglia, Kupffer cells in the liver, red-pulp macrophages in the spleen, and F4/80$^{bright}$ kidney and cardiac macrophages (Perdiguero and Geissmann, 2016). Hashimoto *et al*. (2013) showed through fate-mapping models and parabiosis studies that TRMs are maintained independently of monocytes in the 'steady state' as they have the ability to self-renew through proliferation, even after injury (Hashimoto et al., 2013). Similar results were seen in microglia in mice, where they were shown to maintain in adult tissue independently of circulating haematopoietic precursors (Ginhoux et al., 2010). Furthermore, it has been shown that these macrophages develop in the yolk sac of embryos prior to the development of haematopoietic stem cells (Hoeffel and Ginhoux, 2015, Schulz et al., 2012, Gomez Perdiguero et al., 2015). Common erythro-myeloid progenitors (EMPs) which derive from the embryonic yolk sac on embryonic day 8.5, were also seen to be present in the foetal liver from embryonic day 10.5 had both erythroid and myeloid potential based on the different colony-forming units which were detected (Gomez Perdiguero et al., 2015). These EMPs are the precursors of foetal monocytes and yolk sac macrophages that can develop into microglia independently of the transcription factor *Myb*, which is required for the development of haematopoietic stem cells (Schulz et al., 2012, Gomez Perdiguero et al., 2015). A 'second wave' of late EMPs colonise the foetal liver to generate foetal monocytes which develop into TRMs once recruited to embryonic tissues (but these EMPs are *Myb*$^{+}$); these TRMs have the ability to self-renew into adulthood (Hoeffel et

al., 2015, Ginhoux et al., 2016, Gomez Perdiguero et al., 2015). Thus, TRMs are derived independently of HSCs.

In adult tissues, the amount in which HSCs contribute depends on the organ and this also varies with age. In adult brain, liver and epidermis TRMs for example, HSCs contribute <5%, however in spleen, heart and lungs the contribution of HSCs to TRMs increases with age as these macrophages have a slow turnover (Perdiguero and Geissmann, 2016). Intestinal and dermis macrophages are the main groups of macrophages which are not able to self-renew and therefore would rely on circulating HSCs for renewal and both have an estimated half-life of 4-6 weeks (Ginhoux and Guilliams, 2016).

### 1.6.2 Macrophage activation and polarisation and TAM ontogeny

Macrophages can be broadly classified into M1 (classically activated macrophages), and M2 (alternatively activated macrophages) though there has always been much debate about this classification (Murray et al., 2014, Allavena et al., 2008). These can also be thought of as two 'extremes' of polarisation on a linear scale, and macrophage polarisation can fluctuate in response to stimuli/ signals received from their environment (Sica et al., 2006, Allavena et al., 2008, Mosser and Edwards, 2008, Stout et al., 2005). Since the developments in macrophage ontogeny, new models are also being considered for macrophage activation and origin of TAMs, i.e. monocyte-derived TAM which differentiate upon infiltrating tissues/tumours (Laviron and Boissonnas, 2019). However, as there is not yet a consensus, I have used the older classifications in this thesis.

Despite the overlap, M1 & M2 macrophages have separate phenotypes which are summarised in Table 1.3 (adapted from (Allavena et al., 2008, Sica et al., 2006)) and Figure 1.1

(Sica et al., 2006). TAM are M2-like macrophages but also display pro-tumoural functions (Sica et al., 2006, Mantovani et al., 2002). Many of the polarising stimuli towards an M2-phenotype are expressed in the tumour microenvironment, for example, IL-10, an immunosuppressive cytokine promotes monocyte differentiation to an M2c-like phenotype and is also highly expressed by TAM themselves (Mantovani et al., 2002, Allavena et al., 2008, Sica et al., 2006). Other examples include macrophage colony stimulating factor (M-CSF), prostaglandins, transforming growth factor (TGFβ) and IL-6 (Allavena et al., 2008). The tumour-promoting functions of TAM include their ability to induce angiogenesis mediated by secretion of soluble angiogenic factors such as vascular endothelial growth factor (VEGF) (Mantovani et al., 2006, Murdoch et al., 2008); suppression of adaptive immunity through release of IL-10, TGFβ and chemokines like CCL17, CCL18 and CCL22 to suppress anti-tumour response; release of matrix metalloproteinases (MMPs) and chemokines to promote matrix remodelling, tumour invasion and metastasis and promoting tumour growth and survival (Mantovani et al., 2002, Allavena et al., 2008).

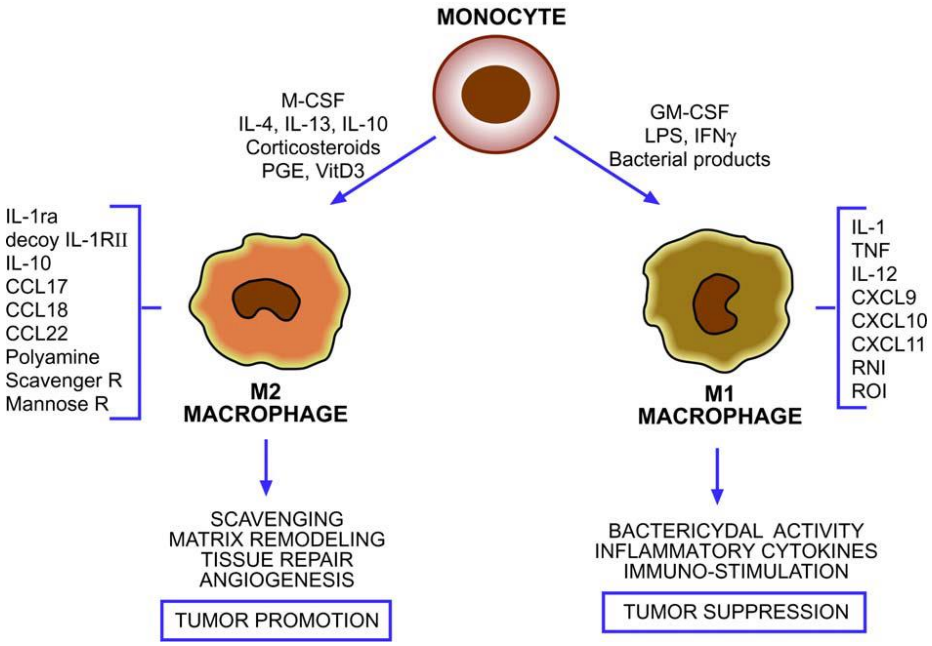


**Figure 1.1 Macrophage polarisation into M1 and M2 macrophages.**

Reprinted from European Journal of Cancer, 42; 717-727. Tumour- associated macrophages are a distinct M2 polarised population promoting tumour progression: potential targets of anti-cancer therapy. Sica et al.,COPYRIGHT (2006), with permission from Elsevier

| | M1 (classically activated) | M2 (alternatively activated) |
|---|---|---|
| **Polarising Stimuli** | IFNγ, LPS, TNF, GM-CSF, Bacterial products | M2a- IL-4, IL-13 |
| | | M2b- IC & LPS or IL-1 or TLR/IL-1R ligands |
| | | M2c- IL-10, glucocorticoids |
| **Main Function** | Tumour Suppression; Th1 Activation, DTH; Killing of intracellular pathogens; immune-stimulation, host defence, tissue destruction | Tumour Promotion; Th2 activation (M2a, M2b); killing and encapsulation of parasites (M2a); Immunosuppression (especially M2b, M2c); wound healing, tissue remodelling, angiogenesis |
| **Cytokine Production** | IL-12$^{HIGH}$, IL-10$^{LOW}$, IL-23; IL-1$^{HIGH}$, TNF, IL-6; signalling IL-1RI$^{HIGH}$; CXCL9, CXCL10, CXCL11 | IL-12$^{LOW}$, IL-10$^{HIGH}$; IL-1$^{LOW}$, TNF, IL-6 (not M2b); TGFβ (M2c); decoy IL-1RII$^{HIGH}$, IL-1R-antagonist; CCL17, CCL18, CCL22, Polyamine, Scavenger R, Mannose R |
| **Toxic Intermediates** | HIGH RNI & ROI | LOW RNI & ROI |
| **Tumour Resistance** | HIGH | POOR |

**Table 1.3 M1 and M2 phenotypes** (adapted from Mosser & Edwards, Nat Rev Immunol., 2008 & Sica et al., Eur J Cancer, 2006) LPS- Lipopolysaccharide; IFNγ- interferon gamma; TNF- tumour necrosis factor; IC- immune complex; TLR- toll-like receptor; IL-1R- IL-1 receptor; DTH- delayed type hypersensitivity; RNI- reactive nitrogen intermediate; ROI- reactive oxygen intermediates.

### 1.6.3 TAM and outcome in cHL

Recent evidence suggests the composition of the tumour microenvironment of cHL is an important determinant of patient outcome (Greaves et al., 2013, Barros et al., 2012b, Chetaille et al., 2009, Tan et al., 2012, Kamper et al., 2011). In particular, increased numbers of CD68 and CD163-expressing tumour-associated macrophages (TAMs) are strongly associated with inferior survival in newly diagnosed cHL patients, in those treated with standard chemotherapy, as well as in those having received autologous stem cell transplant (Tan et al., 2012, Kamper et al., 2011). In these patients, increased CD68 and CD163 expression were also strongly correlated with EBV-positivity in their tumours (Kamper et al., 2011, Tan et al., 2012). Steidl *et al*., used gene expression profiling of the tumour tissues of newly diagnosed cHL patients to show that a gene expression signature of macrophage infiltration was associated with poor prognosis, a finding which was validated using immunohistochemistry to detect TAMs in an independent patient cohort (Steidl et al., 2010). Another study in paediatric cHL showed that those patients with a higher frequency of tumour-associated M1-like macrophages (defined as CD163+pSTAT1+) had better overall survival, whereas patients whose tumours were infiltrated with higher numbers of M2-like macrophages (CD163+CMAF+) had significantly worse progression-free survival (Barros et al., 2015). In 2 studies, EBV-positive cases had a predominantly M1-polarised microenvironment, and a gene signature characteristic of Th1 response, whereas EBV-negative cases had a predominantly M2-polarised microenvironment (Chetaille et al., 2009, Barros et al., 2015). It has been suggested that the microenvironment varies between paediatric and adult cases of cHL such that there appeared to be significantly more Th1-like cells in EBV-positive cases in those under 10 years of age (Barros et al., 2012b). This may reflect age-related differences in the cellular

composition, in particular, a more cytotoxic T-cell infiltrate in younger patients (Barros et al., 2012b, Barros et al., 2012a).

CD68-positive and CD163-positive TAMs are also associated with increased micro-vessel density (MVD) and vascular endothelial growth factor (VEGF) in cHL (Panico et al., 2013, Koh et al., 2014) and MVD correlates with poor outcome in HL patients (Korkolopoulou et al., 2005, Mainou-Fowler et al., 2006, Doussis-Anagnostopoulou et al., 2002), suggesting macrophages contribute to a pro-angiogenic phenotype in HL.

## 1.7 Immune Checkpoints

Immune checkpoints are co-stimulatory or inhibitory pathways involved in regulating T-cell immune responses, as shown in Figure 1.2 (from Pardoll, Nat Rev Cancer, 2012) (Pardoll, 2012). These checkpoints are required to prevent autoimmunity and to protect a host's own tissues from being damaged during the immune response to pathogens (Pardoll, 2012). However, these same checkpoints can be manipulated by tumours to block the anti-tumour immune response (and thus allow tumours to evade detection by a host's immune system) (Pardoll, 2012). Most of these are modulated through ligand-receptor pairs between antigen-presenting cells and T-cells, making the attractive targets for new therapies (Pardoll, 2012).

This is relevant because although HL tissues are known to contain cytotoxic T-lymphocytes (CTL) with specificity for tumour cell epitopes, such as those derived from viral proteins in EBV-positive cases, these CTL are unable to eliminate HRS cells (Chapman et al., 2001). The inhibition of CTL responses in HL is partly mediated by the interaction of programmed death ligand 1 (PD-L1) on tumour cells with PD-1, on T-cells (Green et al., 2012). However, this is just

one of several immune checkpoint pathways that allow tumours to evade detection by the host immune system (Figure 2) (Armand, 2015, Pardoll, 2012).

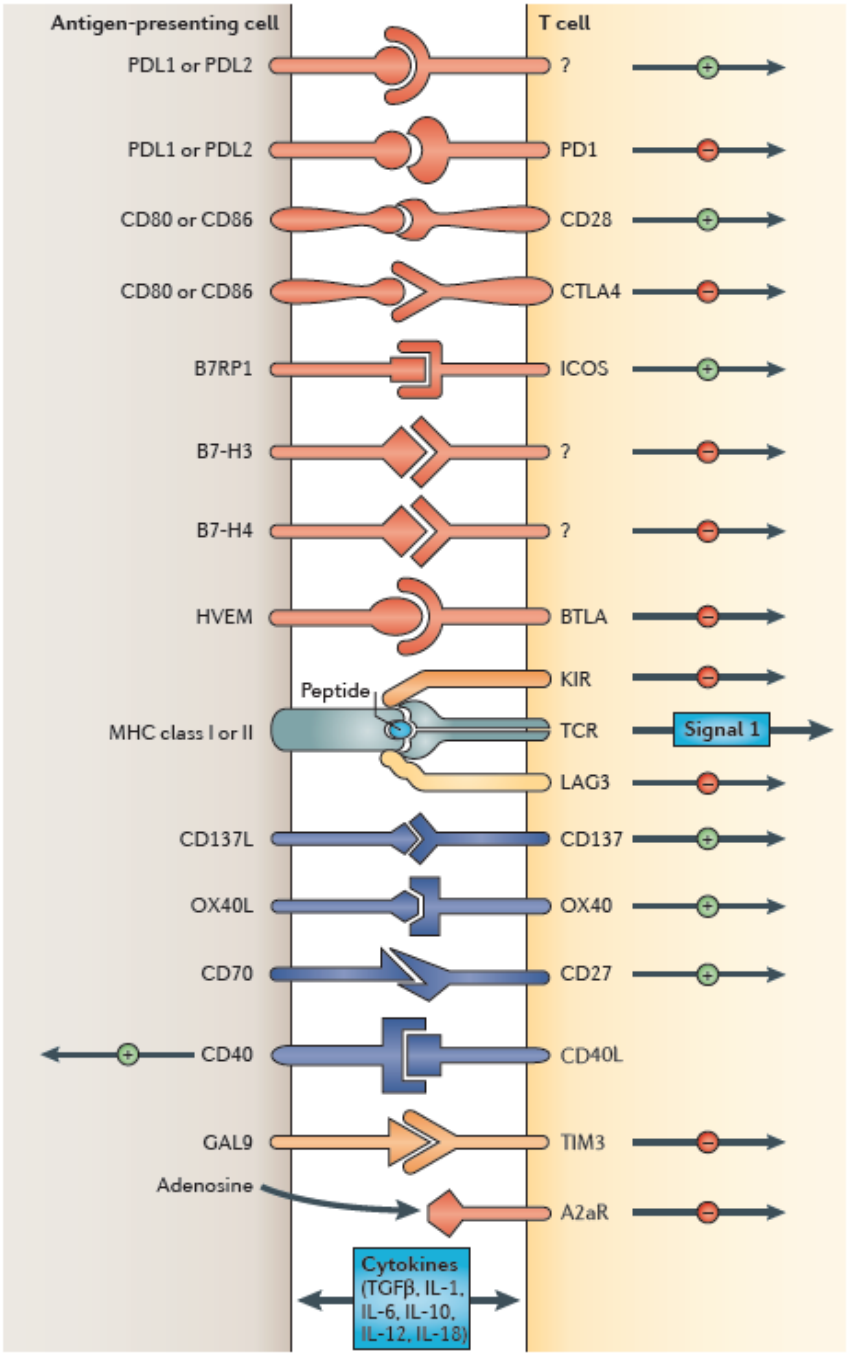


**Figure 1.2**. **Immune checkpoint pathways modulated through T-cells and APCs.** Ligands can bind to different receptors to deliver a co-stimulatory or inhibitory signal. In some cases, the inhibitory receptor on T-cells is only expressed upon activation of T-cells.

## 1.8 Glycoprotein Non-Metastatic Melanoma Protein B (GPNMB)

GPNMB is a trans-membrane protein that is overexpressed in several cancer types including breast cancer, melanoma, lung cancer and glioblastoma [reviewed in (Maric et al., 2013)],(Rose et al., 2010b, Tomihari et al., 2010, Kuan et al., 2006, Li et al., 2014, Oyewumi et al., 2016). It was first cloned in 1995 from low-metastatic melanoma cell lines (and subsequently named 'non-metastatic B', but has since been reported to be expressed in cancers with a more invasive phenotype) (Weterman et al., 1995, Rose et al., 2010a, Oyewumi et al., 2016, Rich et al., 2003, Rose et al., 2007). It is also known as hematopoietic growth factor inducible, neurokinin-1 type (HGFIN) and in its murine form is called Osteoactivin or dendritic cell- associated, heparan sulphate proteoglycan-dependent integrin ligand (DC-HIL) (Shikano et al., 2001, Sheng et al., 2008). GPNMB is a type 1 transmembrane protein and contains several functional domains, including a dileucine motif and half immunoreceptor tyrosine-based activation motif (hemITAM) in the cytoplasmic tail; a single pass transmembrane anchor; a polycystic kidney disease (PKD) domain, integrin binding (RGD) motif and N-terminal signal peptide in the extracellular domain (ECD) of the protein (Figure 1.3A. from Maric et al., Oncotargets Ther. 2013) (Maric et al., 2013). These functional domains interact with other cells in the tumour microenvironment through which it enhances tumour growth and invasiveness, discussed in further detail below and summarised in Figure 1.3B (from Maric et al., Oncotargets Ther. 2013) (Maric et al., 2013).

GPNMB expression is significantly increased following the differentiation of monocytes to macrophages (Dong et al., 2013) and is also reported to be higher in M2 macrophages compared with M1 macrophages (Yu et al., 2016). Proteolytic cleavage of GPNMB by ADAM10 results in the release of a soluble form (sGPNMB) (Rose et al., 2010a) which promotes both

autocrine and paracrine signalling (Maric et al., 2013). Importantly, sGPNMB has been shown to engage its receptor, syndecan-4, to deliver a potent inhibitory signal to CTL and may therefore represent a novel immune checkpoint (Tomihari et al., 2010, Chung et al., 2007). The RGD motif allows GPNMB to bind to integrins, e.g. on endothelial cells, supporting trans-endothelial migration (Maric et al., 2013). sGPNMB promotes endothelial cell survival and migration of breast cancer and glioma cells in vitro and is associated with increased MVD in mammary tumours suggesting it might also directly induce angiogenesis (Rose et al., 2010a, Rich et al., 2003).

### 1.8.1 GPNMB expression in normal tissues

GPNMB is known to be expressed in many normal tissues in the body, but expression levels vary. Transcriptomics analysis (RNA-seq) performed on 95 control human samples covering 27 tissues was published on the NCBI Gene and BioProject websites (Fagerberg et al., 2014, NCBI, NCBI). GPNMB (Gene ID 10457) was most highly expressed in skin, gall bladder and heart tissues, but lymph nodes also had a high expression compared to other tissues (Figure 1.4).

When GPNMB was first cloned in mice, it was shown to be expressed at high levels in bones (including long bones and the skull) as an osteoblast-specific protein, but was subsequently shown to be upregulated in osteoclasts and involved in osteoclast formation and function (Safadi et al., 2001, Sheng et al., 2008). It was then shown that normal human melanocytes express high levels of GPNMB in mature melanosomes, as well as melanoma cells being positive for GPNMB (Hoashi et al., 2010).

GPNMB's role in inflammation and immunity has been explored in multiple inflammatory conditions in humans, mice and rats. As mentioned above, GPNMB is upregulated upon polarisation of monocytes to macrophages, but also appears to act as a negative regulator of proinflammatory responses in macrophages (Ripoll et al., 2007). After acute kidney injury in mice, GPNMB expression was shown to be upregulated, and more specifically was localised to $GPNMB^+$ macrophages infiltrating the injured kidney, compared to relatively low levels of GPNMB in healthy kidney tissue (Zhou et al., 2017). Zhou *et al.* (2017) also showed that knocking down GPNMB inhibited polarisation of macrophages to an M2 phenotype, and promoted M1 polarisation with associated increase in 'pro-inflammatory' cytokine release (e.g. TNF -α) and subsequent decrease in 'anti-inflammatory' cytokine release, (e.g. interleukin-10 (IL-10)). This is in keeping with data from Ripoll *et al*. (2007) that GPNMB is a negative regulator of pro-inflammatory responses. Another study showed GPNMB was widely expressed in the normal brain tissue of adult rats (e.g. cerebrum, cerebellum and spinal cord); more specifically GPNMB was mostly expressed in the microglia/macrophages with some expression in radial glial cells and neuronal nuclei (Huang et al., 2012), Following an injection of LPS into rats (as an inflammatory stimulus), increased numbers of $GPNMB^+$ macrophages infiltrated the area postrema in rat brains, suggesting a role in inflammatory responses in the central nervous system (Huang et al., 2012). In acute liver injury in mice, GPNMB expression increased in the acute recovery phase after 2-4 days post-organ injury; this was predominantly in recruited macrophages (approximately 50% of $CD68^+$ macrophages were also $GPNMB^+$); macrophages which were CD68+GPNMB+ showed enhanced phagocytic activity compared to those which were CD68+GPNMB- (Kumagai et al., 2015).

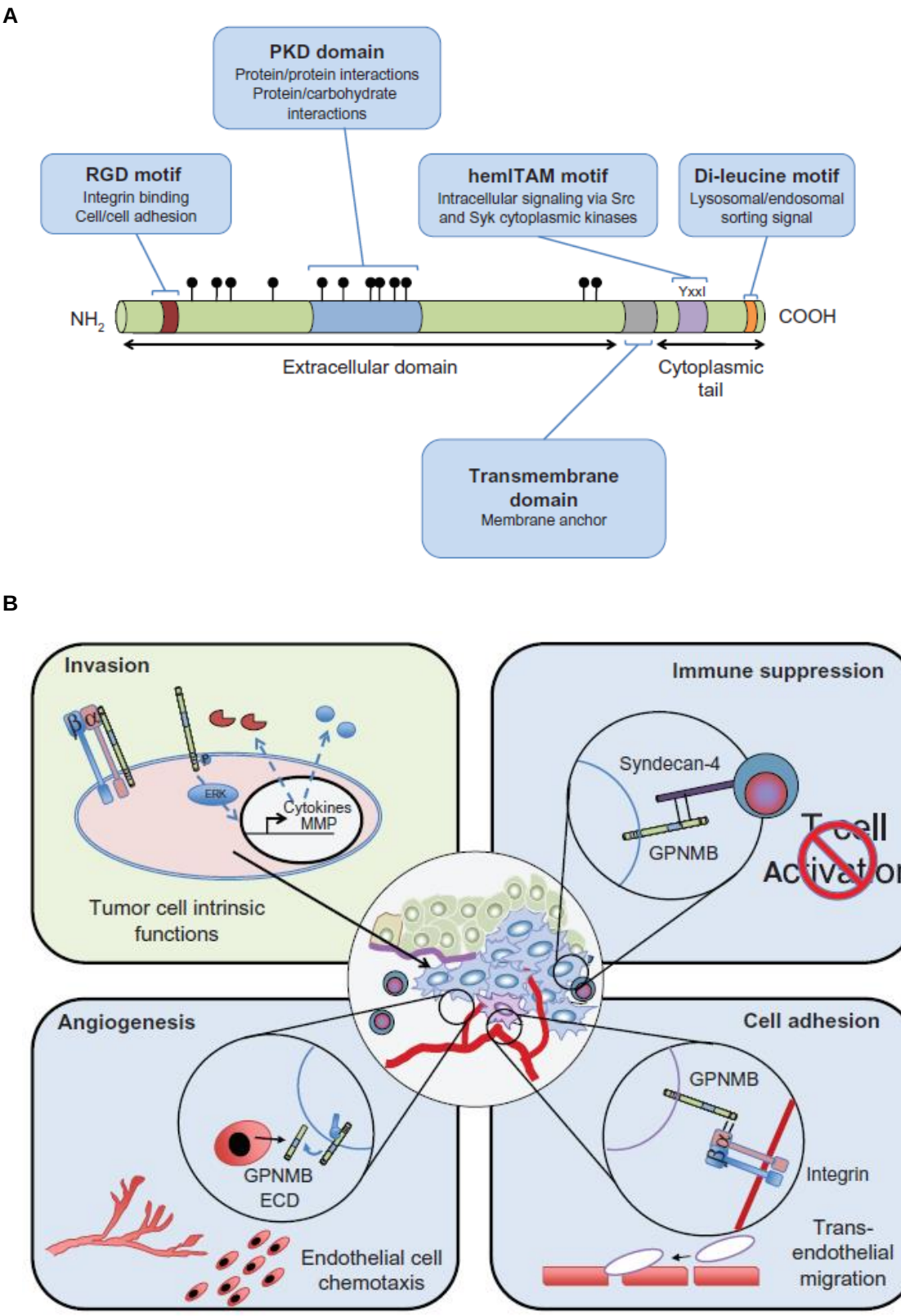


**Figure 1.3. Structure and functions of GPNMB.** (A) Structure of GPNMB protein with functional domains that contribute to tumour growth and invasiveness. (B) Different mechanisms of action of GPNMB.

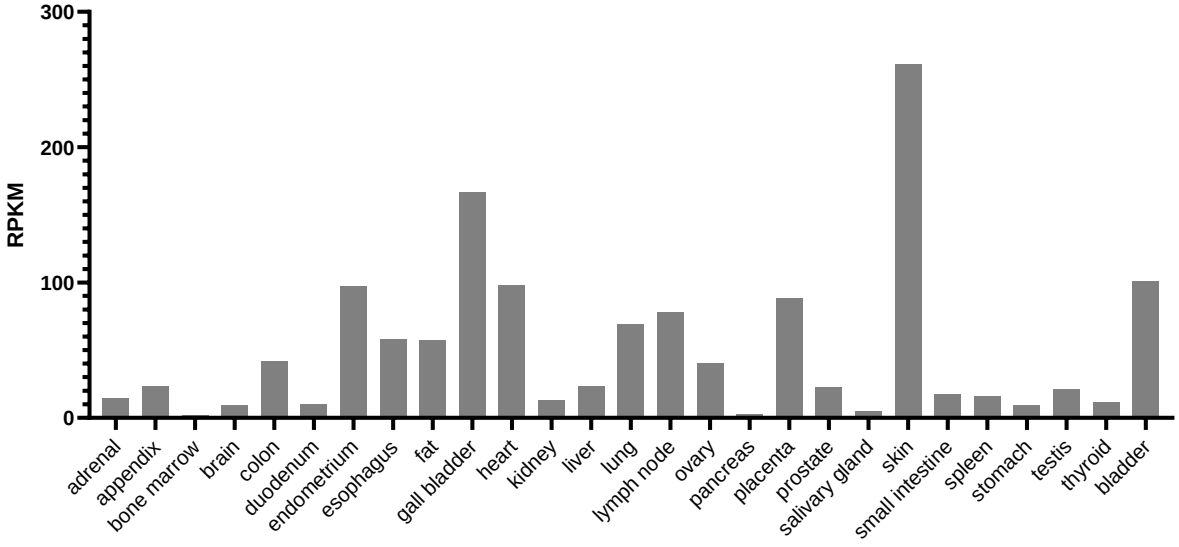


**Figure 1.4 GPNMB expression in normal tissues** (data re-plotted from Fagerberg et al., 2014 and NCBI BioProject PRJEB4337). RNA-seq gene expression data from a total of 95 control samples and 27 tissues showing expression of GPNMB (between 2-7 samples per tissue . RPKM- reads per kilobase per million reads placed.

## 1.9 Hypothesis

My hypothesis is that macrophage-derived GPNMB contributes to the immune evasion of HRS cells and that blocking GPNMB could provide an effective therapeutic approach for patients with cHL. The observation that many other common cancers, including lung cancer, also over-express GPNMB (Tomihari et al., 2010, Li et al., 2014, Oyewumi et al., 2016, Maric et al., 2013, Rose et al., 2010b, Kuan et al., 2006) suggests that the therapeutic targeting of GPNMB might eventually receive more widespread application.

## 1.10 Aims

### 1.10.1 Objective 1: GPNMB expression on patient outcome in cHL

Since it is well established that macrophages are associated with poor outcome in HL, I will investigate if GPNMB expression in macrophages in cHL (by immunohistochemistry for CD68, GPNMB and CD30) can also help refine current outcome prediction models for HL. I have access to clinically annotated paraffin-embedded cHL tissues from adult cases and therefore aim to investigate if there is a relationship between GPNMB expression and clinical outcome.

### 1.10.2 Objective 2: Regulation of GPNMB expression by HRS cells

*In vitro* cultivated M1 and M2 macrophages differentiated from blood monocytes will provide the means to explore if HRS cells can increase GPNMB expression in macrophages; if GPNMB release from macrophages is enhanced by co-culture with HRS cell lines; and if so, which cytokines are responsible for this.

### 1.10.3 Objective 3: Impact of macrophage-derived GPNMB on EBV-specific CTL responses in vitro

I will study the impact of sGPNMB on T-cell activation (in healthy donors) and then on relevant EBV-specific responses *in vitro*. Our lab's established panel of EBV-specific $CD8^+$ T-cell clones will be used to explore the impact of sGPNMB on T-cell recognition of HLA-matched EBV-positive HL-derived and lymphoblastoid cell lines. T-cell recognition of cell lines will be measured by detection of IFN-γ release. sGPNMB will be a commercially available recombinant GPNMB or derived from *in vitro* cultivated M1 and M2 macrophages. To test the

specificity of any effects observed, these experiments will also be done in the presence of commercially available blocking antibodies against GPNMB.

# CHAPTER 2

## MATERIALS AND METHODS

# Chapter 2 Materials and Methods

## 2.1 Cell lines

### 2.1.1 HL cell lines and HEK293 cells

All cell lines (L1236, L428 and L591, HEK293) were obtained from Leibniz Institute DSMZ- German Collection of Microorganisms and Cell Cultures.

All HL cell lines were maintained in 'complete' media: RPMI-1640 + 10% heat-inactivated Foetal Bovine Serum (FBS) (all from Gibco, Life Technologies).

HEK293 cells were maintained in Dulbecco's modified eagle's medium (DMEM) (Sigma-Aldrich, Merck group) + 10% FBS.

All cell lines were incubated at 37°C, 5% $CO_2$ in a humidified atmosphere. Suspension cells were split when at approximately 80% confluency/ $8x10^5$ cells/ml and resuspended at $2\text{-}4x10^5$ cells/ml (2-3 times/week). Adherent cells were split when approximately 80% confluency (assessed by visual microscopic inspection); cells were dissociated using TrypLE Express enzyme (Gibco, Life Technologies); this was neutralised with fresh media after 2 mins, cells resuspended and plated at the required concentration.

L591, L1236 and L428 conditioned media (CM) were prepared by resuspending $1x10^6$ cells/ml in fresh 'complete' media for each cell line and incubating for 24 hours. CM was then harvested by centrifuging cell suspension at 1200 RPM for 10 minutes, and supernatant filtered using 0.2µM sterile syringe filters, then frozen at -20°C until required or used fresh.

### 2.1.2 EBV (B95.8 strain) Lymphoblastoid Cell Lines (LCLs)

All LCLs were maintained in 'LCL Media': RPMI 1640 + 2mM L-glutamine (Sigma-Aldrich, Merck group) + 10% FBS (Labtech) + 50 international units (IU)/ml penicillin + 50µg/ml streptomycin (Gibco, Life Technologies).

Cells were fed twice weekly with fresh media and split depending on confluency (1 in 2 split).

B95.8 LCLs were generated by the Graham Taylor Group.

### 2.1.3 $CD8^+$ T-cell clones

All $CD8^+$ T-cell clones were cultured in 'T-cell media': RPMI-1640 + 2mM L-glutamine (Sigma-Aldrich, Merck group), 30% Monkey Leukocyte Antigen (MLA)-144 supernatant (derived by culturing MLA-144 cells for 2 weeks, supernatant harvested, sterile filtered and stored at -20°C) + 10% FBS (batch tested) (Labtech) + 1% Human Serum (from male AB plasma, batch tested) (Sigma Aldrich, Merck group) + 50IU/ml penicillin + 50µg/ml streptomycin (Gibco, Life Technologies) + 50IU/ml recombinant human Interleukin-2 (Novartis).

Established $CD8^+$ T-cell clones were maintained in 24-well plates (Corning); fed twice weekly by removing 1ml of supernatant and adding 1ml fresh 'T-cell media.' T-cell clones were stimulated every 2-4 weeks as required by culturing with irradiated (4000 rads) allogenic feeder peripheral blood mononuclear cells (PBMCs) ($10^6$ /well from 3 donors) which had been treated with phytohaemagglutinin (PHA) 10µg/ml (Biostat Thermofisher) and irradiated (4000 rads) autologous LCLs ($10^5$ /well).

All T-cell clones were generated by members of the Graham Taylor Group.

## 2.2 Patient and donor samples

### 2.2.1 Ethical approval for research with human tissue

Patient HL blocks (paraffin-embedded tissue) were obtained from Queen Elizabeth Hospital, Birmingham (QE, Birmingham) (RG_15_165). Tonsils were obtained with consent from adult patients from QE, Birmingham through Human Biomaterials Resource Centre (HBRC) and fixed in 10% neutral buffered saline and embedded in paraffin (RG_15_165). Leukocyte cones were obtained with consent through the National Blood Service and used for preparation of monocytes and polarised macrophages (RG_15_165). Whole blood was obtained from healthy donors with consent (RG_13_353) for isolation of PBMCs.

### 2.2.2 cHL Tissue Microarray (TMA)

Paraffin-embedded tissue from 94 adult cHL cases were made into a tissue microarray by Dr Matthew Pugh, a pathologist in our group. Patient and sample details (where available) are given in Table 2.1. Each slide (HL1- HL6) contains 16 samples, each are labelled with their position on the slide (A1-D4).

### 2.2.3 Paraffin embedding of tonsils

Tonsil tissue was cut into 4 pieces, and each fixed in 10% neutral buffered saline (Leica) at 4 time point between 12-48hrs. All 4 pieces of tissue was embedded into 1 paraffin block; then sections were cut and mounted on slides by the Royal Orthopaedic Hospital Pathology Department, Birmingham.

**Table 2.1. cHL TMA- Clinical information from cases (where available)**.

HL2 B3* and C3* are diagnosis and relapse samples from the same patient. HL3 A2* and C2* are diagnosis and relapse samples from another patient. Rows highlighted yellow were excluded from analysis (see section 3.3 for analysis details). PFS- progression-free survival. OS- overall survival. EOT- end of treatment. PD- progressive disease.

| | Age | Sex | Subtype | EBV Status | Type of biopsy | PFS Event | OS Event |
|---|---|---|---|---|---|---|---|
| **HL1** | | | | | | | |
| A1 | 30 | Female | MCCHL | negative | | | |
| A2 | | | | positive | | | |
| A3 | 60 | Male | | negative | | | |
| A4 | 27 | Female | NSCHL | negative | | | |
| B1 | 50 | Male | | negative | | | |
| B2 | 46 | Male | MCCHL | positive | Diagnostic | Death | Died |
| B3 | 62 | Male | MCCHL | positive | | | |
| B4 | 25 | Female | | negative | Diagnostic | Relapse after EOT | |
| C1 | 37 | Female | MCCHL | positive | | | |
| C2 | | | | negative | | | |
| C3 | 24 | Male | | negative | Relapse | Relapse after EOT | |
| C4 | | | | negative | | | |
| D1 | | | | positive | | | |
| D2 | 22 | Male | MCCHL | negative | | | |
| D3 | | | | positive | | | |
| D4 | 62 | Male | MCCHL | positive | | | |
| **HL2** | | | | | | | |
| A1 | 34 | Female | | negative | | | |
| A2 | 22 | Female | | positive | | | |
| A3 | 18 | Female | NSCHL | negative | Diagnostic | PD at EOT | |
| A4 | 31 | Male | MCCHL | negative | Diagnostic | PD at EOT | |
| B1 | 47 | Male | NSCHL | positive | | | |
| B2 | | | | positive | | | |
| B3* | 39 | Male | NSCHL | negative | Diagnostic | Relapse after EOT | |
| B4 | 40 | Male | NSCHL | positive | | | |
| C1 | | | | positive | | | |
| C2 | 32 | Male | NSCHL | negative | | | |
| C3* | 39 | Male | NSCHL | positive | Relapse | Relapse after EOT | |
| C4 | | | | negative | | | |
| D1 | 22 | Male | MCCHL | positive | | | |
| D2 | 36 | Male | NSCHL | negative | | | |
| D3 | 36 | Female | NSCHL | positive | Diagnostic | Relapse after EOT | |
| D4 | | | | negative | | | |
| **HL3** | | | | | | | |

| | Age | Sex | Subtype | EBV Status | Type of biopsy | PFS Event | OS Event |
|---|---|---|---|---|---|---|---|
| A1 | | | | negative | | | |
| A2* | 60 | Female | NSCHL | positive | Relapse | Relapse after EOT | Died |
| A3 | | | | negative | | | |
| A4 | | | | positive | | | |
| B1 | | | | negative | | | |
| B2 | 18 | Female | | negative | Relapse | Relapse after EOT | |
| B3 | | | | negative | | | |
| B4 | | | | positive | | | |
| C1 | 47 | Male | MCCHL | negative | Diagnostic | PD at EOT | |
| C2* | 60 | Female | NSCHL | positive | Diagnostic | Relapse after EOT | Died |
| C3 | 37 | Male | | positive | Diagnostic | PD at EOT | Died |
| C4 | | | | positive | | | |
| D1 | 31 | Male | NSCHL | negative | | | |
| D2 | 73 | Male | MCCHL | positive | Diagnostic | PD at EOT | |
| D3 | | | | positive | | | |
| D4 | 43 | Male | | positive | Diagnostic | Relapse after EOT | |
| **HL4** | | | | | | | |
| A1 | 54 | Male | | positive | Diagnostic | Relapse after EOT | Died |
| A2 | 62 | Male | MCCHL | positive | | | |
| A3 | 32 | Male | NSCHL | negative | | | |
| A4 | 56 | Female | | positive | | | |
| B1 | 51 | Male | MCCHL | negative | | | Died |
| B2 | | | | positive | | | |
| B3 | 25 | Male | NSCHL | positive | | | |
| B4 | 52 | Male | NSCHL | negative | | | |
| C1 | 53 | Female | | negative | | | |
| C2 | | | | negative | | | |
| C3 | 19 | Female | | negative | | | |
| C4 | 28 | Male | MCCHL | positive | | | |
| D1 | 46 | Male | MCCHL | negative | | | |
| D2 | 63 | Female | NSCHL | negative | | | |
| D3 | 52 | Male | NSCHL | negative | | | |
| D4 | 19 | Male | NSCHL | positive | | | |
| **HL5** | | | | | | | |
| A1 | | | | negative | | | |
| A2 | 22 | Female | MCCHL | negative | | | |
| A3 | 17 | Female | | negative | | | |
| A4 | 66 | Male | NSCHL | negative | | | |
| B1 | 68 | Male | NSCHL | negative | | | |
| B2 | 67 | Female | MCCHL | negative | | | |
| B3 | 55 | Male | NSCHL | positive | | | |
| B4 | 23 | Female | NSCHL | negative | | | |
| C1 | 19 | Male | MCCHL | negative | | | |

| | Age | Sex | Subtype | EBV Status | Type of biopsy | PFS Event | OS Event |
|---|---|---|---|---|---|---|---|
| C2 | 53 | Female | NSCHL | negative | | | |
| C3 | 21 | Male | | negative | | | |
| C4 | 27 | Female | NSCHL | negative | | | |
| D1 | 58 | Male | | positive | | | |
| D2 | 41 | Male | | positive | | | |
| D3 | 27 | Female | NSCHL | positive | | | |
| D4 | 41 | Male | NSCHL | negative | | | |
| **HL6** | | | | | | | |
| A1 | 37 | Male | MCCHL | positive | | | |
| A2 | 25 | Female | NSCHL | negative | | | |
| A3 | 61 | Male | MCCHL | positive | | | |
| A4 | 34 | Female | MCCHL | negative | | | |
| B1 | 25 | Male | NSCHL | positive | | | |
| B2 | 65 | Male | | positive | | | |
| B3 | 21 | Female | MCCHL | negative | | | |
| B4 | 72 | Female | MCCHL | negative | | | |
| C1 | 20 | Female | NSCHL | negative | | | |
| C2 | 36 | Female | NSCHL | negative | | | |
| C3 | 30 | Female | NSCHL | negative | | | |
| C4 | 67 | Female | MCCHL | negative | | | |
| D1 | 61 | Male | | negative | | | |
| D2 | 27 | Male | LDCHL | negative | | | |
| D3 | 21 | Male | | positive | | | |
| D4 | 33 | Female | MCCHL | negative | | | |

## 2.3 Transfection of HEK293 cells

HEK293 cells were seeded onto 9mm multi-spot coated microscope slides at a concentration of $2x10^4$cells/spot and incubated overnight to obtain approximately 70% confluency the following day. Cells were washed with Opti-MEM and 70µl Opti-MEM was added to each spot. 10µl of transfection solution was also added to each spot, made up of 100µl Opti-MEM, 2µl lipofectamine reagent, 1µg plasmid DNA (MSCV (Empty vector) or MSCV-GPNMB), kindly provided by Dr Peter Siegel, and incubated together for 15 minutes at room temperature. Cells were incubated with the transfection reagents for 6 hours then this was removed and DMEM added. Cells were incubated for a further 24 hours at 37°C, following which they were washed with PBS then fixed in 10% formal-saline for 10 minutes, left to air-dry and slides stored at -20°C until required.

HEK293 cells were also seeded onto 6-well plates, again aiming to obtain approx. 70% confluency the following day. Cells were washed and 2600µl Opti-MEM was added to each well. In addition, 220µl of transfection mix (2µg plasmid DNA (MSCV or MSCV-GPNMB), 200µl Opti-MEM and 20µl lipofectamine reagent, incubated together for 15 minutes at room temperature) was added per well and incubated for 6 hours at 37°C. After 6 hours, media was replaced with DMEM and cells/ conditioned media (CM) harvested at 24, 48 and 72-hours post-transfection (see 2.5 for protein extraction and western blotting).

## 2.4 RNA extraction and Quantitative real-time polymerase chain reaction (qPCR)

RNA from frozen cell pellets (approx $1x10^6$ cells per sample) of in vitro differentiated macrophages from multiple donors was extracted using the RNeasy Mini Kit (Qiagen) as per manufacturer's protocol with the addition of QIAshredder columns (Qiagen) for homogenisation of cell lysates and on-column DNA digestion with DNase (Qiagen). Concentration of RNA was measured using the NanoDrop-1000 spectrophotometer.

cDNA was made using 200ng or 400ng RNA (depending on amount per sample) and qScript cDNA SuperMix (QuantaBio) using manufacturer's protocol for volumes and incubation times/temperatures in the thermal cycler (Applied Biosystems).

Each cDNA sample was diluted 1:20 with nuclease-free water and 5µl of diluted cDNA was added to a Fast PCR 96-well plate in addition to 10µl FastStart Universal Probe Master Mix (Roche), 3µl nuclease free water, 1µl of 20x GPNMB primer (GPNMB-FAM Hs01095669_m1) & 1µl GAPDH (GAPDH-VIC Hs02786624_g1) endogenous control primer (Taqman gene expression assays, Thermofisher). Each sample was run in triplicate and water was used as a control. Assays were run using the ABI Prism 7700 system and amplified using the thermal-cycling conditions as follows: 50°C for 2 minutes (enzyme activation), 95°C for 10 minutes (denaturation), 40 cycles at 95°C (amplification) and 60°C for 1 minute (extension).

## 2.5 In vitro differentiation of monocytes to macrophages

### 2.5.1 Human PBMC and monocyte isolation from healthy donors

Human PBMCs were isolated from whole blood or leucocyte cones of healthy donors by density gradient centrifugation using Lymphoprep (Axis Shield) and SepMate 50ml tubes (StemCell). 15ml Lymphoprep was pipetted through the filter hole in the SepMate tube until full, with a few mls remaining above the filter. Whole blood was mixed with serum free RPMI-1640 (1:1 ratio, or for leucocyte cones:RPMI 1640 ratio was 1:2), then 20ml of this was carefully layered on top of the Lymphoprep (and repeated in second tube if larger sample) and centrifuged for 10 minutes at 1400 rpm (brake on). The 'buffy coat' white blood cell layer and plasma layer remained above the filter, while the Lymphoprep and RBCs remained at the bottom of the tube under the filter. The 'buffy coat'/plasma layer was poured into a fresh 50ml falcon tube and centrifuged for further 10 minutes at 1400rpm, plasma removed and cell pellet washed with serum-free RPMI-1640. For some donors, whole PBMCs were frozen at this stage in freezing media (FBS supplemented with 10% Dimethyl sulfoxide (DMSO)) for use in T-cell experiments (aliquots of $10x10^6$ cells, stored in -80 then moved to liquid nitrogen once frozen). Monocytes were isolated using CD14 magnetic beads and LS columns as per manufacturer's protocol (Miltenyi). Monocytes on day 0 were stained with CD14/FITC antibody (eBioscience) to check purity by flow cytometry.

### 2.5.2 In vitro differentiation of macrophages

Once isolated, monocytes were counted and plated in 9cm non-TC coated culture plates with 'complete' media supplemented with 1% Glutamax (Gibco) and either 5ng/ml G-MCSF (Peprotech) (to develop into M1-like macrophages) or 25ng/ml M-CSF (Peprotech) (to

develop into M2-like macrophages). Cells were cultured over 7 days and fed on day 5. Cells and CM were both harvested on day 7- cells were either stained (both internal and external staining) for flow cytometry (CD14/FITC, CD45/Pacific Blue, CD68/PE-Texas Red, CD163/APC, CD206/PE-Cy7, CD80/PerCP Cy5.5, GPNMB/PE; all eBioscience) or used in further experiments.

### 2.5.3 Co-culture of macrophages with HL cells or CM

$1x10^5$ M1 and M2 macrophages were pelleted and resuspended in 1ml tumour- CM from L1236, L428 or L591 cell lines (made as previously described) and plated on a 24-well low-binding sterile plate (Corning) for culture in CM alone; or $1x10^5$ macrophages were resuspended in 0.7ml 'complete' RPMI and a 0.4μM cell culture insert/transwell (Corning) was placed on top of the cells. Different numbers of tumour cells from L1236, L428 and L591 cell lines were added at the ratios in Table 2.2. The same number of tumour cells were also added directly into the 24-well plate with M1 or M2 macrophages (i.e. no cell culture insert/transwell was used) for direct cell-cell contact between macrophages and tumour cells.

The tumour cells were resuspended in 0.3ml complete RPMI (1ml total of media which could mix across the membrane) for co-culture with tumour cells. Cells were incubated for 24 hours, after which time both macrophages and CM were harvested- macrophages were stained for flow cytometry with the same panel of antibodies as above and CM was stored at -20°C for use in GPNMB ELISA.

| Macrophages:tumour cells | No. of tumour cells added to $1x10^5$ macrophages |
|---|---|
| 10:1 | $1x10^4$ |
| 1:1 | $1x10^5$ |
| 1:10 | $1x10^6$ |

**Table 2.2** Ratios of macrophages:tumour cells in HL co-culture

## 2.5.4 Co-culture with cytokines

Macrophages were plated as in 2.5.5 with HL CM or 1:1 ratio of macrophages:HL cells of each cell line as controls for the cytokines. $1x10^5$ M1 and M2 macrophages were pelleted and resuspended in 100µl, then added to 900µl of relevant cytokine (diluted in 'complete' media with 1% glutamax) individually or all together as per Table 2.3.

Cells were incubated for 24 hours, after which time both macrophages and CM were harvested- macrophages were stained for flow cytometry with the same panel of antibodies as above and CM was stored at -20°C for use in GPNMB ELISA.

| Cytokine | Stock concentration | Working concentration (in 900µl) | Final concentration in well (total volume 1ml) | Vol. of stock |
|---|---|---|---|---|
| Angiogenin (R&D) | 10µg/ml (10ng/µl) | 0.78µg/ml=1in12.8 dilution | 0.7µg/ml | 470µl in 6016µl MM |
| CD147/emmprin (R&D) | 100µg/ml (100ng/µl) | 2.22µg/ml=1in45 dilution | 2µg/ml | 123µl in 5535µl MM |
| CD54/ ICAM-1 (Peprotech) | 500µg/ml (500ng/µl) | 2.78µg/ml=1in180 dilution | 2.5µg/ml | 31µl in 5580µl MM |
| CCL5/ RANTES (Peprotech) | 50µg/ml (50ng/µl) | 111.11ng/ml = 1in450 dilution | 100ng/ml | 13µl in 5850µl MM |
| MIF (Peprotech) | 50µg/ml (50ng/µl) | 111.11ng/ml = 1in450 dilution | 100ng/ml | 13µl in 5850µl MM |
| ALL cytokines | Angiogenin 469µl; emmprin 133µl; ICAM-1 33.33µl; CCL5 13.33µl; MIF 13.33µl (662µl) in 6000µl Media | | | |

**Table 2.3 Dilutions of each recombinant cytokine used in co-culture**. Cytokines diluted in 'complete' media + 1% glutamax.. Each cytokine made up in 900µl, added to 100µl of cells. Total volume = 1ml per well.

## 2.6 T-cell Activation and Treatment with GPNMB

PBMCs were isolated from whole blood of 10 donors as described in 2.4.1, and taken out of liquid nitrogen storage.

### 2.6.1 T-cell activation and treatment with recombinant GPNMB (rGPNMB)

PBMCs were recounted from each donor (donors 1-10). The experiment was set up in one 96-well TC-coated sterile plate per donor (Corning). After counting, 5.5 x $10^6$ cells per

donor were washed with PBS and resuspended at 1 x $10^6$ cells/ml in 5.5ml of T-cell Media (StemCell 10981). 100µl of cells were added to all control/vehicle wells in duplicate, followed by 8.5µl PBS per well to vehicle wells.

Six concentrations of T-cell activator were to be tested. For each concentration, Immunocult Human CD3/CD28 T-cell activator (StemCell 10971) was added to 850µl of PBMCs at 1 x $10^6$ cells/ml at the volumes in table 2.4 to give the final concentration per ml. 100µl of PBMCs plus T-cell activator mix at each concentration were added to 8 wells per row for duplicates of each condition (see Figure 2.1 for plate layout). Then rGPNMB (recombinant human GPNMB Fc Chimera Protein- R&D 2550-AC) stock was added at the volumes in Table 2.5 to 12 wells per column to achieve the final concentrations of rGPNMB ranging between 0.04µg/ml- 1µg/ml per well, in duplicate on the plate.

The plates were incubated at 37°C for 24 hours, following which both PBMCs and CM were harvested. Cells were stained with Live/dead/APC Cy7, CD4/APC, CD8/PerCP Cy5.5, CD45/Pacific Blue (all eBioscience), CD69/FITC (Biolegend), FMO CD69 unstained for flow cytometry. CM was tested for interferon-γ release using ELISA.

| Concentration (µl/ml) | Volume CD3/CD28 activator to add to 850µl (µl) |
|---|---|
| 0.125 | 1.06 of 1in10 dilution in PBS |
| 0.25 | 2.125 of 1in10 dilution |
| 0.5 | 4.25 of 1in10 dilution |
| 1 | 8.5 of 1in10 dilution |
| 2 | 1.7 |
| 5 | 4.25 |

**Table 2.4 Dilutions of Immunocult CD3/CD28 T-cell activator**

| Concentration (µg/ml) | Volume of rGPNMB stock (100µg/ml) to add per 100µl well |
|---|---|
| 0.04 | 4µl of 1in100 dilution |
| 0.2 | 2µl of 1in10 dilution |
| 1 | 1µl |

**Table 2.5 Dilutions rGPNMB**

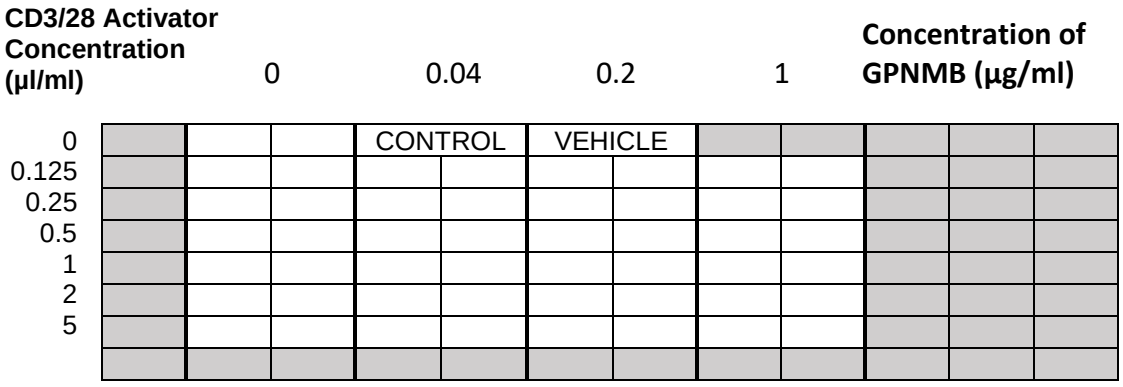


**Figure 2.1 Plate layout for each donor (1-10)**

## 2.6.2 Treatment of activated T-cells with anti-GPNMB antibodies

Donor 5 PBMCs were used in this experiment; they were activated with 1µl/ml Immunocult CD3/CD28 T-cell activator (dilutions and conditions as in 2.6.1)- 1 x $10^5$ PBMCs were plated per well on a 96-well plate in triplicate for each condition. 0.5µg/ml and 5µg/ml of each anti-GPNMB antibody was added (each made up to a total of 10µl , other than antibody 2 which was too dilute), or 10µl PBS was added as a control (Table 2.6 shows antibodies used). 4µl of stock rGPNMB (R&D 2550-AC, 100µg/ml) was added to give a final concentration of 0.04µg/ml per well, or 4µl PBS was added (vehicle).

Each antibody and rGPNMB were incubated at 37°C for 1 hour prior to adding to the plate. The plate was incubated for 24 hours at 37°C, then CM harvested and tested for interferon-γ release using ELISA.

| **Anti-GPNMB Antibody** | **(a) Volume of antibody required for 500ng + volume of PBS (total 10µl/well)** | **(b) Volume of antibody required for 5µg + volume of PBS (total 10µl/well)** |
|---|---|---|
| 1. **R&D MAB2550** Mouse monoclonal; concentration 0.5mg/ml | 1µl antibody + 9µl PBS | 10µl antibody + 0 PBS |
| 2. **R&D AF2550** (from ELISA Kit)- Polyclonal Goat; 216ug/ml | 2.3µl antibody + 7.7µl PBS | 23µl= 5µg antibody + 0 PBS |
| 3. **Abcam ab56584** Mouse monoclonal; 0.48mg/ml | 1.04µl antibody + 9µl PBS | 10.4µl= 5 µg antibody + 0 PBS |
| 4. **Abcam ab175427** Mouse monoclonal (7C10E5); 1mg/ml (lot 8) | 0.5µl antibody + 9.5µl PBS | 5µl antibody + 5µl PBS |
| 5. **Abcam ab125898** Rabbit polyclonal; 1mg/ml, lot GR87297-11 (Lot 11) | 0.5µl antibody + 9.5µl PBS | 5µl antibody + 5µl PBS |

**Table 2.6. Anti-GPNMB antibodies**

### 2.6.3 Macrophage and T-cell co-culture

PBMCs and $CD14^+$ monocytes were isolated from 3 donor leucocyte cones and differentiated into M1 and M2 macrophages as described in section 2.5.1-2.5.2, except that they were plated onto 24-well plates instead of 9cm plates (number of cells scaled down and 1ml of media added (containing G-MCSF or M-CSF for M1 or M2 macrophages), fed on day 5 as previously and grown for 7 days.

The remaining $CD14^-$ PBMCs from these donors were initially frozen in liquid nitrogen on D0 and thawed on D7 of M1/M2 culture in order to be added to the macrophages. The number of PBMCs and reagents for T-cell activation to be added were scaled up by factor 6 due to 6 X increase in surface area from a 96-well plate to a 24-well plate.

On day 7 of M1/M2 culture, media from all macrophage wells was removed and wells washed carefully with PBS to avoid losing cells attached to the bottom of the plates. $6x10^5$ $CD14^-$ PBMCs were resuspended in 600µl T-cell media and added to matched M1 or M2 macrophages (from the same donor) in 24-well plates. Soluble CD3/CD28 activator was added at the following concentrations: vehicle, 0.25µl/ml, 0.5µl/ml and 1µl/ml of activator (total volume 600µl/well). In separate 24-well plates (i.e. without macrophages), PBMCs from each donor were plated with the same concentrations of CD3/CD28 activator, and rGPNMB 0.04µg/ml as controls for the experiment.

Plates were incubated at 37°C for 24 hours; supernatants were harvested and interferon-γ release measured by ELISA.

## 2.7 CD8+ EBV specific T-cell clone recognition of HL cell lines and LCLs

EBV-negative HL cell lines (L1236, KMH2, L540) and L591 were used. The HL cells or LCLs were the target cells, and epitope-specific CD8+ T-cell clones were used as effector cells (identified by the first 3 letters of the peptide sequence)- see Table 5.2 for full details of all matched cells used.

$1x10^6$ HL cells or HLA-matched LCLs were infected with Modified vaccinia Ankara (MVA) recombinant expressing LMP2A (MVA- LMP2A) 10 multiplicity of infection (MOI), 1 MOI, 0.1MOI or pulsed with epitope peptide (500ng/ml), or their respective controls- MVA-pSC11 (empty vector) at 10MOI or dimethyl sulfoxide (DMSO) (1in10,000 dilution with media). HLA-mismatched LCLs were exposed to the same epitope peptide as a negative control. For L591 cells, MVA-E1ΔGA (expresses EBNA1 protein with deleted GA-rich region), EBNA1 HPV peptide or their respective controls- MVA-pSC11 or DMSO as above. MVA pSC11, LMP2A and E1ΔGA were made by Graham Taylor's group. Peptides were synthesised by Alta Biosciences and resuspended in DMSO at 5mg/ml. HL cells or LCLs were pelleted, and then either virus or peptide added and the pellet resuspended in the minimum volume of media remaining in the tube. Cells were incubated at 37°C for 1 hour, but pellets were resuspended every 20 minutes. Cells were washed 3 times with RPMI-1640 + 10% FCS + 1% P/S to ensure excess peptide was washed off; cells were counted and resuspended at $10^6$cells/ml. HL cells or LCLs were plated in triplicate at 100µl/well in a 96-well V-bottom plate (Thermofisher). T-cell clones were counted (10,000 per well in triplicate per cell line), washed with media and resuspended at $10^5$cells/ml. 100µl of T-cell clones was added to the

HL cells or LCLs in triplicate and plates incubated at 37°C for 18 hours. Supernatants were harvested onto a new 96-well plate and frozen at -20°C. Supernatants were tested for interferon-γ by ELISA.

When rGPNMB (R&D 2550-AC, stock 100µg/ml) was tested, this was added at the same time as HL cells/ LCLs and T-cell clones just prior to incubation, but cells were resuspended in half the volume and 50µl of each were added to the well (to keep final volume the same as in previous experiments after GPNMB added). Concentrations of 1ng/ml, 5ng/ml, 10ng/ml, 20ng/ml, 40ng/ml, 200ng/ml and 1000ng/ml of rGPNMB were used. PBS was used as vehicle. Each required concentration was made up at double the required concentration and 100µl added per well to give the final required concentration as above (final volume in well= 200µl).

## 2.8 Enzyme-linked immunosorbent assays (ELISA)

GPNMB and M-CSF ELISA Duoset kits (R&D) were used to measure the quantity of each substance in CM harvested from experiments. GPNMB or M-CSF ELISAs were carried out as per manufacturer's protocols using all other reagents from R&D. Absorbance was read at 450nm using the BioRad iMark microplate reader.

Interferon-γ ELISA (developed by G. Taylor's group) was used to measure interferon-γ release from activated T-cells using the following protocol:

- Coat Nunc MaxiSorp Immuno 96-well flat-bottom plates (Thermo Scientific) with Capture antibody: anti-human Interferon-γ (Clone 2G1) Antibody stock (1µg/ml, Invitrogen M700A) diluted in 1X coating buffer (10X stock: $NaHCO_3$ 1.36g; $KHCO_3$ 7.35g; make up to

100ml with dH2O, adjust to pH 9.2 with 1M HCl/ 1M NaOH, then dilute to 1X with $dH_2O$) at 0.75µg/ml- Add 50µl/well (Add 3.7µl Ab per 5ml coating buffer for 1 96-well plate). Cover plate and incubate overnight for 18 hours at 4°C

- Wash plate 6 times with 0.05% PBST and blot dry on tissue
- Block plate with 200µl/well blocking buffer (Add 5g Bovine Serum Albumin (BSA) (Sigma) and 250µl Tween to 500ml PBS). Incubate at room temperature (RT) for 1 hour
- Wash plate 6 times with 0.05% PBST and blot dry on tissue
- Prepare standards: two-fold serial dilutions from 20,000pg/ml (2µl/ml of recombinant Interferon-γ (Sigma)) down to 31.25pg/ml, diluted in RPMI 1640 medium, plus RPMI 1640 medium alone as 'blank' and defrost samples if needed
- Add standards and CM samples to plate, noting plate layout (50µl/well in triplicate). Incubate at room temperature for 2 hours
- Wash plate 6 times with 0.05% PBST
- Add Detection antibody: biotinylated interferon-γ antibody (Invitrogen M701B B133.5), diluted 1/1333 in blocking buffer (Add 3.75µl antibody to 5ml blocking buffer for 1 96-well plate), add 50µl/well. Cover and incubate at RT for 1 hour
- Wash plate 6 times with 0.05% PBST
- Dilute ExtrAvidin Peroxidase (Sigma E2886) with blocking buffer (1/1000), add 50µl/well. Cover and incubate at RT for 30 minutes
- Wash plate 8 times with 0.05% PBST
- Add 100µl TMB substrate (Life Technologies)/well. Incubate at RT for 20 minutes
- Stop reaction with 100µl of 1M HCl/well

Absorbance was measured at 450nm and 655nm (subtract 655nm measurement from 450nm measurement) using the BioRad iMark microplate reader.

All standard curves were created using ELISA Analysis (www.elisaanalysis.com) to work out the concentration of each protein in samples tested.

## 2.9 Western blotting

### 2.9.1 Protein extraction

HEK293 cells on 6-well plates were washed with PBS and then lysed by adding 200µl of lysis buffer per well and incubating plate on ice for 30 minutes. Cell-scrapers were used to detach the remaining cells from the bottom of the plates and lysates transferred to 1.5ml eppendorfs and centrifuged at 13,000 rpm for 15 minutes at 4°C. Protein supernatant was transferred to a new eppendorf and kept at -20°C until needed.

### 2.9.2 Quantification of protein concentration

BSA (Sigma) standards were made up at 100, 200, 300, 400 and 500µg/ml. Each sample was diluted 1:10 with distilled $H_2O$ and 10µl of standard or sample was loaded in duplicate into a 96-well plate. Bio-Rad Protein Assay Reagent was diluted 1:5 with distilled $H_2O$ and 200µl added per well and incubated at room temperature for 5 minutes. Absorbance was read at 595nm using a Bio-Rad 680 microplate reader. A standards curve was plotted using absorbance readings for BSA standards and this was used to calculate the protein concentration of samples.

### 2.9.3 Gel electrophoresis

10% SDS-PAGE gels were made as per protocol in the Roche diagnostics Lab FAQs booklet. Once set, gels were loaded into a mini Trans-Blot tank which was filled with Tris/glycine/SDS buffer. 30µg of each sample was mixed with Laemmli sample buffer (1:1 dilution) and denatured at 95°C for 10 minutes before loading into separate wells in the gel. Spectra multi-colour broad range protein ladder was also added to the gel. Samples were run at 120V, 400mAmp for approximately 90-120minutes to separate proteins (GPNMB has different isoforms and I wanted to try and detect all of them).

### 2.9.4 Protein transfer

The Bio-Rad Trans-Blot Turbo Transfer system was used to transfer proteins onto PVDF membranes using Bio-Rad Trans-Blot Turbo Mini PVDF Transfer Packs using the recommended program for mixed molecular weight proteins (1.3Amp, 25V, 7minutes).

### 2.9.5 Immunoblotting

After transfer of proteins to the PVDF membrane, membranes were blocked in 5% w/v skimmed milk/ TBST for 1 hour at room temperature, then membrane was washed in TBST for 3x5 minutes. The membrane was incubated in primary antibody (anti-human GPNMB antibody (mouse monoclonal, Abcam 7C10E5), diluted in 5% w/v skimmed milk at 1:250) overnight at 4°C on a roller or 16 hours. Following this, the membrane was washed 3x5 minutes in TBST and then incubated in secondary HRP-conjugated anti-mouse antibody (Dako PO447, 1:1000 dilution in 5% w/v skimmed milk) for 1 hour. The membrane was washed 3x5 minutes before incubating for 1 minute with Bio-Rad clarity western enhanced chemiluminescence substrate buffer and then using the ChemiDoc MP machine to develop

the blot. The membrane was washed again for 3x5 minutes in TBST and incubated with β-actin (Cell signalling, 1:1000 in 5% w/v milk) for 1 hour at room temperature and re-developed as before to act as a protein loading control.

## 2.10 Immunohistochemistry (IHC)

### 2.10.1 Dewaxing of formalin-fixed paraffin-embedded HL and tonsil sections

Paraffin-embedded sections were dewaxed by placing into Histoclear (National Diagnostics) for 10 mins, followed by rehydration in 100% ethanol for 10 minutes and then in running tap water for 5 minutes.

HEK293 cells grown and transfected on spot slides were thawed and placed into running water for 5 minutes.

All slides are ready for the next steps in 2.10.2.

### 2.10.2 IHC using Citric-acid antigen retrieval method

All slides were then placed in 0.3% hydrogen peroxide (Sigma) for 15 minutes to block endogenous peroxidases. Slides were immersed in tap water until citrate buffer was heated up. Citrate buffer was prepared by adding 1L distilled $H_2O$ to 1.26g sodium citrate and 0.25g citric acid, pH was adjusted to 6 with sodium hydroxide. The citrate buffer was heated in a large 2L beaker for 10min on High heat in the microwave, after which the slides were immersed into the buffer and heated for further 10 mins on medium heat and 10 minutes on low heat. Slides/buffer were cooled before removing slides and running in tap

water for 5 minutes. After this, slides were placed on a metal staining tray and washed with PBST for 5 minutes.

To reduce non-specific background staining, slides were blocked with 5X Casein (Vector labs) for 10 minutes and this was drained off prior to adding primary antibody 1:100 dilution (diluted in PBS) (anti-human GPNMB antibody (mouse monoclonal [7C10E5], Abcam ab175427) then incubating at 4°C for 16-18 hours overnight. Slides were washed with PBST 5 minutes and then secondary HRP-conjugated anti-mouse/rabbit IgG antibody (ImmPRESS universal antibody, Vector labs) was applied and incubated for 30 minutes at room temperature.

Slides were washed with PBST for 5 minutes and then diaminobenzidine (DAB) (Vector labs) was applied to slides for 3-5mins until the brown precipitate develops (substrate reacts with peroxidase from secondary antibody) which represents antigens bound to the antibody. Slides were washed in running tap water for 5 mins then counter-stained with Mayer's Haematoxylin (Sigma-Aldrich) for 5 minutes. Slides were washed in warm running water for 5 minutes. Slides were dehydrated by placing in 100% ethanol for 10 minutes, histoclear for 10 minutes then mounted with glass coverslips using Omnimount (National Diagnostics) mounting medium. Once dry, slides were visualised using a light microscope.

### 2.10.3 Multiplex fluorescent IHC

The Opal 4-plex kit (Perkin Elmer) was used for multiplex fluorescent IHC. The initial part of the protocol is the same as above for IHC, apart from the primary GPNMB antibody was used at 1:1000 for 1 hour at room temperature. Universal secondary antibody was applied as

above for 30 minutes. After washing slides with PBST, Cy3 fluorophore was diluted to 1:200 in amplification diluent (in kit) and added to slides- these were incubated for 10 minutes at room temperature in the dark and slides were once again washed with PBST for 5 mins.

1L of citrate buffer is made up as previously and heated for 5 minutes on High. At this point, slides are once again immersed into the buffer and heated for 15 minutes on Low, then left to cool. The protocol is then restarted from the point of blocking with 5X casein. The slides were subsequently labelled with either CD68 (Dako, 1:1200 for 1 hour at room temperature, with FITC fluorophore) or CD30 (Dako Flex Ready-to-use, 1 hour at room temperature, with FITC fluorophore) antibodies having already been stained with GPNMB/ Cy3. After the second fluorophore has been applied, slides are once again put into citrate buffer and heated for 15 minutes on low setting. After allowing the slides to cool, they are placed under running distilled water for 5 mins, counterstained with DAPI (1in1000, Life technologies) for 10 minutes before mounting using Vectashield hard-set mounting medium (Vector labs). Once stained and mounted, slides are stored at 4°C or -20°C in the dark until visualised using a fluorescent microscope.

### 2.10.4 Duplex Automated IHC

Automated IHC was carried out by Dr Matthew Pugh using the Leica Bond-Max using the machine standard IHC protocol with a 20-minute antigen retrieval using the Epitope retrieval 2 solution (all solutions as recommended from Leica Biosystems). Antibodies were used at the following dilutions: CD30 (Dako, 1:100), CD68 (Dako, 1:500), GPNMB (abcam 125898 1:1000). Sequential double staining of GPNMB and CD30 was carried out- Protocol F was done using GPNMB primary antibody (1-hour incubation) followed by Protocol J with

CD30 antibody (30-minute incubation). Sequential double staining of GPNMB and CD68 was carried out- Protocol F was done using GPNMB primary antibody (1 hour incubation) followed by Protocol J with CD68 antibody (30-minute incubation). Detection of GPNMB was with bond polymer refined detection kit. CD30 and CD68 were detected using ond polymer refined red detection kit. Slides were dehydrated by placing in 100% ethanol for 10 minutes, histoclear for 10 minutes then mounted with vectamount permanent mounting medium (Vector labs).

## 2.11 Cytokine array

The Human XL Cytokine Array Kit (R&D ARY022B) was used as per manufacturer's instructions with IRDye 800CW Streptavidin (Li-COR) at a 1:2000 dilution using Array Buffer 6 (instead of Streptavidin-HRP provided in kit, instructions available on R&D website). Images were taken with the Li-COR Odyssey Scanner and analysed using Image Studio software.

Samples tested were: 'complete' media supplemented with 1% glutamax (control) and CM from L1236, L428 and L591.

## 2.12 Bioinformatics analysis of publicly available transcriptional data from primary cHL

The microarray data were downloaded from the Gene Expression Omnibus website- a public functional genomics repository (NCBI) (www.ncbi.nlm.nih.gov/geo/).

Twelve cHL microarray data were from GSE12453 (Weniger et al., 2018, Brune et al., 2008):

https://www.ncbi.nlm.nih.gov/geo/query/acc.cgi?acc=GSE12453

Four tcr-cHL microarray data were from GSE14879 (Weniger et al., 2018):

https://www.ncbi.nlm.nih.gov/geo/query/acc.cgi?acc=GSE14879

Five non geminal centre CD30 positive B cell microarray data were from GSE83441 (Weniger et al., 2018):

https://www.ncbi.nlm.nih.gov/geo/query/acc.cgi?acc=GSE83441

The following analysis was done by Dr Wenbin Wei. Probe level quantile normalisation (Bolstad et al., 2003) and robust multi-array analysis (RMA) (Irizarry et al., 2003) were performed using the 'affy' package from the Bioconductor website (Gautier et al., 2004, Bioconductor) (https://bioconductor.org/). Probe sets that were differentially expressed between the 16 cHL and five non-GC CD30 positive B cell samples were identified using limma (Smyth, 2004) with the criteria of absolute fold change > 1.5 and limma p value < 0.05. Probe set annotation was from Affymetrix "HG-U133_Plus_2.na35.annot.csv" and reannotated according to the NCBI gene database (NCBI) (www.ncbi.nlm.nih.gov/gene). Probe sets with "Negative Strand Matching Probes" were removed. Probe sets with "Present" calls in less than 3 samples were removed. Genes appearing in both significantly up- and down- regulated lists were removed from differentially expressed genes lists. The list of genes was sorted by fold change.

# CHAPTER 3

## EXPRESSION OF GPNMB IN HODGKIN LYMPHOMA

# Chapter 3 Expression of GPNMB in Hodgkin lymphoma

As outlined in Chapter 1, there is an urgent need to develop new therapies for patients with classic Hodgkin lymphoma. *GPNMB* was identified as a potential target when it was shown to be amongst the most over-expressed genes in HL and functionally acts as a suppressor of T-cell function (Chung et al., 2007), which we postulated could contribute to the immunosuppressive microenvironment in cHL and therefore could function as a novel immune checkpoint target in cHL.

## 3.1 Analysis of publicly available transcriptional data from primary cHL

The starting point for my study was a re-analysis of transcriptional data from primary HL; the purpose being to identify genes over-expressed in cHL that might serve as targets for existing drugs or for drugs in clinical development. The initial experiment was a re-analysis of a microarray experiment performed by the Kuppers group (Brune et al., 2008, Weniger et al., 2018) in which gene expression was measured in micro-dissected HRS cells, as well as in different isolated B cell subsets, including CD30-positive extrafollicular (EF) B cells, the presumed progenitors of cHL. Gene expression was measured using Affymetrix HG-U133 Plus2 array and normalised using RMA as described in section 2.12 (Irizarry et al., 2003). This re-analysis was done by Dr Wenbin Wei in our group who derived a set of genes differentially expressed in HRS cells vs $CD30^+$ EF B cells. Table 3.1 shows the top 50 genes that were over-expressed in this re-analysis. *CCL18* is on the list twice (number 1 and number 15); this is because the Affymetrix GeneChip has two different probe sets for this gene (Probe set IDs

209924_at and 32128_at). That both probe sets are upregulated is reassuring (Table 3.1 and Figure 3.1A). Variation in the levels of gene expression observed for different probe sets from the same gene is expected. There is no consensus on how to deal with this. Some suggest taking the average of all probe sets for a given gene. However, it is known that some probe sets do not perform as well as others and taking an average may reduce sensitivity. I adopted a more conservative approach by treating each probe set individually (Stalteri and Harrison, 2007).

From this list of over-expressed genes in HRS cells, *GPNMB* was of interest because it was a novel target that had not previously been shown to be overexpressed in cHL.

Figure 3.1B shows the gene expression data for *GPNMB* plotted for each HRS sample compared to CD30+EF cells. *GPNMB* gene expression is variable amongst patient samples.

**Table 3.1 Top 50 over-expressed genes in HRS cells compared to CD30+ EF cells**

(data from Brune *et al.,* 2008, and Wenniger *et al.*,2018, reanalysis by Dr Wenbin Wei)

*CCL18* represented twice due to two probe sets in the microarray.

| | Entrez Gene ID | Gene Symbol | Description | Adjusted P Value | Fold Change |
|---|---|---|---|---|---|
| 1 | 6362 | CCL18 | chemokine (C-C motif) ligand 18 (pulmonary and activation-regulated) | 1.52E-09 | 147.66 |
| 2 | 4318 | MMP9 | matrix metallopeptidase 9 | 1.66E-10 | 99.19 |
| 3 | 170575 | GIMAP1 | GTPase, IMAP family member 1 | 5.85E-11 | 77.53 |
| 4 | 4321 | MMP12 | matrix metallopeptidase 12 | 8.86E-05 | 69.74 |
| 5 | 1116 | CHI3L1 | chitinase 3-like 1 (cartilage glycoprotein-39) | 1.62E-05 | 63.59 |
| 6 | 5168 | ENPP2 | ectonucleotide pyrophosphatase/phosphodiesterase 2 | 4.31E-10 | 62.50 |
| 7 | 4837 | NNMT | nicotinamide N-methyltransferase | 5.64E-07 | 59.65 |
| 8 | 55340 | GIMAP5 | GTPase, IMAP family member 5 | 1.91E-12 | 57.76 |
| 9 | 341 | APOC1 | apolipoprotein C-I | 8.72E-11 | 55.83 |
| 10 | 1475 | CSTA | cystatin A (stefin A) | 1.54E-07 | 55.71 |
| 11 | 56833 | SLAMF8 | SLAM family member 8 | 7.84E-10 | 55.36 |
| 12 | 10202 | DHRS2 | dehydrogenase/reductase (SDR family) member 2 | 0.001369 | 45.70 |
| 13 | 7850 | IL1R2 | interleukin 1 receptor, type II | 8E-08 | 44.96 |
| 14 | 713 | C1QB | complement component 1, q subcomponent, B chain | 2.07E-05 | 44.24 |
| 15 | 6362 | CCL18 | chemokine (C-C motif) ligand 18 (pulmonary and activation-regulated) | 2.21E-07 | 42.64 |
| 16 | 3490 | IGFBP7 | insulin-like growth factor binding protein 7 | 4.67E-06 | 41.89 |
| 17 | 1277 | COL1A1 | collagen, type I, alpha 1 | 1.74E-07 | 39.67 |
| **18** | **10457** | **GPNMB** | **glycoprotein (transmembrane) nmb** | **4.53E-05** | **38.94** |
| 19 | 5730 | PTGDS | prostaglandin D2 synthase 21kDa (brain) | 6.85E-07 | 35.12 |
| 20 | 6678 | SPARC | secreted protein, acidic, cysteine-rich (osteonectin) | 1.86E-07 | 34.46 |
| 21 | 6361 | CCL17 | chemokine (C-C motif) ligand 17 | 0.000664 | 31.30 |
| 22 | 5730 | PTGDS | prostaglandin D2 synthase 21kDa (brain) | 3.17E-06 | 29.65 |
| 23 | 84419 | C15orf48 | chromosome 15 open reading frame 48 | 1.8E-07 | 27.53 |
| 24 | 915 | CD3D | CD3d molecule, delta (CD3-TCR complex) | 4.55E-10 | 26.62 |
| 25 | 3575 | IL7R | interleukin 7 receptor | 6.15E-09 | 25.90 |

| | Entrez Gene ID | Gene Symbol | Description | Adjusted P Value | Fold Change |
|---|---|---|---|---|---|
| 26 | 9935 | MAFB | v-maf avian musculoaponeurotic fibrosarcoma oncogene homolog B | 1.39E-08 | 25.50 |
| 27 | 7262 | PHLDA2 | pleckstrin homology-like domain, family A, member 2 | 1.67E-06 | 25.33 |
| 28 | 4094 | MAF | v-maf avian musculoaponeurotic fibrosarcoma oncogene homolog | 1.29E-06 | 25.00 |
| 29 | 6348 | CCL3 | chemokine (C-C motif) ligand 3 | 1.29E-07 | 24.29 |
| 30 | 347733 | TUBB2B | tubulin, beta 2B class IIb | 0.000341 | 23.97 |
| 31 | 57451 | TENM2 | teneurin transmembrane protein 2 | 0.000176 | 23.14 |
| 32 | 929 | CD14 | CD14 molecule | 7.61E-07 | 22.74 |
| 33 | 2017 | CTTN | Cortactin | 1.91E-10 | 22.72 |
| 34 | 7980 | TFPI2 | tissue factor pathway inhibitor 2 | 0.024467 | 22.60 |
| 35 | 718 | C3 | complement component 3 | 2.49E-08 | 22.59 |
| 36 | 5328 | PLAU | plasminogen activator, urokinase | 4.7E-08 | 22.27 |
| 37 | 1191 | CLU | Clusterin | 1.46E-07 | 20.06 |
| 38 | 914 | CD2 | CD2 molecule | 1.84E-08 | 19.39 |
| 39 | 118932 | ANKRD22 | ankyrin repeat domain 22 | 9.39E-08 | 19.13 |
| 40 | 341 | APOC1 | apolipoprotein C-I | 1.67E-11 | 19.05 |
| 41 | 3957 | LGALS2 | lectin, galactoside-binding, soluble, 2 | 1.87E-07 | 18.61 |
| 42 | 27299 | ADAMDEC1 | ADAM-like, decysin 1 | 4.62E-07 | 18.30 |
| 43 | 2034 | EPAS1 | endothelial PAS domain protein 1 | 4.19E-05 | 17.63 |
| 44 | 7045 | TGFBI | transforming growth factor, beta-induced, 68kDa | 8.83E-07 | 16.82 |
| 45 | 1514 | CTSL | cathepsin L | 4.19E-08 | 16.35 |
| 46 | 1052 | CEBPD | CCAAT/enhancer binding protein (C/EBP), delta | 4.22E-07 | 16.29 |
| 47 | 1116 | CHI3L1 | chitinase 3-like 1 (cartilage glycoprotein-39) | 3.01E-05 | 15.81 |
| 48 | 6279 | S100A8 | S100 calcium binding protein A8 | 0.007155 | 15.67 |
| 49 | 1281 | COL3A1 | collagen, type III, alpha 1 | 0.012016 | 15.47 |
| 50 | 3490 | IGFBP7 | insulin-like growth factor binding protein 7 | 2.25E-06 | 15.38 |

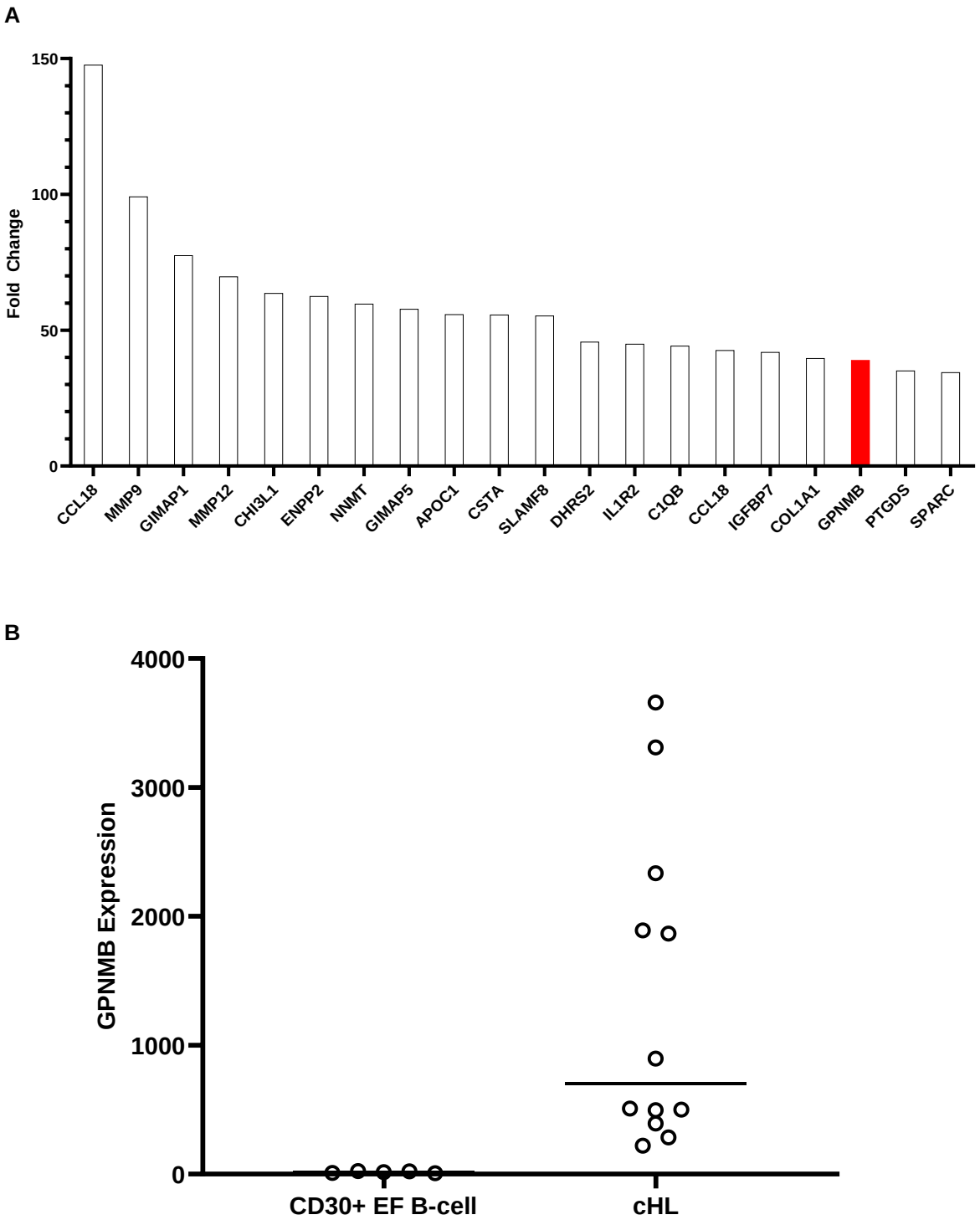


**Figure 3.1. GPNMB expression in HRS cells compared to CD30$^+$ EF cells** (data from Brune *et al.,* 2008 and Wenniger *et al.*, 2018, reanalysis by Dr Wenbin Wei). Gene expression measured using Affymetrix HG-U133 Plus2 array and normalised using RMA. A) Top 20 most over-expressed genes in HRS cells compared to CD30$^+$ EF cells by microarray (B) GPNMB gene expression by microarray from 12 cHL patients compared to CD30$^+$ EF cells with median of samples plotted

## 3.2 Validation of anti-GPNMB antibody

Having shown that GPNMB is over-expressed in primary HRS cells in publicly available transcriptional data, I next wanted to study the expression of GPNMB at the protein level in primary cHL. I first attempted to validate a mouse monoclonal antibody (Abcam ab175427 [7C10E5]) against GPNMB using HEK293 cells that I transfected either with GPNMB expression plasmid or with an empty vector (EV) (both gifts from Peter Siegel). Having first confirmed that HEK293 cells transfected with GPNMB expression plasmid, but not the empty vector, expressed GPNMB mRNA (Figure 3.2), I then performed immunoblotting on cells cultured for 24, 48 and 72-hours post-transfection. In Figure 3.3A, it is shown that GPNMB was detected as two isoforms (mature- 115kDa, precursor- 90kDa) as previously described (Hoashi et al., 2010). Of note, the expression of GPNMB appeared to decline over time post-transfection. IHC revealed strong expression of GPNMB in a subset of the transfected cell population as expected (Figure 3.3B).

Unfortunately, after initial testing of this antibody, two subsequent new vials (with different lot numbers) did not work when used in IHC. Therefore, further anti-GPNMB antibodies were obtained and validated. One of these, a rabbit polyclonal anti-GPNMB antibody (Abcam ab125898) was shown to be specific when tested in IHC (Figure 3.4). Tonsil was used a positive control as GPNMB is known to be expressed in lymphoid tissues and macrophages in healthy/inflamed tissues (see section 1.8.1).

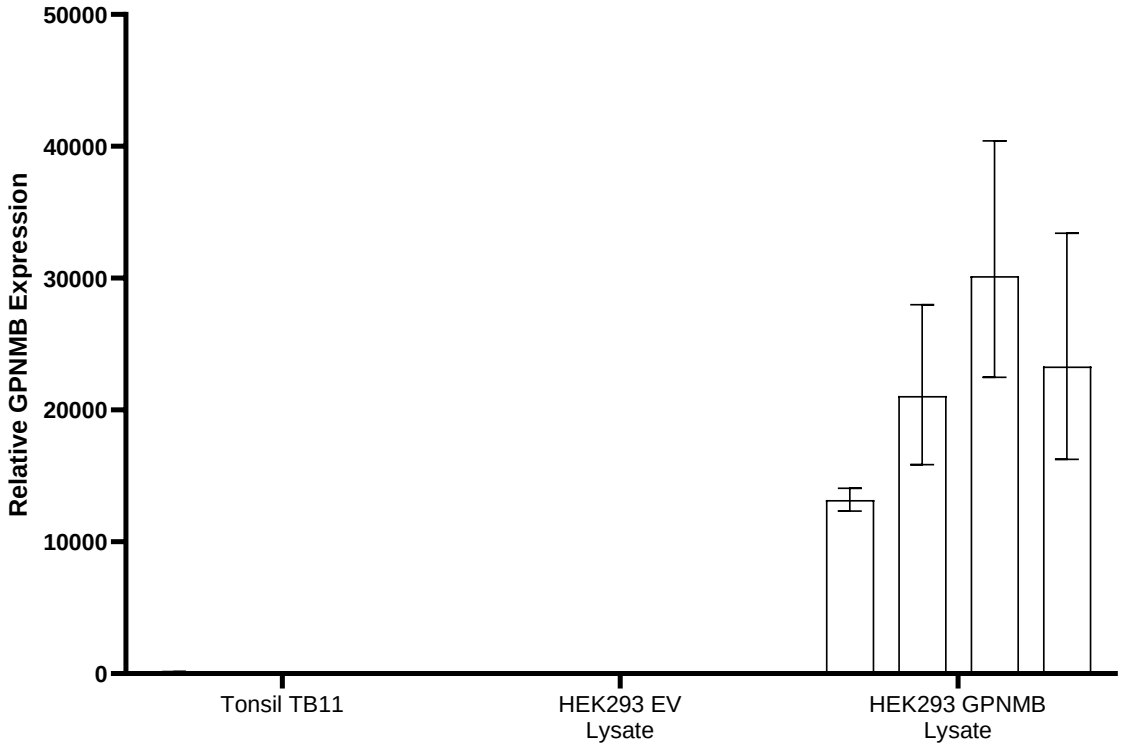


**Figure 3.2. Detection of GPNMB mRNA in transfected cells** (normalised to tonsil TB11)**.** qPCR using a GPNMB-specific probe was used to detect high levels of GPNMB mRNA in cells transfected with GPNMB expression plasmid, but not in cells transfected with EV (data shown is the mean of 3 replicates from 4 transfection experiments).

**A**

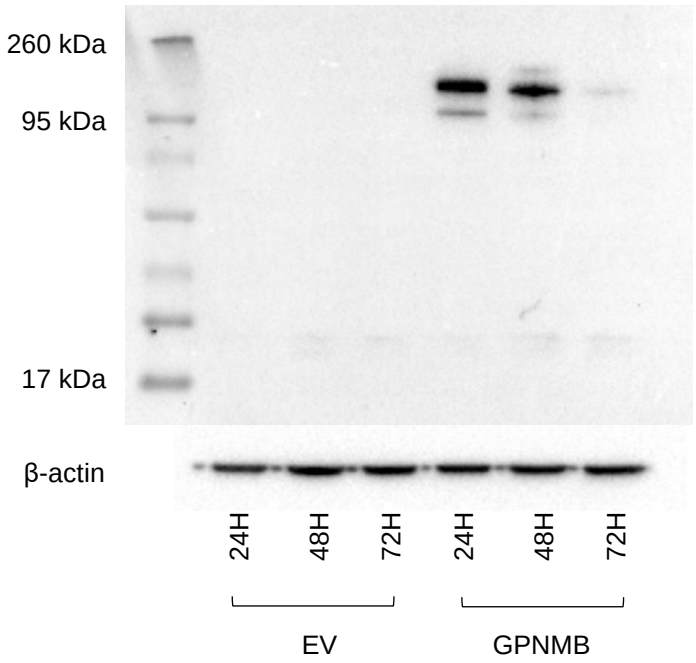


**B**

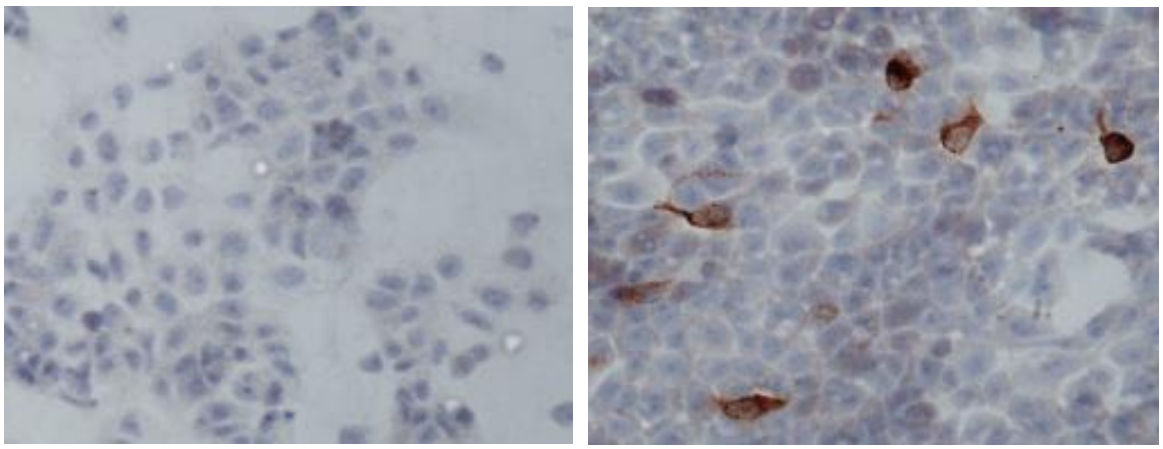

**Figure 3.3 Validation of monoclonal anti-GPNMB antibody (Abcam ab175427 [7C10E5]).**

(A) Western blot of HEK293 cells transfected with empty vector (EV) or GPNMB expression plasmid. (B) Immunohistochemistry (IHC) of HEK293 cells transfected with EV (left panel) or GPNMB expression plasmid (right panel).

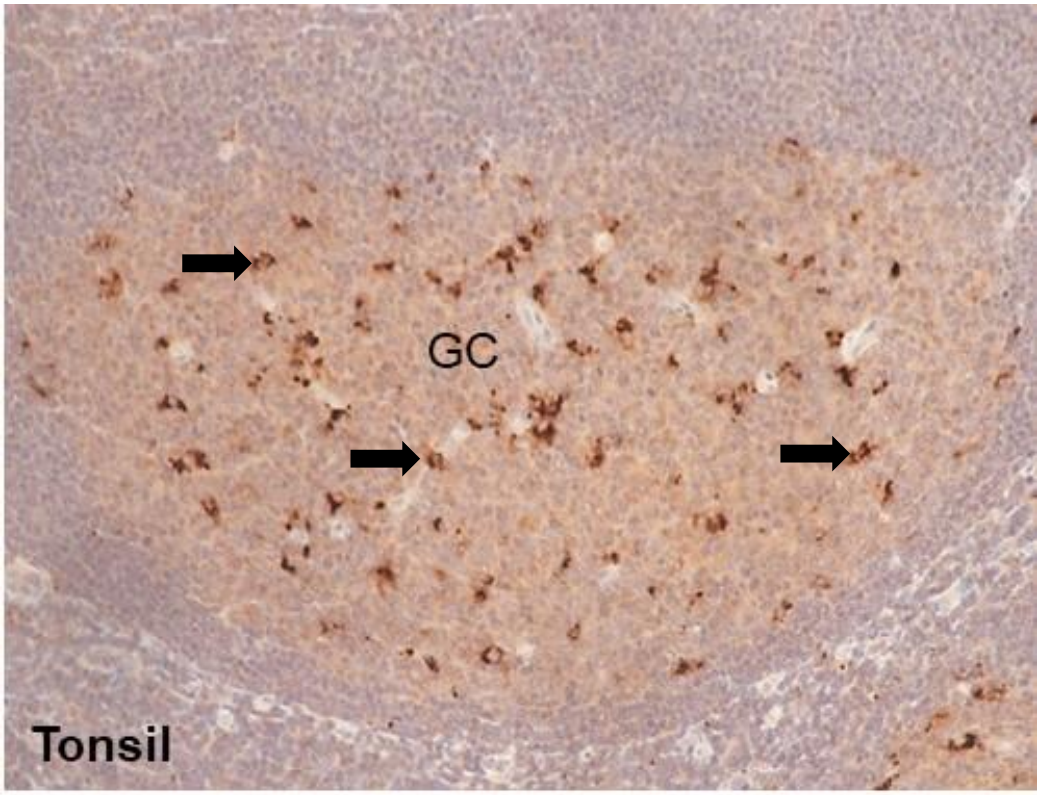


**Figure 3.4 Validation of polyclonal anti-GPNMB antibody (Abcam ab125898)**. IHC of tonsil section stained with the antibody. Specific staining of macrophages can be seen in the germinal centre (GC) marked by arrows. GPNMB is known to be expressed in macrophages in multiple normal tissues inflamed tissue and also lymphoid tissues (see section 1.8.1).

## 3.3 GPNMB expression in primary cHL

The first anti-GPNMB antibody (ab175425 [7C10E5]) was used to stain paraffin-embedded sections from 20 adult cases of cHL. Surprisingly, GPNMB expression was not observed in HRS cells in most cases; only the occasional HRS cell in 1-2 cases showed GPNMB expression (Figure 3.5). However, all cases showed strong staining of GPNMB in what appeared to be macrophages (Figure 3.5). Germinal centre B cells expressed only low levels of GPNMB expression, whereas macrophages in the GC were strongly stained (Figure 3.5).

To confirm this observation, I performed multiplex immunofluorescence on 14 cHL cases to investigate the co-expression of GPNMB with either CD30 or CD68 (Figure 3.6). All 14 cases showed prominent staining of GPNMB in CD68 positive tumour-associated macrophages (TAM). Very few HRS cells expressed GPNMB.

A tissue microarray (TMA) of 94 adult cHL cases (containing samples at initial diagnosis or relapse; paired samples from diagnosis and relapse were available for 2 patients) was stained for GPNMB (using the new anti-GPNMB antibody ab125898) and CD68 or GPNMB and CD30. Slides were also stained for EBER for EBV status. The TMA IHC was done by Dr Matthew Pugh. Eight cases were excluded from analysis due to insufficient tissue, absence of lesional tissue or one case due to high background staining. To obtain $GPNMB^+$ cell density for the remaining 86 cases, the number of $GPNMB^+$ cells in three 40X high power fields (HPF) per case were counted, and an average taken per case. The area per HPF was $230mm^2$. This analysis was performed with Dr Matthew Pugh. Table 3.2 shows the $GPNMB^+$ cell density/HPF.

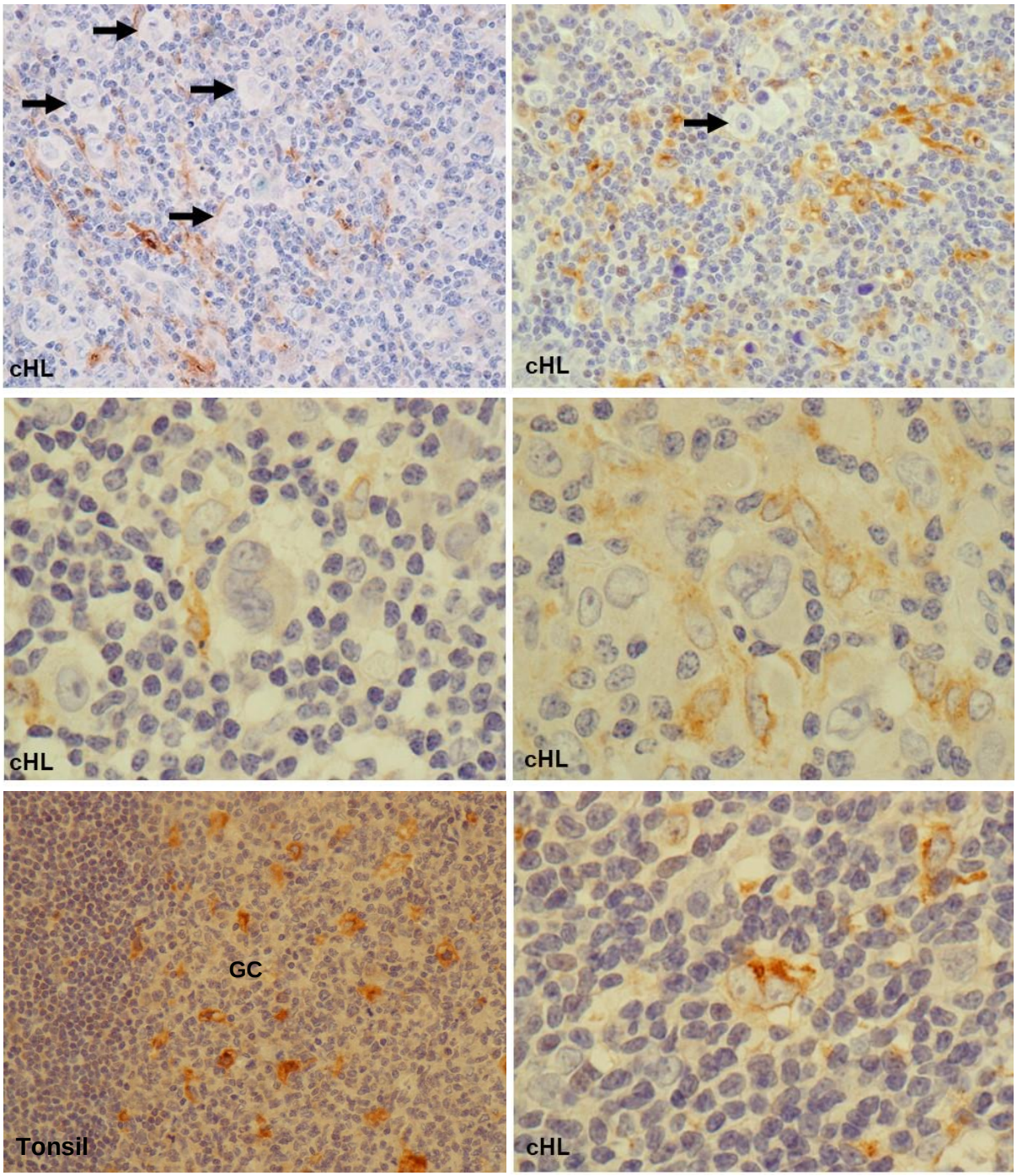


**Figure 3.5. GPNMB expression in cHL.** Top panels- HRS cells (arrows) do not express GPNMB, but GPNMB-expressing cells appear to be macrophages. Middle 2 panels- higher power images showing GPNMB$^-$ HRS cells with GPNMB$^+$ cells in close proximity. Bottom right panel- GPNMB$^+$ HRS cell. Bottom left panel- GPNMB$^+$ macrophages in the GC of tonsil.

A

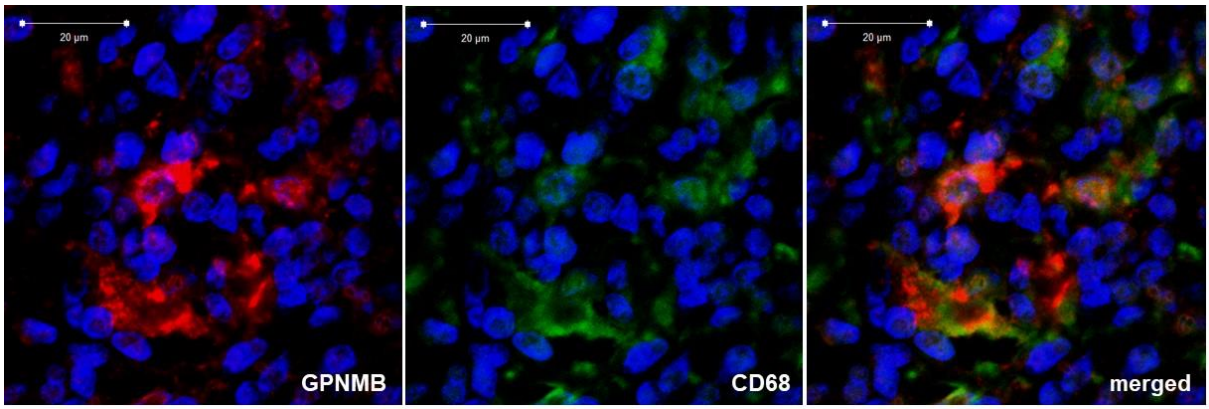


B

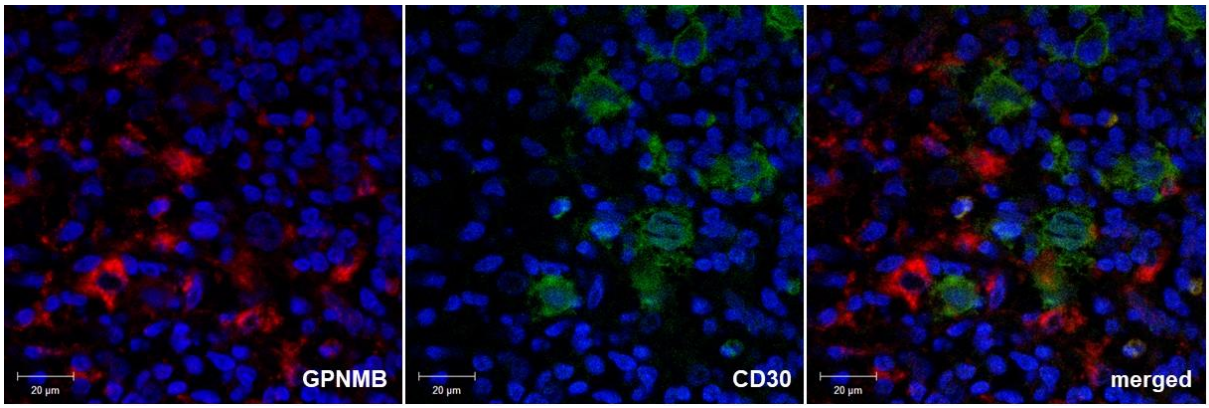


C

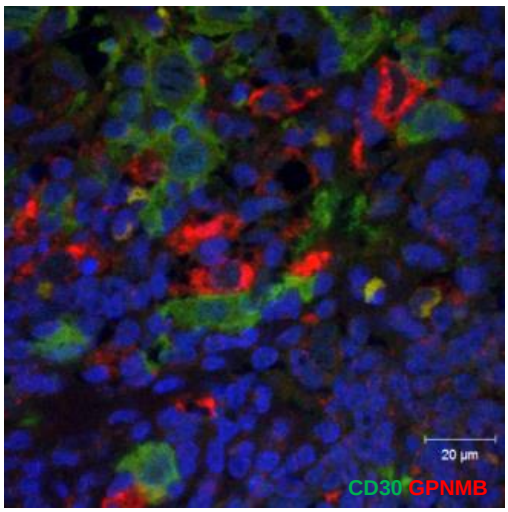


**Figure 3.6. GPNMB is expressed by TAM in cHL.** (A) Co-expression of CD68 (green) and GPNMB (red) in TAM in cHL (B) Double staining of CD30-positive HRS cells (green) and GPNMB (red)- no co-expression is seen here (C) Double staining of CD30-positive HRS cells (green) and GPNMB (red)- no co-expression is seen but HRS cells and GPNMB$^{+}$ TAM are in close proximity.

**Table 3.2. cHL TMA cell density/HPF.** Average of 3 $GPNMB^+$ cells/HPF (40X) was taken. Each slide (HL1- HL6) contains 16 samples, labelled with their position on the slide. HL2 B3* and C3* are diagnosis and relapse samples from the same patient. HL3 A2* and C2* are diagnosis and relapse samples from another patient. Rows highlighted grey were excluded.

| | Count 1 | Count 2 | Count 3 | Mean count/ HPF | Description/ Comment |
|---|---|---|---|---|---|
| **HL1** | | | | | |
| A1 | 17 | 3 | 3 | 7.67 | sparse, diffuse |
| A2 | | | | | No lesional tissue |
| A3 | 10 | 11 | 7 | 9.33 | sparse, diffuse |
| A4 | 28 | 18 | 17 | 21.00 | loosely aggregated |
| B1 | 9 | 20 | 1 | 10.00 | nodular aggregates, overall sparse |
| B2 | 102 | 105 | 114 | 107.00 | dense, diffuse |
| B3 | 40 | 39 | 37 | 38.67 | moderate, geographical |
| B4 | 15 | 8 | 15 | 12.67 | sparse, aggregation within nodules |
| C1 | 22 | 30 | 36 | 29.33 | diffuse, sparse- moderate |
| C2 | 40 | 64 | 50 | 51.33 | geographical, moderate- dense |
| C3 | | | | | No lesional tissue |
| C4 | 1 | 10 | 5 | 5.33 | sparse, diffuse |
| D1 | 21 | 21 | 2 | 14.67 | aggregated, mod-sparse |
| D2 | 13 | 19 | 17 | 16.33 | diffuse, moderate |
| D3 | 27 | 22 | 46 | 31.67 | aggregated in small nodules |
| D4 | 77 | 79 | 46 | 67.33 | dense, diffuse, some expression in spindled cells |
| **HL2** | | | | | |
| A1 | 38 | 26 | 24 | 29.33 | moderate, loosely aggregated |
| A2 | 27 | 22 | 33 | 27.33 | loose aggregation, sparse- moderate |
| A3 | 21 | 11 | 12 | 14.67 | sparse-moderate, diffuse |
| A4 | 49 | 50 | 44 | 47.67 | diffuse, moderate |
| B1 | | | | | High background |
| B2 | | | | | Insufficient tissue |
| B3* | 28 | 24 | 38 | 30.00 | Diagnosis sample. sparse, small aggregations |
| B4 | 27 | 37 | 25 | 29.67 | aggregated, moderate |
| C1 | 81 | 39 | 24 | 48.00 | aggregated in periphery of follicles |
| C2 | 33 | 12 | 10 | 18.33 | aggregated to periphery of lymphoid nodules |
| C3* | 23 | 16 | 20 | 19.67 | Relapse sample. moderate, diffuse |
| C4 | | | | | Insufficient tissue |
| D1 | 42 | 74 | 32 | 49.33 | dense, aggregations in periphery of follicles |
| D2 | 8 | 9 | 9 | 8.67 | sparse |
| D3 | 30 | 42 | 33 | 35.00 | overall diffuse, aggregations around blood vessels |
| D4 | 11 | 2 | 20 | 11.00 | diffuse and sparse |

| | Count 1 | Count 2 | Count 3 | Mean count/ HPF | Description/ Comment |
|---|---|---|---|---|---|
| **HL3** | | | | | |
| A1 | 42 | 9 | 19 | 23.33 | patchy distribution |
| A2* | 66 | 79 | 86 | 77.00 | relapse sample. Avoiding follicles, high density |
| A3 | 30 | 37 | 38 | 35.00 | aggregated, moderate density |
| A4 | 14 | 11 | 25 | 16.67 | sparse aggregated expression, co-localises to cd30 in nodules |
| B1 | 18 | 8 | 12 | 12.67 | diffuse sparse distribution |
| B2 | 38 | 24 | 35 | 32.33 | loosely aggregated, moderate density |
| B3 | 32 | 21 | 26 | 26.33 | very fibrotic, sparse-moderate diffuse within nodule |
| B4 | 39 | 48 | 68 | 51.67 | geographical distribution, moderate density |
| C1 | 45 | 19 | 29 | 31.00 | diffuse within nodules |
| C2* | 16 | 17 | 13 | 15.33 | diagnosis sample. diffuse within nodules, low-moderate density |
| C3 | 37 | 20 | 30 | 29.00 | aggregated |
| C4 | 33 | 80 | 40 | 51.00 | loosely aggregated, moderate density |
| D1 | 50 | 95 | 65 | 70.00 | aggregated, moderate to high density |
| D2 | 84 | 65 | 51 | 66.67 | diffuse expression, moderate-high density |
| D3 | 48 | 63 | 17 | 42.67 | geographical distribution, moderate-high density, co-localised with spindled areas |
| D4 | 20 | 44 | 37 | 33.67 | concentrated in spindle areas and outside GCs |
| **HL4** | | | | | |
| A1 | 31 | 25 | 29 | 28.33 | mostly concentrated outside follicles; a few in the follicle |
| A2 | 28 | 37 | 39 | 34.67 | diffuse, variable expression in macrophages |
| A3 | 2 | 4 | 8 | 4.67 | sparse diffuse density |
| A4 | 51 | 24 | 18 | 31.00 | sparse-moderate, loosely aggregated |
| B1 | 25 | 66 | 45 | 45.33 | very strong expression, sparse-moderate density |
| B2 | 66 | 51 | 60 | 59.00 | |
| B3 | 26 | 44 | 19 | 29.67 | sparse to moderate, diffuse |
| B4 | 40 | 76 | 40 | 52.00 | expression in spindled cells and spindles areas- ?expression in fibroblasts |
| C1 | 45 | 26 | 23 | 31.33 | loosely aggregated, around outside of HRS aggregates, and within some of them |
| C2 | 49 | 23 | 38 | 36.67 | moderate, in spindled areas excluded from follicles. Closely associated to HRS cells |
| C3 | 69 | 52 | 62 | 61.00 | moderate to dense, diffuse with some loose aggregates. Strong expression |
| C4 | 38 | 13 | 29 | 26.67 | sparse to moderate, noticeable numbers of negative macrophages |
| D1 | 38 | 53 | 34 | 41.67 | aggregates within the nodules |
| D2 | | | | | Insufficient tissue |
| D3 | 64 | 73 | 67 | 68.00 | dense with geographic distribution |
| D4 | 46 | 10 | 5 | 20.33 | nodular, sparse overall, but dense in one area- aggregates of macrophages focal to this area |

| | Count 1 | Count 2 | Count 3 | Mean count/ HPF | Description/ Comment |
|---|---|---|---|---|---|
| **HL5** | | | | | |
| A1 | | | | | Insufficient tissue |
| A2 | 23 | 15 | 31 | 23.00 | low-moderate, 50:50 gpnmb +/- macrophages |
| A3 | 36 | 18 | 19 | 24.33 | low-moderate, diffuse |
| A4 | 29 | 42 | 35 | 35.33 | diffuse, some exclusion from follicles, reactive tissue next to tumour |
| B1 | 48 | 34 | 17 | 33.00 | diffuse, moderate expression |
| B2 | 43 | 56 | 65 | 54.67 | high expression in tumour |
| B3 | 54 | 50 | 43 | 49.00 | moderate density, geographic distribution, some denser areas |
| B4 | 6 | 13 | 11 | 10.00 | sparse, gathered around blood vessels |
| C1 | 119 | 179 | 196 | 164.67 | high expression, expression in spindle shaped cells and macrophages |
| C2 | | | | | Insufficient tissue |
| C3 | 23 | 16 | 24 | 21.00 | present within nodules, diffuse but sparse to moderate density, closely associated with HRS cells |
| C4 | 52 | 70 | 72 | 64.67 | moderate density, positive spindle shaped cells |
| D1 | 41 | 36 | 28 | 35.00 | diffuse, moderate-high density, occasional spindle positive cells |
| D2 | 42 | 37 | 29 | 36.00 | moderate, diffuse staining |
| D3 | 109 | 106 | 94 | 103.00 | dense |
| D4 | 18 | 15 | 11 | 14.67 | sparse, abundant $GPNMB^-$ macrophages |
| **HL6** | | | | | |
| A1 | 51 | 46 | 44 | 47.00 | dense |
| A2 | 22 | 14 | 25 | 20.33 | sparse-moderate, spindle cells expressing GPNMB, abundant $GPNMB^-$ macrophages |
| A3 | 15 | 13 | 10 | 12.67 | diffuse, mod-sparse |
| A4 | 38 | 48 | 32 | 39.33 | nodular, moderate |
| B1 | 20 | 22 | 27 | 23.00 | relatively sparse |
| B2 | 16 | 32 | 29 | 25.67 | diffuse, sparse-moderate |
| B3 | 27 | 21 | 14 | 20.67 | diffuse, sparse, close to hrs cells |
| B4 | 39 | 29 | 54 | 40.67 | diffuse, spindled form expression, moderate |
| C1 | 6 | 4 | 8 | 6.00 | sparse |
| C2 | 23 | 30 | 18 | 23.67 | expression in spindle cells, close association with HRS cells |
| C3 | 17 | 22 | 22 | 20.33 | diffuse within nodules, some spindle cells |
| C4 | 36 | 30 | 34 | 33.33 | vague aggregates, abundant $GPNMB^-$ neg macrophages |
| D1 | 50 | 58 | 43 | 50.33 | moderate-dense, diffuse |
| D2 | 25 | 18 | 38 | 27.00 | diffuse, sparse |
| D3 | 35 | 25 | 37 | 32.33 | diffuse, moderate density |
| D4 | 7 | 10 | 18 | 11.67 | sparse, diffuse |

All cases showed some GPNMB expression, though this expression was variable as seen in Table 3.2, even within each sample. Mean cell density/HPF for all 86 cases analysed is shown in Figure 3.7. Representative cases from the cohort showing GPNMB/CD68 and GPNMB/CD30 expression are shown in Figure 3.8. Morphologically, some macrophages were noted to be 'HRS-like'; large, binucleate and pleomorphic (Figure 3.9). Cases were then grouped by EBV status (through EBER staining) (Figure 3.10).

Clinical data was available for 70 cases (including 2 patients where diagnosis and relapse sample were tested) so further analysis only includes these cases. Median age was 36 years (range 17-73 years) (Figure 3.11A). Cases were split into 2 age groups (17-36 and 37-73 years); there was no significant difference in mean cell density between the 2 groups, but the mean number of $GPNMB^+$ cells/HPF was slightly higher in the 37-73 age group (unpaired t-test) (Figure 3.11B). I then looked at cases by progression-free survival (PFS) and overall survival (OS) (Figure 3.12). There were only 13 cases where disease had progressed/relapsed, and in this group the mean number of $GPNMB^+$ cells/HPF was slightly higher than in the progression-free group (but not significant, unpaired t-test) (Figure 3.12A). There were 5 patients who died, and similarly the mean cell density was 50 cells/HPF compared to 34 cells/HPF in the group who survived but was not significant and this group was very small (unpaired t-test) (Figure 3.12B). For the 13 cases with progressive disease/relapsed cHL, I compared the diagnostic biopsies to those taken when relapse occurred (Figure 3.12C). There were 2 paired patient samples; in one case the mean cell density of $GPNMB^+$ cells/HPF increased in the relapse biopsy compared to the diagnostic sample; in another the mean cell density decreased. More samples (ideally paired diagnosis/relapse biopsies from the same patient) are required to further assess this.

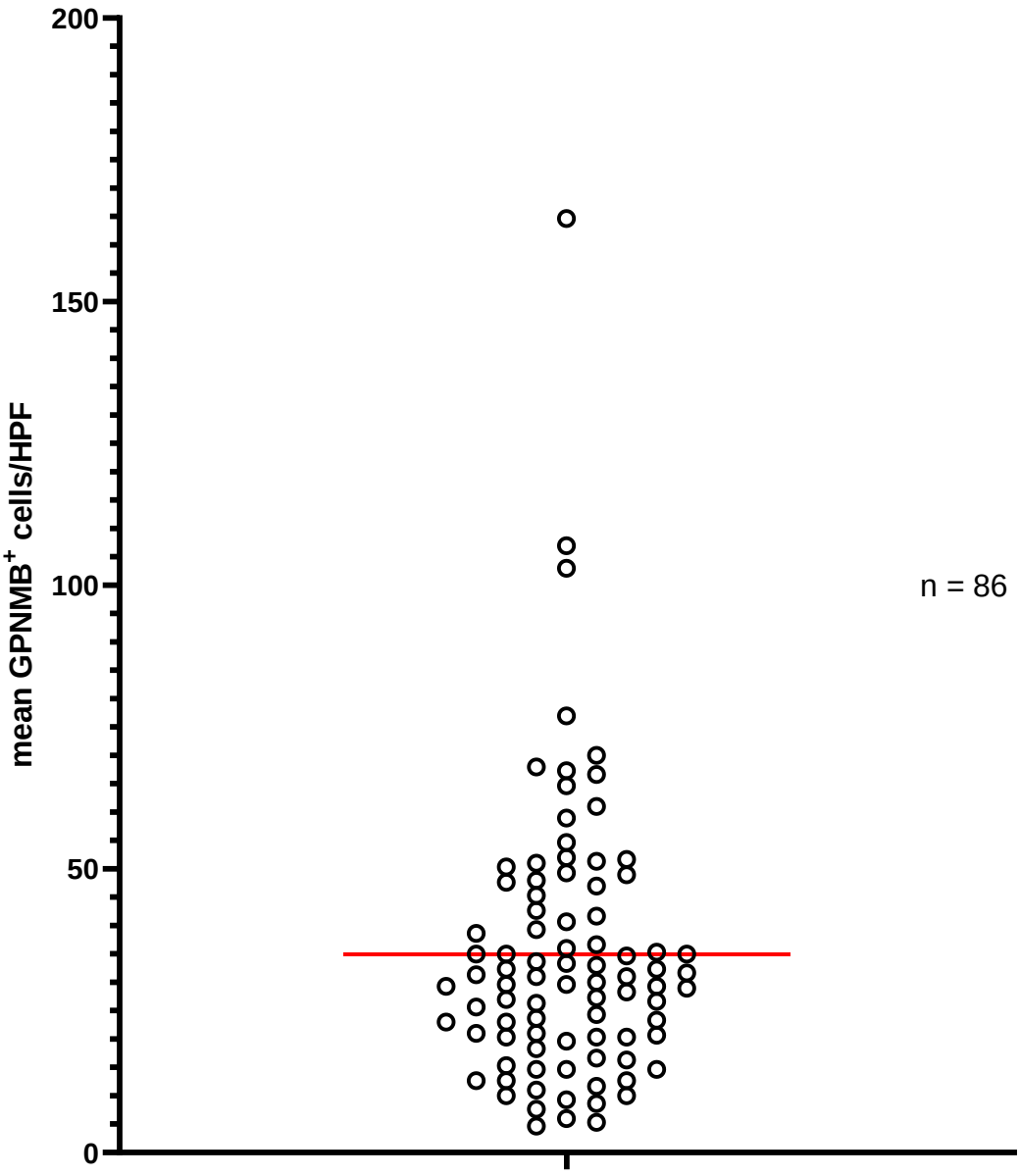


**Figure 3.7. GPNMB cell density in cHL.** Average cell density of GPNMB$^+$ cells in all 86 cases (average count from 3 HPF per case) with mean plotted.

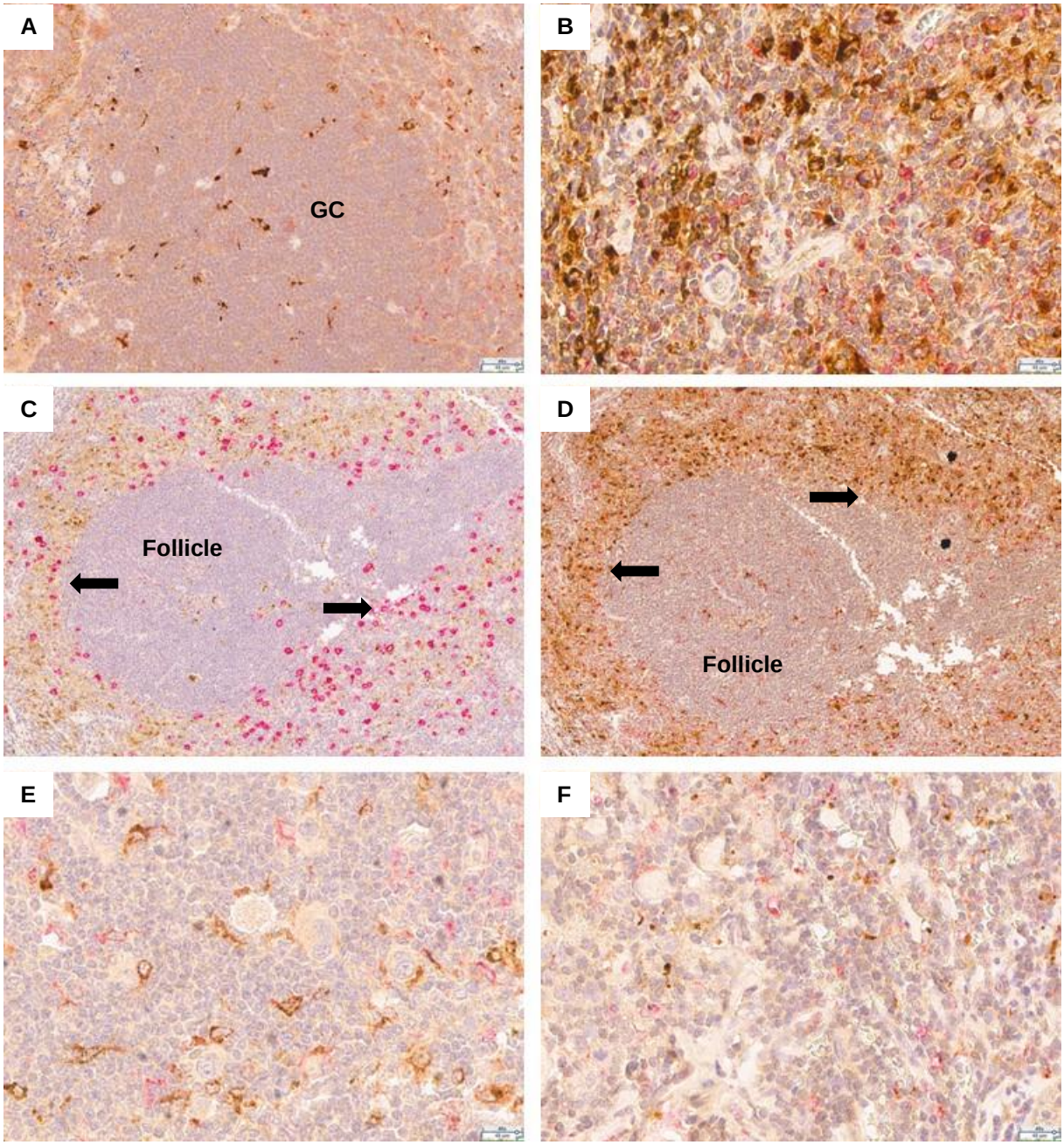


**Figure 3.8. GPNMB/CD68 and GPNMB/CD30 expression in cHL.** GPNMB (brown), CD68/CD30 (red). (A) Tonsil- GPNMB & CD68 in macrophages in the GC. (B)-(D) are from the same case. (B) dense expression of GPNMB in macrophages in a HPF (C) GPNMB/CD30 expression- aggregations of macrophages and HRS cells in periphery of follicle (arrows) (D) GPNMB/CD68 expression around periphery of follicle (arrows) (E) diffuse moderate GPNMB expression (F) sparse GPNMB expression.

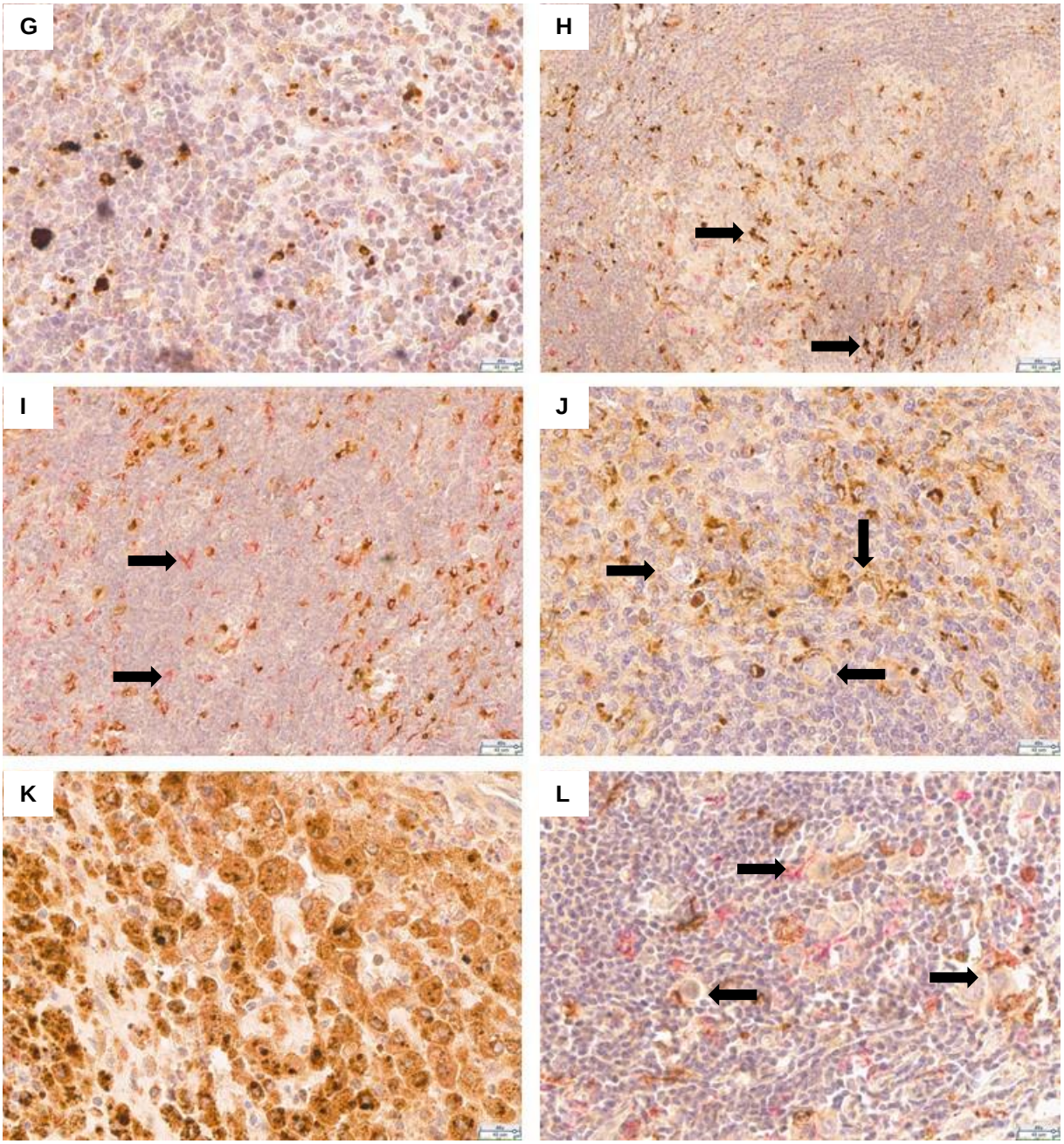


**Figure 3.8. GPNMB/CD68 and GPNMB/CD30 expression in cHL.** Continued. GPNMB (brown), CD68 (red). (G) Sparse but very strong expression of GPNMB in macrophages (H) loosely aggregated GPNMB$^+$ cells (arrows) (I) Proportion of CD68$^+$ macrophages do not express GPNMB (arrows) (J) GPNMB+ macrophages closely associated with HRS cells (arrows) (K) Highest GPNMB$^+$ cell density/HPF (L) Close association of HRS cells to GPNMB$^+$ macrophages (arrows).

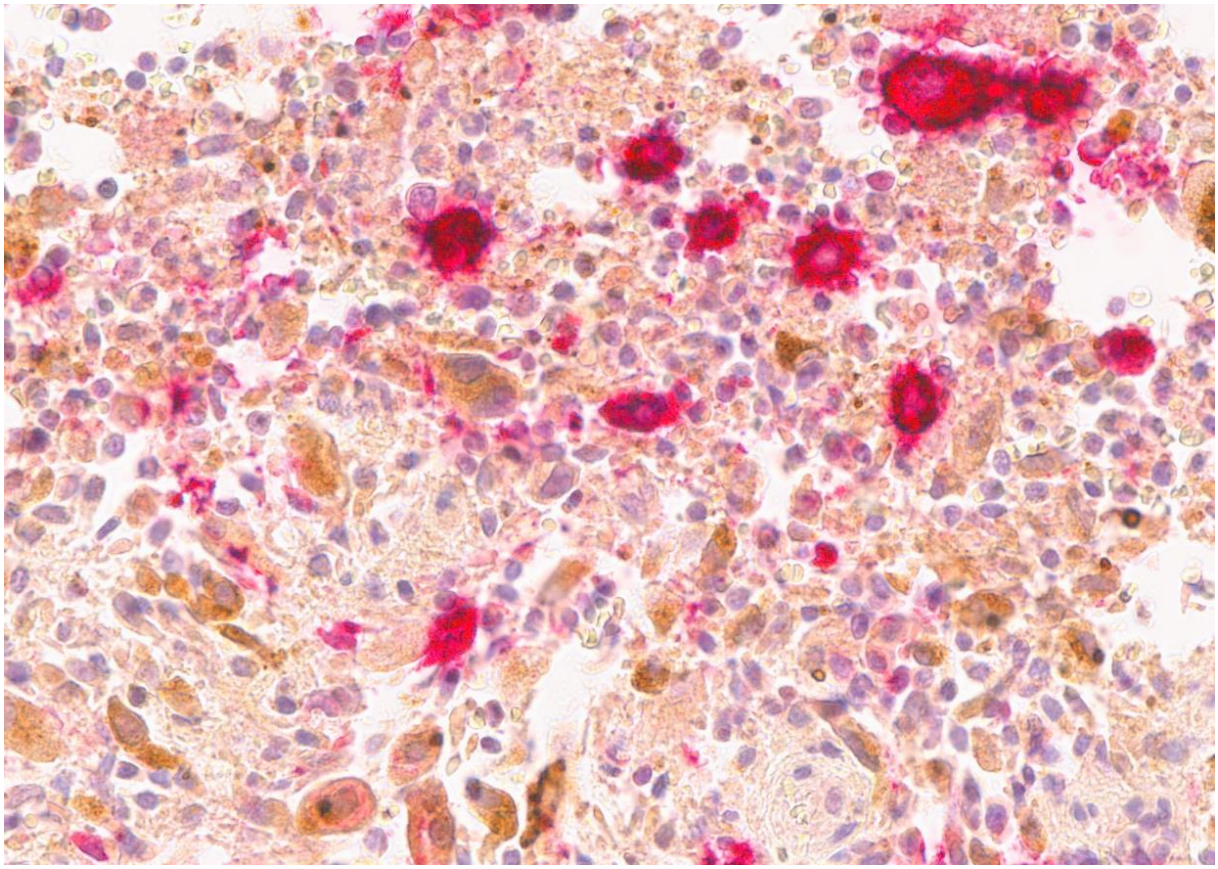

**Figure 3.9. 'HRS-like' macrophages in cHL.** This case from the cHL TMA is stained for CD30 (red) and GPNMB (brown). There are several large, pleomorphic, binucleate $GPNMB^{+}$ macrophages (which are $CD30^{-}$) that look very similar to HRS cells.

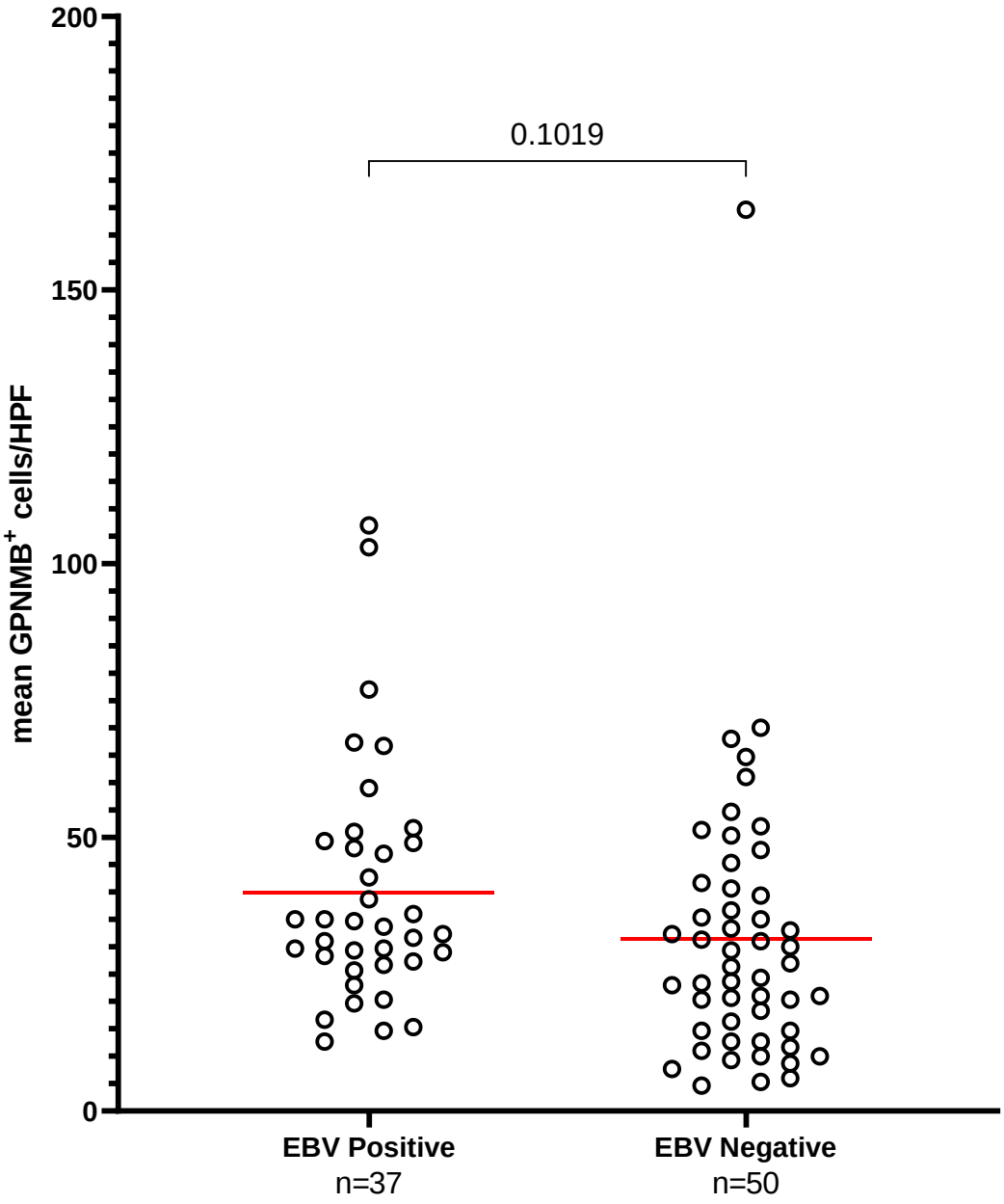


**Figure 3.10. GPNMB cell density in cHL by EBV status.** (n=87) There are 86 patients but 88 samples (2 patients have 2 samples each). One of the patient's diagnostic biopsy was EBV negative and the relapse biopsy was EBV positive (hence n=87 here). There was no significant difference in mean number of GPNMB$^+$ cells/HPF, but on average, there were more GPNMB$^+$ cells in EBV positive cases (mean=39.9 cells/HPF) compared to EBV negative cases (mean=31.4cells/HPF).

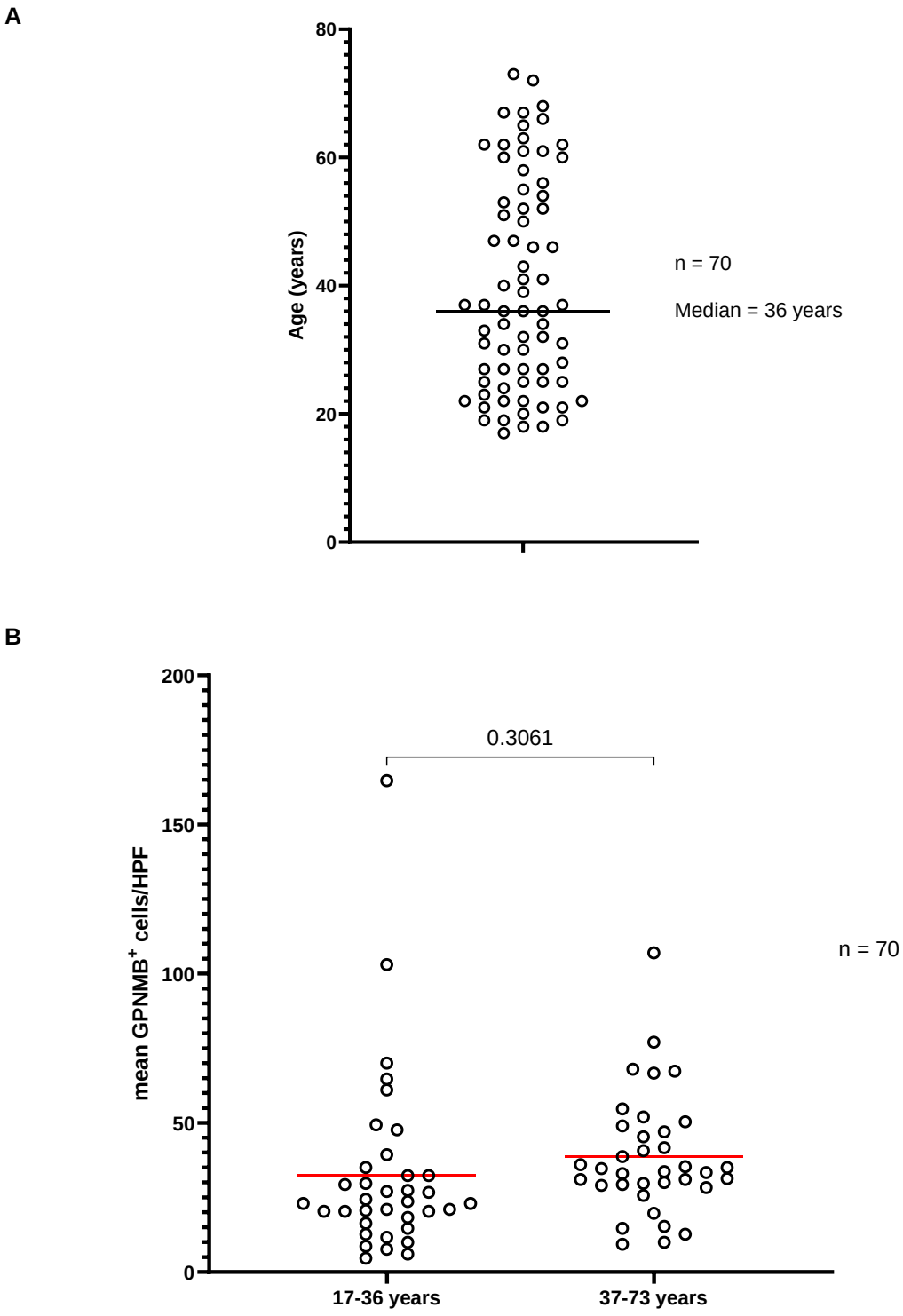


**Figure 3.11. GPNMB cell density in cHL by age group.** n=70 (A) Median age of cases (with clinical data available) = 36 (B) Average cell density of GPNMB$^+$ cells, grouped by age (average count from 3 HPF per case) with group mean plotted. No statistical difference in mean cell density, however, the mean number of GPNMB$^+$ cells/HPF is slightly higher in the 37-73 years age group (unpaired t-test).

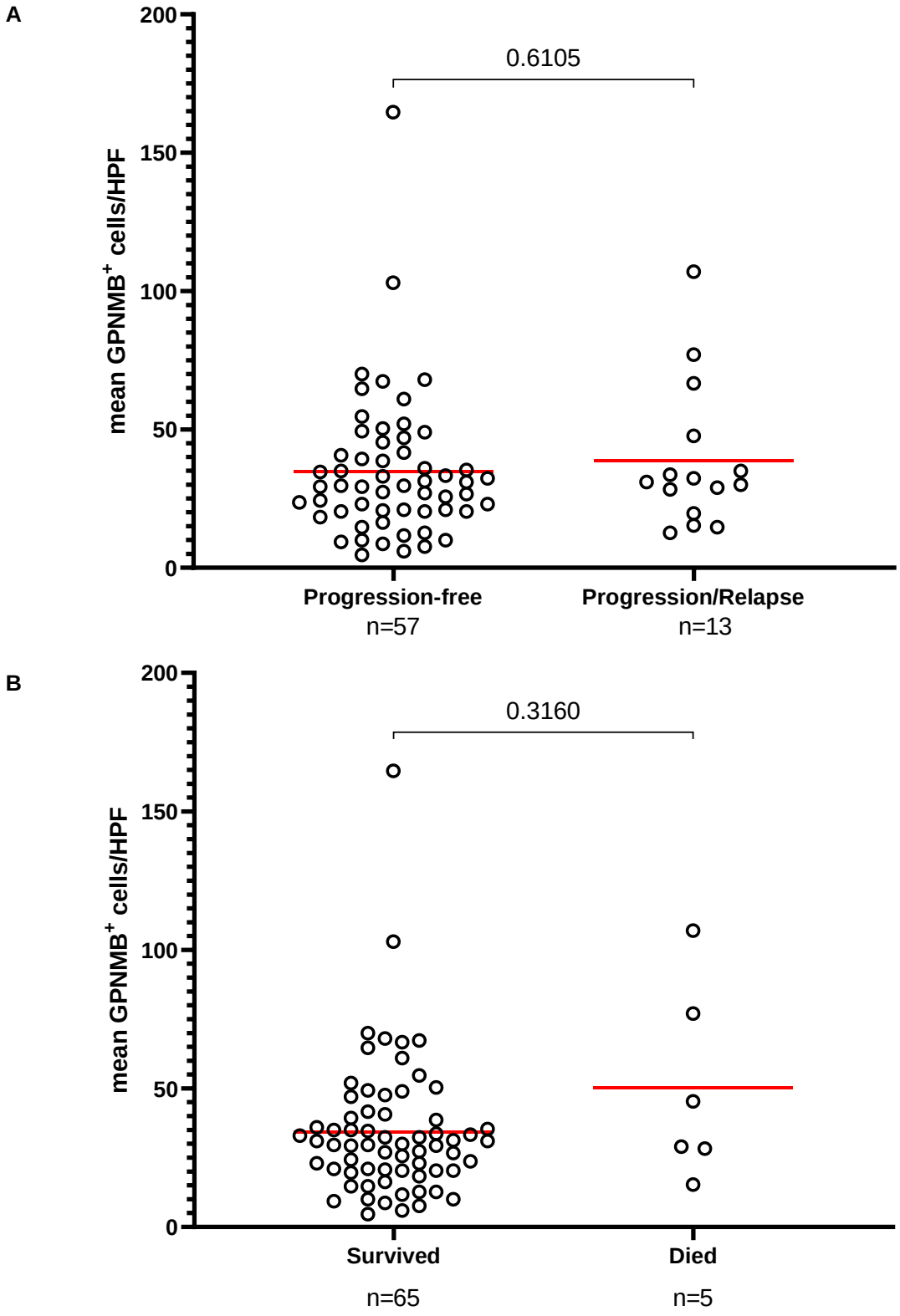


**Figure 3.12. GPNMB mean cell density in cHL by Progression Free Survival (PFS) and Overall Survival (OS).** n=70 (A) mean GPNMB$^+$ cell density grouped by PFS (B) mean GPNMB$^+$ cell density grouped by OS (for the 2 patients with 2 samples, both samples were plotted).

C

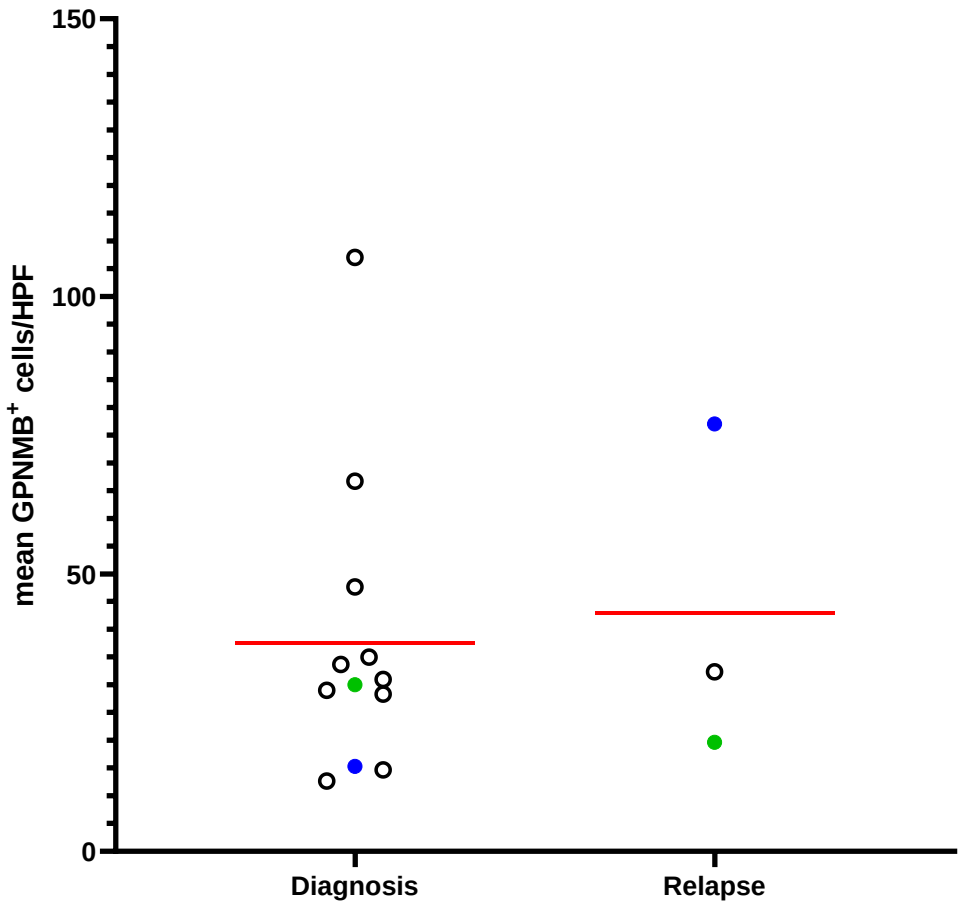


**Figure 3.12. GPNMB mean cell density in cHL by Progression Free Survival (PFS) and Overall Survival (OS).** Continued. n=70 (C) For the cases which relapsed/progressed, comparing mean cell density in diagnostic vs relapse samples. 2 paired samples are colour-coded.

## 3.4 GPNMB expression in HL cell lines and LCLs

I next studied the expression of GPNMB in cHL-derived cell lines and EBV-transformed primary B cells (lymphoblastoid cell lines; LCLs) using quantitative real-time polymerase chain reaction (qPCR), normalising expression against samples of isolated GC B cells taken from the tonsils of three donors. While GPNMB was detected in all three normal GC B cell samples, it was either expressed at very low levels or was undetectable in all five HL cell lines and all five LCLs tested (Figure 3.13). Thus, the results of this qPCR analysis would appear to support my observations that GPNMB is not generally expressed in the tumour cells of cHL. However, the TAM of cHL consistently express high levels of GPNMB.

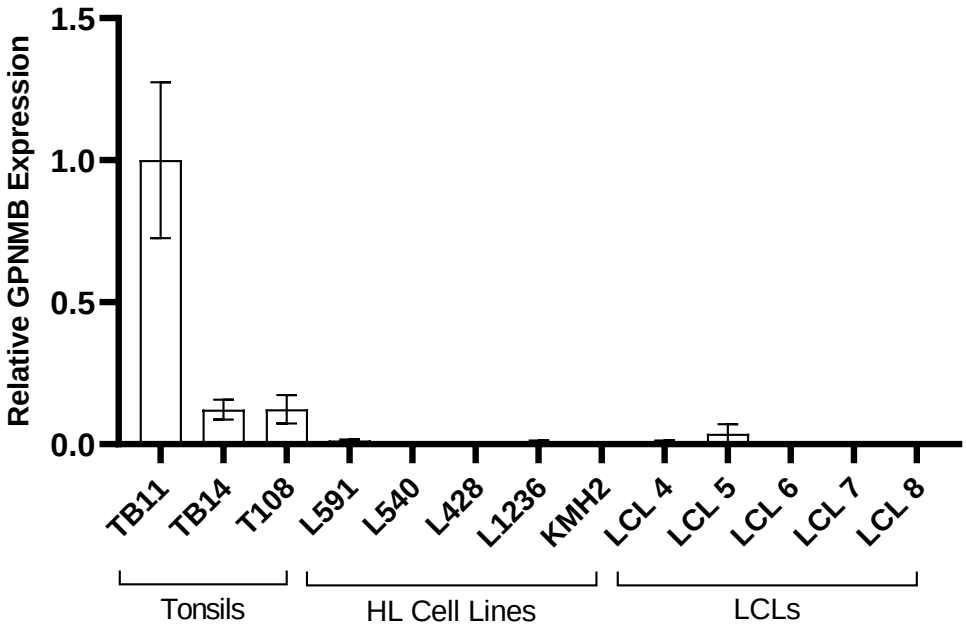


**Figure 3.13. Relative GPNMB expression in normal GC B cells, HL cell lines and LCLs** (normalised to tonsil TB11). GPNMB is expressed either in very low levels or not expressed by HL cell lines or LCLs (mean of 3 replicates).

## 3.5 Soluble GPNMB (sGPNMB) is released into conditioned media (CM) from GPNMB-expressing cells

Having shown that GPNMB expression in transfected HEK293 cells declined over time post-transfection, I next tested if this was the result of the release of a soluble form of GPNMB from these cells. It has previously been shown that the extracellular domain of GPNMB can be proteolytically cleaved by ADAM10 as sGPNMB, and this soluble form acts to promote endothelial cell migration (Rose et al., 2010). To do this, I used a GPNMB Duoset ELISA kit (R&D) to measure GPNMB protein in the cell lysates and conditioned media of transfected cells (Figure 3.14). I found that the concentration of GPNMB was generally higher in cell lysates than in conditioned media. However, over time, the GPNMB levels decreased in cell lysates but increased in conditioned media. I conclude that this is most likely the result of the release of soluble GPNMB from transfected cells.

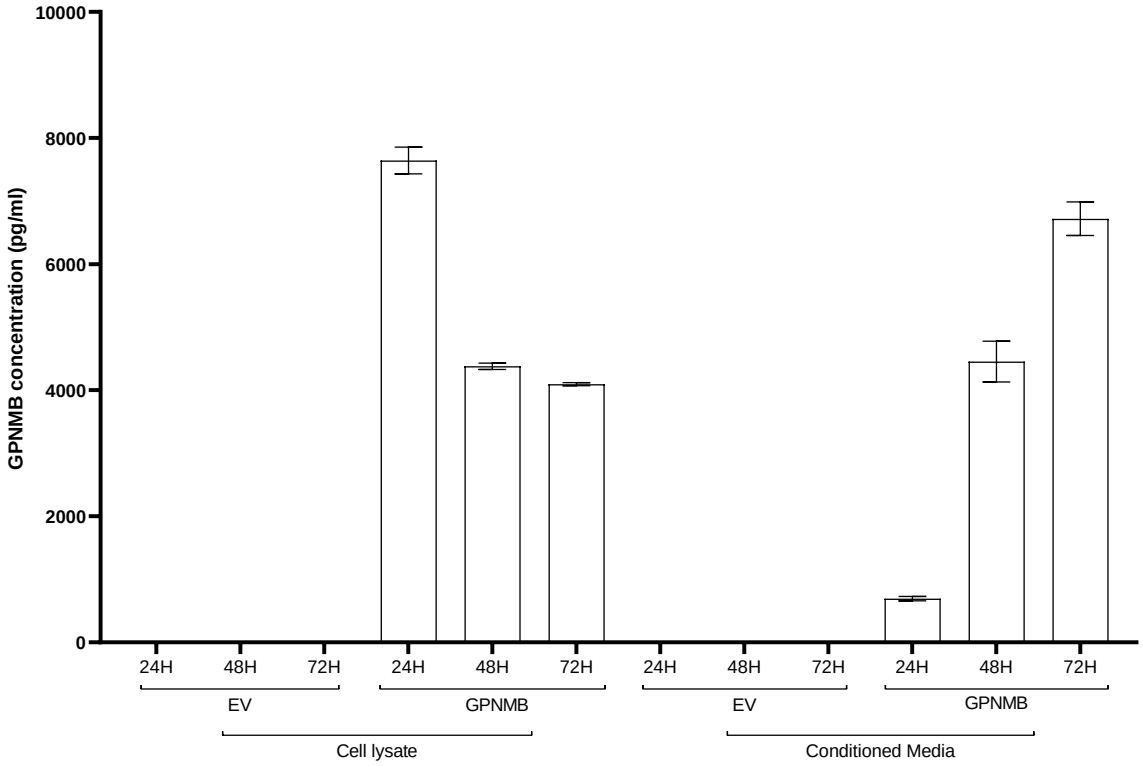


**Figure 3.14. sGPNMB is detectable in conditioned media from GPNMB-expressing cells.** A GPNMB-specific ELISA was used to quantify the amount of GPNMB in cell lysates or conditioned media from HEK293 cells transfected with either EV or GPNMB. The amount of GPNMB in lysate decreased over the 72-hour time course, while levels of GPNMB increased in the conditioned media (mean of 3 replicates, result is one representative experiment out of 4).

## 3.6 Summary

In this chapter, I have shown the following:

- Although GPNMB appeared on a list of overexpressed genes by HRS cells based on gene expression data from micro-dissected HRS cells, it is mostly expressed in the TAMs within cHL
- All cHL cases tested so far expressed GPNMB in TAMs, but expression levels and $GPNMB^{+}$ cell density was variable
- Soluble GPNMB is released into conditioned media of GPNMB-expressing cells and this was detectable using a commercially available ELISA kit for GPNMB

# CHAPTER 4

## GPNMB EXPRESSION IS INDUCED BY POLARISATION OF MACROPHAGES

# Chapter 4 GPNMB expression is induced by polarisation of macrophages

## 4.1 Introduction

GPNMB expression has been reported to be significantly increased following the differentiation of monocytes to M2 macrophages (Dong et al., 2013) and to be higher in M2 macrophages compared with M1 macrophages (Yu et al., 2016). In the previous chapter I showed that GPNMB is expressed by CD68+ macrophages in HL.

The aims of this chapter are to; 1) study GPNMB expression in *in vitro* polarised macrophages; 2) explore the effect of HL cells on the polarisation of macrophages and on the expression of GPNMB expression, and; 3) identify the cytokines involved in the GPNMB pathway/ regulation of GPNMB expression by macrophages.

In the following experiments, each donor represents a biological replicate. Cells from 2-3 donors were co-cultured in one experiment, and the experiment repeated multiple times on separate occasions with freshly isolated monocytes which were differentiated into M1 or M2 macrophages each time. Thus, each graph contains donors which may have been co-cultured in different experiments, but each experiment was set up in the same way, with each donor acting as a 'biological replicate.'

## 4.2 GPNMB expression by *in vitro* polarised M1 and M2 macrophages

### 4.2.1 Polarisation of monocytes to M1 and M2 macrophages

Having shown that GPNMB is expressed by tumour-associated macrophages in the microenvironment of HL, I next wanted to study the expression of GPNMB following the polarisation of $CD14^{+}$ monocytes *in vitro* using GM-CSF and M-CSF. These Monocytes were isolated from the leukocyte cones of healthy donors and cultured with GM-CSF or M-CSF for 7 days. The $CD14^{+}$ isolated cells were subjected to flow cytometry to measure the surface expression of a panel of markers by flow cytometry (CD14, CD68, CD163, CD206, GPNMB) to check the purity of isolation and cell phenotype (Figure 4.1 A).

Day 7 cultured macrophages were also stained for the same panel of markers as above (Figure 4.1 B). All macrophages were defined as being $CD45^{positive}CD68^{positive}$; this population was gated for CD163 and CD206 positivity and surface expression of GPNMB: M1 macrophages (treated with GM-CSF) were mostly $CD163^{negative}CD206^{positive}$; M2 macrophages (treated with M-CSF) had a population of $CD163^{positive}CD206^{positive}$ cells, but there were also populations of $CD163^{negative}CD206^{negative}$ cells and $CD163^{positive}CD206^{positive}$ as in the M1 macrophage population. The proportion of $CD163^{positive}CD206^{positive}$ cells across donors is shown in Figure 4.1 C.

To assess cytokine expression of *in vitro* polarised M1 and M2 macrophages, cells were treated with LPS for 24 hours and IL-10 and IL-12(p70) secretion measured in conditioned media (CM) by enzyme-linked immunosorbent assays (ELISAs) measuring IL-10 and IL-12(p70) secretion (performed by Dr Tracey Perry using Human IL-10 and IL-12 ELISA kits from

BioLegend as per manufacturer's instructions, other than assays were done in 96-well plates with ¼ well volumes (Corning)) (Figure 4.1 D). CM from GM-CSF-treated macrophages CM showed IL-$10^{low}$ and IL-12(p70)$^{high}$ secretion after LPS treatment, typical of M1 macrophages; M-CSF-treated macrophage CM showed IL-$10^{high}$ and IL-12(p70)$^{low}$ secretion after LPS treatment, typical of M2 macrophages.

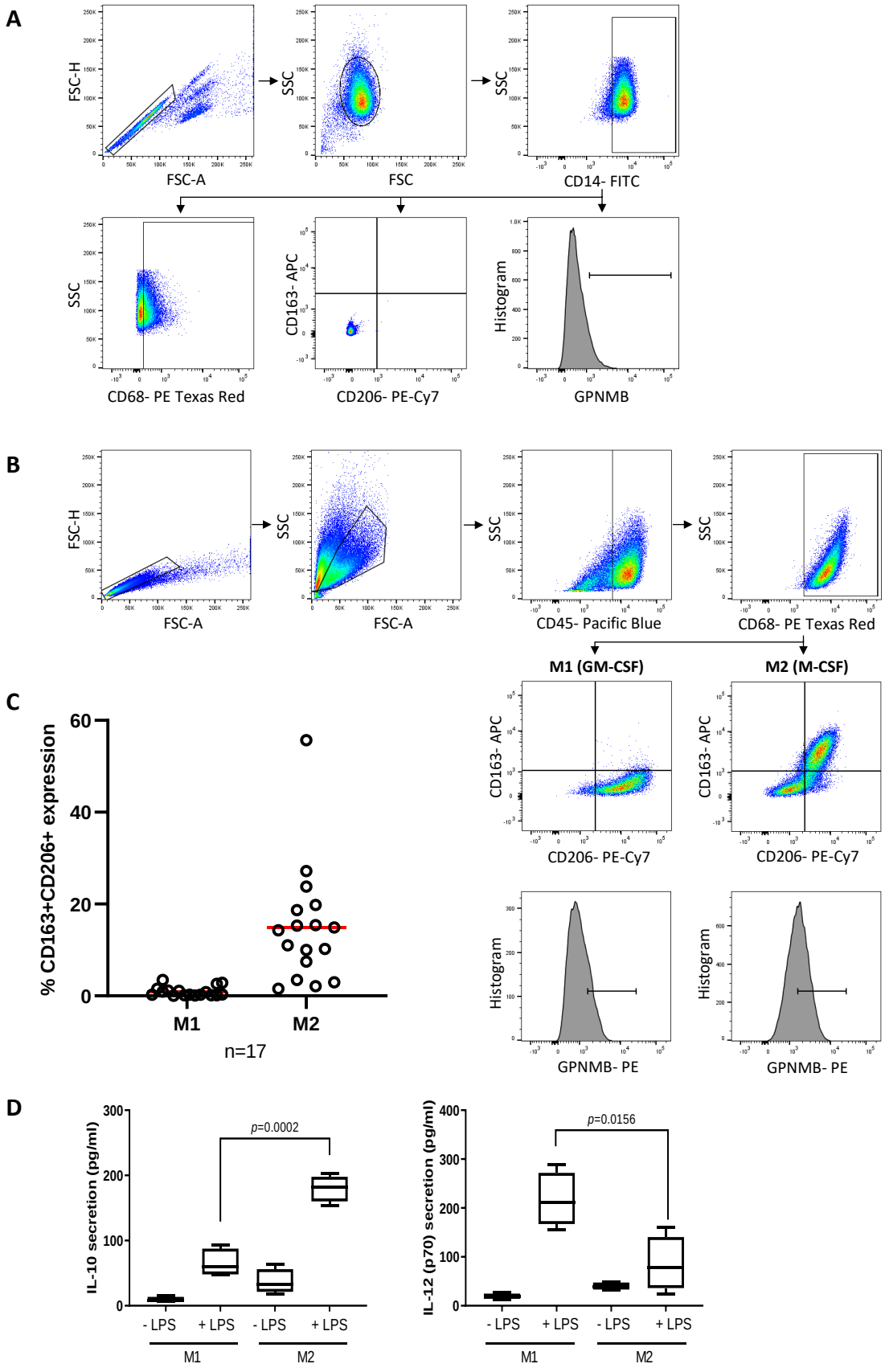


**Figure 4.1 Surface expression of macrophage markers in polarised M1 and M2 macrophages by flow cytometry.** (A) Gating strategy for CD14+ monocytes by flow cytometry (B) Gating strategy for D7 cultured macrophages to assess surface expression of CD163, CD206 and GPNMB in the M1 or M2 populations. (C) CD163/CD206 expression in D7 M1 or M2 macrophages across donors (D) IL-10 and IL-12(p70) secretion following stimulation of *in vitro* polarised M1 or M2 macrophages with LPS for 24 hours measured by ELISA. Figure 4.1D from Dr Tracey Perry (Adams Perry, 2019)

### 4.2.2 M1 and M2 macrophages have a higher expression of GPNMB than monocytes

GPNMB expression was measured in the *in vitro* differentiated macrophage populations by quantitative real-time polymerase chain reaction (qPCR) and flow cytometry. ELISA was used to measure sGPNMB levels in CM from $1x10^5$cells/ml for 24 hours (cell numbers were adjusted to account for differences in proliferation between M1 and M2 macrophages).

GPNMB expression by qPCR was seen to increase significantly in both M1 and M2 macrophages compared to monocytes (Day 0 CD14+ cells) following 7 days of differentiation (Figure 4.2 A). Although M2 macrophages had a slightly higher mean expression level, there was no significant difference in GPNMB expression between M1 and M2 cells. The three tested HL cell lines did not express GPNMB. All samples were normalised to THP-1 cell line.

Surface expression of GPNMB was also measured by flow cytometry and there was no significant difference in overall expression levels between M1 and M2 macrophages (as part of the gating strategy in Figure 4.1 B) (Figure 4.2 B). When GPNMB expression levels were compared between matched M1s and M2s from individual donors, there was no consistent difference, in keeping with qPCR data.

sGPNMB levels in CM from M1 and M2 macrophages were similar between the 2 groups and no significant difference was seen once cell number was accounted for (Figure 4.2 C), though M2s tended to proliferate more rapidly so CM collected from cells on day 7 showed slightly higher sGPNMB levels in M2 CM than in M1 CM (data not shown). CM from 3 HL cell

lines used in subsequent experiments were checked for sGPNMB and none was detected (Figure 4.2 B).

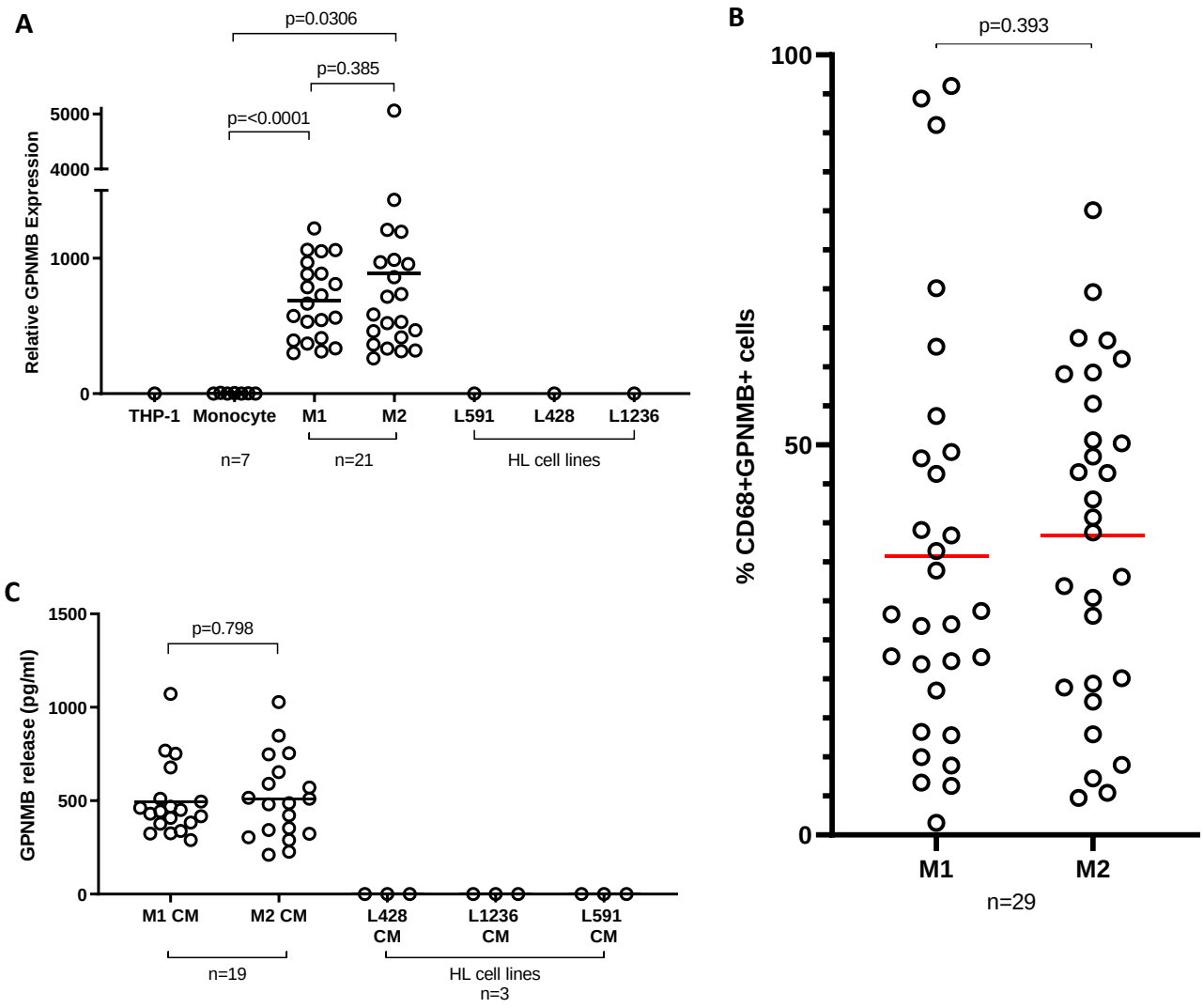


**Figure 4.2 GPNMB expression in polarised M1 and M2 macrophages.** (A) Relative GPNMB expression (normalised to THP-1 cells) measured by qPCR increases significantly upon differentiation of monocytes to both M1 and M2 macrophages, but expression levels between M1 and M2 macrophages did not differ significantly. HL cell lines do not express GPNMB (B) Surface expression of GPNMB measured by flow cytometry. There was no significant difference in GPNMB surface expression between M1 and M2 macrophages (C) sGPNMB release from $1x10^5$ cells (M1 or M2) into CM after 24 hours measured by ELISA. There was no significant difference between sGPNMB release between M1 and M2 macrophages. No sGPNMB was detectable in CM made from HL cell lines (used in subsequent experiments)

## 4.3 Co-culture with Hodgkin cells induces GPNMB expression in M1 and M2 macrophages

### 4.3.1 Hodgkin cell line CM contains M-CSF

In order to determine which HL cell lines to use in co-culture with M1 and M2 macrophages, I measured M-CSF release across HL cell lines by ELISA as this is the cytokine added to monocytes to induce M2 macrophage polarisation, which more closely resemble the tumour-associated macrophage (TAM) phenotype (Mantovani et al., 2002, Rey-Giraud et al., 2012). CM from $1x10^6$cells/ml was collected after 24 hours on three separate occasions and M-CSF levels measured. CM from L1236 and L428 lines had the highest levels of M-CSF and L591 CM and media alone did not contain detectable M-CSF (figure 4.3).

L1236 and L428 cell lines were therefore selected for use in subsequent co-culture experiments, along with L591 as this cell line did not release detectable M-CSF to see if there are any differences in macrophage polarisation and GPNMB expression following co-culture with these cell lines or their CM. Interestingly, L591 is also the only EBV-positive cell line.

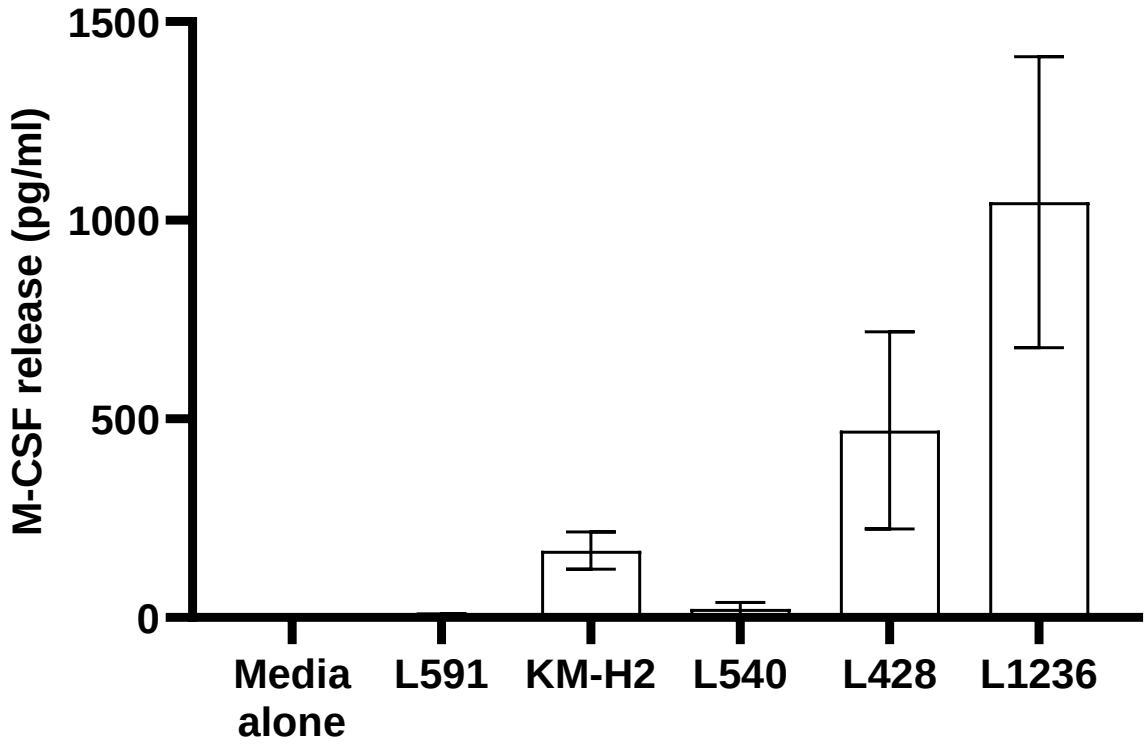


**Figure 4.3 M-CSF release across Hodgkin lymphoma cell lines.** M-CSF release was measured in CM from HL cell lines (harvested from $1x10^6$ cells/ml after 24 hours) and media alone by ELISA, collected on 3 separate occasions. L1236 and L428 cell lines showed the highest levels of M-CSF release. M-CSF was not detectable in L591 CM.

### 4.3.2 Co-culture of *in vitro* polarised macrophages with Hodgkin cells induces macrophage polarisation and GPNMB expression

3 HL cell lines (L428, L1236 and L591) were chosen to be co-cultured with in vitro polarised macrophages for 24 hours. CM from each cell line (harvested from $1x10^6$cells/ml after 24 hours) or HL cells were used in different ratios to macrophages to determine if this affected the degree of polarisation or GPNMB expression. This was important to know because HL is an unusual tumour insofar as there are relatively few HRS cells within the TME in comparison to other cells, including macrophages. The following ratios of macrophages:HL cells were used; 10 macrophages: 1 HL cells (M1/M2: HL 10:1 on graphs); 1 macrophage:1 HL cell (M1/M2:HL 1:1); 1 macrophage: 10 HL cells (M1/M2:HL 1:10). Some of the co-cultures were carried out with a 0.4µm transwell insert to keep HL cells separate from macrophages, and in others no transwell was used so the cells were in direct contact with each other. This was to determine if direct cell-cell contact was required for any observed effects, or if soluble factors released by HL cells were enough to exert the effect, in comparison to culture with HL CM alone. As well as soluble factors, other intercellular mechanisms of communication could be occurring in the transwell experiments. Extracellular vesicles, e.g. exosomes and ectosomes could be released by tumour cells, which promote and contribute to various aspects of the cancer phenotype, e.g. growth, angiogenesis, migration, metastasis and immune evasion; some of these could cross a 0.4µm membrane even if tumour cells cannot (Möller and Lobb, 2020). Several studies have reported that tumour-derived exosomes can induce macrophage activation and polarisation in multiple cancers, e.g. melanoma and pancreatic cancer [reviewed in (Moradi-Chaleshtori et al., 2019)]. Tumour microtubes or tunnelling nanotubes are membranous channels made from F-actin that connect different cell types over longer

distances of up to 100µm (Roehlecke and Schmidt, 2020). In cancer, they have been shown to be involved with cancer cell-macrophage interactions in a breast cancer model as a means of promoting tumour cell invasion in vitro (Hanna et al., 2019).

Co-culture of macrophages and HL cells with direct cell-cell contact (i.e. when no transwells were used) induced the polarisation of M1 to M2 macrophages and further polarisation of M2 macrophages along the spectrum (Figures 4.4 A&B, 4.5 A&B and 4.6 A&B). However, when cells were co-cultured with transwells, only a modest increase in CD163+CD206+ cells in both M1 and M2 macrophages was observed (Figures 4.4 C&D, 4.5 C&D and 4.6 C&D).

I next wanted to determine if GPNMB expression was induced in macrophages co-cultured with HL cells or CM. Surface expression of GPNMB was compared between cell lines +/- transwells using the gating strategy as before (Figure 4.1 B). Co-culture with all 3 HL cell lines and CM induced surface GPNMB expression with and without transwells compared to expression in control M1 or M2 cells (Day 7 post- GMCSF or -MCSF culture respectively) and this was significant across all co-culture conditions tested and for both M1 and M2 macrophages (Figures 4.7-4.9). This increase in GPNMB expression appears to be greatest following co-culture of M1 macrophages with transwells across all 3 HL cell lines (Figures 4.7C, 4.8C and 4.9C) compared to the donors where no transwells were used (Figures 4.7A, 4.8A and 4.9A), despite direct cell-cell contact being necessary for robust macrophage polarisation. Different donors had to be used between experiments with and without transwells, so whilst it is not possible to directly compare donors between experiments, an overall difference in

GPNMB expression can be seen even when a concurrent increase in CD163+CD206+ expression was not observed where transwells were used (Figures 4.4B-4.6 B vs. 4.7B-4.9B).

I then wanted to compare GPNMB surface expression after co-culture to sGPNMB release into macrophage CM at 24 hours post co-culture and look at differences in 3 representative individual donors (co-cultured in one experiment). GPNMB surface expression was measured by flow cytometry as previously, and sGPNMB release was measured by ELISA (Figure 4.10). For each donor, M1 and M2 macrophages were co-cultured with all 3 cell lines and these have been combined by co-culture condition (n=3 cell lines). Across all 3 donors, M2 macrophages expressed more GPNMB than M1 macrophages and each cell line had a very similar effect on GPNMB surface expression and sGPNMB release; both surface expression and sGPNMB release increased across all co-culture conditions to similar levels between donors. GPNMB expression levels and sGPNMB release was similar at a ratio of 10 macrophages:1 HL cell compared to 1 macrophage:10 HL cells.

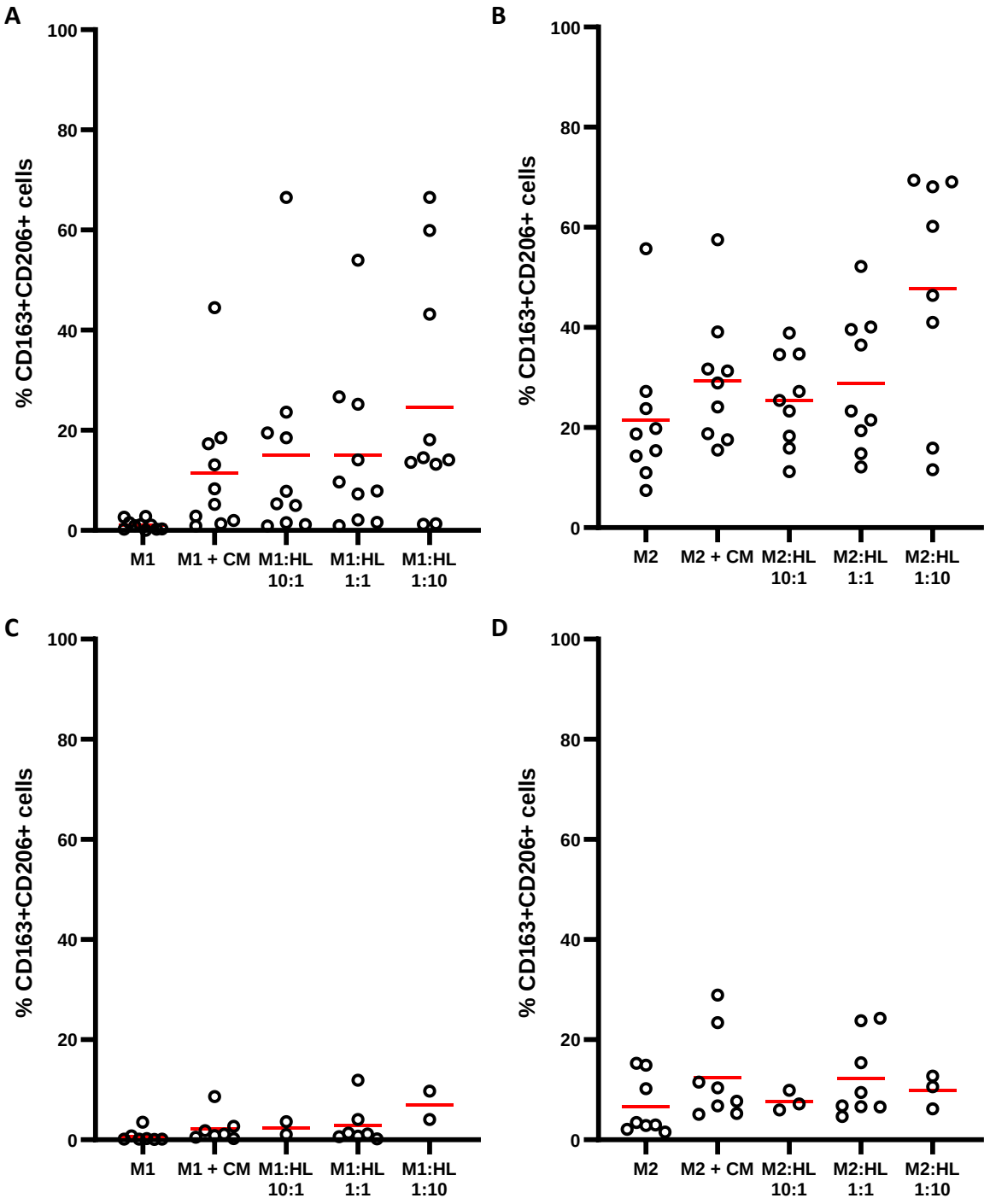


**Figure 4.4 CD163+CD206+ expression following co-culture of macrophages with L428 cells.** (A) & (B) No transwell was used. When macrophages and HL cells are in direct contact in co-culture in the well, this induces polarisation of M1s to M2s and it further polarises M2s (seen as an increase in % of CD163+CD206+ cells compared to the control levels on day 7 following culture with GM-CSF or MSCF in M1 or M2 macrophages respectively. (C) & (D) Transwells were used in co-culture. In these donors, there is only a slight increase in CD163+CD206+ cells in both groups following co-culture compared to when no transwell was used.

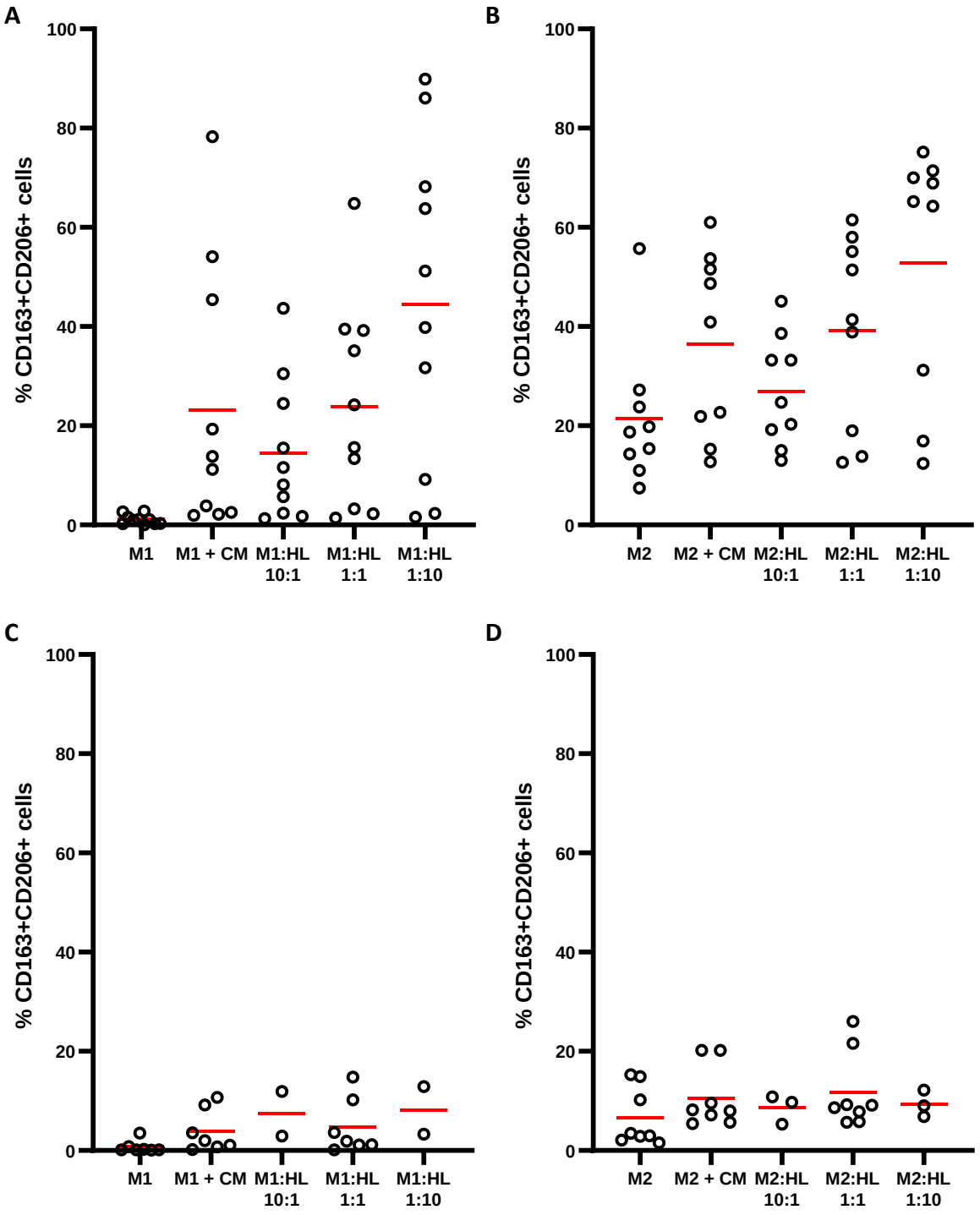


**Figure 4.5 CD163+CD206+ expression following co-culture of macrophages with L1236 cells.** (A) & (B) No transwell was used. When macrophages and HL cells are in direct contact in co-culture in the well, this induces polarisation of M1s to M2s and it further polarises M2s (seen as an increase in % of CD163+CD206+ cells compared to the control levels on day 7 following culture with GM-CSF or MSCF in M1 or M2 macrophages respectively. (C) & (D) Transwells were used in co-culture. In these donors, there is only a slight increase in CD163+CD206+ cells in both groups following co-culture compared to when no transwell was used.

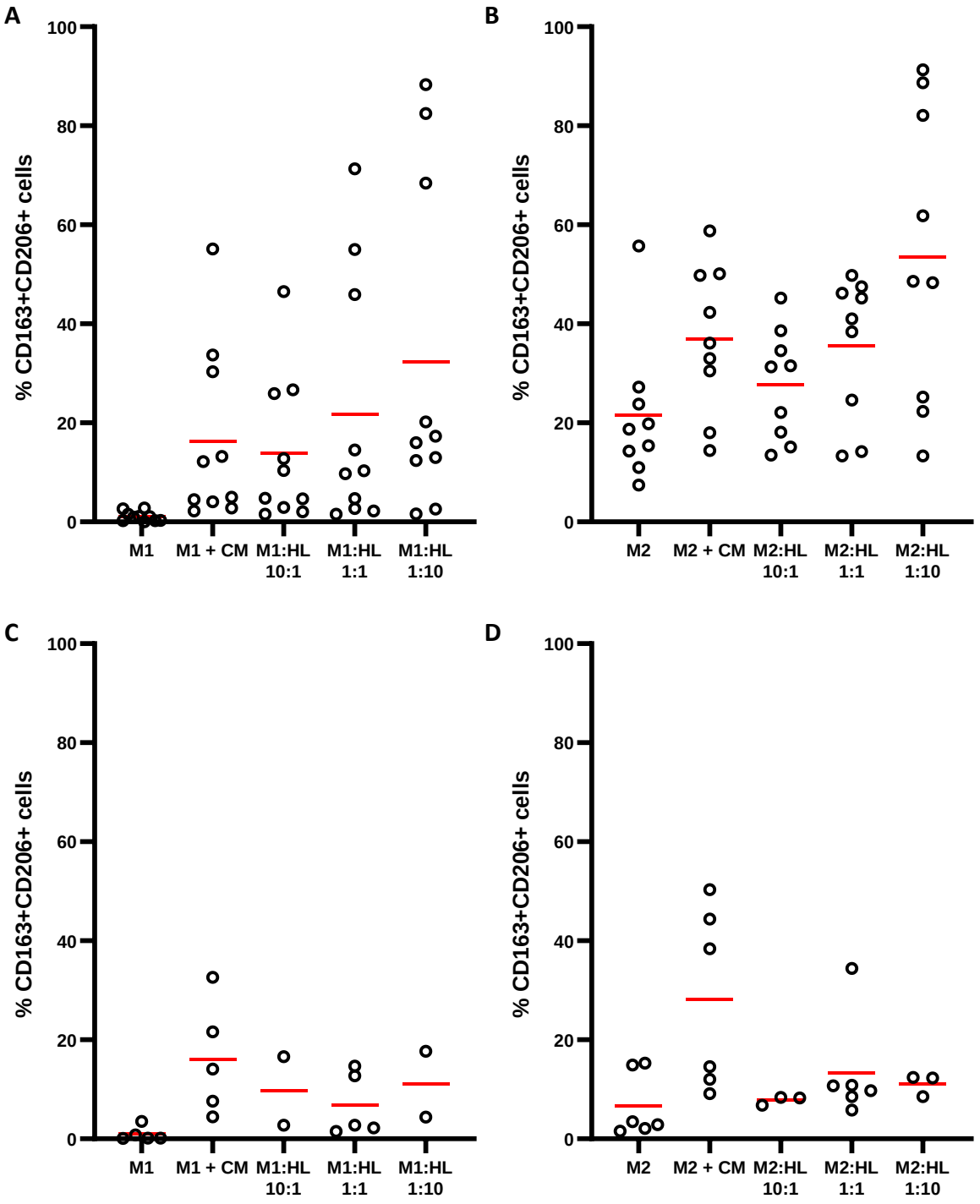


**Figure 4.6 CD163+CD206+ expression following co-culture of macrophages with L591 cells.** (A) & (B) No transwell was used. When macrophages and HL cells are in direct contact in co-culture in the well, this induces polarisation of M1s to M2s and it further polarises M2s (seen as an increase in % of CD163+CD206+ cells compared to the control levels on day 7 following culture with GM-CSF or MSCF in M1 or M2 macrophages respectively. (C) & (D) Transwells were used in co-culture. In these donors, there is only a slight increase in CD163+CD206+ cells in both groups following co-culture compared to when no transwell was used.

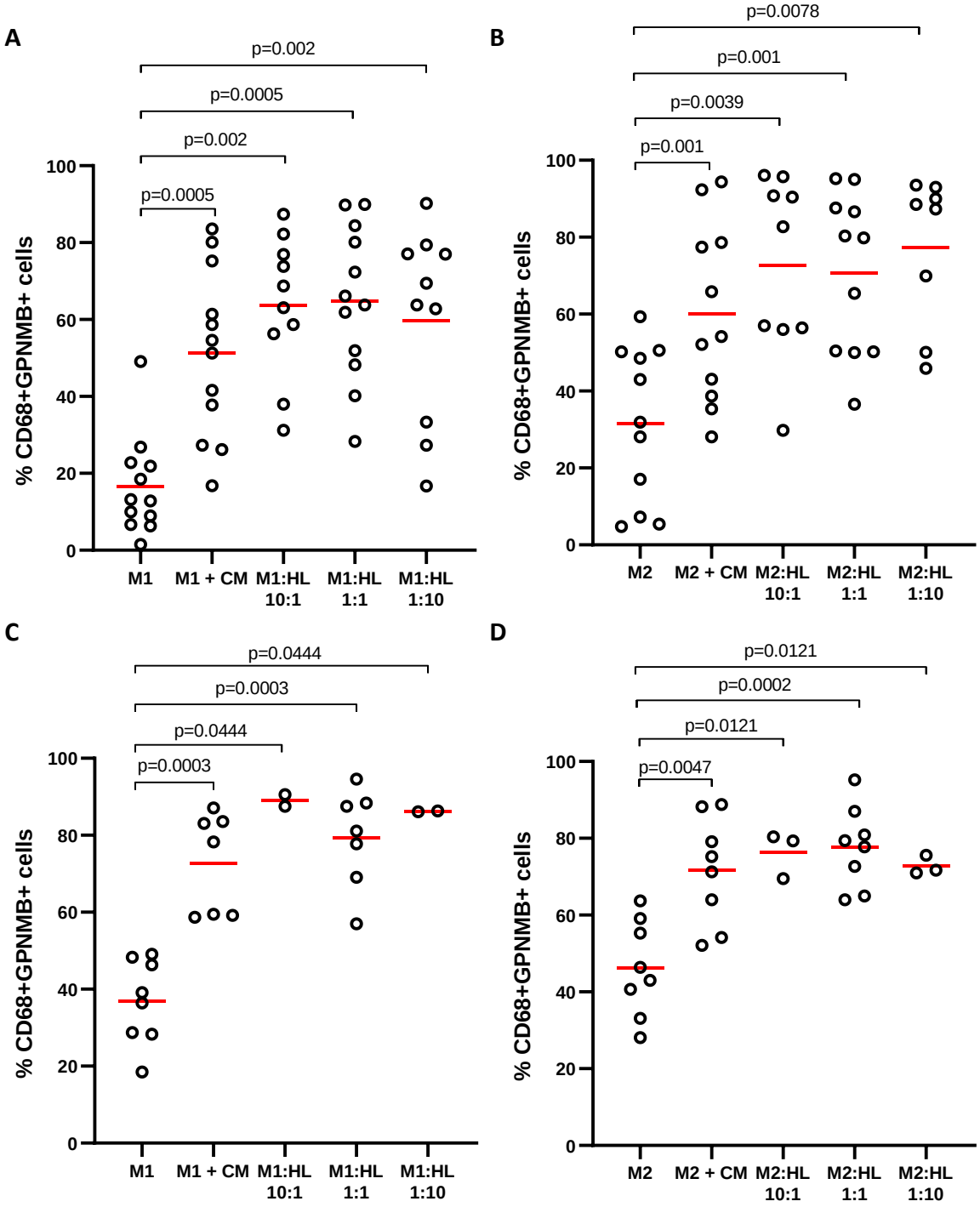


**Figure 4.7 GPNMB expression increases upon co-culture of macrophages with L428 cells.** (A) & (B) No transwells used. In these donors, there was a significant increase in surface GPNMB expression following direct co-culture of macrophages with L428 CM or cells for 24 hours compared to the control M1 or M2 macrophages (7 days post-culture with GM-CSF or MCSF respectively). Differences were significant across all ratios of macrophages:HL cells (Wilcoxon matched pairs signed rank test). (C) & (D) Transwells used. In these donors, there was also a significant increase in surface GPNMB expression following co-culture of macrophages with L428 CM or cells using transwells for 24 hours, compared to control M1 or M2 macrophages. Differences were significant across all ratios of macrophages:HL cells (Mann-Whitney test).

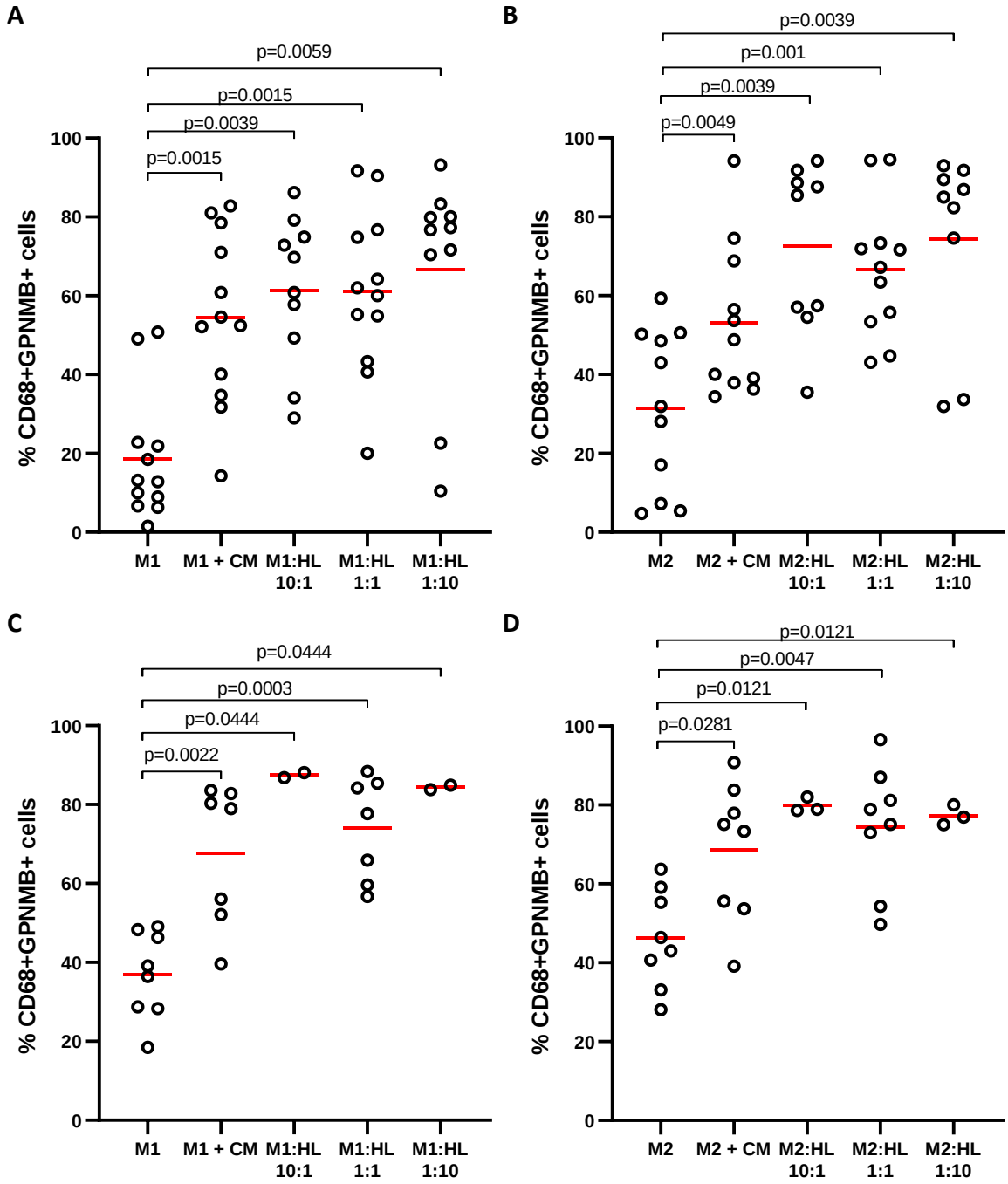


**Figure 4.8 GPNMB expression increases upon co-culture of macrophages with L1236 cells.** (A) & (B) No transwells used. In these donors, there was a significant increase in surface GPNMB expression following direct co-culture of macrophages with L1236 CM or cells for 24 hours compared to the control M1 or M2 macrophages (7 days post-culture with GM-CSF or MCSF respectively). Differences were significant across all ratios of macrophages:HL cells (Wilcoxon matched pairs signed rank test). (C) & (D) Transwells used. In these donors, there was also a significant increase in surface GPNMB expression following co-culture of macrophages with L1236 CM or cells using transwells for 24 hours, compared to control M1 or M2 macrophages. Differences were significant across all ratios of macrophages:HL cells (Mann-Whitney test).

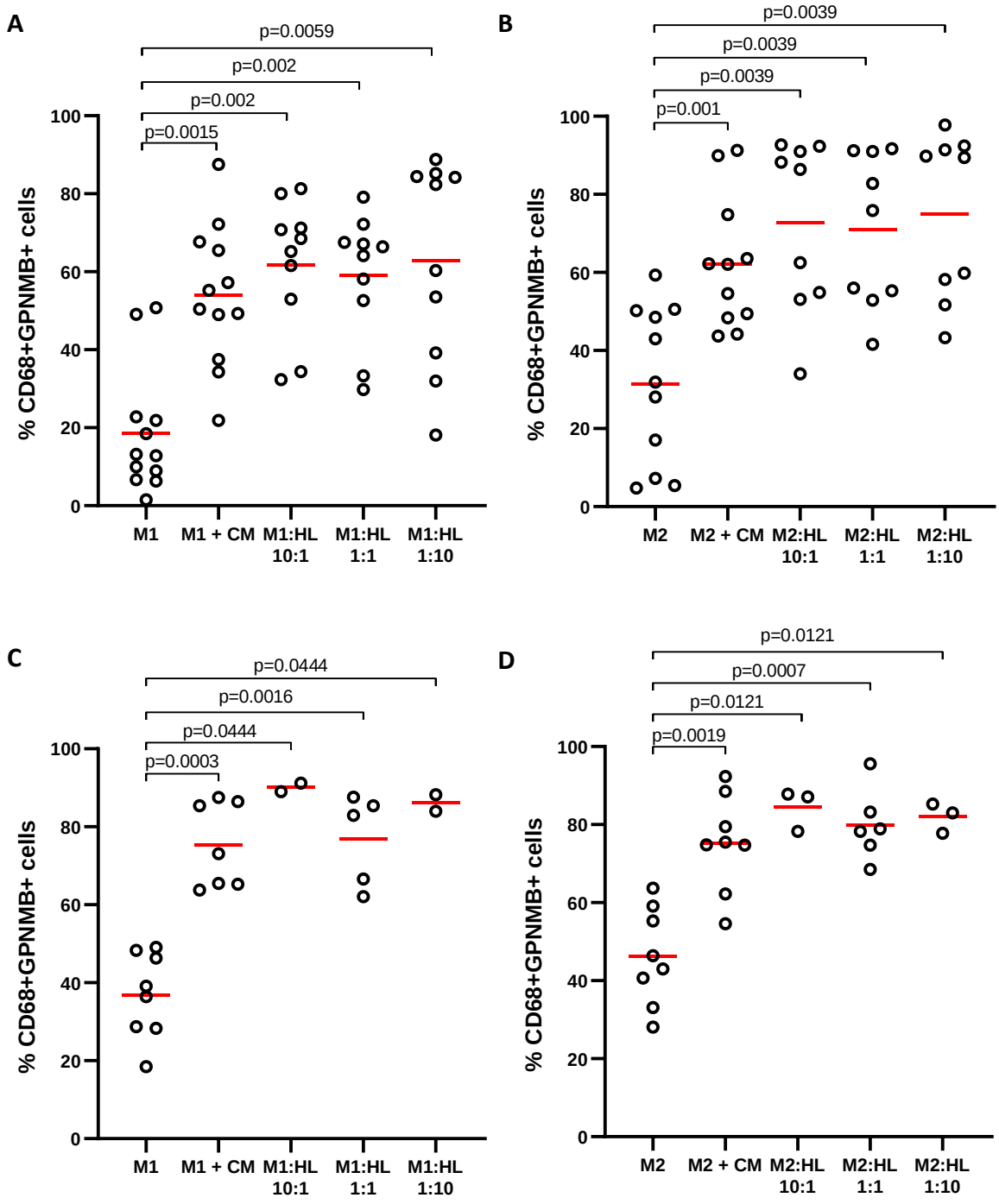


**Figure 4.9 GPNMB expression increases upon co-culture of macrophages with L591 cells.** (A) & (B) No transwells used. In these donors, there was a significant increase in surface GPNMB expression following direct co-culture of macrophages with L591 CM or cells for 24 hours compared to the control M1 or M2 macrophages (7 days post-culture with GM-CSF or MCSF respectively). Differences were significant across all ratios of macrophages:HL cells (Wilcoxon matched pairs signed rank test). (C) & (D) Transwells used. In these donors, there was also a significant increase in surface GPNMB expression following co-culture of macrophages with L591 CM or cells using transwells for 24 hours, compared to control M1 or M2 macrophages. Differences were significant across all ratios of macrophages:HL cells (Mann-Whitney test).

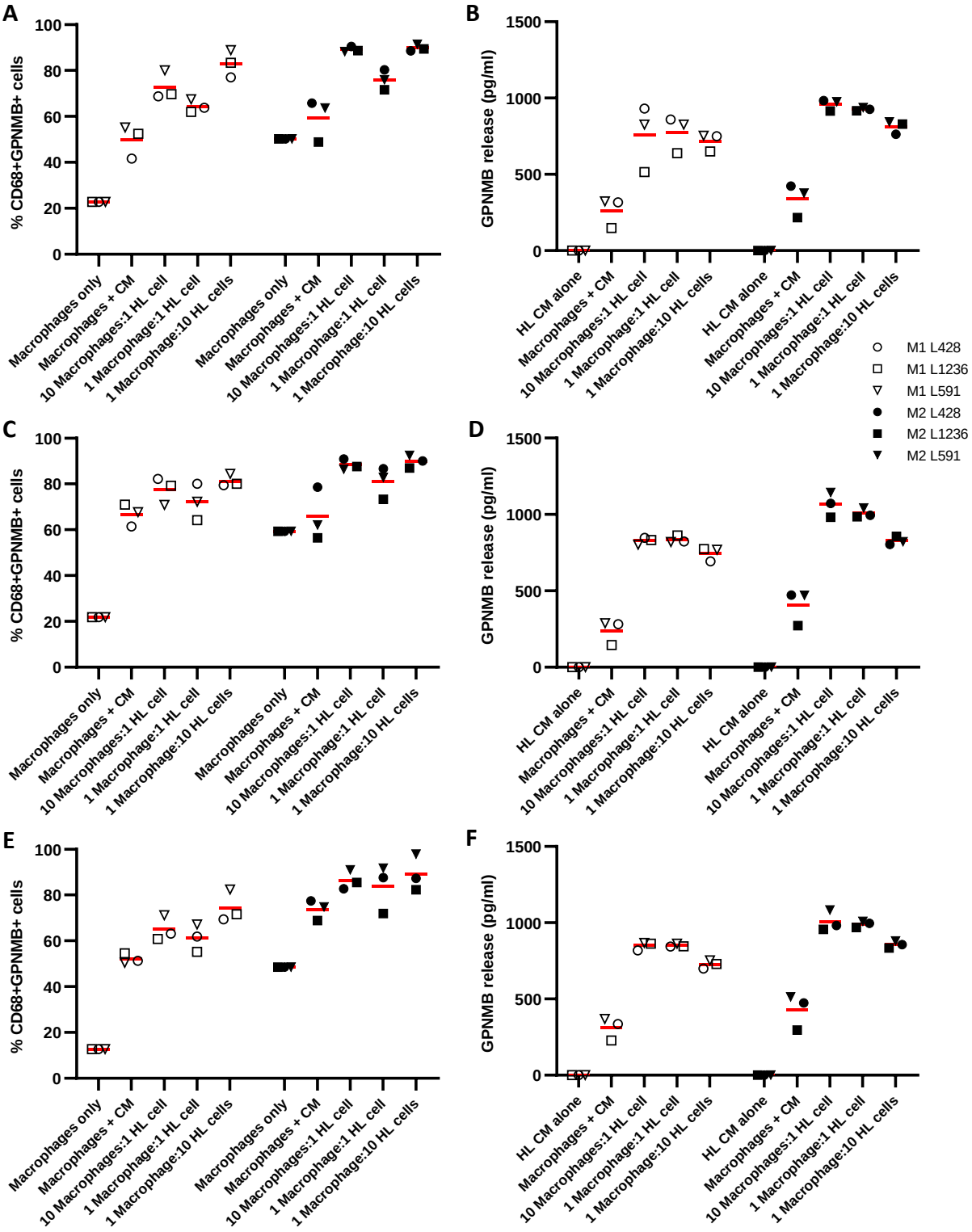


**Figure 4.10 GPNMB surface expression and sGPNMB release after co-culture with 3 cell lines across 3 donors.** No transwells were used in these 3 donors; n= 3 HL cell lines, macrophages were co-cultured for 24 hours with HL CM or HL cells and macrophages and CM collected. Surface GPNMB expression measured by flow cytometry; sGPNMB release measured by ELISA. (A) Donor Y3 surface GPNMB expression (B) Donor Y3 sGPNMB release (C) Donor Z3 surface GPNMB expression (D) Donor Z3 sGPNMB release (E) Donor A4 surface GPNMB release (F) Donor A4 sGPNMB release.

## 4.4 Which cytokines are responsible for the induction of GPNMB expression in macrophages?

Having seen that GPNMB expression can be induced when macrophages were co-cultured with either CM alone and when transwells were used with 3 HL cell lines, I wanted to identify the cytokines responsible for this effect. A commercially available cytokine array kit (R&D) was used to test for 102 human cytokines in complete media supplemented with glutamax (RPMI-1640 + 10% FBS + 1X glutamax) compared to CM from L428, L1236 and L591 cell lines (harvested after 24 hours culture at $1x10^6$cells/ml). Each membrane represents a different sample/conditioned media (Figure 4.11 A, B and C). As a similar effect was seen in co-cultures with all 3 cell lines, I focussed on the top 5 cytokines present in all 3 CMs (Figure 4.11 B and D), which are shaded on the corresponding membrane diagram and intensities graphed. These were angiogenin, emmprin/ CD147, ICAM-1/CD54, MIF and CCL5.

I next wanted to determine which, if any, of these cytokines are responsible for inducing GPNMB expression in macrophages. Recombinant human angiogenin, emmprin, ICAM-1, MIF and CCL5 were cultured with M1 and M2 macrophages separately and all together for 24 hours; the effects were compared to HL cells or CM from all 3 cell lines (positive controls) (Figure 4.12). The cytokine control was 0.1% BSA/PBS (recombinant cytokine diluent). This experiment was only done once with 3 donors and requires further optimisation.

For M1 macrophages, all cytokines individually and combined appeared to induce GPNMB expression to a higher level than any of the HL CM or cell line controls. GPNMB expression was highest following culture with emmprin. In M2s, all cytokines individually and

combined induced GPNMB expression to high levels, similar to those seen by HL cell line/ CM co-culture. Emmprin and MIF induced highest levels of GPNMB expression, however, the cytokine control also induced GPNMB expression in M2s in 2 donors therefore the experiment would need to be repeated to further explore this.

## 4.5 Summary

In this chapter, I have shown the following:

- GPNMB expression is induced by polarisation of human monocytes to macrophages in vitro and sGPNMB is detectable in the conditioned media of these polarised M1 and M2 macrophages
- There was no significant difference in GPNMB expression levels of M1 vs M2 macrophages
- Co-culture of M1 and M2 macrophages with CM from cHL cell lines or directly with Hodgkin cells induced polarisation of M1 to M2 macrophages and further polarisation of M2 macrophages, however co-culture using transwells did not have the same effect on macrophage polarisation
- Co-culture of M1 and M2 macrophages with CM or cHL cell lines (via transwell or direct co-culture) significantly induced surface expression of GPNMB in both M1 and M2 macrophages
- Cytokines which may be responsible for induction of GPNMB expression include CD147, CD54, MIF, CCL5 and angiogenin as identified by a cytokine array of cHL CM but these need to be studied in further detail

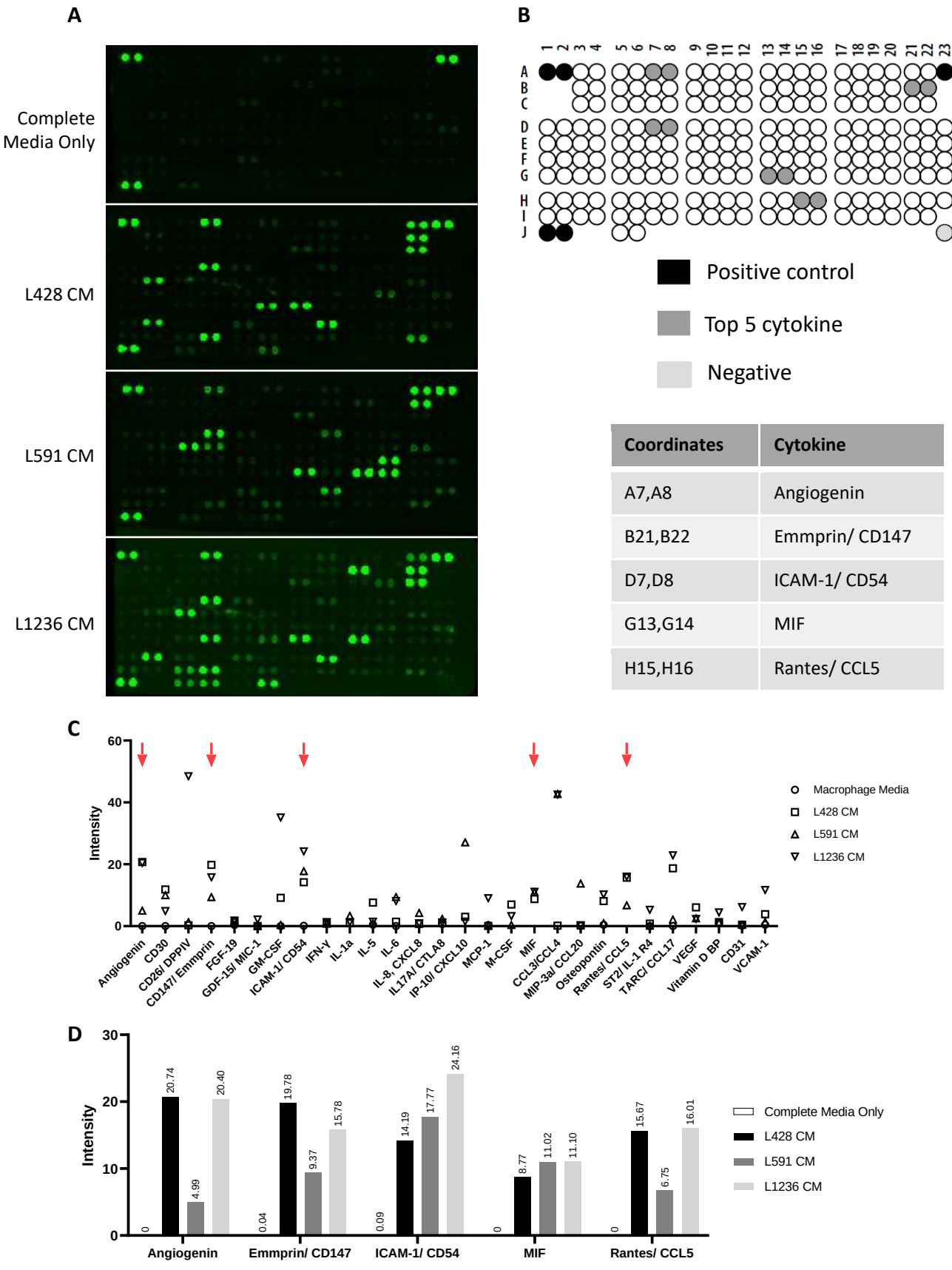


| Coordinates | Cytokine |
|---|---|
| A7,A8 | Angiogenin |
| B21,B22 | Emmprin/ CD147 |
| D7,D8 | ICAM-1/ CD54 |
| G13,G14 | MIF |
| H15,H16 | Rantes/ CCL5 |

**Figure 4.11 Cytokine array of HL CM looking at 102 different human cytokines.** (A) Each pair of dots represents one cytokine in duplicate. The brighter the intensity the higher the level of cytokine in CM. (B) Positive and negative controls marked on diagram. The 5 most highly expressed cytokines present in all 3 HL cell line CM are shaded for comparison with each membrane and corresponding names of these are listed. (C) All cytokines present in the HL CMs. Red arrows represent the top 5. (D) Intensity of each pair of dots for these 5 cytokines was measured in all CM.

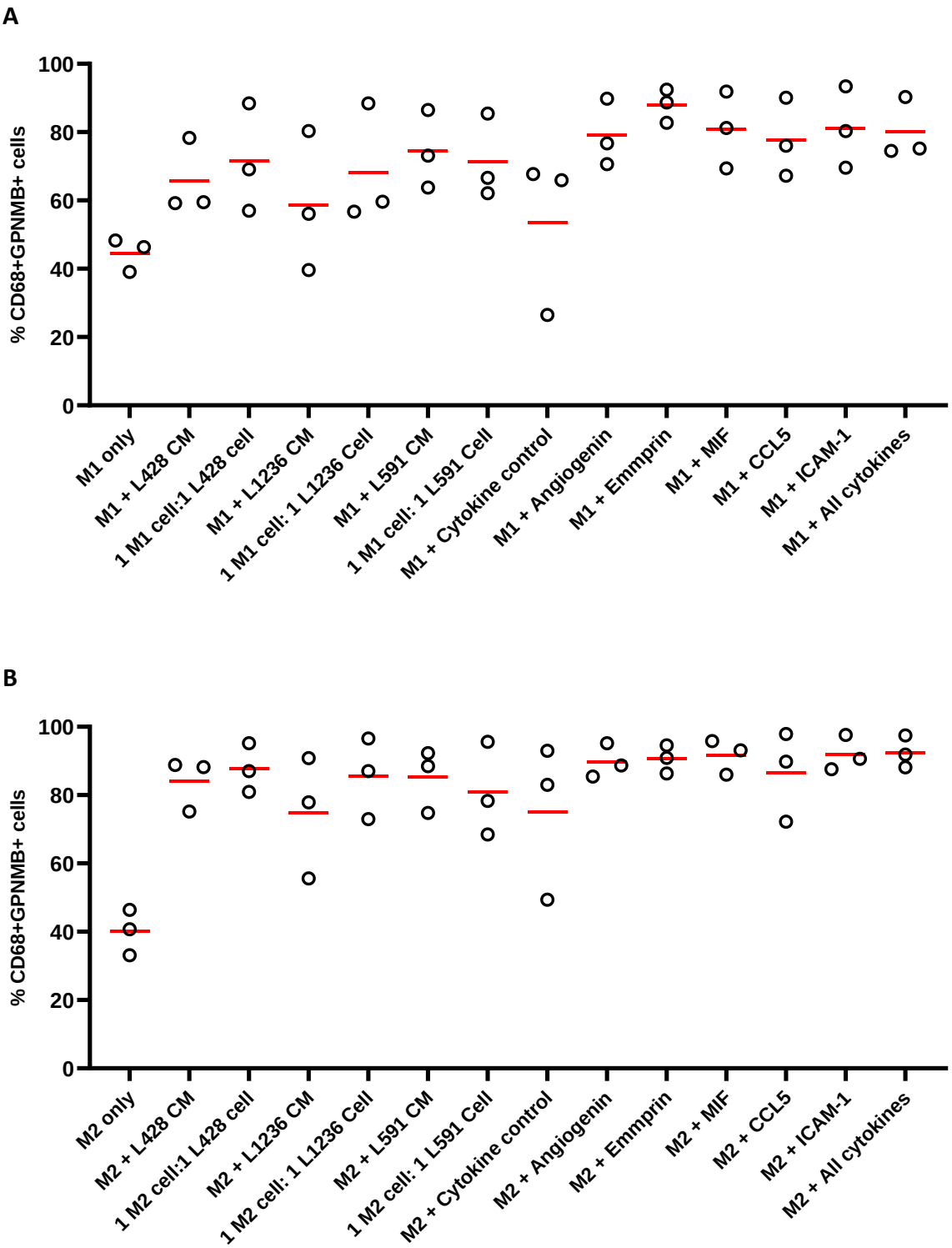


**Figure 4.12 Recombinant cytokine culture with macrophages.** 3 donor macrophages cultured with GM-CSF or MCSF for 7 days; followed by: (A) M1 co-culture with 3 HL cell lines or CM (positive controls) and recombinant human cytokines separately or all together. (B) M2 co-culture with 3 HL cell lines or CM (positive controls) and recombinant human cytokines separately or all together.

# CHAPTER 5

## GPNMB BLOCKS T-CELL ACTIVATION AND T-CELL RECOGNITION OF EBV-SPECIFIC EPITOPES

# Chapter 5 GPNMB blocks T-cell activation and T-cell recognition of EBV-specific epitopes

## 5.1 Introduction

GPNMB has previously been suggested to act by inhibiting T-cell activation (Chung et al., 2007b, Chung et al., 2009, Chung et al., 2013). The Ariizumi group suggested that GPNMB inhibits activation of already activated T-cells (but not resting T-cells). These experiments were initially done in mice, on the basis that GPNMB in mice and humans share 70% amino acid sequence homology, therefore this pathway would likely be functional in humans too. Later this was confirmed in human T-cells. They observed that immobilised GPNMB (5µg/ml) blocked T-cell activation whereas soluble GPNMB, when used at concentrations between 2.6-20µg/ml, did not (Chung et al., 2007b).

The aims of this chapter are to: 1) study if GPNMB influences T-cell activation *in vitro;* 2) Explore if any effects seen can be reversed using a specific neutralising antibody; 3) Determine if macrophage-derived GPNMB can block T-cell activation, and 4) study if GPNMB can block T-cell recognition of EBV-latent gene derived epitopes in HL cells.

## 5.2 Optimisation of T-cell activation assays

Initially, I used anti-human functional grade CD3 and CD28 antibodies (microplate wells coated with CD3 antibody and soluble CD28 antibody) to achieve suboptimal activation of T-cells within PBMCs. Activation was measured as the percentage of $CD3^{+}CD69^{+}$ cells by flow cytometry (Figure 5.1 A and B) and interferon-γ release by ELISA. However, I noticed variability in the levels of activation between experiments represented as donor 1 and donor 2. No

difference in the percentage of $CD3^+CD69^+$ cells was seen in 'donor 1' but was observed in 'donor 2' using the same activation method (Figure 5.1 A). I also saw variability in the activation of T-cells from the same donor using the same activation method (Figure 5.1 B).

Therefore, in subsequent experiments, a combined soluble CD3/CD28 activator was used to achieve more consistent T-cell activation. Interferon-γ release by activated T-cells was chosen to be the most appropriate read-out given that it was less time consuming and more suited to higher throughput analysis.

### 5.2.1 Syndecan-4

Syndecan-4 is a transmembrane heparan-sulphate-bearing proteoglycan, and the only identified ligand for GPNMB, found by the Ariizumi group to be upregulated on activated (but not resting) T-cells (Chung et al., 2007b, Chung et al., 2007a). I had attempted to further explore the syndecan-4- GPNMB interaction and syndecan-4 expression during T-cell activation and expression in cHL. I tried optimising several anti-syndecan-4 antibodies using IHC, western blotting and flow cytometry (Santa Cruz, R&D and Sigma) under various experimental conditions to detect the protein (including activating T-cells); unfortunately none of the antibodies were specific enough to detect the protein and therefore I did not investigate this further (Figure 5.2)

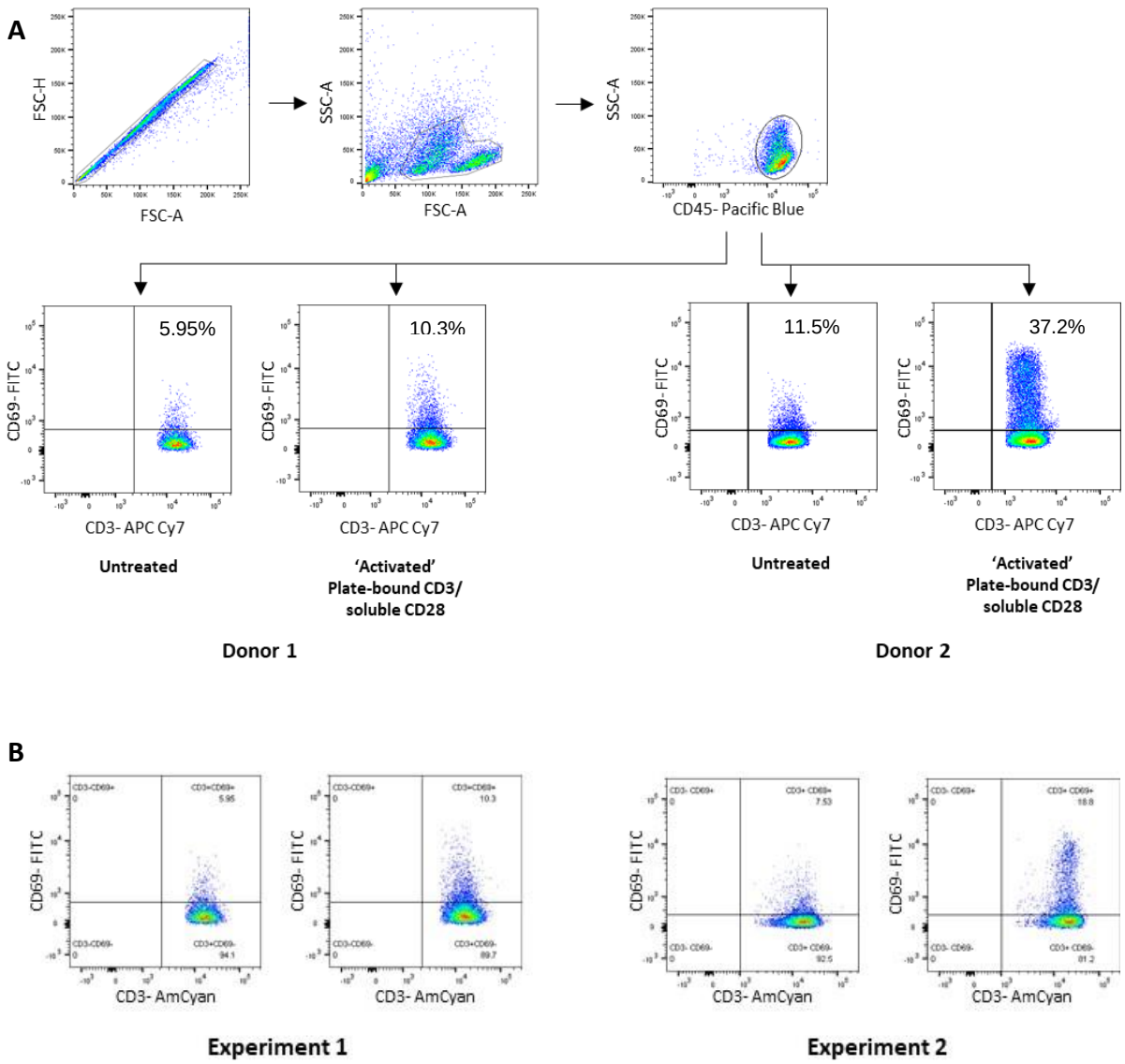


**Figure 5.1. Variation in T-cell activation by flow cytometry.** Gating strategy- upper panel shows the gating strategy to obtain live CD45+ cells. Lower panels show 2 representative donors, showing levels of CD69 in CD3 + cells. Figure shows that the addition of CD3 and CD28 antibodies resulted in an increased number of CD69+ cells indicating activation of the T-cell. This figure illustrates the observed variation in T-cell activation between donors. (A) Anti-human functional grade CD3 (OKT3) antibody (bound to microplate well) and CD28 antibodies (soluble) used to activate T-cells. Activation measured as the percentage of $CD3^{+}CD69^{+}$ cells by flow cytometry (seen here) and interferon-γ release by ELISA. Variability in activation was observed between experiments (represented as donor 1 and donor 2); no difference in % of $CD3^{+}CD69^{+}$ cells was seen in 'donor 1' but was seen in 'donor 2' using the same activation method. (B) Variation in activation was also observed within the same donor using plate-bound CD3 antibody and soluble CD28 antibody as above.

A

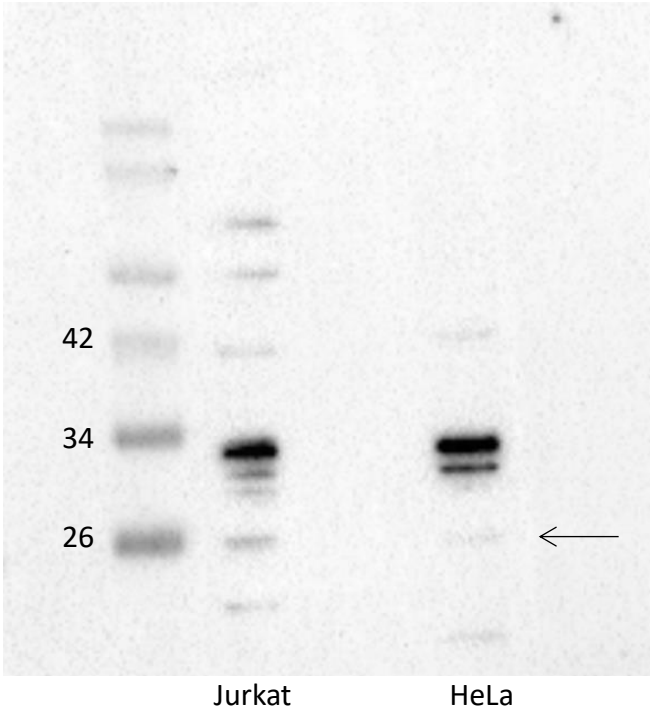


B

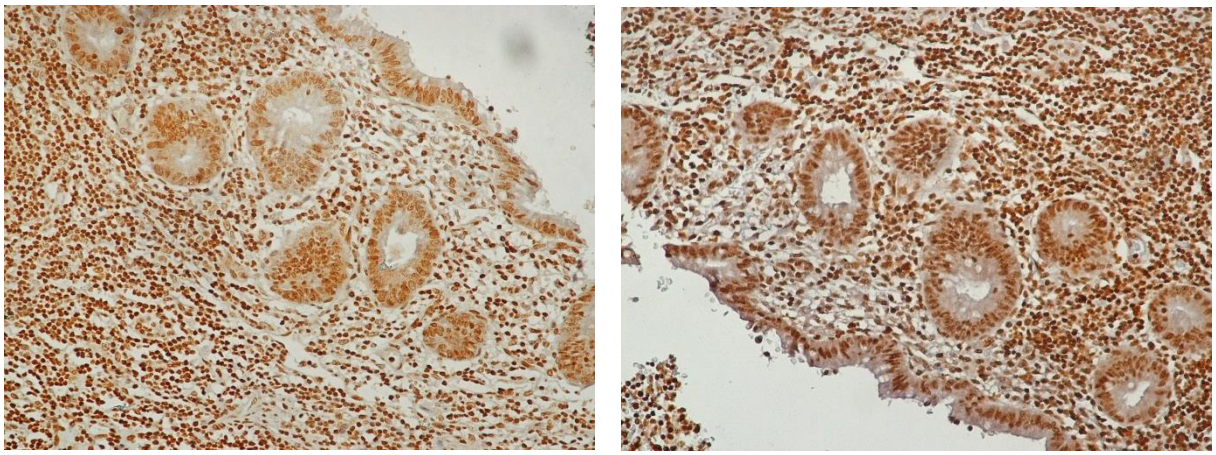

**Figure 5.2. Optimisation of anti-Syndecan-4 antibodies.** (A) Western blot of Jurkat and HeLa cell lysates using anti-Syndecan-4 (5G9) antibody (Santa Cruz sc-12766). HeLa cell lysate was the positive control, expected protein size 24kDa (arrow) (B) IHC of appendix (positive control) stained with anti-Syndecan-4 antibody (Sigma HPA005716) using two antigen retrieval methods: Citric acid antigen retrieval, pH 6.0 (left) vs. EDTA antigen retrieval, pH 9 (right). Using both methods there was non-specific staining and high background staining.

## 5.3 GPNMB blocks T-cell activation *in vitro*

### 5.3.1 Recombinant GPNMB (rGPNMB) blocks T-cell activation

Initial experiments were done using the activation method described in Figure 5.1 A and B (plate-bound anti-CD3 Ab and soluble anti-CD28 Ab); T-cell activation was measured as the percentage of CD3+CD69+ PBMCs (by flow cytometry) and interferon-γ release by ELISA. rGPNMB at varying concentrations (1.25-10μg/ml) was added to determine the effect of these treatments on T-cell activation. To show that the effect was specific to rGPNMB, once rGPNMB was added to cell media, this was then removed using a rabbit anti-human GPNMB Ab and MACs magnetic separation microbeads (Anti-Rabbit IgG microbeads, Miltenyi Biotec) to make 'GPNMB deplete media,' and either this or rGPNMB-containing media were added to PBMCs for 24 hours (Figure 5.3).

At all concentrations of rGPNMB (1.25μg/ml-10μg/ml) used, I observed a reduction in the percentage of CD3+CD69+ PBMCs, but when 'GPNMB-deplete' media was added, the percentage of CD3+CD69+ PBMCs increased to a level greater than the control activated T-cells, indicating that this effect was specific to rGPNMB. Corresponding levels of interferon-γ from the same samples did not show the same effect, except at 10μg/ml of rGPNMB (but interferon-γ levels were not very high in these experiments) (Figure 5.3).

This initial experiment showing an effect of rGPNMB on T-cell activation prompted me to investigate this further.

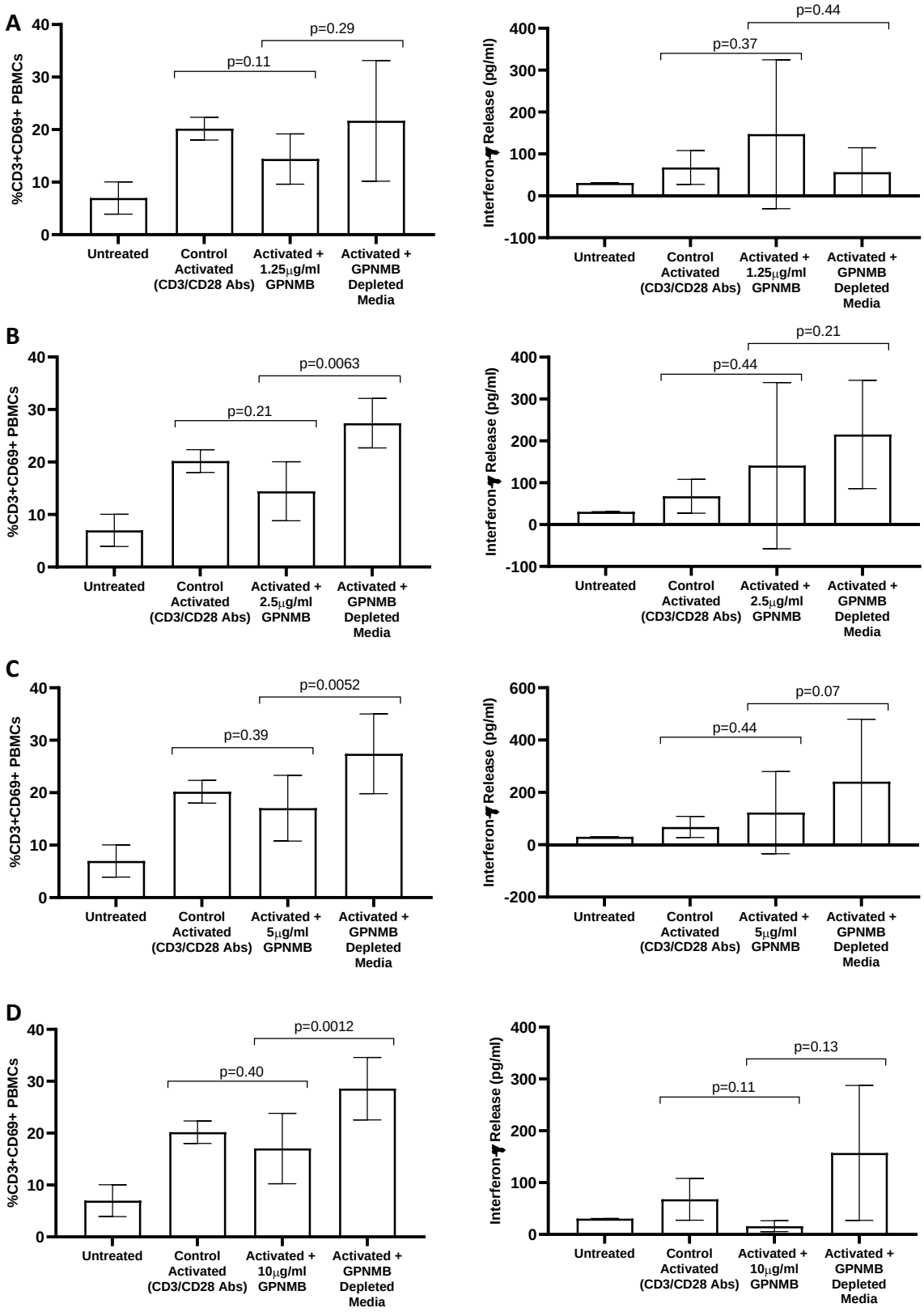


**Figure 5.3. GPNMB specifically blocks T-cell activation.** Left $CD3^{+}CD69^{+}$ cells measured by flow cytometry. Right- interferon-γ production measured by ELISA. (A) 1.25μg/ml GPNMB. (B) 2.5μg/ml GPNMB. (C) 5μg/ml GPNMB. (D) 10μg/ml GPNMB. Mean of 3 separate experiments. Paired t-tests applied.

### 5.3.2 Recombinant GPNMB (rGPNMB) blocks T-cell activation in the majority of healthy donors

In initial experiments, I had seen variability in amount of T-cell activation using bound anti-CD3 Ab and soluble anti-CD28 Ab. In subsequent experiments, soluble CD3/CD28 activator was used (as in Figure 5.1 C). I had also observed inter-donor variation in the levels of activation when trying to titrate the amount of soluble CD3/CD28 activator to use, and as also might be expected, inter-donor variation in the degree of T-cell activation response after adding rGPNMB. To evaluate the inter-donor variability seen in both amount of CD3/CD28 activator needed and also effect of varying concentrations of rGPNMB on T-cell activation, PBMCs were isolated and tested from 10 healthy donors; 6 concentrations of soluble CD3/CD28 activator were used (0.25µl/ml-5µl/ml) (Figure 5.3); 3 concentrations of rGPNMB were used, having titrated the dose down in other experiments (five-fold dilutions from 0.04µg/ml to 1µg/ml).

T-cell activation for all 10 donors is shown in Figure 5.4, measured as interferon-γ release vs relative interferon-γ (each donor normalised to its own 'baseline' level of activation in the Vehicle). It can be seen that the amount of CD3/CD28 activator required to stimulate T-cells is donor-dependent. I was aiming for 'sub-optimal' T-cell activation for the response to be as close to a physiological response as possible.

Figure 5.5 shows each donor's individual response to rGPNMB following activation at all concentrations of activator. Figure 5.6 A-F shows the response from all 10 donors to all concentrations of rGPNMB, plotted by increasing dose of CD3/CD28 activator so all donors

can be compared to each other. Figure 5.6 G shows the mean interferon-γ release across all 10 donors at each concentration of activator.

The lowest concentration of rGPNMB tested (0.04µg/ml) significantly blocks T-cell activation at 3 concentrations of CD3/28 activator (0.5µl/ml, 1µl/ml and 5µl/ml) across all donors, and rGPNMB 1µg/ml significantly blocks T-cell activation at 0.5µl/ml of CD3/28 activator (paired t-tests applied) (figure 5.6 A-F). When the means from all donors are plotted at each concentration of CD3/28 activator, blocking of T-cell activation is significant at all concentrations, but is most significant at 0.04µg/ml (Figure 5.6G).

The overall response to rGPNMB is a blocking of T-cell activation at doses as low as 0.04µg/ml, but this response is donor-dependent. Some donors do not respond as well as others and for some donors, when the level of activation is very high, this blocking of T-cell activation is not as effective as at the lower levels of activation and is sometimes overcome by higher doses of rGPNMB.

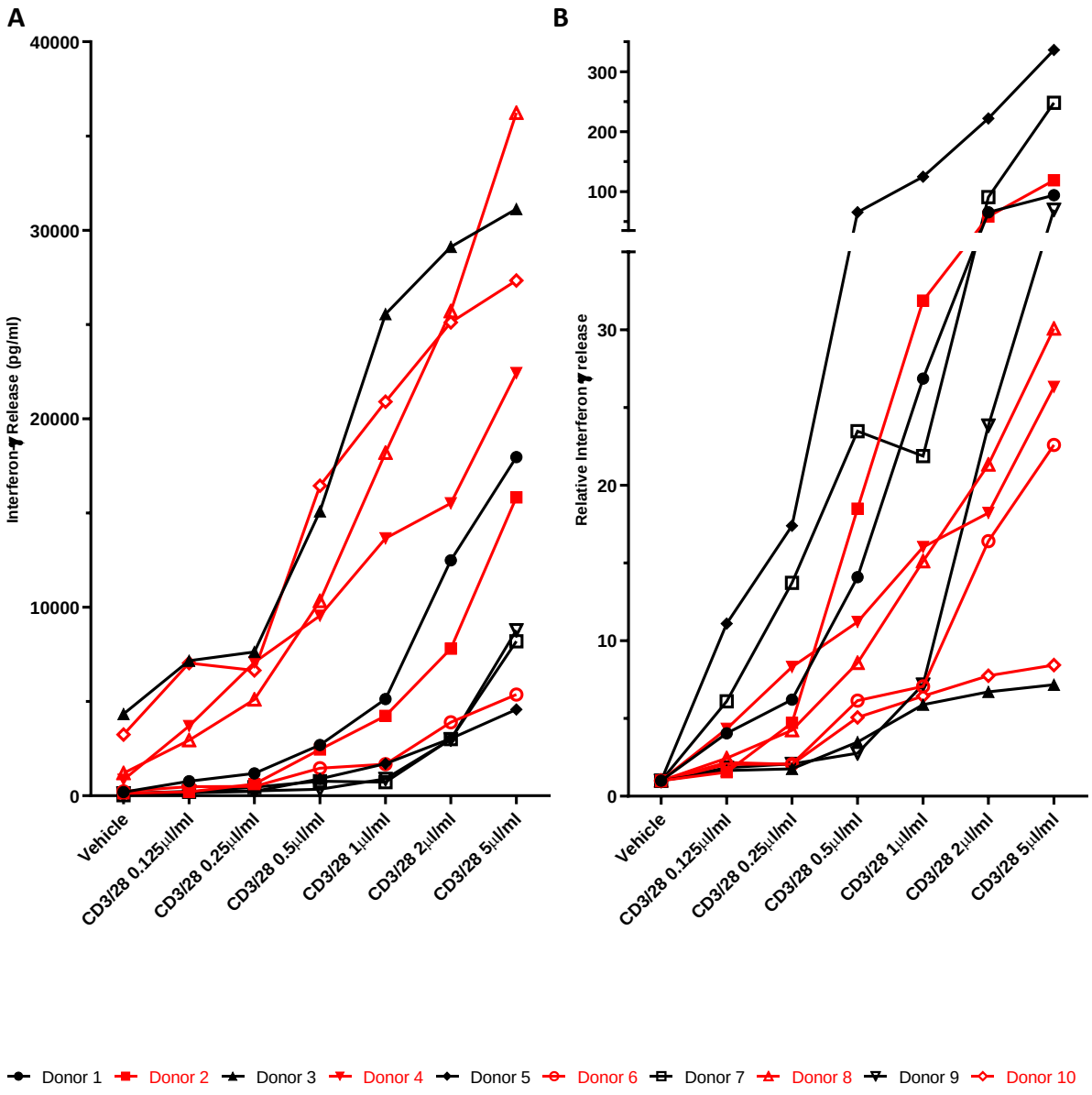


**Figure 5.4 T-cell activation in healthy donors.** (A) Raw interferon- γ production and (B) Relative Interferon-γ production by 10 healthy donors upon activation with different concentrations of CD3/28 activator, aiming to achieve sub-optimal activation.

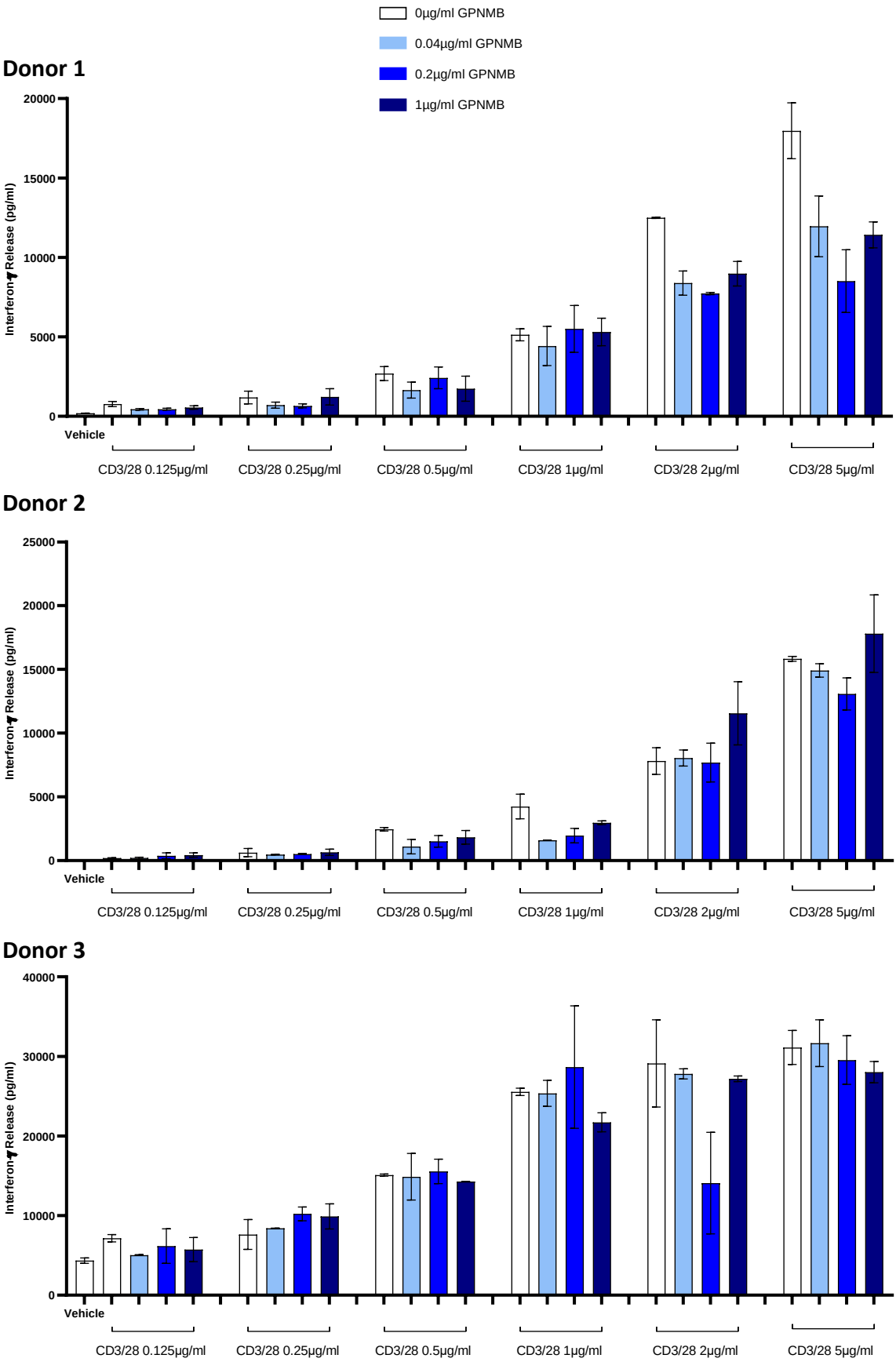


**Figure 5.5. GPNMB blocks T-cell activation in most healthy donors.** Donors 1-3

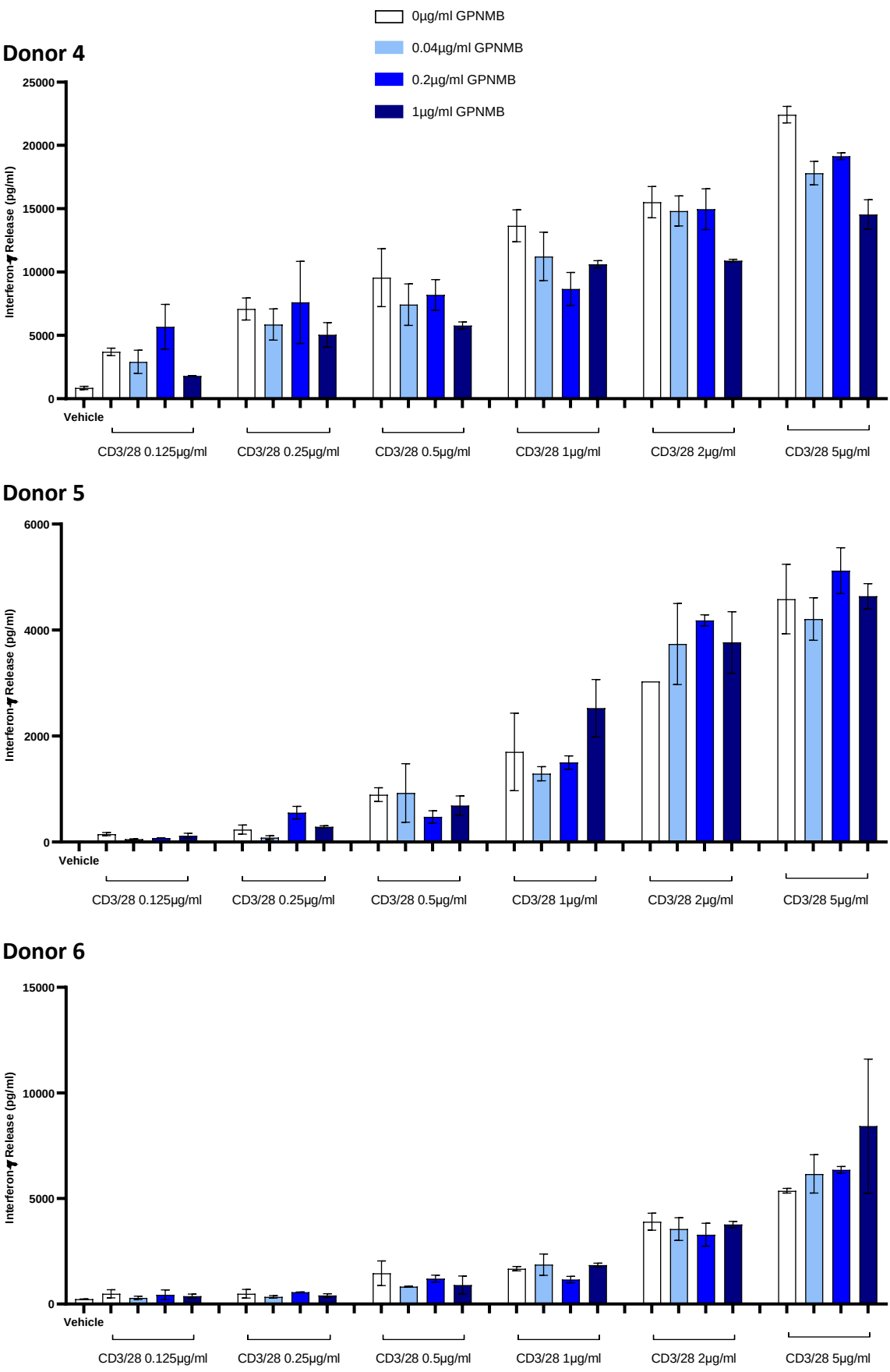


**Figure 5.5. GPNMB blocks T-cell activation in most healthy donors.** Continued. Doors 4-6

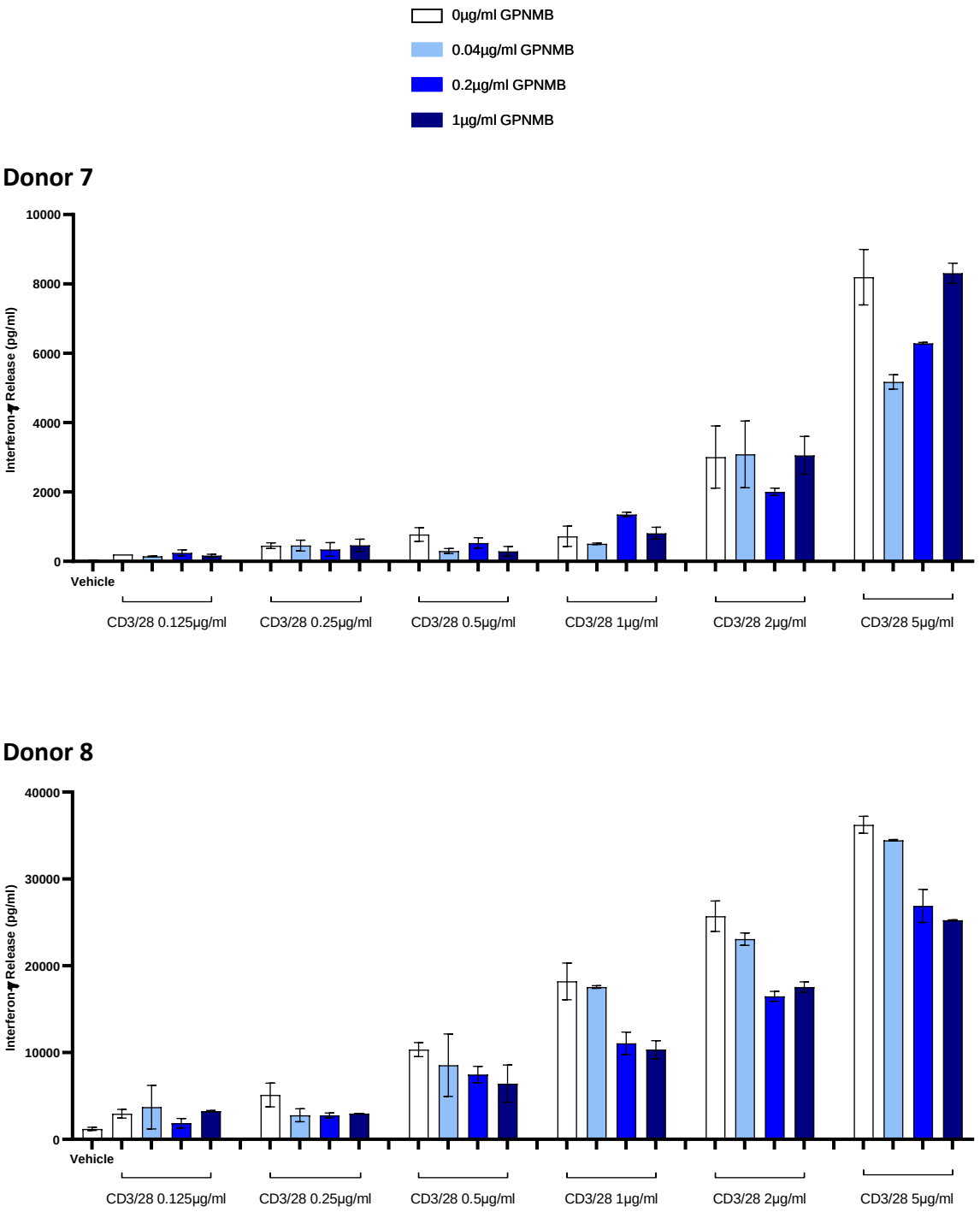


**Figure 5.5. GPNMB blocks T-cell activation in most healthy donors.** Continued. Donors 7-8

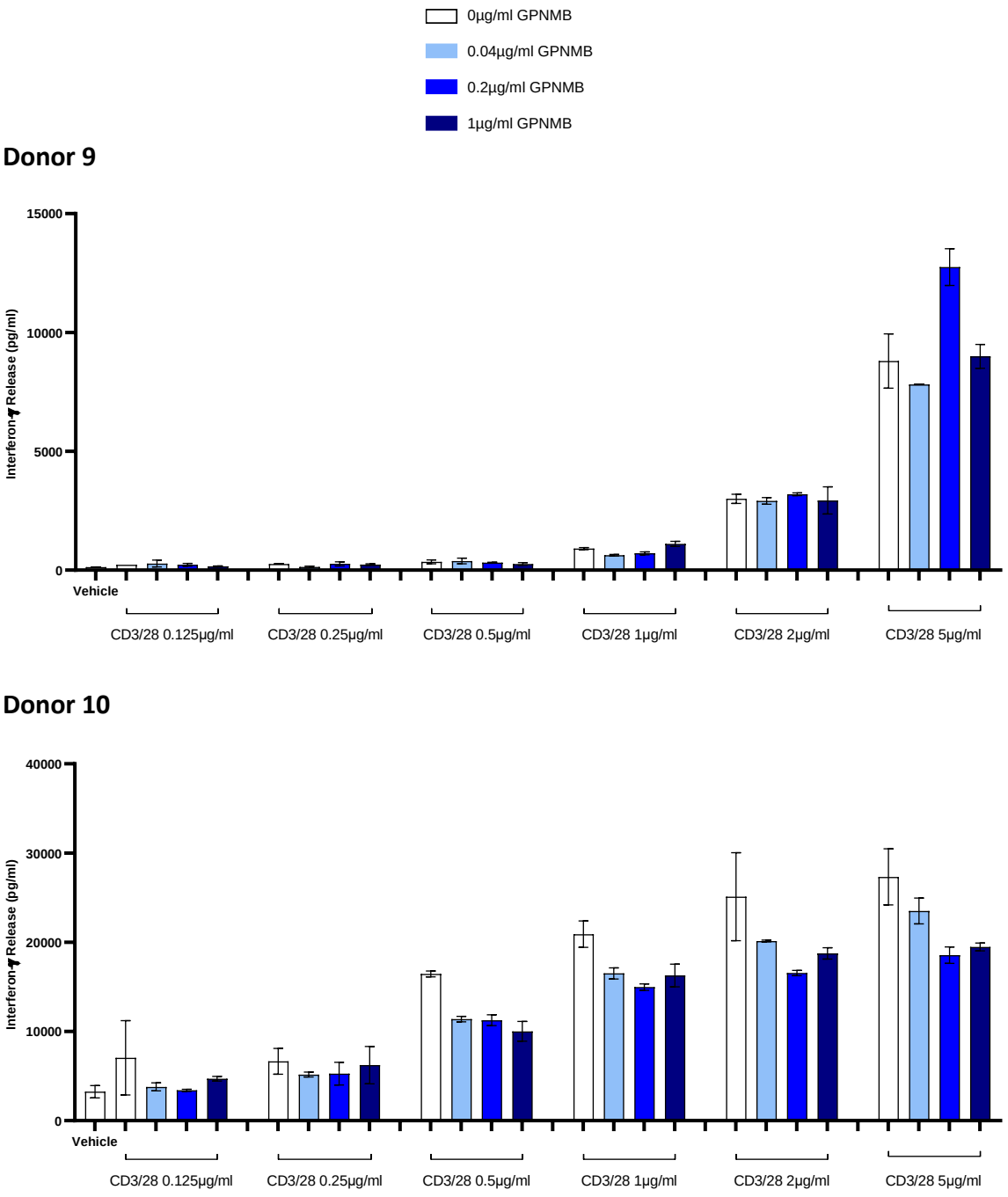


**Figure 5.5. GPNMB blocks T-cell activation in most healthy donors.** Continued. Donors 9-10

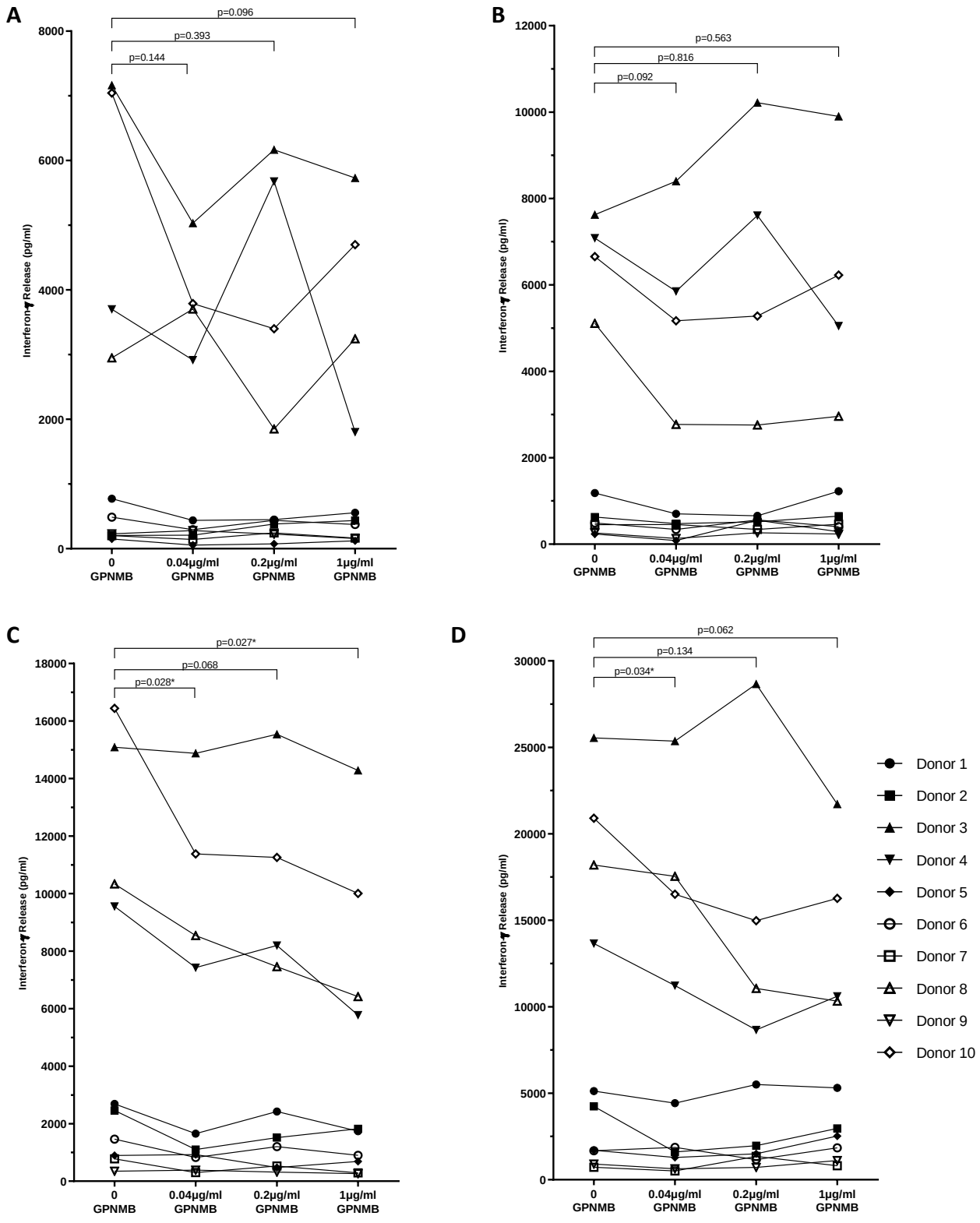


**Figure 5.6 Effect of GPNMB on T-cell activation in 10 donors at multiple concentrations of CD3/28 activator** (A) 0.125µl/ml CD3/28 activator (B) 0.25µl/ml CD3/28 activator (C) 0.5µl/ml CD3/28 activator (D) 1µl/ml CD3/28 activator.

Continued on next page.

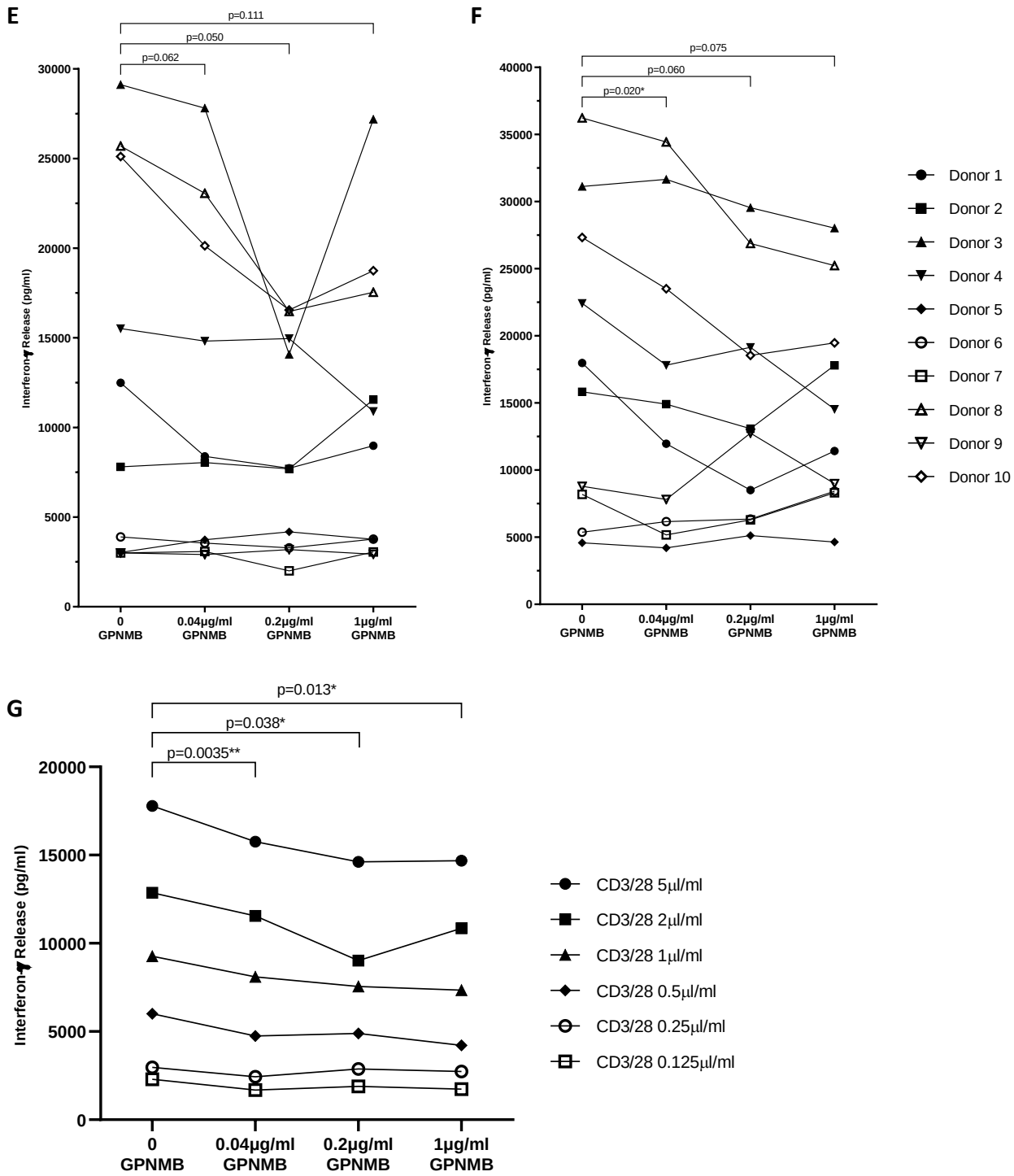


**Figure 5.6 Effect of GPNMB on T-cell activation in 10 donors at multiple concentrations of CD3/28 activator** continued. (E) 2µl/ml CD3/28 activator (F) 5µl/ml CD3/28 activator (G) Mean from all donors at each concentration of activator. The lowest concentration of rGPNMB tested (0.04µg/ml) significantly blocks T-cell activation at 3 concentrations of CD3/28 activator across all donors, and rGPNMB of 1µg/ml significantly blocks T-cell activation at 0.5µl/ml of CD3/28 activator (measured by interferon-γ release, paired t-tests applied). When the mean from all donors is plotted at each concentration of CD3/28 activator, blocking of T-cell activation is significant at all concentrations.

## 5.4 Anti-GPNMB antibody prevents inhibition of T-cell activation *in vitro*

Having shown that rGPNMB can block T-cell activation in vitro, I wanted to see if an anti-GPNMB antibody could prevent this inhibition. I used PBMCs from one of the donors above (Donor 5, where cells were known to activate and respond to rGPNMB), 1μg/ml of CD3/CD28 activator and 0.04μg/ml rGPNMB. I tested 5 commercially available anti-human GPNMB antibodies (Table 5.1). None of them were previously tested or sold as 'neutralising' antibodies so all were tested for neutralising ability at 2 doses (0.5μg/ml and 5μg/ml).

Antibody 1 was effective at preventing inhibition of T-cell activation and a significant increase in interferon-γ release was seen at both concentrations of anti-GPNMB antibody (unpaired t-test) (Figure 5.7 A). Antibody 3 did have an effect at 5μg/ml but there was a decrease in interferon-γ production in the control (Figure 5.7 C). Antibody 4 was the most effective at preventing inhibition of T-cell activation and the result was significant at both doses (Figure 5.7 D). Not only that, but at both concentrations, activation was much higher than in the controls after addition of this antibody (Figure 5.7D).

So far, I have only tested these antibodies on one donor. They need to be tested on more donors to confirm the effect seen by antibody 4. I would also use an isotype control when repeating the experiment.

| | |
|---|---|
| Antibody 1 | MAB2550 (R&D Mouse Monoclonal Clone #303802) |
| Antibody 2 | AF2550 (R&D Goat Polyclonal) |
| Antibody 3 | ab56584 (Abcam Mouse Monoclonal) |
| Antibody 4 | ab175427 (Abcam Mouse Monoclonal [7C10E5]) |
| Antibody 5 | ab125898 (Abcam Rabbit Polyclonal) |

**Table 5.1 Anti-Human GPNMB Antibodies**

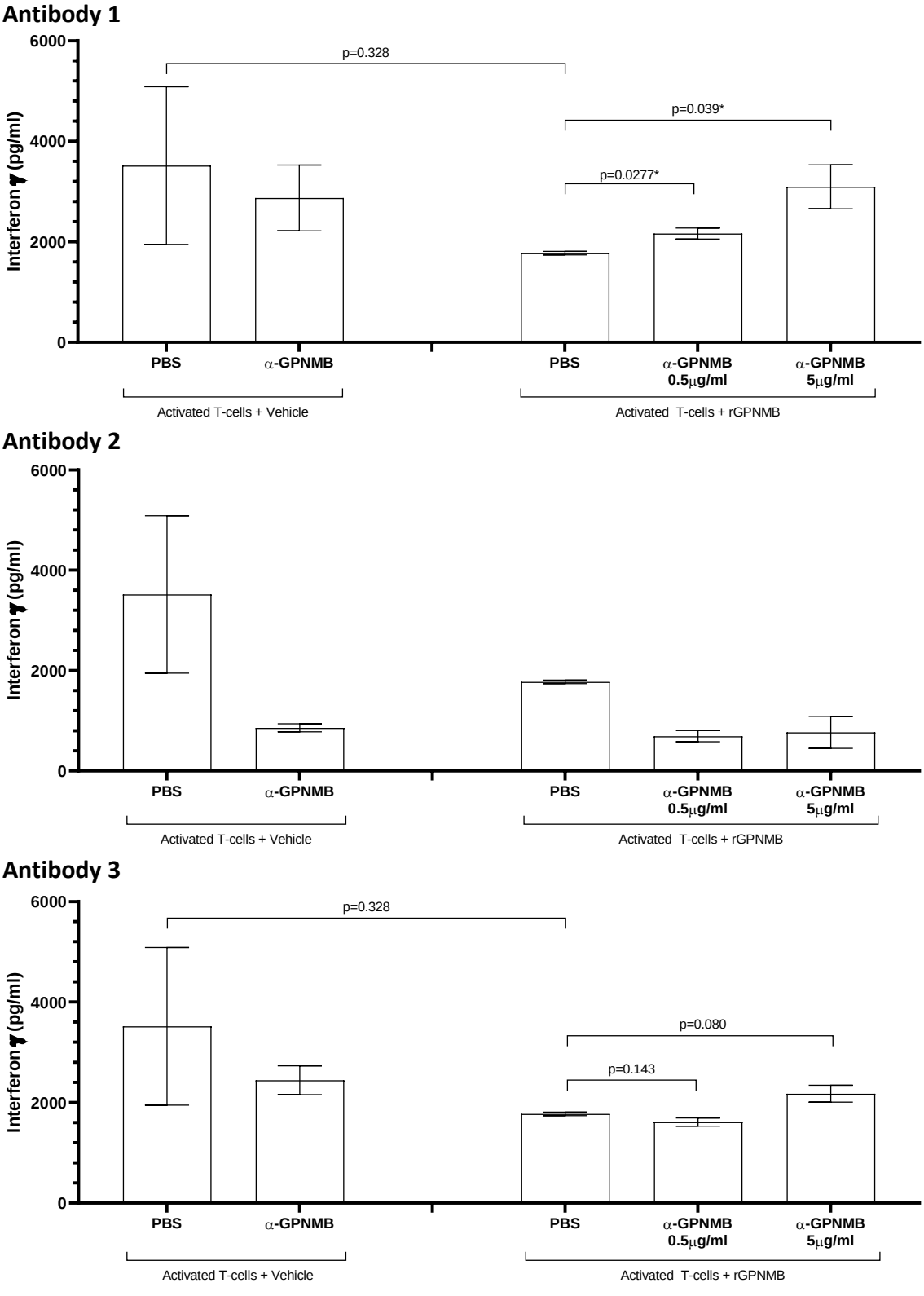


**Figure 5.7 Anti-GPNMB antibody prevents inhibition of T-cell activation by GPNMB.** 5 different anti-human GPNMB antibodies were tested for their ability to prevent inhibition of T-cell activation *in vitro* (Table 5.1). Activated T-cells (PBMCs) were treated with PBS (vehicle) or anti-GPNMB antibody alone (control); then with 0.04μg/ml rGPNMB + PBS (vehicle) or 2 concentrations of each anti-GPNMB antibody. Antibody 1 did significantly prevent inhibition of T-cell activation. Antibody 3- there was some prevention of inhibition at the higher dose of this antibody (unpaired t-tests used).

**Antibody 4**

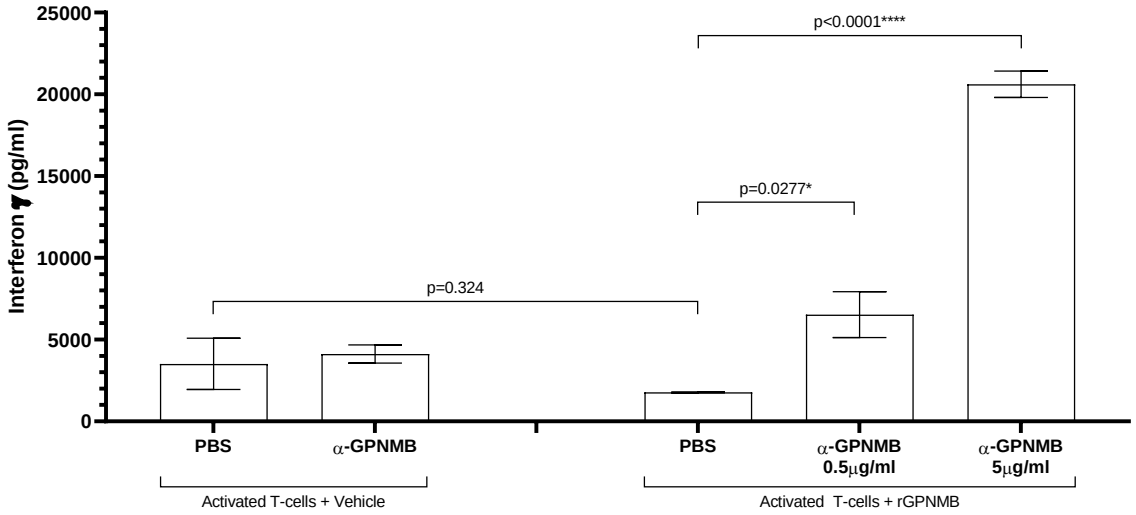


**Antibody 5**

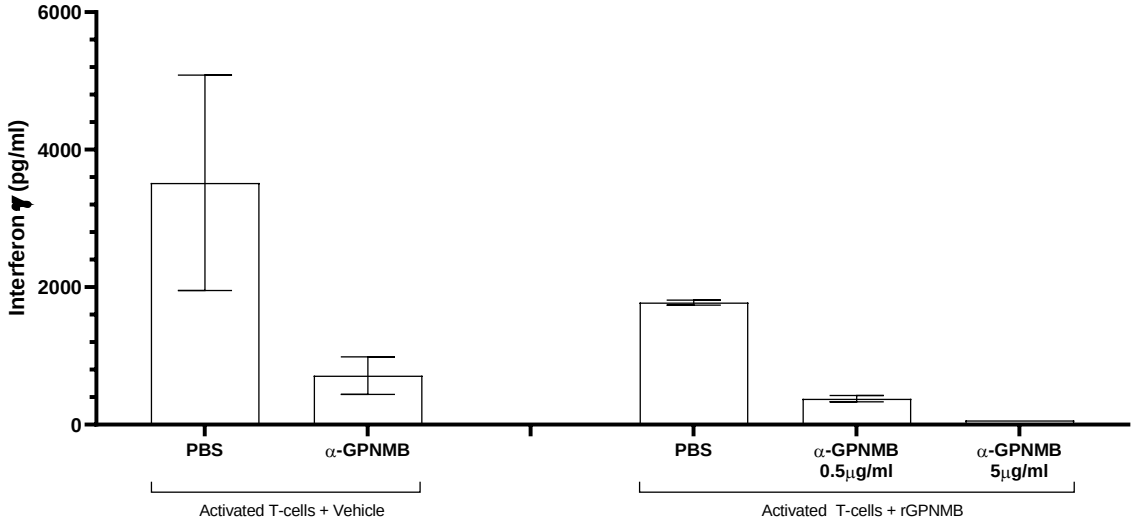


**Figure 5.7 Anti-GPNMB antibody prevents inhibition of T-cell activation by GPNMB.** Continued. 5 different anti-human GPNMB antibodies were tested for their ability to prevent inhibition of T-cell activation *in vitro* (Table 5.1). Activated T-cells (PBMCs) were treated with PBS (vehicle) or anti-GPNMB antibody alone (control); then with 0.04μg/ml rGPNMB + PBS (vehicle) or 2 concentrations of each anti-GPNMB antibody. Antibody 4 was the most effective neutralising antibody. It prevented inhibition of T-cell activation significantly (unpaired t-tests used).

## 5.5 Does macrophage-derived GPNMB block T-cell activation?

In chapter 4, I showed that CD14+- derived M1 or M2 macrophages express GPNMB on their cell surface (by flow cytometry), at RNA level and also release sGPNMB into their CM. I wanted to see if macrophage-derived GPNMB would be able to block T-cell activation in PBMCs from matched donors. To do this, I performed a preliminary experiment using three donors.

PBMCs were isolated and CD14+ cells differentiated into M1 or M2 macrophages (grown on 24-well plates), then matched CD14- PBMCs were added to these cells with CD3/CD28 activator (0.25µl/ml, 0.5µl/ml and 1µl/ml) to see if macrophage-derived GPNMB could block activation in a similar way to 0.04µg/ml rGPNMB (control) (Figure 5.8).

In donor 11, there was blocking of activation by rGPNMB, and also by M1 and M2 macrophage-derived GPNMB. In donor 12, the initial level of activation was not that high, but no response was seen in the control (rGPNMB) or with M2-derived GPNMB, but there was some blocking with M1-derived GPNMB. In donor 13, baseline activation was low, but then there was an increase in activation seen in all groups (Figure 5.8).

More donors need to be tested to further evaluate this.

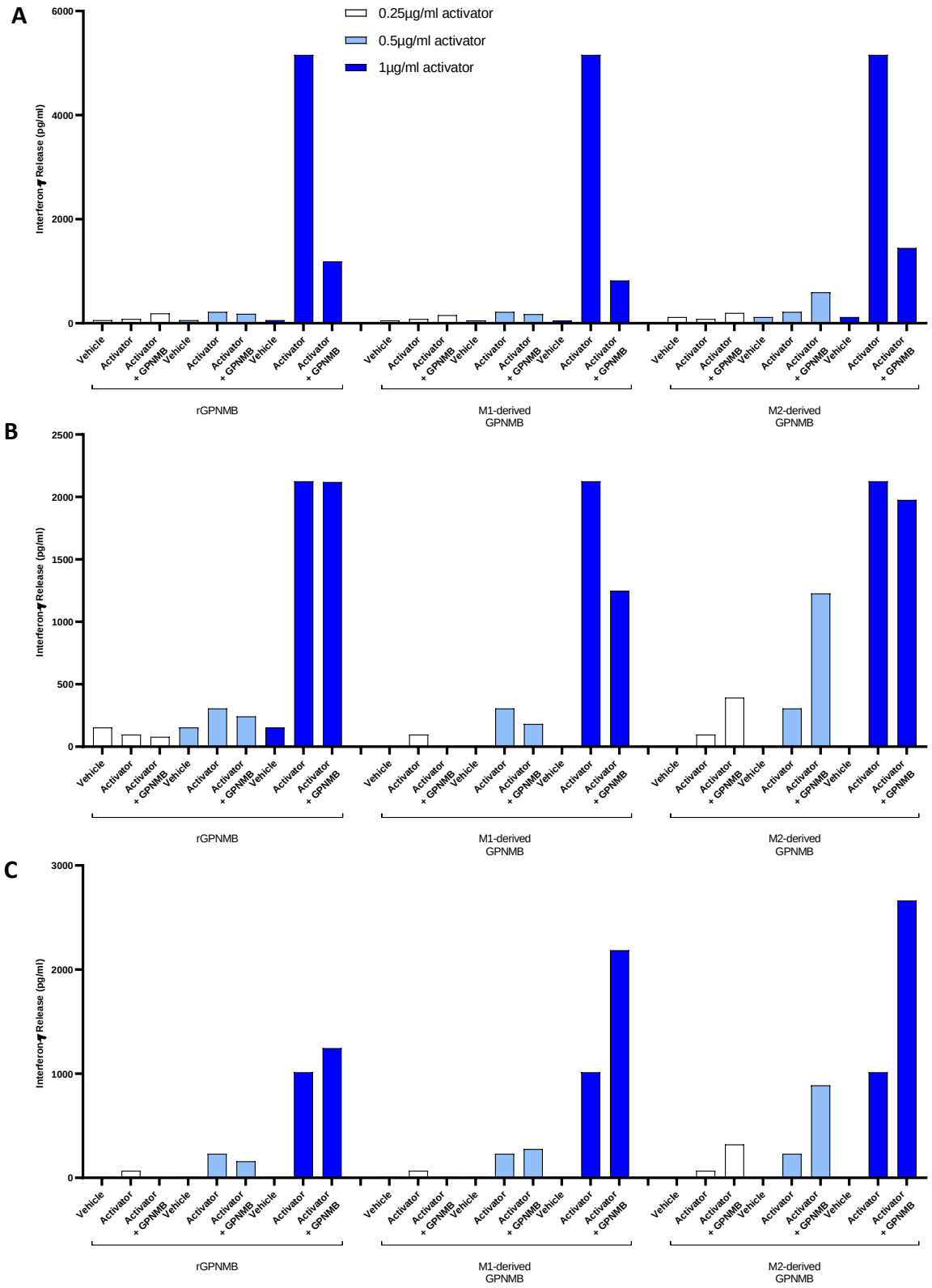


**Figure 5.8 Effect of Macrophage-derived GPNMB on 3 donors.** PBMCs from each donor were isolated, CD14+ cells differentiated into M1 or M2 macrophages in 24-well plates, then remaining PBMCs from that donor were activated (with 3 different concentrations of activator) and either rGPNMB (0.04µg/ml) added, or CD14- PBMCs co-cultured with M1 or M2 macrophages derived from the same donor (macrophage-derived GPNMB) (A) Donor 11 (B) Donor 12 (C) Donor 13

## 5.6 GPNMB blocks T-cell recognition of EBV-specific epitopes in Hodgkin lymphoma *in vitro*

Having assessed the effect of GPNMB on T-cell activation, next I wanted to look at the effect of GPNMB on cytotoxic T-lymphocyte (CTL) recognition of EBV-specific epitopes in HL *in vitro*., given that 40-50% of HL cases are EBV- positive.

The ability of HL cell lines to process and present EBV proteins to HLA- Class I- restricted EBV-specific CTL clones has previously been shown (Lee et al., 1998). Three of the HL cell lines used were EBV-negative (L1236, KMH2, L540) and so EBV proteins were expressed either by exposing the cells with modified vaccinia Ankara (MVA) recombinant expressing LMP2A (MVA-LMP2A) (which requires the HL cells to process and present the protein on their cell surface), or epitope peptide (which binds to class I HLA on the cell surface), or their respective controls- MVA-pSC11 (empty vector) or dimethyl sulfoxide (DMSO). As positive controls, LCLs matched by HLA-type were exposed to MVA-LMP2A or epitope peptide in the same way. HLA-mismatched LCLs were exposed to the same epitope peptide as a negative control. The HL cells or LCLs were the target cells, and epitope-specific CD8+ T-cell clones were used as effector cells (identified by the first 3 letters of the peptide sequence)- see Table 5.2 for full details of all cells used. L591 cell line is the only EBV-positive HL cell line so I also wanted to test this cell line. However, the cells may not have expressed the EBNA1 HPV epitopes to be recognised by the HLA-matched T-cell clones and therefore they were exposed to MVA-E1ΔGA (expresses EBNA1 protein with deleted GA-rich region; deletion of this region makes the protein easier to process), EBNA1 HPV peptide or their respective controls- MVA-pSC11 or

DMSO (Table 5.2). Interferon-γ release was used to measure CD8+ T-cell recognition of EBV proteins on HL cells or LCLs.

| HL Cell line | HLA Type(s) | HLA- Matched LCLs | T-cell clones |
|---|---|---|---|
| KMH2 | A11, A24, B51, B62 | LCL 1 (A11)<br>LCL 2 (A24) | SSC (A11-restricted epitope, LMP2 amino acids 340-350)<br>TYG (A24-restricted epitope, LMP2 amino acids 419-427) |
| L1236 | A2, B51 | LCL 3 (A2) | FLY (A2-restricted epitope, LMP2 amino acids 356-364)<br>CLG (A2-restricted epitope, LMP2 amino acids 426-434) |
| L540 | A3, A11, B51 | LCL 1 (A11) | SSC (A11-restricted epitope, LMP2 amino acids 340-350) |
| L591 | A1, A33, B8, B35 | LCL 1 (B35) | HPV clone 35 (B35.01-restricted epitope, EBNA1 amino acids 407-417)<br>HPV clone 41 (B35.01-restricted epitope, EBNA1 amino acids 407-417) |

**Table 5.2 HL cell lines, HLA-matched LCLs and T-cell clones**

Initially, all cell lines and LCLs were tested with all matched T-cell clones to test the response to relevant MVA virus (multiplicity of infections (MOI) of 10, 1 and 0.1 were used) and peptide to ensure they were all able to process and present EBV proteins which are recognised by the matched T-cell clones and to use those which responded the best in subsequent experiments. KMH2 cells and matched LCLs were recognised by both SSC and TYG t-cell clones (Figure 5.9). L540 cells and matched LCLs were recognised by SSC cells (Figure 5.10). L1236 cells and LCLs were recognised by FLY and CLG clones (Figure 5.11). There was very minimal recognition of L591 cells by both EBNA1 HPV clones (c35 and c41) compared to the matched LCL positive controls (Figure 5.12). Therefore, only LCLs and matched EBNA1 HPV clones were used in subsequent experiments.

Prior to testing if rGPNMB influences T-cell recognition of EBV-specific epitopes in HL, CM from a sample of HL cell lines, LCLs, T- cell clones (before and after exposure to MVA or peptide were tested to see if they expressed GPNMB (by ELISA). Very minimal amounts were detected in 2 of the samples (Figure 5.13).

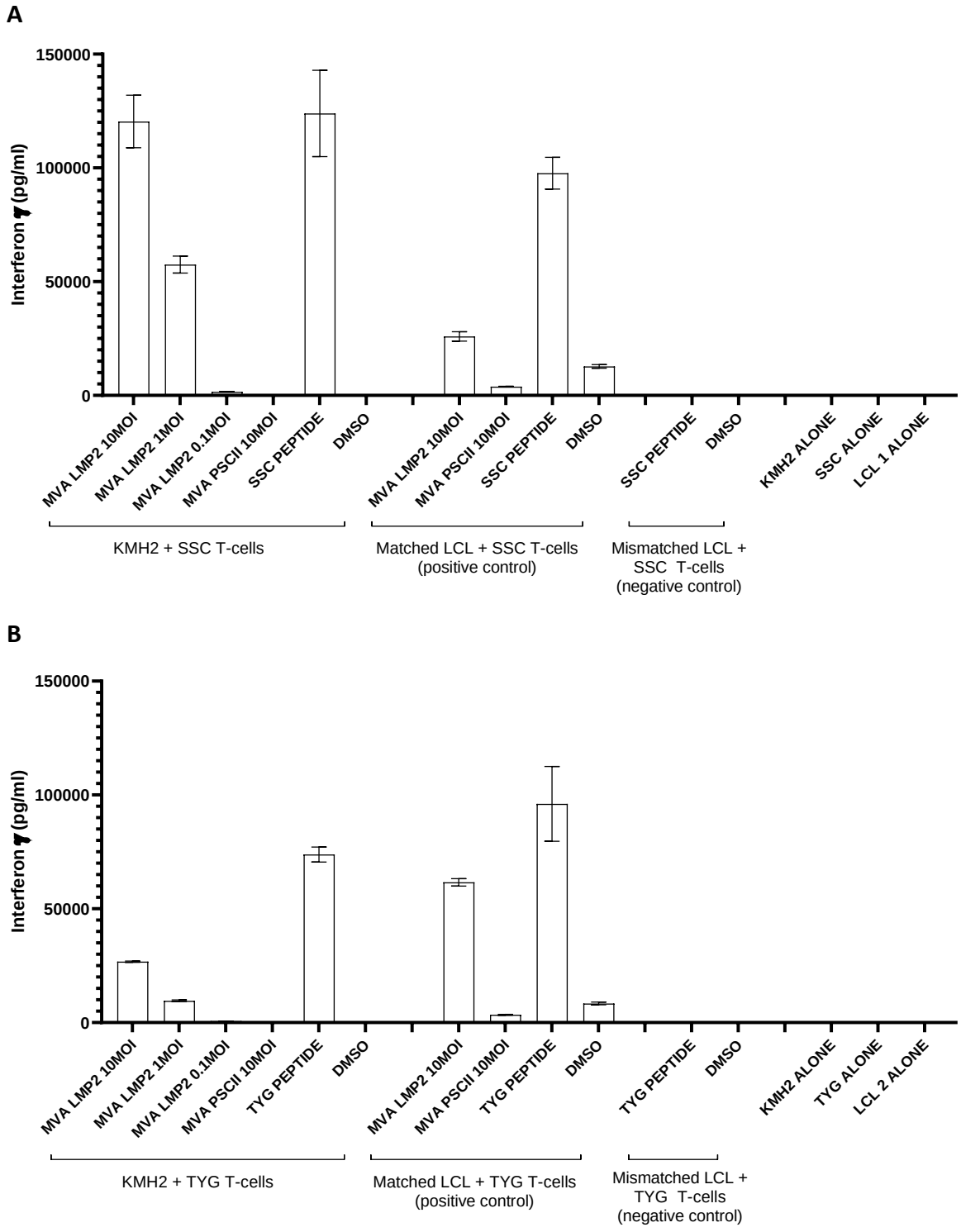


**Figure 5.9 Recognition of EBV-specific epitopes in KMH2 (a HL cell line) and matched LCLs by T-cell clones.** Initially, 4 HL cell lines were tested to assess recognition of EBV-specific epitopes by matched T-cell clones, along with corresponding LCLs and matched T-cell clones (positive controls). KMH2 and matched LCLs recognised by (A) SSC T-cell clones and (B) TYG T-cell clones.

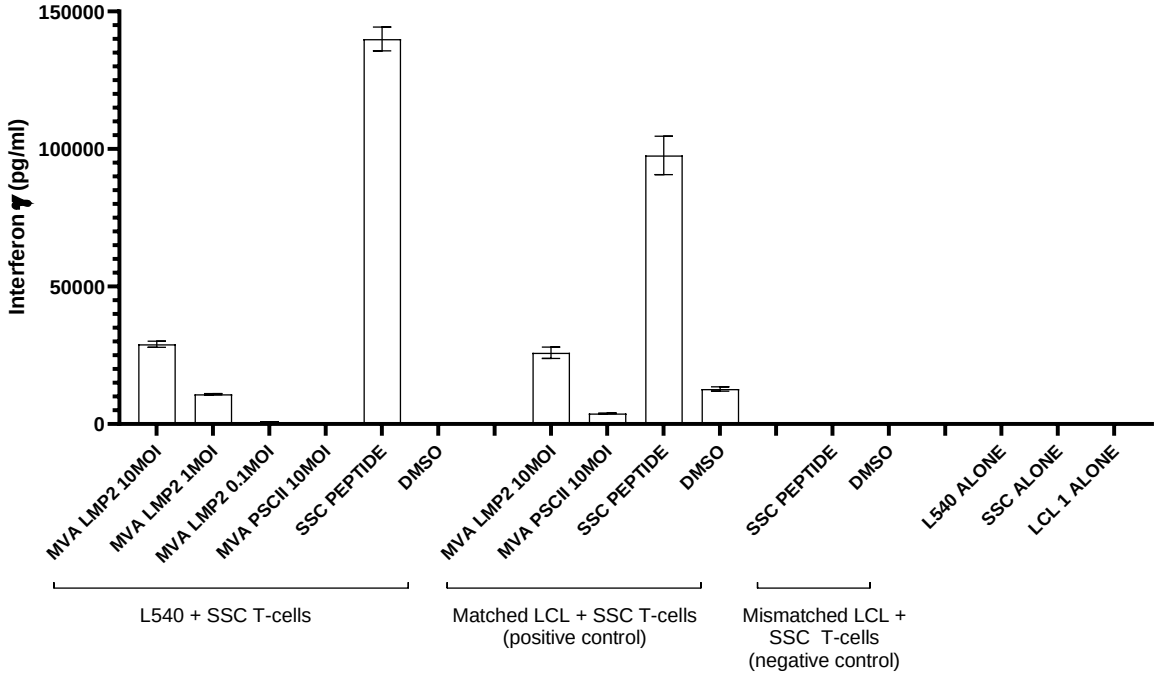


**Figure 5.10 Recognition of EBV-specific epitopes in L540 (a HL cell line) and matched LCLs by T-cell clones.** Initially, 4 HL cell lines were tested to assess recognition of EBV-specific epitopes by matched T-cell clones, along with corresponding LCLs and matched T-cell clones (positive controls). L540 and matched LCLs are recognised by SSC T-cell clones.

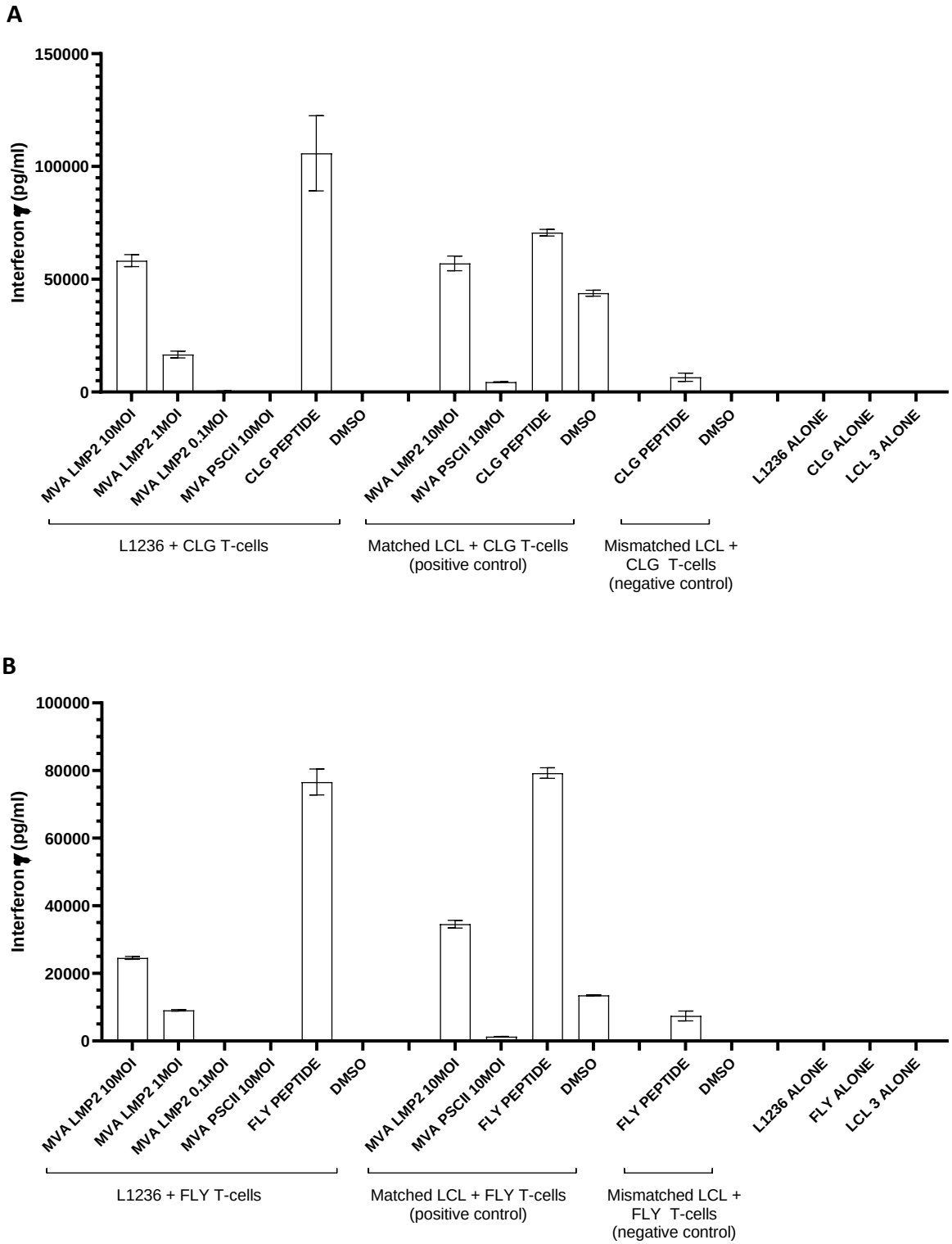


**Figure 5.11 Recognition of EBV-specific epitopes in L1236 (a HL cell line) and matched LCLs by T-cell clones.** Initially, 4 HL cell lines were tested to assess recognition of EBV-specific epitopes by matched T-cell clones, along with corresponding LCLs and matched T-cell clones (positive controls). L1236 and matched LCLs are recognised by (A) CLG T-cell clones and (B) FLY T-cell clones.

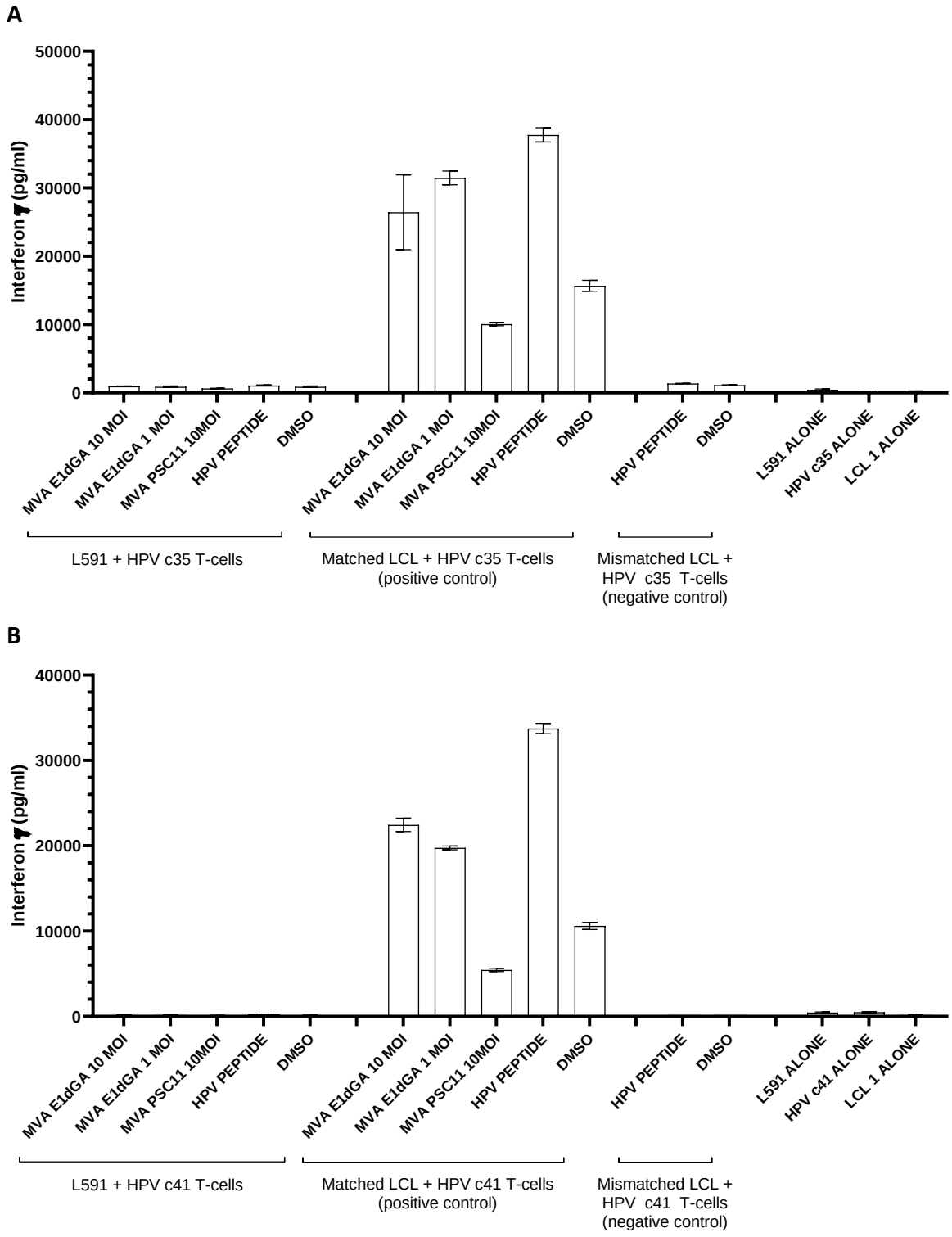


**Figure 5.12 Recognition of EBV-specific epitopes in L591 (a HL cell line) and matched LCLs by T-cell clones.** Initially, 4 HL cell lines were tested to assess recognition of EBV-specific epitopes by matched T-cell clones, along with corresponding LCLs and matched T-cell clones (positive controls). There was minimal recognition of L591 cells but matched LCLs were recognised by (A) HPV c35 T-cell clones and (B) HPV c41 T-cell clones.

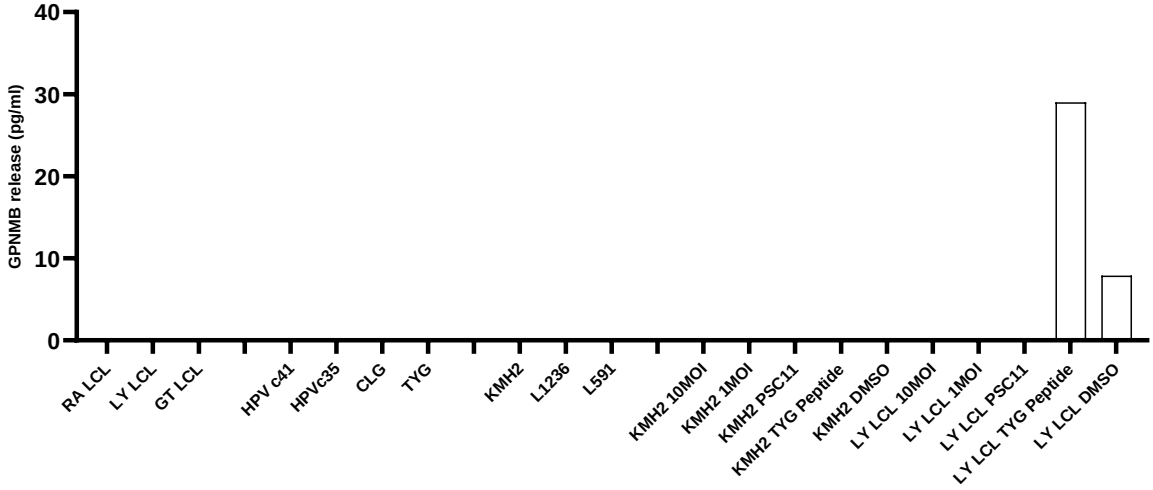


**Figure 5.13 GPNMB levels in CM from HL cell lines, LCLs and T-cell clones** (measured by ELISA)

Having tested the T-cell response to HL cell lines and matched LCLs, I wanted to see if this recognition of EBV-specific epitopes could be blocked by GPNMB. Initially, 0.04μg/ml rGPNMB was added to either HL cell line + T-cell clones or LCLs + T-cell clones (the lowest concentration used in previous experiments where an effect was seen) and interferon-γ release measured (Figures 5.14 – 5.17). Blocking of T-cell recognition of 3 HL cell lines tested (KMH2, L1236 and L540) by rGPNMB was seen, but this did not reach statistical significance (paired student t-test). Blocking of T-cell recognition of LCLs by rGPNMB was also seen, however this was statistically significant in the SSC T-cell clones and CLG T-cell clones (paired student t-test) (Figures 5.14 and 5.15). In the HPV clones, blocking was only seen when LCLs were pulsed with peptide but not MVA virus (Figure 5.17). All paired t-tests were done comparing untreated vs 0.04μg/ml rGPNMB across all conditions tested (i.e. 2 MVA virus concentrations, pSC11, peptide and DMSO).

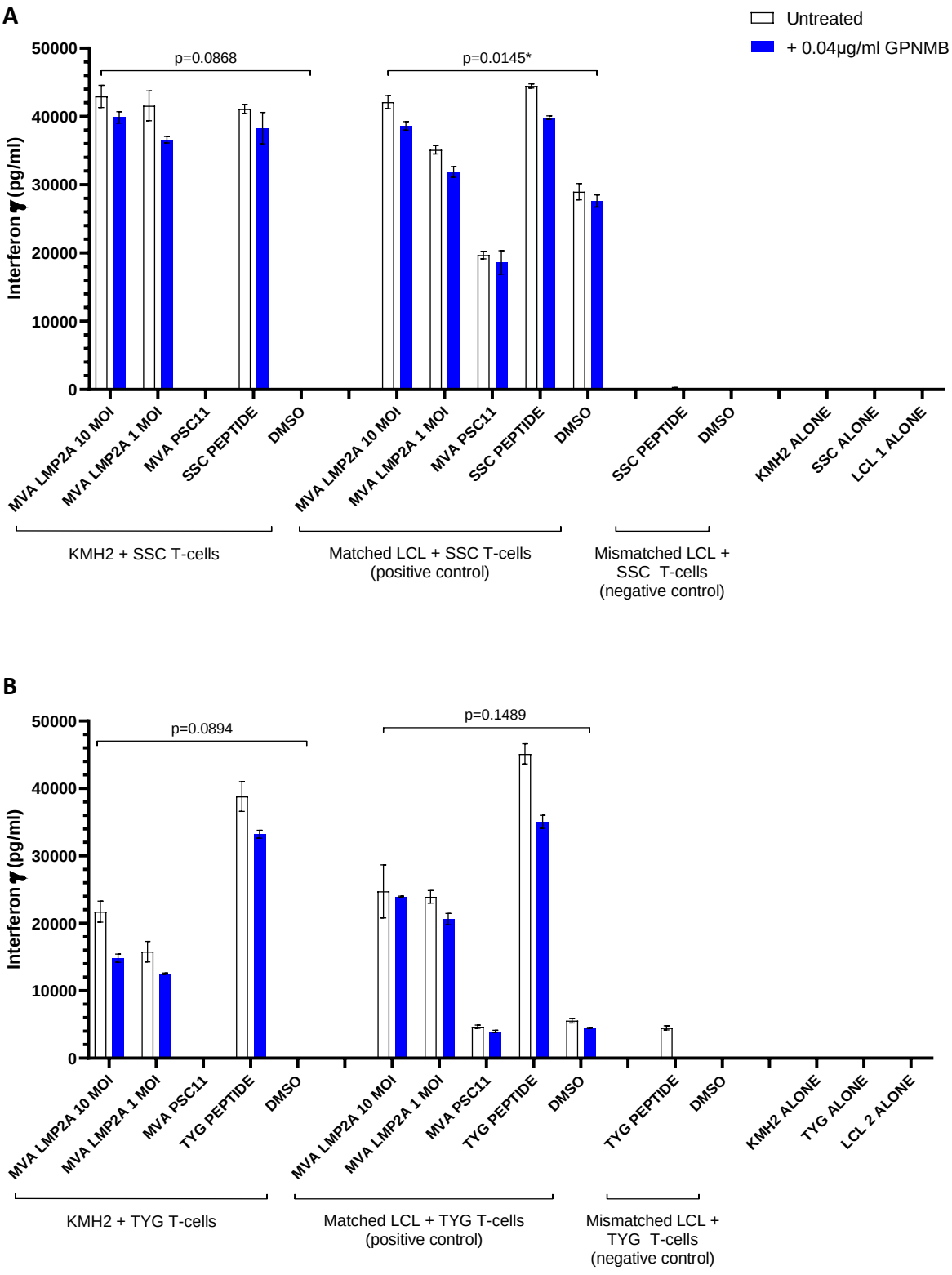


**Figure 5.14 Recognition of EBV-specific epitopes in HL cell lines and matched LCLs by T-cell clones is partially blocked by GPNMB.** (A) SSC and (B) TYG T-cell recognition of KMH2 or matched LCLs was partially blocked by the addition of rGPNMB 0.04µg/ml. The blocking of recognition of LCLs by the SSC T-cell clones was significant (A) (paired t-test).

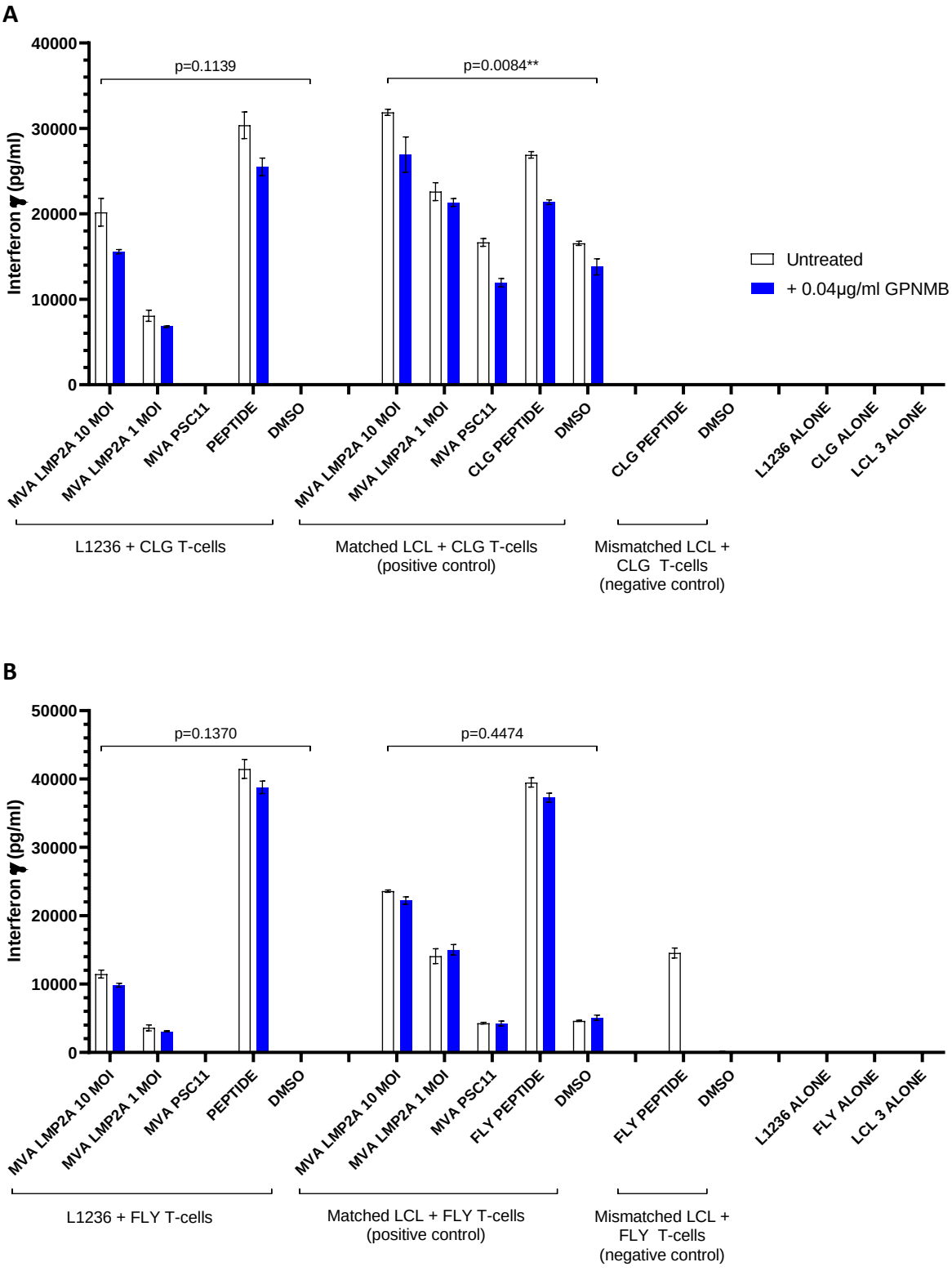


**Figure 5.15 Recognition of EBV-specific epitopes in HL cell lines and matched LCLs by T-cell clones is partially blocked by GPNMB.** (A) CLG and (B) FLY T-cell recognition of L1236 HL cells or matched LCLs was partially blocked by the addition of rGPNMB 0.04µg/ml. The blocking of recognition of LCLs by the CLG T-cell clones was significant (A) (paired t-test).

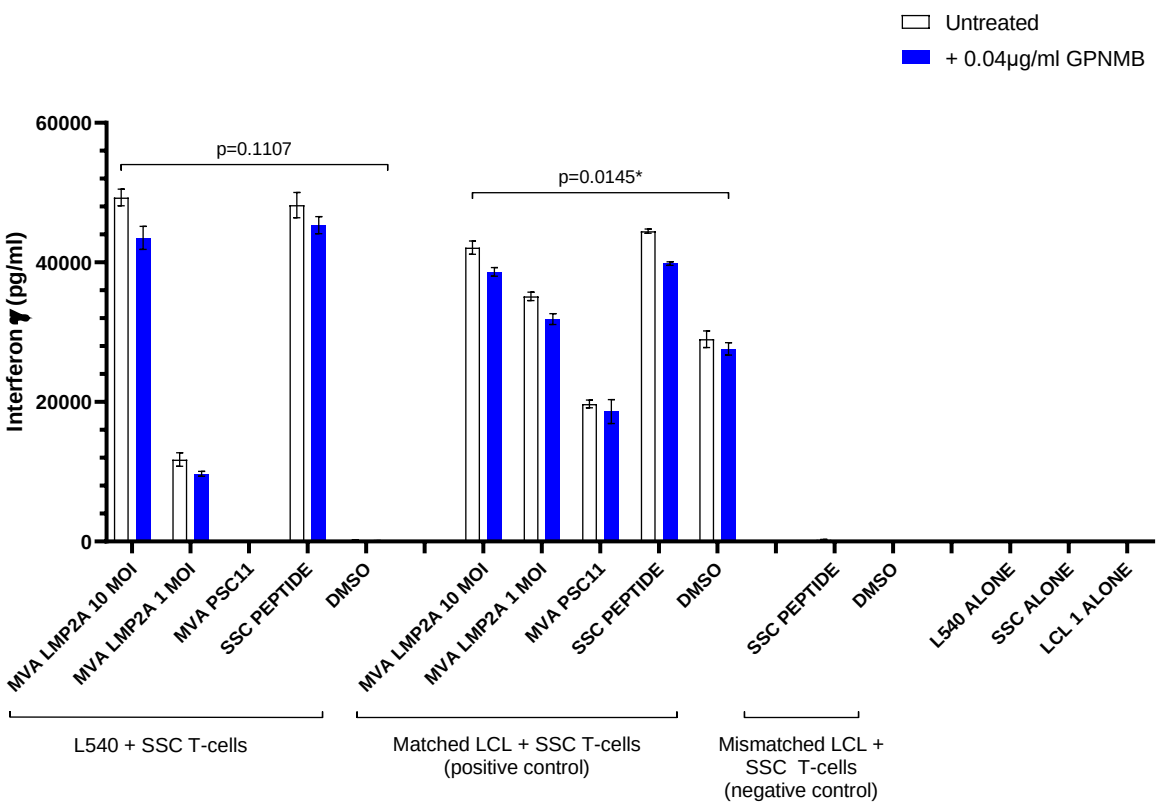


**Figure 5.16 Recognition of EBV-specific epitopes in HL cell lines and matched LCLs by T-cell clones is partially blocked by GPNMB.** SSC T-cell recognition of L540 or matched LCLs was partially blocked by the addition of rGPNMB 0.04µg/ml. The blocking of recognition of LCLs by the SSC T-cell clones was significant (paired t-test).

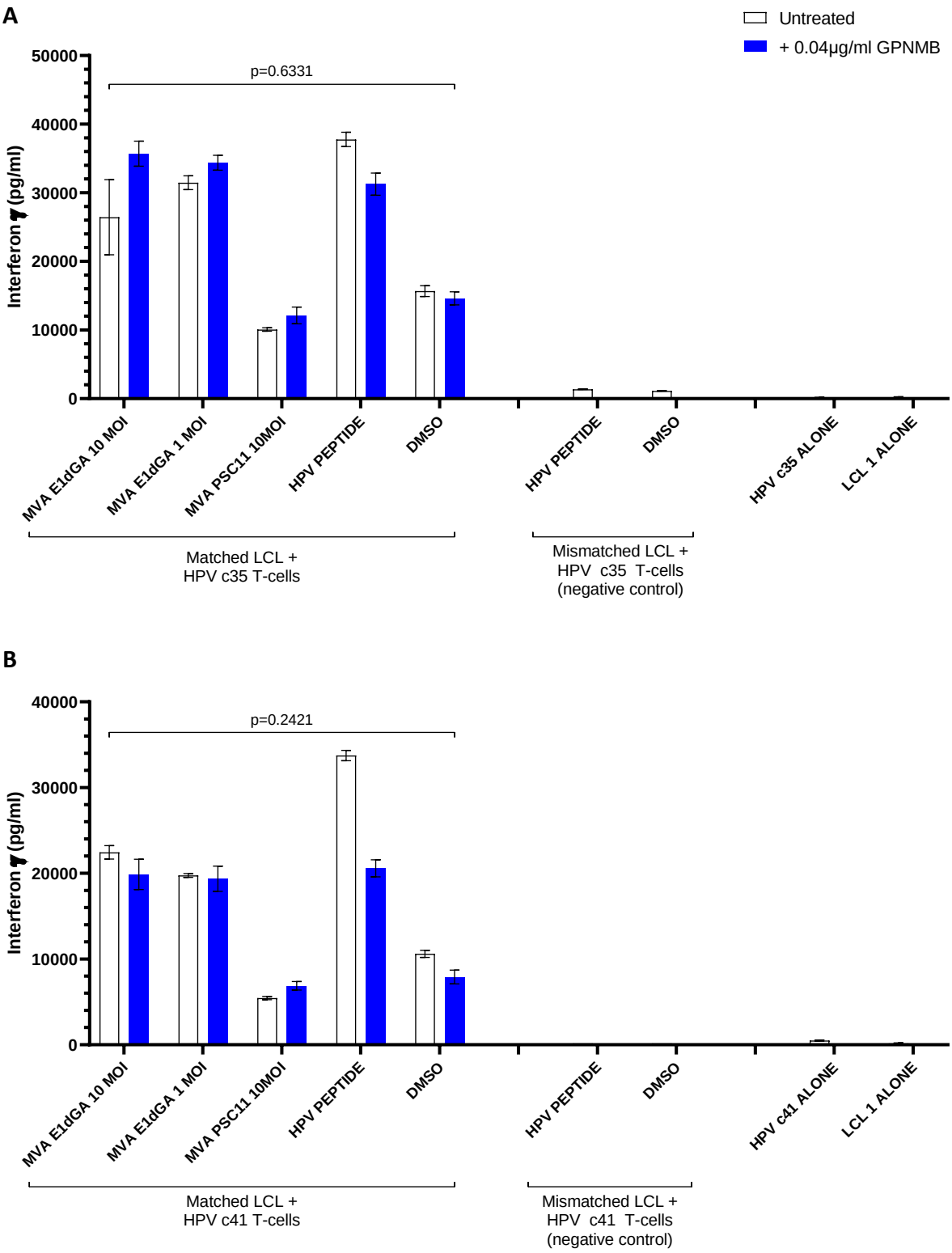


**Figure 5.17 Recognition of EBV-specific epitopes in matched LCLs by T-cell clones is partially blocked by GPNMB.** (A) HPV c35 and (B) HPV c41 T-cell recognition of matched LCLs loaded with peptide was partially blocked by the addition of rGPNMB 0.04µg/ml (paired t-test).

As I saw a partial blocking of T-cell recognition with 0.04µg/ml rGPNMB (based on the lowest amount required to block T-cell activation previous experiments), I decided to repeat the assay, this time using both a higher and a lower concentration of rGPNMB.

First, I used 2 HL cell lines and matched LCLs and the HPV clones and a range of 0.04µg/ml-1µg/ml of rGPNMB. There was significant partial blocking of TYG T-cell recognition of KMH2 cells at 0.04µg/ml, 0.08µg/ml and 0.2µg/ml of rGPNMB, with the largest blocking effect seen at 0.04µg/ml of rGPNMB (unpaired t-tests) (Figure 5.18 A). Blocking of matched LCLs by TYG T-cell clones was seen at 0.04µg/ml, 0.08µg/ml and 0.2µg/ml of rGPNMB, this was significant at all three concentrations (unpaired t-tests) (Figure 5.18 B). CLG T-cell recognition of L1236 was partially blocked by the addition of rGPNMB 0.04µg/ml-0.2µg/ml, and the greatest effect was seen at both 0.04µg/ml and 0.08µg/ml (Figure 5.19 A). The blocking of recognition of matched LCLs by CLG T-cell clones was significant at 0.04µg/ml, 0.08µg/ml and 0.2µg/ml of rGPNMB with some variation between MVA and peptide (unpaired t-tests) (Figure 5.19 B). HPV c35 T-cell recognition of matched LCLs loaded with peptide was partially blocked by the addition of rGPNMB 0.04µg/ml-0.2µg/ml (Figure 5.20 A). At 1µg/ml of rGPNMB there was a significant increase in T-cell recognition of matched LCLs. HPV c41 T-cell recognition of matched LCLs was partially blocked by the addition of rGPNMB 0.04µg/ml-0.2µg/ml (unpaired t-tests) (Figure 5.20 B). All unpaired t-tests were done between 0 rGPNMB and all other concentrations tested.

The blocking of LCL recognition by EBV-specific T-cell clones by rGPNMB at multiple concentrations was greater than the blocking of HL cell line recognition by the same T-cell clones.

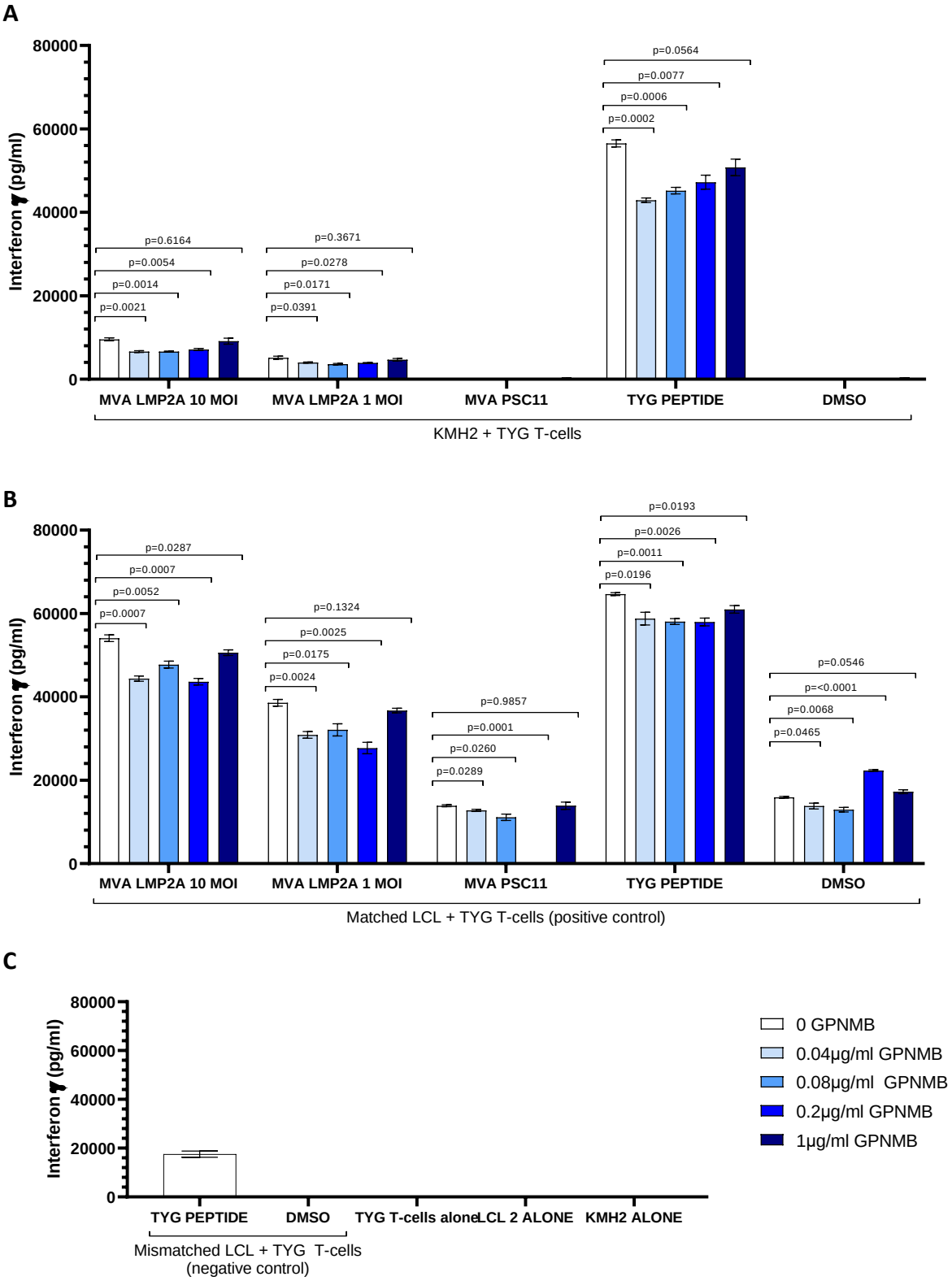


**Figure 5.18 Recognition of EBV-specific epitopes in HL cell lines and matched LCLs by T-cell clones is partially blocked by GPNMB- titration of rGPNMB concentrations.** TYG T-cell recognition of KMH2 or matched LCLs was partially blocked by the addition of rGPNMB 0.04µg/ml-0.2µg/ml. The blocking of recognition of LCLs by the TYG T-cell clones was significant at 0.04µg/ml, 0.08µg/ml and 0.2µg/ml (unpaired t-tests). (C) Mismatched LCL + TYG and other controls.

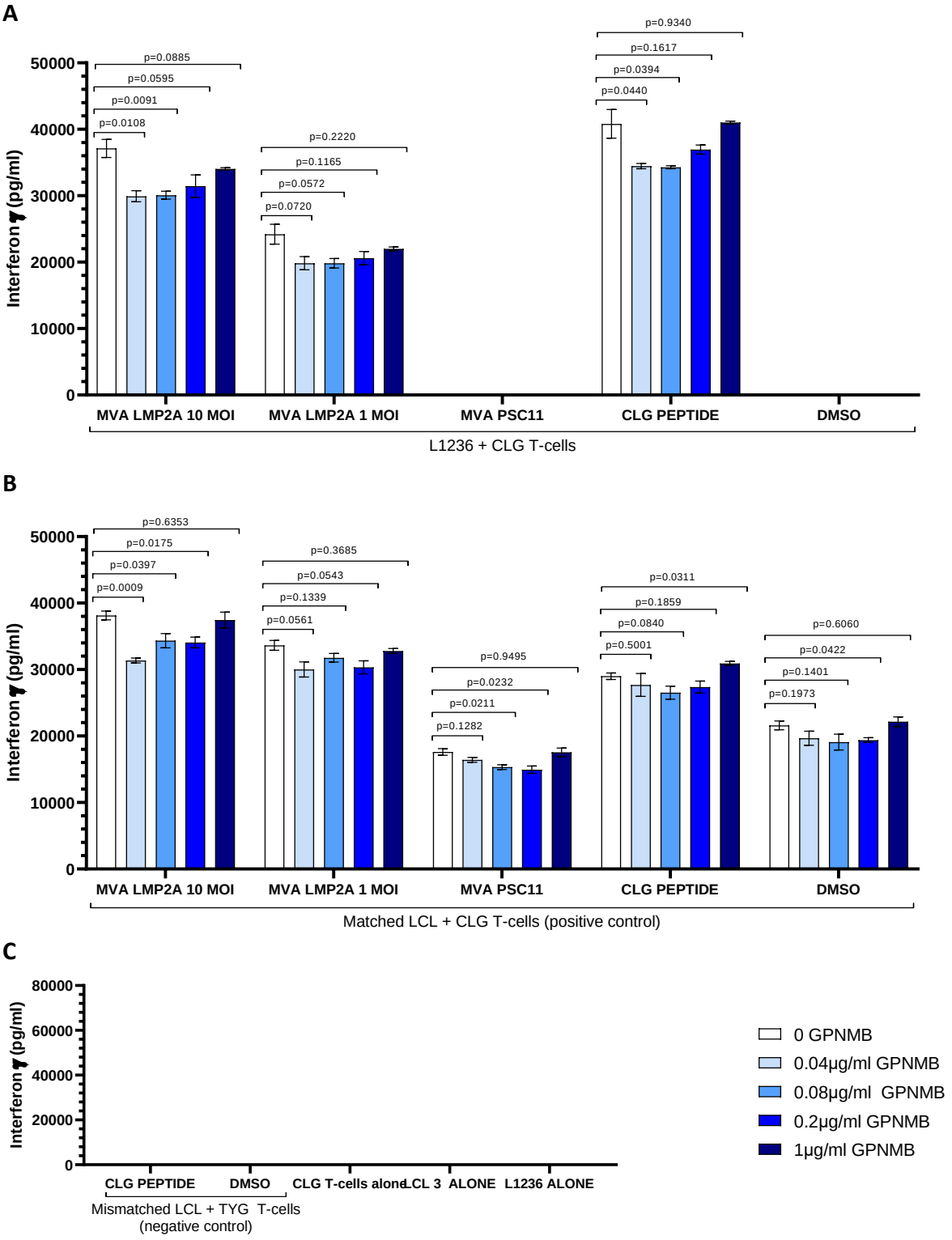


**Figure 5.19 Recognition of EBV-specific epitopes in HL cell lines and matched LCLs by T-cell clones is partially blocked by GPNMB- titration of rGPNMB concentrations.** CLG T-cell recognition of L1236 (A) or matched LCLs (B) was partially blocked by the addition of rGPNMB 0.04µg/ml-0.2µg/ml. The blocking of recognition of both L1236 and LCLs by the CLG T-cell clones was significant at 0.04µg/ml +/- 0.08µg/ml and 0.2µg/ml of rGPNMB with some variation between MVA and peptide (unpaired t-tests) (C) Mismatched LCL + CLG and other controls.

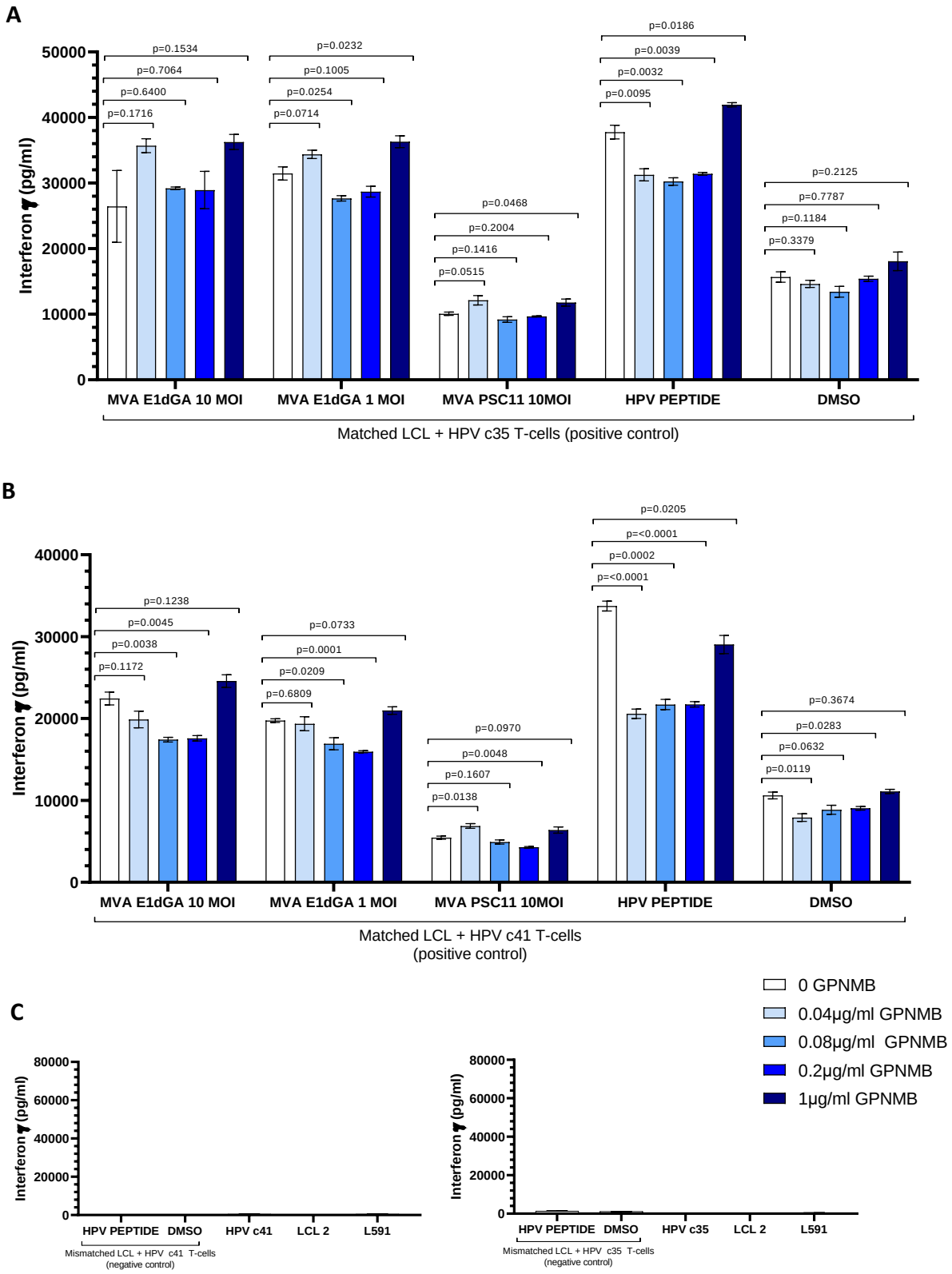


**Figure 5.20 Recognition of EBV-specific epitopes in matched LCLs by T-cell clones is partially blocked by GPNMB.** (A) HPV c35 (A) or HPV c41 (B) T-cell recognition of matched LCLs loaded with peptide was partially blocked by the addition of rGPNMB 0.04µg/ml-0.2µg/ml. At 1µg/ml of rGPNMB there was a significant increase in HPV c35 T-cell recognition (unpaired t-tests) (C) Mismatched LCL + HPV c35 or HPV c41 and other controls.

Having seen an effect at 0.04μg/ml-0.2μg/ml of rGPNMB, I wanted to test lower concentrations of rGPNMB as 0.4μg/ml was the lowest concentration used across all experiments. I used a range from 1ng/ml-1000ng/ml of rGPNMB in the next set of experiments. TYG T-cell clones (with KMH2 or LCL 2), CLG T-cell clones (with L1236 or LCL 3) and HPV c41 T-cell clones (with LCL 1) were tested. To present EBV proteins to T-cells, HL cell lines and LCLs were pulsed with peptide (overall this had a better response than infecting with MVA-LMP2A or MVA-E1ΔGA) or DMSO control prior to treating with rGPNMB.

Nearly all concentrations of rGPNMB (other than 10ng/ml) caused significant blocking of T-cell responses of TYG T-cell clones against KMH2 cells and matched LCLs; all concentrations of rGPNMB caused significant blocking of CLG recognition of L1236 cells but not matched LCLs; concentrations of 40ng/ml and above led to significant blocking of HPV c41 recognition of matched LCLs (unpaired t-tests at each concentration of GPNMB tested in HL cell lines or LCLs in Figure 5.21 A-C). Mismatched LCL controls and other controls are in Figure 5.21 D.

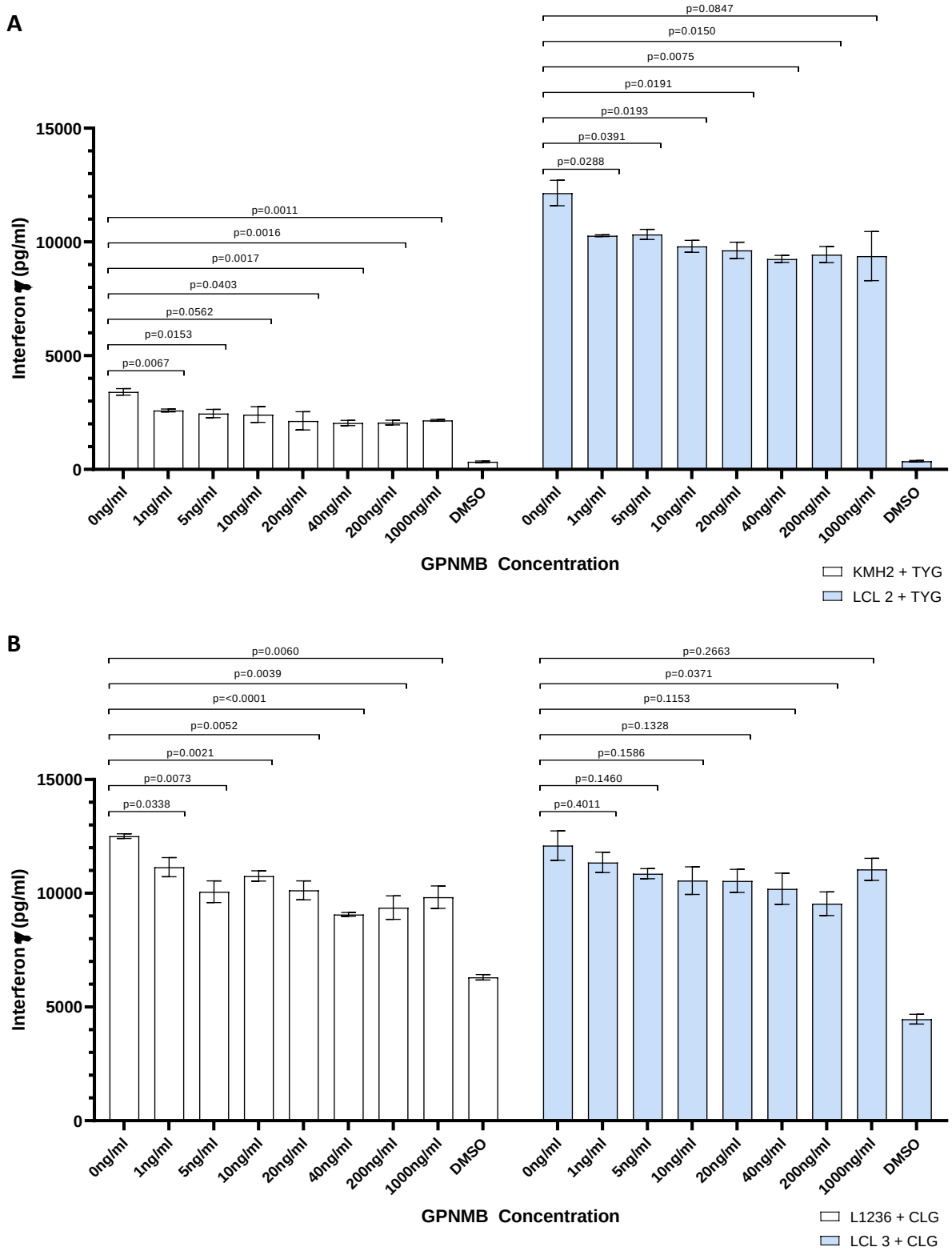


**Figure 5.21 Recognition of EBV-specific epitopes in HL cell lines and matched LCLs by T-cell clones is partially blocked by GPNMB at 1ng/ml-1000ng/ml.** (A) TYG T-cell recognition of KMH2 or matched LCLs was partially blocked by the addition of rGPNMB 1ng/ml-1000ng/ml (B) CLG T-cell recognition of L1236 or matched LCLs was partially blocked by the addition of rGPNMB 1ng/ml-1000ng/ml. Nearly all concentrations of rGPNMB showed significant blocking of TYG recognition of KMH2 and matched LCLs, and all concentrations of rGPNMB showed significant blocking of CLG T-cell recognition of L1236 cells but not matched LCLs (unpaired t-test).

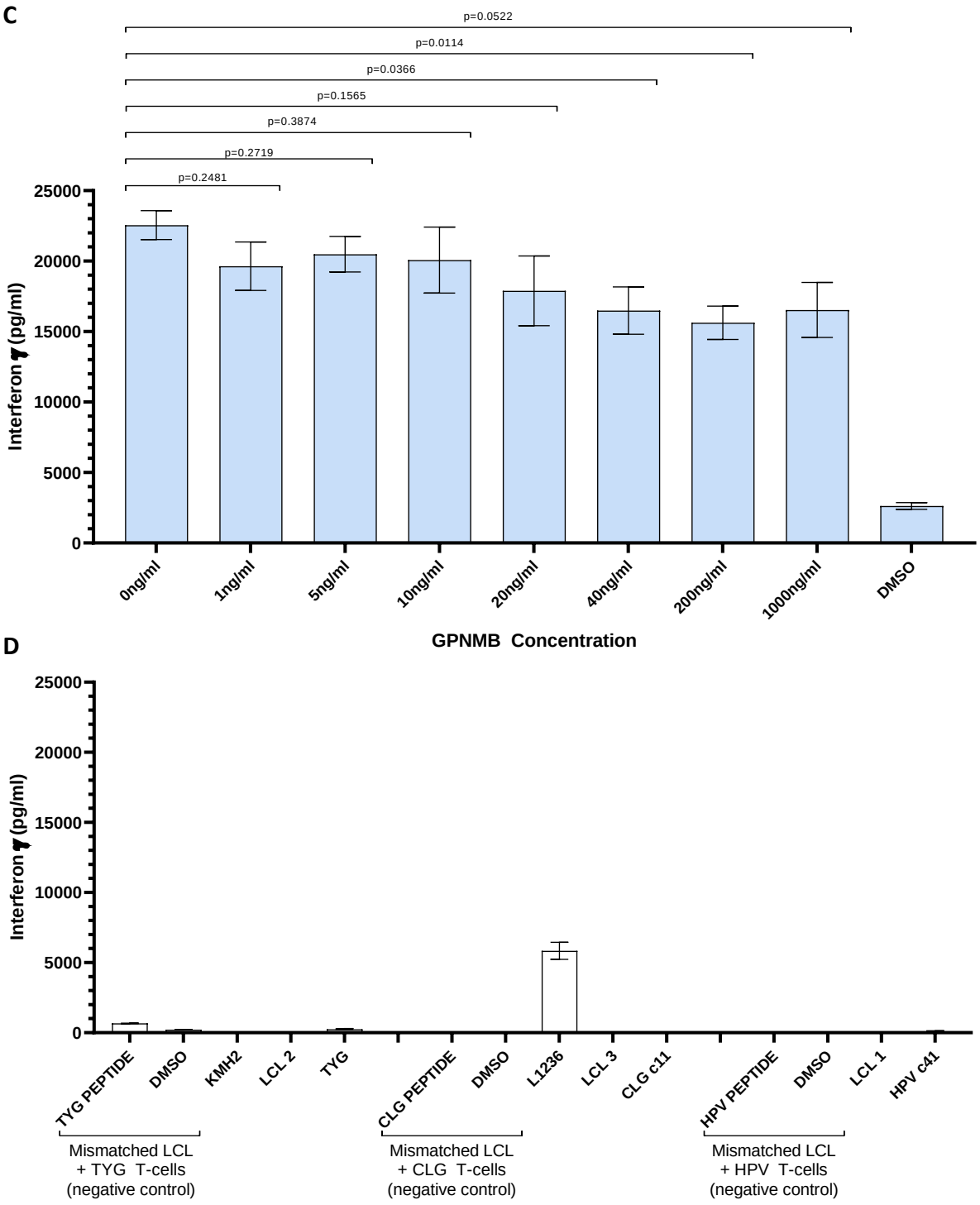


**Figure 5.21 Recognition of EBV-specific epitopes in matched LCLs by T-cell clones is partially blocked by GPNMB at 1ng/ml-1000ng/ml.** Continued. (C) HPV c41 T-cell recognition of matched LCLs was partially blocked by the addition of rGPNMB 1ng/ml-1000ng/ml. Concentrations of 40ng/ml and above rGPNMB showed significant blocking across all T-cell clones tested (unpaired t-test). (D) Mismatched LCL controls and individual cell line controls for all 3 T-cell clones, matched LCLs and HL cell lines.

## 5.7 Chapter Summary

In this chapter I have shown:

- rGPNMB partially blocks T-cell activation of healthy donors *in vitro*
- preliminary data suggesting anti-GPNMB antibodies can prevent inhibition of T-cell activation by GPNMB but this needs to be confirmed in more donors
- rGPNMB partially blocks t-cell recognition of EBV-specific epitopes in HL tumour cell lines

# CHAPTER 6

## DISCUSSION

# Chapter 6 Discussion

New treatment targets are needed for cHL patients, especially to improve outcomes in those with relapsed/refractory disease and to reduce long-term side effects in children and young adults. GPNMB has recently emerged as a novel therapeutic target in gastric cancer, osteosarcoma and lung cancer, in addition to breast cancer and melanoma where it is being targeted in clinical trials (Rose et al., 2017, Ren et al., 2020, Oyewumi et al., 2016, Jin et al., 2018).

A monoclonal antibody-drug conjugate (ADC), glembatumumab vedotin (CDX-011; CR-011-vc-MMAE) conjugates a human monoclonal antibody directed against the extracellular domain of GPNMB to monomethyl auristatin E (MMAE); this leads to death of cells expressing GPNMB by microtubule inhibition (Naumovski and Junutula, 2010, Tse et al., 2006). Initial phase I/II clinical trials showed an acceptable safety profile and clinical activity in heavily pre-treated patients with advanced melanoma and breast cancer (Bendell et al., 2014, Ott et al., 2014). Moreover, a further phase II study in GPNMB-expressing triple negative breast cancer showed an increased overall response rate (ORR) in tumours with GPNMB overexpression (≥25% tumour cells) compared to standard chemotherapy, albeit in a small sample size (Yardley et al., 2015). Since then, a further phase II randomised clinical trial assessing response of glembatumumab vedotin vs. capecitabine in GPNMB-overexpressing triple-negative breast cancer in heavily-pre-treated patients has recently been published (Vahdat et al., 2021). The primary endpoint of PFS was not met (2.9 months for glembatumumab vedotin vs 2.8 months for capecitabine), nor was there an increased relative risk/benefit in terms of side-effects and toxicity (Vahdat et al., 2021). In advanced melanoma, the most recent phase II study looked at response to glembatumumab vedotin after disease progression on immune-checkpoint

inhibitors and BRAF/MEK inhibitors, with limited treatment options (Ott et al., 2019). In this patient group, the ORR was 11% (not significant); median PFS was 4.4 months; median OS was 9 months but the safety profile was acceptable (Ott et al., 2019). Main adverse effects include rash, neutropenia/leucopenia, neuropathy, alopecia and fatigue. Interestingly, in this study, those who developed a treatment-related rash in the first cycle had a better ORR than those who did not (Ott et al., 2019). The only study carried out in a younger population was a phase II trial of glembatumumab vedotin in adolescents/young adults with recurrent osteosarcoma, in whom prognosis is poor (Kopp et al., 2019). Although the drug was well-tolerated (most common adverse event was rash), and some anti-tumour activity was seen, this was insufficient overall to proceed to the next stage of the trial (Kopp et al., 2019). In both studies by Ott *et al*. (2019) and Kopp *et al*. (2019), GPNMB expression was not correlated with response to glembatumumab vedotin. Additionally, bearing in mind all patients had advanced disease and had been heavily pretreated, some response to glembatumumab vedotin was seen (with no alternative treatment available in some cases), and therefore GPNMB could still be a viable target in these diseases. It is not known what the response in untreated patients would be; maybe a microtubule inhibitor is not the most appropriate 'active' agent in those tumours, or further stratification of patients (and therefore identification of relevant biomarkers) is required to determine who would benefit from anti-GPNMB therapy the most.

GPNMB has many different mechanisms of action through which it can promote tumour growth, therefore in cHL where tumour cells themselves are very rare, I wanted to explore its contribution to the immunosuppressive TME.

My initial objectives were to:

1) To investigate if GPNMB expression is related to patient outcome in cHL

2) To explore the relationship between HRS cells and GPNMB expression
3) To study the impact of macrophage-derived GPNMB on EBV-specific CTL responses in vitro

## 6.1 Objective 1: GPNMB expression on patient outcome in HL

I first identified GPNMB as a potential target through a re-analysis of a dataset which compared gene expression in micro-dissected HRS cells compared to $CD30^+$ EF B cells (Brune et al., 2008, Weniger et al., 2018). Dr Wenbin Wei produced a list of over-expressed genes in HRS cells vs $CD30^+$ EF B cells and *GPNMB* was $18^{th}$ on this list, with a 38.9 fold-change increase in expression. However, I found that GPNMB was absent in HRS cells in most cases but was expressed in TAMs. In tonsils (positive control), GPNMB was expressed by macrophages within the GC (Figure 3.5B). In cHL, some macrophages looked large, binucleate and pleomorphic (which can be described as 'HRS-like' by pathologists); these would be difficult to differentiate from actual HRS cells on morphology alone (Figure 3.9). In the experiments performed by the Kuppers group, HRS cells were identified and micro-dissected only by morphology; it is possible that macrophages were dissected instead of HRS cells, which could have increased the overall expression of GPNMB in these experiments. I also showed that HL cell lines have very low or undetectable levels of GPNMB expression (compared to GC B cells) using qPCR (Figure 3.13), which supports the observation that HRS cells do not generally express GPNMB.

After staining the first set of cHL cases and tonsils for GPNMB, expression appeared to be in macrophages within GCs of tonsils and in TAMs in cHL. This was confirmed with multiplex IHC, showing co-expression of CD68 and GPNMB by TAM in cHL and macrophages in tonsil. In the 86 cHL cases stained in the TMA, GPNMB was expressed in all 86 cases, but the amount of expression and density of $GPNMB^+$ cells was variable. Co-staining with CD68 confirmed co-

expression of GPNMB in TAMs in all cases, however there were a few cases where only a proportion of $CD68^+$ macrophages expressed GPNMB, and a few cases which had a low cell density of $GPNMB^+$ cells/HPF but they were strongly GPNMB+ positive (Figure 3.8G). Another interesting observation was that whereas macrophages are usually present in the GC of normal lymphoid tissue, in some cHL cases TAMs appeared to aggregate around the periphery of follicles within the tumour; in some cases, with HRS cells too (Figure 3.8C-D). Sometimes TAMs appeared to be forming loose aggregates within the tumour (Figure 3.8H) +/- being closely associated or clustered around HRS cells (Figure 3.L). Having made these observations, in future experiments I would like to do additional analysis of the stained cHL cases to assess the proportion of $GPNMB^+$ macrophages and their association with HRS cells. A recent study by Zheng *et al.* (2020) explored how spatial density and distribution of TAMs was related to survival in non-small cell lung cancer. They compared TAMs in the tumour centre to those at the invasive margin and adjacent non-tumour tissue by RNA-sequencing and then used multiplex immunofluorescence to analyse tumour cells/TAM proximity (Zheng et al., 2020). They showed that hypoxia was linked to an increased accumulation of M2 TAMs, which were more prevalent than M1s, especially at the invasive margin; higher proximity of tumour cells to M2 TAMs at the invasive margins than M1 TAMs; and that poor survival was associated with a reduced density of M1 TAMs in the tumour centre, increased proximity of M2 TAMs to tumour cells at the invasive margin and reduced proximity of M1 TAMs to tumour cells at the invasive margin (Zheng et al., 2020). Although non-small cell lung cancer and cHL are very different tumours, my observation that TAMs appear to aggregate around the periphery of follicles and sometimes around HRS cells suggests the location of TAMs within the tumour could be a predictive marker of survival in cHL, and therefore worth investigating further.

Clinical data were available for only 70 cases, including patients who progressed, relapsed or died, Only 3 samples were from relapse (the rest were all initial diagnostic biopsies), although there were paired diagnostic and relapse biopsies in two patients. From the clinical data available, no clear conclusions can be made about whether increased GPNMB expression in cHL is associated with a worse outcome or whether the proportion of GPNMB+ TAMs is higher at relapse versus diagnosis (this was the case in one of the patients, but not the other (Figure 3.11C). More cases are required to study this further, ideally from both adult and paediatric cohorts to fully evaluate if GPNMB could be a predictive biomarker in cHL.

It has previously been suggested that increased numbers of TAMs are associated with a worse outcome/ poor survival in cHL in both paediatric and adult patients and therefore may provide a means to further risk stratify patients; this is particularly relevant in those with progressive disease, but could also be used as a biomarker to stratify patients at diagnosis to receive more intense chemotherapy or determine if these patients might respond better to immune checkpoint inhibitors (Cencini et al., 2021, Steidl et al., 2010, Barros et al., 2015, Guo et al., 2016). It has also been reported previously that higher numbers of M2-like macrophages are associated with worse PFS in paediatric cHL and additionally, $EBV^{+}$ cHL was associated with increased numbers of M1-like macrophages (Barros et al., 2015). Therefore, further classification of TAM in cHL to M1-like or M2-like TAM would be beneficial to see if the $GPNMB^{+/-}$ TAMs belong to particular subsets. The main challenge highlighted from several studies has been which macrophage markers to use in immunohistochemistry or immunofluorescence and which specific clones of CD68 and CD163 antibodies are more specific for macrophages (vs. other cells, e.g. fibroblasts or myeloid cells) for example (Guo et

al., 2016, Barros et al., 2015, Cencini et al., 2021). The markers used in further studies would need to be carefully considered.

## 6.2 Objective 2: Regulation of GPNMB expression by HRS cells

Previously, it has been shown that GPNMB is upregulated upon polarisation of monocytes to macrophages and also that GPNMB expression is higher in M2 compared to M1 macrophages (Yu et al., 2016, Dong et al., 2013). In one experiment, human monocytes were polarised to macrophages by culturing with M-CSF for 7 days, in a similar way to my experiments (Dong et al., 2013). They saw significant upregulation of GPNMB during monocyte to macrophage differentiation by RNA sequencing (Dong et al., 2013). The other group looked at GPNMB expression in M1 vs M2 macrophages; there was a 3-fold increase in GPNMB mRNA expression and protein expression (measured by ELISA) in M2s compared to M1s (normalised to M1s), however these experiments were done with bone-marrow derived macrophages from mice, which were further stimulated with LPS and IFNγ for an M1 phenotype and IL-4 for an M2 phenotype (Yu et al., 2016). In my experiments, using up to 29 healthy donors as biological replicates, I found GPNMB expression to be variable amongst the macrophages derived from different donors. Although GPNMB mRNA expression was slightly higher in M2 macrophages than M1 macrophages, this was not significantly different. However, I did observe a significant increase in GPNMB mRNA expression upon differentiation of monocytes to both M1 and M2 macrophages. This is consistent with data from Dong *et al*. (2013) who also saw a significant increase in GPNMB expression upon differentiation of monocytes to macrophages; it should be noted that their data used monocytes and monocyte-derived macrophages from one donor only, whereas I have compared mRNA expression levels in 21 donors. The differences seen

with Yu *et al*.'s work (2016) could be due to the fact they used murine macrophages and different cytokines to stimulate further polarisation towards an M1 or M2 phenotype, rather than just GM-CSF or M-CSF. They also did not compare GPNMB expression levels between bone marrow cells (prior to differentiation) and M1 or M2 macrophages to see if GPNMB was upregulated during differentiation, or compare between bone-marrow macrophages (prior to further polarisation) and M1 or M2 macrophages to see if further polarisation increased expression levels (Yu et al., 2016). Ripoll *et al*. (2007) also showed that GPNMB expression was induced during macrophage differentiation. They compared murine bone marrow cells to bone marrow-macrophages, human monocytes to monocyte-derived macrophages and THP-1 monocyte-like cells to differentiated cells (in the presence of PMA) (Ripoll et al., 2007). GPNMB mRNA expression was increased upon differentiation to macrophages across all 3 cell types (Ripoll et al., 2007). I also consistently saw surface expression of GPNMB in both M1 and M2 macrophages, but the number of GPNMB+ cells was variable and overall there were similar expression levels in both groups. sGPNMB was also detectable in the supernatant of M1 and M2 after 24 hours of cultivation (once monocytes were differentiated for 7 days).

Two HL cell lines were chosen for their ability to express M-CSF, which is the cytokine used to differentiate monocytes into M2-like macrophages. L591 cells were chosen as an M-CSF negative cell line for comparison. Experiments were done +/- transwells to determine the effect of either exposure to supernatant or direct cell contact between HRS cells and M1 or M2 macrophages. A significant increase in GPNMB expression was seen on macrophages when they were co-cultured with all three HL cell lines or exposed to CM+/- transwells despite only a slight increase in CD163+CD206+ cells in the same donors. This is suggests that direct cell-cell contact between HRS cells and macrophages is required for them to be further

polarised along the M1-M2 spectrum, but not for GPNMB expression to be increased. Given that tumour cells are very rare in cHL, I tested different ratios of macrophages:HL cells and HL CM. There was more of an increase in average GPNMB expression when macrophages were co-cultured with HL cells compared to CM, the result was significant across all groups and similar results were also seen across all ratios of macrophages:HL cells, indicating that the number of tumour cells does not affect their ability to induce GPNMB expression; the data also suggest that a soluble factor released by HRS cells may be responsible for inducing GPNMB expression.

Initially, two of the HL cell lines (L428 and L1236) were chosen for co-culture experiments because they release M-CSF into their CM, but L591 was chosen because their CM contained very little M-CSF. L591 CM induced similar levels of GPNMB expression in both M1 and M2 macrophages, compared with the other two cell lines which did produce M-CSF, suggesting that other cytokines may be involved in up-regulating GPNMB expression. A cytokine array was used to measure cytokine levels in the HL cell lines. Five cytokines were highly expressed- angiogenin, emmprin/CD147, ICAM-1, MIF and CCL5. Recombinant versions of each of these proteins were added to M1 and M2 macrophages (separately and all together to 3 donors). An effect was seen with each cytokine individually and when all were used in combination. However, a similar effect on GPNMB expression was seen with the cytokine control (0.1% BSA/PBS) and the whole experiment was only done once with 3 donors due to time constraints. Therefore, this would need to be repeated and further optimised to see which of these proteins, if any, are involved in the upregulation of GPNMB in macrophages.

## 6.3 Objective 3: Impact of macrophage-derived GPNMB on EBV-specific CTL responses in vitro

Eventually I settled on an approach to activate T-cells which utilised a combination of soluble CD3/CD28 activator (Stemcell). I used Interferon-gamma release to measure the extent of activation. I observed considerable inter-donor variation both in terms of the degree of T-cell activation and also the response to soluble GPNMB.

In my initial experiments using high concentrations of rGPNMB based on results from other groups, I observed an initial 'blocking' effect was seen by a reduction in number of CD3+CD69+ PBMCs, but the interferon-γ levels were not very high overall, and thus it was hard to assess if there was an effect. It is difficult to gauge what constitutes a 'physiological' concentration of GPNMB given that it is impossible to measure the local concentrations produced by a macrophage *in vivo*, however, if thinking about the amount of GPNMB surrounding a macrophage and the close proximity of macrophages to other cells for example, the concentration within that space could be much higher than 10µg/ml, but the overall concentration of GPNMB within the TME might be much lower. Having said that, 10µg/ml might be considered a very high concentration for *in vitro* experiments. For this reason, I tested lower concentrations of rGPNMB; 0.04µg/ml rGPNMB blocked T-cell activation across 3 different concentrations of activator (0.5µl/ml- 5µl/ml) and 1µg/ml rGPNMB blocked T-cell activation at 0.5µl/ml of activator. Looking at the mean interferon-γ levels across the whole experiment, I observed that rGPNMB significantly blocked T-cell activation overall, but this effect was most significant at 0.04µg/ml of rGPNMB (Figure 5.5G). At each concentration of CD3/CD28 activator separately, between 7-8 donors showed some blocking response to rGPNMB, especially at the lower concentrations, but this effect could apparently be

'overcome' by higher concentrations of rGPNMB (Figure 5.5 A-F). This result contrasts with previous observations by another group (Chung et al., 2007, Chung et al., 2009, Chung et al., 2013) who showed that sGPNMB did not block T-cell activation whereas immobilised GPNMB) did. Chung *et al*. and the Ariizumi group did most of their experiments using murine T-cells and DC-HIL (the murine form of GPNMB) (Chung et al., 2007, Chung et al., 2013), with human T-cells only used in one publication (Chung et al., 2009). In all their experiments (both human and murine), they activated isolated T-cells with anti-CD3 antibody alone, blocked activation with immobilised GPNMB/ DC-HIL (up to 40µg/ml), and used anti-CD28 antibody to rescue inhibition (Chung et al., 2007, Chung et al., 2009, Chung et al., 2013). In mice, using concentrations of soluble DC-HIL upto 20µg/ml, no blocking of T-cell activation was seen, in contrast to 5µg/ml of immobilised DC-HIL which did block T-cell activation (Chung et al., 2007). In my initial experiments I used higher concentrations of soluble rGPNMB upto 10µg/ml, where I saw variable effects, but it is possible that using too high concentrations of GPNMB could over-saturate the T-cells, and that could be why Chung *et al*. saw no effect using soluble GPNMB, whereas this is less likely to happen if it is immobilised; the lowest documented dose of soluble DC-HIL used by Chung *et al*. was 1.25µg/ml but I used 0.04µg/ml of rGPNMB (Chung et al., 2007). I also used a combination of anti-CD3 and anti-CD28 antibodies to activate T-cells within whole PBMCs, both of which I considered to be more 'physiological' than using isolated T-cells and anti-CD3 antibody alone (Chung et al., 2007, Chung et al., 2009).

Multiple commercially available anti-Human GPNMB antibodies are available, but none of them has previously been tested for their neutralising ability. I tested these on one donor at 2 concentrations. Antibodies MAB2550 (R&D #303802) and ab175427 (Abcam [7C10E5]) were both effective at neutralising rGPNMB and reversing the inhibition of T-cell

activation. Future experiments will be directed to further testing of these antibodies and also other antibodies which have recently become available commercially.

I tested if macrophage-derived GPNMB could block T-cell activation. Although the initial results were promising, this experiment would need to be repeated.

As 40-50% of cHL cases are EBV-positive, I wanted to see if GPNMB could also block T-cell recognition of EBV-specific epitopes in HL. HLA-matched $CD8^+$ T-cell clones were used to test this in HL cell lines, and as LCLs are known to be efficiently recognised by T-cell clones they acted as a positive control in the experiment. KMH2, L540 and L1236 cells were all able to be recognised by matched T-cell clones following pulsing with epitope peptide, or infection with MVA-LMP2A, indicating these HL cells were able to process and present the relevant peptides to the cell surface. L591 HL cells, which are EBV positive, were also treated with MVA-E1ΔGA or HPV peptide but these cells were not recognised by the EBNA1 HPV clones; only the matched LCLs were recognised, which suggests the T-cell clones were acting appropriately. L591 cell line is not known to contain mutations in *B2M* (Liu et al., 2014) but it could be that L591 cells have low levels of class I expression; this could be evaluated in future experiments. I could also attempt to upregulate class I expression by treating the cells with interferon-γ if levels are low. For the experiments here, only matched LCLs and 2 HPV clones were used.

Initially I used 0.04μg/ml of rGPNMB to see if any blocking of T-cell recognition of LCLs or HL cells could be seen (and although some blocking of recognition of HL cell lines was seen, this was not significant). Blocking of T-cell recognition of LCLs was significant using two of the CD8+ T-cell clones (SSC and CLG). HPV clone blocking was only seen when cells were pulsed with peptide (exogenous processing of EBV). Having seen an effect with 0.04μg/ml of rGPNMB, I wanted to test higher and lower concentrations of rGPNMB to see if the response

was similar to that seen in T-cell activation, i.e. variable response or 'overcoming' of blocking at higher concentrations of rGPNMB. I observed a significant partial blocking of T-cell recognition at all concentrations of rGPNMB used, as low as 1ng/ml.

Although complete blocking of T-cell activation or complete blocking of T-cell recognition was not seen, a significant partial response of both to sGPNMB was seen, and therefore further investigation into targeting GPNMB as an immune checkpoint is required. In more recent clinical trials in HL and other cancers, e.g melanoma and hepatocellular carcinoma, combination immune checkpoint therapy has been used (Cheng et al., 2020, Larkin et al., 2019, Herrera et al., 2018), raising the possibility of combining anti-GPNMB therapy with existing treatment for cHL (chemotherapy and radiation therapy) so that lower doses can be used, or combining an anti-GPNMB therapy with PD-1 blockade for example. It would also be interesting to study GPNMB expression in patients who do not respond to PD-1 blockade therapy.

The ADC glembatumumab vedotin which targets GPNMB is in trials as single agent therapy in other cancers; in these cancers GPNMB is mainly expressed by malignant cells within the tumour, therefore targeting these cells with an ADC is appropriate (Rose et al., 2017). cHL is an unusual tumour to begin with, in that malignant HRS cells are very rare and the bulk of the tumour is made up of immune/inflammatory cells; thus disrupting the immunosuppressive TME that supports HRS cells would be beneficial. In addition to immune suppression, GPNMB has other possible mechanisms of action through which it could be exerting effects in cHL. sGPNMB is associated with increased MVD in mammary tumours and promotes endothelial cell migration both as a direct chemoattractant for endothelial cells, but

also through indirect VEGF upregulation (Rose et al., 2010). TAMs have been shown to be significantly correlated with MVD, VEGF expression and poor outcomes in cHL, so macrophage-derived sGPNMB could also be driving angiogenesis though upregulation of VEGF and endothelial cell migration in cHL (Koh et al., 2014, Panico et al., 2013, Korkolopoulou et al., 2005, Rose et al., 2010). In cHL, where GPNMB appears to be predominantly expressed by macrophages, blocking GPNMB with a neutralising antibody would be preferential.

# References


ADAMS PERRY, T. 2019. The role of sphingosine-1-phosphate in macrophage recruitment and function in diffuse large B-cell lymphoma. Doctor of Philosophy, University of Birmingham.

ALDINUCCI, D., GLOGHINI, A., PINTO, A., DE FILIPPI, R. & CARBONE, A. 2010. The classical Hodgkin's lymphoma microenvironment and its role in promoting tumour growth and immune escape. *J Pathol,* 221**,** 248-63.

ALLAVENA, P., SICA, A., SOLINAS, G., PORTA, C. & MANTOVANI, A. 2008. The inflammatory micro-environment in tumor progression: the role of tumor-associated macrophages. *Crit Rev Oncol Hematol,* 66**,** 1-9.

ANSELL, S. M. 2015. Hodgkin Lymphoma: Diagnosis and Treatment. *Mayo Clinic Proceedings,* 90**,** 1574-1583.

ANSELL, S. M., LESOKHIN, A. M., BORRELLO, I., HALWANI, A., SCOTT, E. C., GUTIERREZ, M., SCHUSTER, S. J., MILLENSON, M. M., CATTRY, D., FREEMAN, G. J., RODIG, S. J., CHAPUY, B., LIGON, A. H., ZHU, L., GROSSO, J. F., KIM, S. Y., TIMMERMAN, J. M., SHIPP, M. A. & ARMAND, P. 2015. PD-1 blockade with nivolumab in relapsed or refractory Hodgkin's lymphoma. *N Engl J Med,* 372**,** 311-9.

ARAI, S., FANALE, M., DEVOS, S., ENGERT, A., ILLIDGE, T., BORCHMANN, P., YOUNES, A., MORSCHHAUSER, F., MCMILLAN, A. & HORNING, S. J. 2013. Defining a Hodgkin lymphoma population for novel therapeutics after relapse from autologous hematopoietic cell transplant. *Leuk Lymphoma,* 54**,** 2531-3.

ARMAND, P. 2015. Immune checkpoint blockade in hematologic malignancies. *Blood,* 125**,** 3393-400.

BARROS, M. H., HASSAN, R. & NIEDOBITEK, G. 2012a. Tumor-associated macrophages in pediatric classical Hodgkin lymphoma: association with Epstein-Barr virus, lymphocyte subsets, and prognostic impact. *Clin Cancer Res,* 18**,** 3762-71.

BARROS, M. H., SEGGES, P., VERA-LOZADA, G., HASSAN, R. & NIEDOBITEK, G. 2015. Macrophage polarization reflects T cell composition of tumor microenvironment in pediatric classical Hodgkin lymphoma and has impact on survival. *PLoS One,* 10**,** e0124531.

BARROS, M. H., VERA-LOZADA, G., SOARES, F. A., NIEDOBITEK, G. & HASSAN, R. 2012. Tumor microenvironment composition in pediatric classical Hodgkin lymphoma is modulated by age and Epstein-Barr virus infection. *Int J Cancer,* 131**,** 1142-52.

BENDELL, J., SALEH, M., ROSE, A. A., SIEGEL, P. M., HART, L., SIRPAL, S., JONES, S., GREEN, J., CROWLEY, E., SIMANTOV, R., KELER, T., DAVIS, T. & VAHDAT, L. 2014. Phase I/II study of the antibody-drug conjugate glembatumumab vedotin in patients with locally advanced or metastatic breast cancer. J Clin Oncol, 32, 3619-25.

BIOCONDUCTOR. affy- Methods for Affymetrix Oligonucleotide Arrays [Online]. Available: https://bioconductor.org/packages/release/bioc/html/affy.html [Accessed 20/09/2021].

BOLSTAD, B. M., IRIZARRY, R. A., ASTRAND, M. & SPEED, T. P. 2003. A comparison of normalization methods for high density oligonucleotide array data based on variance and bias. Bioinformatics, 19, 185-93.

BOND, D. A. & ALINARI, L. 2017. Emerging treatment options for the management of Hodgkin's lymphoma: clinical utility of nivolumab. *J Blood Med,* 8**,** 41-54.

BRUNE, V., TIACCI, E., PFEIL, I., DÖRING, C., ECKERLE, S., VAN NOESEL, C. J. M., KLAPPER, W., FALINI, B., VON HEYDEBRECK, A., METZLER, D., BRÄUNINGER, A., HANSMANN, M.-L. & KÜPPERS, R. 2008. Origin and pathogenesis of nodular lymphocyte–predominant Hodgkin lymphoma as revealed by global gene expression analysis. *Journal of Experimental Medicine,* 205**,** 2251-2268.

BRUNE, M. M., JUSKEVICIUS, D., HASLBAUER, J., DIRNHOFER, S. & TZANKOV, A. 2021. Genomic Landscape of Hodgkin Lymphoma. *Cancers,* 13**,** 682.

CENCINI, E., FABBRI, A., SICURANZA, A., GOZZETTI, A. & BOCCHIA, M. 2021. The Role of Tumor-Associated Macrophages in Hematologic Malignancies. Cancers, 13, 3597.

CHENG, A.-L., HSU, C., CHAN, S. L., CHOO, S.-P. & KUDO, M. 2020. Challenges of combination therapy with immune checkpoint inhibitors for hepatocellular carcinoma. Journal of Hepatology, 72, 307-319

CHAPMAN, A. L., RICKINSON, A. B., THOMAS, W. A., JARRETT, R. F., CROCKER, J. & LEE, S. P. 2001. Epstein-Barr virus-specific cytotoxic T lymphocyte responses in the blood and tumor site of Hodgkin's disease patients: implications for a T-cell-based therapy. *Cancer Res,* 61**,** 6219-26.

CHETAILLE, B., BERTUCCI, F., FINETTI, P., ESTERNI, B., STAMATOULLAS, A., PICQUENOT, J. M., COPIN, M. C., MORSCHHAUSER, F., CASASNOVAS, O., PETRELLA, T., MOLINA, T., VEKHOFF, A., FEUGIER, P., BOUABDALLAH, R., BIRNBAUM, D., OLIVE, D. & XERRI, L. 2009. Molecular profiling of classical Hodgkin lymphoma tissues uncovers variations in the tumor microenvironment and correlations with EBV infection and outcome. *Blood,* 113**,** 2765-3775.

CHUNG, J. S., DOUGHERTY, I., CRUZ, P. D., JR. & ARIIZUMI, K. 2007a. Syndecan-4 mediates the coinhibitory function of DC-HIL on T cell activation. *J Immunol,* 179**,** 5778-84.

CHUNG, J. S., SATO, K., DOUGHERTY, II, CRUZ, P. D., JR. & ARIIZUMI, K. 2007. DC-HIL is a negative regulator of T lymphocyte activation. *Blood,* 109**,** 4320-7.

CHUNG, J. S., BONKOBARA, M., TOMIHARI, M., CRUZ, P. D., JR. & ARIIZUMI, K. 2009. The DC-HIL/syndecan-4 pathway inhibits human allogeneic T-cell responses. *Eur J Immunol,* 39**,** 965-74.

CHUNG, J. S., TOMIHARI, M., TAMURA, K., KOJIMA, T., CRUZ, P. D., JR. & ARIIZUMI, K. 2013. The DC-HIL ligand syndecan-4 is a negative regulator of T-cell allo-reactivity responsible for graft-versus-host disease. *Immunology,* 138**,** 173-82.

DOJCINOV, S. D., FEND, F. & QUINTANILLA-MARTINEZ, L. 2018. EBV-Positive Lymphoproliferations of B- T- and NK-Cell Derivation in Non-Immunocompromised Hosts. *Pathogens (Basel, Switzerland),* 7**,** 28.

DONG, C., ZHAO, G., ZHONG, M., YUE, Y., WU, L. & XIONG, S. 2013. RNA sequencing and transcriptomal analysis of human monocyte to macrophage differentiation. *Gene,* 519**,** 279-87.

DOUSSIS-ANAGNOSTOPOULOU, I. A., TALKS, K. L., TURLEY, H., DEBNAM, P., TAN, D. C., MARIATOS, G., GORGOULIS, V., KITTAS, C. & GATTER, K. C. 2002. Vascular endothelial growth factor (VEGF) is expressed by neoplastic Hodgkin-Reed-Sternberg cells in Hodgkin's disease. *J Pathol,* 197**,** 677-83.

FAGERBERG, L., HALLSTRÖM, B. M., OKSVOLD, P., KAMPF, C., DJUREINOVIC, D., ODEBERG, J., HABUKA, M., TAHMASEBPOOR, S., DANIELSSON, A., EDLUND, K., ASPLUND, A., SJÖSTEDT, E., LUNDBERG, E., SZIGYARTO, C. A., SKOGS, M., TAKANEN, J. O., BERLING, H., TEGEL, H., MULDER, J., NILSSON, P., SCHWENK, J. M., LINDSKOG, C., DANIELSSON, F., MARDINOGLU, A., SIVERTSSON, A., VON FEILITZEN, K., FORSBERG, M., ZWAHLEN, M., OLSSON, I., NAVANI, S., HUSS, M., NIELSEN, J., PONTEN, F. & UHLÉN, M. 2014. Analysis of the human tissue-specific expression by genome-wide integration of transcriptomics and antibody-based proteomics. Mol Cell Proteomics, 13, 397-406.

GAUTIER, L., COPE, L., BOLSTAD, B. M. & IRIZARRY, R. A. 2004. affy--analysis of Affymetrix GeneChip data at the probe level. Bioinformatics, 20, 307-315.

GINHOUX, F., GRETER, M., LEBOEUF, M., NANDI, S., SEE, P., GOKHAN, S., MEHLER, M. F., CONWAY, S. J., NG, L. G., STANLEY, E. R., SAMOKHVALOV, I. M. & MERAD, M. 2010. Fate mapping analysis reveals that adult microglia derive from primitive macrophages. Science, 330, 841-5.

GINHOUX, F. & GUILLIAMS, M. 2016. Tissue-Resident Macrophage Ontogeny and Homeostasis. Immunity, 44, 439-449.

GINHOUX, F., SCHULTZE, J. L., MURRAY, P. J., OCHANDO, J. & BISWAS, S. K. 2016. New insights into the multidimensional concept of macrophage ontogeny, activation and function. Nat Immunol, 17, 34-40.

GOMEZ PERDIGUERO, E., KLAPPROTH, K., SCHULZ, C., BUSCH, K., AZZONI, E., CROZET, L., GARNER, H., TROUILLET, C., DE BRUIJN, M. F., GEISSMANN, F. & RODEWALD, H. R. 2015. Tissue-resident macrophages originate from yolk-sac-derived erythro-myeloid progenitors. Nature, 518, 547-51.

GOODMAN, K. A., RIEDEL, E., SERRANO, V., GULATI, S., MOSKOWITZ, C. H. & YAHALOM, J. 2008. Long-term effects of high-dose chemotherapy and radiation for relapsed and refractory Hodgkin's lymphoma. *J Clin Oncol,* 26**,** 5240-7.

GREAVES, P., CLEAR, A., COUTINHO, R., WILSON, A., MATTHEWS, J., OWEN, A., SHANYINDE, M., LISTER, T. A., CALAMINICI, M. & GRIBBEN, J. G. 2013. Expression of FOXP3, CD68, and CD20 at diagnosis in the microenvironment of classical Hodgkin lymphoma is predictive of outcome. *J Clin Oncol,* 31**,** 256-62.

GREEN, M. R., RODIG, S., JUSZCZYNSKI, P., OUYANG, J., SINHA, P., O'DONNELL, E., NEUBERG, D. & SHIPP, M. A. 2012. Constitutive AP-1 activity and EBV infection induce PD-L1 in Hodgkin lymphomas and posttransplant lymphoproliferative disorders: implications for targeted therapy. *Clin Cancer Res,* 18**,** 1611-8.

GUO, B., CEN, H., TAN, X. & KE, Q. 2016. Meta-analysis of the prognostic and clinical value of tumor-associated macrophages in adult classical Hodgkin lymphoma. BMC Medicine, 14.

HANNA, S. J., MCCOY-SIMANDLE, K., LEUNG, E., GENNA, A., CONDEELIS, J. & COX, D. 2019. Tunneling nanotubes, a novel mode of tumor cell-macrophage communication in tumor cell invasion. Journal of Cell Science, 132, jcs223321.

HASHIMOTO, D., CHOW, A., NOIZAT, C., TEO, P., MARY, LEBOEUF, M., CHRISTIAN, SEE, P., PRICE, J., LUCAS, D., GRETER, M., MORTHA, A., SCOTT, E, TANAKA, M., NICO, GARCÍA-SASTRE, A., E, GINHOUX, F., PAUL & MERAD, M. 2013. Tissue-Resident Macrophages Self-Maintain Locally throughout Adult Life with Minimal Contribution from Circulating Monocytes. Immunity, 38, 792-804.

HERRERA, A. F., MOSKOWITZ, A. J., BARTLETT, N. L., VOSE, J. M., RAMCHANDREN, R., FELDMAN, T. A., LACASCE, A. S., ANSELL, S. M., MOSKOWITZ, C. H., FENTON, K., OGDEN, C. A., TAFT, D., ZHANG, Q., KATO, K., CAMPBELL, M. & ADVANI, R. H. 2018. Interim results of brentuximab vedotin in combination with nivolumab in patients with relapsed or refractory Hodgkin lymphoma. Blood, 131, 1183-1194.

HOASHI, T., SATO, S., YAMAGUCHI, Y., PASSERON, T., TAMAKI, K. & HEARING, V. J. 2010. Glycoprotein nonmetastatic melanoma protein b, a melanocytic cell marker, is a melanosome-specific and proteolytically released protein. *The FASEB Journal,* 24**,** 1616-1629.

HOEFFEL, G., CHEN, J., LAVIN, Y., LOW, D., ALMEIDA, F. F., SEE, P., BEAUDIN, A. E., LUM, J., LOW, I., FORSBERG, E. C., POIDINGER, M., ZOLEZZI, F., LARBI, A., NG, L. G., CHAN, J. K., GRETER, M., BECHER, B., SAMOKHVALOV, I. M., MERAD, M. & GINHOUX, F. 2015.

C-Myb(+) erythro-myeloid progenitor-derived fetal monocytes give rise to adult tissue-resident macrophages. Immunity, 42, 665-78.

HOEFFEL, G. & GINHOUX, F. 2015. Ontogeny of Tissue-Resident Macrophages. Front Immunol, 6, 486.

HUANG, J. J., MA, W. J. & YOKOYAMA, S. 2012. Expression and immunolocalization of Gpnmb, a glioma-associated glycoprotein, in normal and inflamed central nervous systems of adult rats. Brain and Behavior, 2, 85-96.

IRIZARRY, R. A., HOBBS, B., COLLIN, F., BEAZER-BARCLAY, Y. D., ANTONELLIS, K. J., SCHERF, U. & SPEED, T. P. 2003. Exploration, normalization, and summaries of high density oligonucleotide array probe level data. Biostatistics, 4, 249-64.

JAFFE, E. S., PITTALUGA, S. & ANASTASI, J. 2018. The Pathologic Basis for the Classification of Non-Hodgkin and Hodgkin Lymphomas. Elsevier.

JIN, R., JIN, Y. Y., TANG, Y. L., YANG, H. J., ZHOU, X. Q. & LEI, Z. 2018. GPNMB silencing suppresses the proliferation and metastasis of osteosarcoma cells by blocking the PI3K/Akt/mTOR signaling pathway. Oncol Rep, 39, 3034-3040.

KAMPER, P., BENDIX, K., HAMILTON-DUTOIT, S., HONORE, B., NYENGAARD, J. R. & D'AMORE, F. 2011. Tumor-infiltrating macrophages correlate with adverse prognosis and Epstein-Barr virus status in classical Hodgkin's lymphoma. *Haematologica,* 96**,** 269-76.

KANZLER, H., KÜPPERS, R., HANSMANN, M. L. & RAJEWSKY, K. 1996. Hodgkin and Reed-Sternberg cells in Hodgkin's disease represent the outgrowth of a dominant tumor clone derived from (crippled) germinal center B cells. *Journal of Experimental Medicine,* 184**,** 1495-1505.

KASAMON, Y. L., DE CLARO, R. A., WANG, Y., SHEN, Y. L., FARRELL, A. T. & PAZDUR, R. 2017. FDA Approval Summary: Nivolumab for the Treatment of Relapsed or Progressive Classical Hodgkin Lymphoma. *Oncologist,* 22**,** 585-591.

KOH, Y. W., PARK, C. S., YOON, D. H., SUH, C. & HUH, J. 2014. CD163 expression was associated with angiogenesis and shortened survival in patients with uniformly treated classical Hodgkin lymphoma. *PLoS One,* 9**,** e87066.

KOPP, L. M., MALEMPATI, S., KRAILO, M., GAO, Y., BUXTON, A., WEIGEL, B. J., HAWTHORNE, T., CROWLEY, E., MOSCOW, J. A., REID, J. M., VILLALOBOS, V., RANDALL, R. L., GORLICK, R. & JANEWAY, K. A. 2019. Phase II trial of the glycoprotein non-metastatic B-targeted antibody-drug conjugate, glembatumumab vedotin (CDX-011), in recurrent osteosarcoma AOST1521: A report from the Children's Oncology Group. Eur J Cancer, 121, 177-183.

KORKOLOPOULOU, P., THYMARA, I., KAVANTZAS, N., VASSILAKOPOULOS, T. P., ANGELOPOULOU, M. K., KOKORIS, S. I., DIMITRIADOU, E. M., SIAKANTARIS, M. P., ANARGYROU, K., PANAYIOTIDIS, P., TSENGA, A., ANDROULAKI, A., DOUSSIS-ANAGNOSTOPOULOU, I. A., PATSOURIS, E. & PANGALIS, G. A. 2005. Angiogenesis in Hodgkin's lymphoma: a morphometric approach in 286 patients with prognostic implications. *Leukemia,* 19**,** 894-900.

KUAN, C. T., WAKIYA, K., DOWELL, J. M., HERNDON, J. E., 2ND, REARDON, D. A., GRANER, M. W., RIGGINS, G. J., WIKSTRAND, C. J. & BIGNER, D. D. 2006. Glycoprotein nonmetastatic melanoma protein B, a potential molecular therapeutic target in patients with glioblastoma multiforme. *Clin Cancer Res,* 12**,** 1970-82.

KUMAGAI, K., TABU, K., SASAKI, F., TAKAMI, Y., MORINAGA, Y., MAWATARI, S., HASHIMOTO, S., TANOUE, S., KANMURA, S., TAMAI, T., MORIUCHI, A., UTO, H., TSUBOUCHI, H. & IDO, A. 2015. Glycoprotein Nonmetastatic Melanoma B (Gpnmb)-Positive Macrophages Contribute to the Balance between Fibrosis and Fibrolysis during the Repair of Acute Liver Injury in Mice. PLoS One, 10, e0143413.

KUPPERS, R. 2009. The biology of Hodgkin's lymphoma. *Nat Rev Cancer,* 9**,** 15-27.

KÜPPERS, R. 2018. Chapter 74 - Origin of Hodgkin Lymphoma. *In:* HOFFMAN, R., BENZ, E. J., SILBERSTEIN, L. E., HESLOP, H. E., WEITZ, J. I., ANASTASI, J., SALAMA, M. E. & ABUTALIB, S. A. (eds.) *Hematology (Seventh Edition).* Elsevier.

LARKIN, J., CHIARION-SILENI, V., GONZALEZ, R., GROB, J.-J., RUTKOWSKI, P., LAO, C. D., COWEY, C. L., SCHADENDORF, D., WAGSTAFF, J., DUMMER, R., FERRUCCI, P. F., SMYLIE, M., HOGG, D., HILL, A., MÁRQUEZ-RODAS, I., HAANEN, J., GUIDOBONI, M., MAIO, M., SCHÖFFSKI, P., CARLINO, M. S., LEBBÉ, C., MCARTHUR, G., ASCIERTO, P. A., DANIELS, G. A., LONG, G. V., BASTHOLT, L., RIZZO, J. I., BALOGH, A., MOSHYK, A., HODI, F. S. & WOLCHOK, J. D. 2019. Five-Year Survival with Combined Nivolumab and Ipilimumab in Advanced Melanoma. New England Journal of Medicine, 381, 1535-1546.

LAVIRON, M. & BOISSONNAS, A. 2019. Ontogeny of Tumor-Associated Macrophages. Frontiers in Immunology, 10.

LEE, S. P., CONSTANDINOU, C. M., THOMAS, W. A., CROOM-CARTER, D., BLAKE, N. W., MURRAY, P. G., CROCKER, J. & RICKINSON, A. B. 1998. Antigen presenting phenotype of Hodgkin Reed-Sternberg cells: analysis of the HLA class I processing pathway and the effects of interleukin-10 on epstein-barr virus-specific cytotoxic T-cell recognition. *Blood,* 92**,** 1020-30.

LI, Y. N., ZHANG, L., LI, X. L., CUI, D. J., ZHENG, H. D., YANG, S. Y. & YANG, W. L. 2014. Glycoprotein nonmetastatic B as a prognostic indicator in small cell lung cancer. *APMIS,* 122**,** 140-6.

LIU, Y., ABDUL RAZAK, F. R., TERPSTRA, M., CHAN, F. C., SABER, A., NIJLAND, M., VAN IMHOFF, G., VISSER, L., GASCOYNE, R., STEIDL, C., KLUIVER, J., DIEPSTRA, A., KOK, K. & VAN DEN BERG, A. 2014. The mutational landscape of Hodgkin lymphoma cell lines determined by whole-exome sequencing. *Leukemia,* 28**,** 2248-2251

MAINOU-FOWLER, T., ANGUS, B., MILLER, S., PROCTOR, S. J., TAYLOR, P. R. & WOOD, K. M. 2006. Micro-vessel density and the expression of vascular endothelial growth factor (VEGF) and platelet-derived endothelial cell growth factor (PdEGF) in classical Hodgkin lymphoma (HL). *Leuk Lymphoma,* 47**,** 223-30.

MANTOVANI, A., SCHIOPPA, T., PORTA, C., ALLAVENA, P. & SICA, A. 2006. Role of tumor-associated macrophages in tumor progression and invasion. *Cancer Metastasis Rev,* 25**,** 315-22.

MANTOVANI, A., SOZZANI, S., LOCATI, M., ALLAVENA, P. & SICA, A. 2002. Macrophage polarization: tumor-associated macrophages as a paradigm for polarized M2 mononuclear phagocytes. *Trends Immunol,* 23**,** 549-55.

MARIC, G., ROSE, A. A., ANNIS, M. G. & SIEGEL, P. M. 2013. Glycoprotein non-metastatic b (GPNMB): A metastatic mediator and emerging therapeutic target in cancer. *Onco Targets Ther,* 6**,** 839-52.

MARQUEZ-RODAS, I., CEREZUELA, P., SORIA, A., BERROCAL, A., RISO, A., GONZALEZ-CAO, M. & MARTIN-ALGARRA, S. 2015. Immune checkpoint inhibitors: therapeutic advances in melanoma. *Ann Transl Med,* 3**,** 267.

MARTIN, A., CHAHWAN, R., PARSA, J. Y. & SCHARFF, M. D. 2015. Chapter 20 - Somatic Hypermutation: The Molecular Mechanisms Underlying the Production of Effective High-Affinity Antibodies. *In:* ALT, F. W., HONJO, T., RADBRUCH, A. & RETH, M. (eds.) *Molecular Biology of B Cells (Second Edition).* London: Academic Press.

MEYER, R. M., GOSPODAROWICZ, M. K., CONNORS, J. M., PEARCEY, R. G., WELLS, W. A., WINTER, J. N., HORNING, S. J., DAR, A. R., SHUSTIK, C., STEWART, D. A., CRUMP, M., DJURFELDT, M. S., CHEN, B. E., SHEPHERD, L. E., GROUP, N. C. T. & EASTERN COOPERATIVE ONCOLOGY, G. 2012. ABVD alone versus radiation-based therapy in limited-stage Hodgkin's lymphoma. *N Engl J Med,* 366**,** 399-408.

MÖLLER, A. & LOBB, R. J. 2020. The evolving translational potential of small extracellular vesicles in cancer. Nature Reviews Cancer, 20, 697-709.

MORADI-CHALESHTORI, M., HASHEMI, S. M., SOUDI, S., BANDEHPOUR, M. & MOHAMMADI-YEGANEH, S. 2019. Tumor-derived exosomal microRNAs and proteins as modulators of macrophage function. Journal of Cellular Physiology, 234, 7970-7982.

MOSKOWITZ, C. H., NADEMANEE, A., MASSZI, T., AGURA, E., HOLOWIECKI, J., ABIDI, M. H., CHEN, A. I., STIFF, P., GIANNI, A. M., CARELLA, A., OSMANOV, D., BACHANOVA, V., SWEETENHAM, J., SUREDA, A., HUEBNER, D., SIEVERS, E. L., CHI, A., LARSEN, E. K.,

HUNDER, N. N., WALEWSKI, J. & GROUP, A. S. 2015. Brentuximab vedotin as consolidation therapy after autologous stem-cell transplantation in patients with Hodgkin's lymphoma at risk of relapse or progression (AETHERA): a randomised, double-blind, placebo-controlled, phase 3 trial. *Lancet,* 385**,** 1853-62.

MOSSER, D. M. & EDWARDS, J. P. 2008. Exploring the full spectrum of macrophage activation. *Nat Rev Immunol,* 8**,** 958-69.

MURDOCH, C., MUTHANA, M., COFFELT, S. B. & LEWIS, C. E. 2008. The role of myeloid cells in the promotion of tumour angiogenesis. *Nat Rev Cancer,* 8**,** 618-31.

MURRAY, P. J., ALLEN, J. E., BISWAS, S. K., FISHER, E. A., GILROY, D. W., GOERDT, S., GORDON, S., HAMILTON, J. A., IVASHKIV, L. B., LAWRENCE, T., LOCATI, M., MANTOVANI, A., MARTINEZ, F. O., MEGE, J. L., MOSSER, D. M., NATOLI, G., SAEIJ, J. P., SCHULTZE, J. L., SHIREY, K. A., SICA, A., SUTTLES, J., UDALOVA, I., VAN GINDERACHTER, J. A., VOGEL, S. N. & WYNN, T. A. 2014. Macrophage activation and polarization: nomenclature and experimental guidelines. *Immunity,* 41**,** 14-20.

NAGPAL, P., DESCALZI-MONTOYA, D. B. & LODHI, N. 2020. The circuitry of the tumor microenvironment in adult and pediatric Hodgkin lymphoma: cellular composition, cytokine profile, EBV , and exosomes. Cancer Reports

NAUMOVSKI, L. & JUNUTULA, J. R. 2010. Glembatumumab vedotin, a conjugate of an anti-glycoprotein non-metastatic melanoma protein B mAb and monomethyl auristatin E for the treatment of melanoma and breast cancer. Curr Opin Mol Ther, 12, 248-57.

NCBI. BioProject [Online]. Available: www.ncbi.nlm.nih.gov/bioproject [Accessed 20/09/2021].

NCBI. Gene [Online]. Available: www.ncbi.nlm.nih.gov/gene [Accessed 20/09/2021].

NCBI. Gene Expression Omnibus [Online]. Available: www.ncbi.nlm.nih.gov/geo/ [Accessed 20/09/2021].

OTT, P. A., HAMID, O., PAVLICK, A. C., KLUGER, H., KIM, K. B., BOASBERG, P. D., SIMANTOV, R., CROWLEY, E., GREEN, J. A., HAWTHORNE, T., DAVIS, T. A., SZNOL, M. & HWU, P. 2014. Phase I/II study of the antibody-drug conjugate glembatumumab vedotin in patients with advanced melanoma. J Clin Oncol, 32, 3659-66.

OTT, P. A., PAVLICK, A. C., JOHNSON, D. B., HART, L. L., INFANTE, J. R., LUKE, J. J., LUTZKY, J., ROTHSCHILD, N. E., SPITLER, L. E., COWEY, C. L., ALIZADEH, A. R., SALAMA, A. K., HE, Y., HAWTHORNE, T. R., BAGLEY, R. G., ZHANG, J., TURNER, C. D. & HAMID, O. 2019. A phase 2 study of glembatumumab vedotin, an antibody-drug conjugate targeting glycoprotein NMB, in patients with advanced melanoma. Cancer, 125, 1113-1123.

OYEWUMI, M. O., MANICKAVASAGAM, D., NOVAK, K., WEHRUNG, D., PAULIC, N., MOUSSA, F. M., SONDAG, G. R. & SAFADI, F. F. 2016. Osteoactivin (GPNMB) ectodomain

protein promotes growth and invasive behavior of human lung cancer cells. *Oncotarget,* 7**,** 13932-44.

PANICO, L., RONCONI, F., LEPORE, M., TENNERIELLO, V., CANTORE, N., DELL'ANGELO, A. C., FERBO, U. & FERRARA, F. 2013. Prognostic role of tumor-associated macrophages and angiogenesis in classical Hodgkin lymphoma. *Leuk Lymphoma,* 54**,** 2418-25.

PARDOLL, D. M. 2012. The blockade of immune checkpoints in cancer immunotherapy. *Nat Rev Cancer,* 12**,** 252-64.

PERDIGUERO, E. G. & GEISSMANN, F. 2016. The development and maintenance of resident macrophages. Nature Immunology, 17, 2-8.

PÉRICART, S., TOSOLINI, M., GRAVELLE, P., ROSSI, C., TRAVERSE-GLEHEN, A., AMARA, N., FRANCHET, C., MARTIN, E., BEZOMBES, C., LAURENT, G., BROUSSET, P., FOURNIÉ, J.-J. & LAURENT, C. 2018. Profiling Immune Escape in Hodgkin's and Diffuse large B-Cell Lymphomas Using the Transcriptome and Immunostaining. Cancers, 10, 415.

REN, F., ZHAO, Q., LIU, B., SUN, X., TANG, Y., HUANG, H., MEI, L., YU, Y., MO, H., DONG, H., ZHENG, P. & MI, Y. 2020. Transcriptome analysis reveals GPNMB as a potential therapeutic target for gastric cancer. J Cell Physiol, 235, 2738-2752.

REY-GIRAUD, F., HAFNER, M. & RIES, C. H. 2012. In Vitro Generation of Monocyte-Derived Macrophages under Serum-Free Conditions Improves Their Tumor Promoting Functions. *PLoS ONE,* 7**,** e42656.

RICH, J. N., SHI, Q., HJELMELAND, M., CUMMINGS, T. J., KUAN, C. T., BIGNER, D. D., COUNTER, C. M. & WANG, X. F. 2003. Bone-related genes expressed in advanced malignancies induce invasion and metastasis in a genetically defined human cancer model. *J Biol Chem,* 278**,** 15951-7.

RIPOLL, V. M., IRVINE, K. M., RAVASI, T., SWEET, M. J. & HUME, D. A. 2007. Gpnmb is induced in macrophages by IFN-gamma and lipopolysaccharide and acts as a feedback regulator of proinflammatory responses. J Immunol, 178, 6557-66.

ROEHLECKE, C. & SCHMIDT, M. H. H. 2020. Tunneling Nanotubes and Tumor Microtubes in Cancer. Cancers, 12, 857.

ROSE, A. A., ANNIS, M. G., DONG, Z., PEPIN, F., HALLETT, M., PARK, M. & SIEGEL, P. M. 2010a. ADAM10 releases a soluble form of the GPNMB/Osteoactivin extracellular domain with angiogenic properties. *PLoS One,* 5**,** e12093.

ROSE, A. A., GROSSET, A. A., DONG, Z., RUSSO, C., MACDONALD, P. A., BERTOS, N. R., ST-PIERRE, Y., SIMANTOV, R., HALLETT, M., PARK, M., GABOURY, L. & SIEGEL, P. M. 2010b. Glycoprotein nonmetastatic B is an independent prognostic indicator of recurrence and a novel therapeutic target in breast cancer. *Clin Cancer Res,* 16**,** 2147-56.

ROSE, A. A., PEPIN, F., RUSSO, C., ABOU KHALIL, J. E., HALLETT, M. & SIEGEL, P. M. 2007. Osteoactivin promotes breast cancer metastasis to bone. *Mol Cancer Res,* 5**,** 1001-14.

ROSE, A. A. N., BIONDINI, M., CURIEL, R. & SIEGEL, P. M. 2017. Targeting GPNMB with glembatumumab vedotin: Current developments and future opportunities for the treatment of cancer. *Pharmacology & Therapeutics,* 179**,** 127-141.

SAFADI, F. F., XU, J., SMOCK, S. L., RICO, M. C., OWEN, T. A. & POPOFF, S. N. 2001. Cloning and characterization of osteoactivin, a novel cDNA expressed in osteoblasts. J Cell Biochem, 84, 12-26.

SCHULZ, C., GOMEZ PERDIGUERO, E., CHORRO, L., SZABO-ROGERS, H., CAGNARD, N., KIERDORF, K., PRINZ, M., WU, B., JACOBSEN, S. E., POLLARD, J. W., FRAMPTON, J., LIU, K. J. & GEISSMANN, F. 2012. A lineage of myeloid cells independent of Myb and hematopoietic stem cells. Science, 336, 86-90

SCOTT, D. W. & STEIDL, C. 2014. The classical Hodgkin lymphoma tumor microenvironment: macrophages and gene expression-based modeling. *Hematology Am Soc Hematol Educ Program,* 2014**,** 144-50.

SHENG, M. H., WERGEDAL, J. E., MOHAN, S. & LAU, K. H. 2008. Osteoactivin is a novel osteoclastic protein and plays a key role in osteoclast differentiation and activity. *FEBS Lett,* 582**,** 1451-8.

SHIKANO, S., BONKOBARA, M., ZUKAS, P. K. & ARIIZUMI, K. 2001. Molecular cloning of a dendritic cell-associated transmembrane protein, DC-HIL, that promotes RGD-dependent adhesion of endothelial cells through recognition of heparan sulfate proteoglycans. *J Biol Chem,* 276**,** 8125-34.

SICA, A., SCHIOPPA, T., MANTOVANI, A. & ALLAVENA, P. 2006. Tumour-associated macrophages are a distinct M2 polarised population promoting tumour progression: potential targets of anti-cancer therapy. *Eur J Cancer,* 42**,** 717-27.

SMITH, K., CHIU, A., PARIKH, R., YAHALOM, J. & YOUNES, A. 2018. Chapter 75 - Hodgkin Lymphoma: Clinical Manifestations, Staging, and Therapy. *In:* HOFFMAN, R., BENZ, E. J., SILBERSTEIN, L. E., HESLOP, H. E., WEITZ, J. I., ANASTASI, J., SALAMA, M. E. & ABUTALIB, S. A. (eds.) *Hematology (Seventh Edition).* Elsevier.

SMYTH, G. K. 2004. Linear Models and Empirical Bayes Methods for Assessing Differential Expression in Microarray Experiments. Statistical Applications in Genetics and Molecular Biology, 3, 1-25.

STALTERI, M. A. & HARRISON, A. P. 2007. Interpretation of multiple probe sets mapping to the same gene in Affymetrix GeneChips. BMC Bioinformatics, 8.

STATISTICS, O. F. N. 2015. Cancer survival in England: adults diagnosed in 2009-2013, followed up in 2014. *Newport:ONS*.

STATISTICS, O. F. N. 2016. Cancer survival in England- Patients diagnosed between 2010 and 2014 and folowed up to 2015.

STEIDL, C., LEE, T., SHAH, S. P., FARINHA, P., HAN, G., NAYAR, T., DELANEY, A., JONES, S. J., IQBAL, J., WEISENBURGER, D. D., BAST, M. A., ROSENWALD, A., MULLER-HERMELINK, H. K., RIMSZA, L. M., CAMPO, E., DELABIE, J., BRAZIEL, R. M., COOK, J. R., TUBBS, R. R., JAFFE, E. S., LENZ, G., CONNORS, J. M., STAUDT, L. M., CHAN, W. C. & GASCOYNE, R. D. 2010. Tumor-associated macrophages and survival in classic Hodgkin's lymphoma. *N Engl J Med,* 362**,** 875-85.

STOUT, R. D., JIANG, C., MATTA, B., TIETZEL, I., WATKINS, S. K. & SUTTLES, J. 2005. Macrophages sequentially change their functional phenotype in response to changes in microenvironmental influences. *J Immunol,* 175**,** 342-9.

TAN, K. L., SCOTT, D. W., HONG, F., KAHL, B. S., FISHER, R. I., BARTLETT, N. L., ADVANI, R. H., BUCKSTEIN, R., RIMSZA, L. M., CONNORS, J. M., STEIDL, C., GORDON, L. I., HORNING, S. J. & GASCOYNE, R. D. 2012. Tumor-associated macrophages predict inferior outcomes in classic Hodgkin lymphoma: a correlative study from the E2496 Intergroup trial. *Blood,* 120**,** 3280-7.

TAYLOR, G. S., LONG, H. M., BROOKS, J. M., RICKINSON, A. B. & HISLOP, A. D. 2015. The immunology of Epstein-Barr virus-induced disease. *Annu Rev Immunol,* 33**,** 787-821.

TOMIHARI, M., CHUNG, J. S., AKIYOSHI, H., CRUZ, P. D., JR. & ARIIZUMI, K. 2010. DC-HIL/glycoprotein Nmb promotes growth of melanoma in mice by inhibiting the activation of tumor-reactive T cells. *Cancer Res,* 70**,** 5778-87.

TSE, K. F., JEFFERS, M., POLLACK, V. A., MCCABE, D. A., SHADISH, M. L., KHRAMTSOV, N. V., HACKETT, C. S., SHENOY, S. G., KUANG, B., BOLDOG, F. L., MACDOUGALL, J. R.,RASTELLI, L., HERRMANN, J., GALLO, M., GAZIT-BORNSTEIN, G., SENTER, P. D., MEYER, D. L., LICHENSTEIN, H. S. & LAROCHELLE, W. J. 2006. CR011, a fully human monoclonal antibody-auristatin E conjugate, for the treatment of melanoma. Clin Cancer Res, 12, 1373-82.

VAHDAT, L. T., SCHMID, P., FORERO-TORRES, A., BLACKWELL, K., TELLI, M. L., MELISKO, M., MOBUS, V., CORTES, J., MONTERO, A. J., MA, C., NANDA, R., WRIGHT, G. S., HE, Y., HAWTHORNE, T., BAGLEY, R. G., HALIM, A. B., TURNER, C. D. & YARDLEY, D. A. 2021. Glembatumumab vedotin for patients with metastatic, gpNMB overexpressing, triple-negative breast cancer ("METRIC"): a randomized multicenter study. NPJ Breast Cancer, 7, 57.

VAN FURTH, R., COHN, Z. A., HIRSCH, J. G., HUMPHREY, J. H., SPECTOR, W. G. & LANGEVOORT, H. L. 1972. The mononuclear phagocyte system: a new classification of macrophages, monocytes, and their precursor cells. Bull World Health Organ, 46, 845-52.

WENIGER, M. A., TIACCI, E., SCHNEIDER, S., ARNOLDS, J., RÜSCHENBAUM, S., DUPPACH, J., SEIFERT, M., DÖRING, C., HANSMANN, M.-L. & KÜPPERS, R. 2018. Human CD30+ B cells represent a unique subset related to Hodgkin lymphoma cells. *Journal of Clinical Investigation,* 128**,** 2996-3007.

WENIGER, M. A. & KÜPPERS, R. 2021. Molecular biology of Hodgkin lymphoma. *Leukemia*.

WETERMAN, M. A., AJUBI, N., VAN DINTER, I. M., DEGEN, W. G., VAN MUIJEN, G. N., RUITTER, D. J. & BLOEMERS, H. P. 1995. nmb, a novel gene, is expressed in low-metastatic human melanoma cell lines and xenografts. *Int J Cancer,* 60**,** 73-81.

WIENAND, K., CHAPUY, B., STEWART, C., DUNFORD, A. J., WU, D., KIM, J., KAMBUROV, A., WOOD, T. R., CADER, F. Z., DUCAR, M. D., THORNER, A. R., NAG, A., HEUBECK, A. T., BUONOPANE, M. J., REDD, R. A., BOJARCZUK, K., LAWTON, L. N., ARMAND, P., RODIG, S. J., FROMM, J. R., GETZ, G. & SHIPP, M. A. 2019. Genomic analyses of flow-sorted Hodgkin Reed-Sternberg cells reveal complementary mechanisms of immune evasion. *Blood Advances,* 3**,** 4065-4080.

YARDLEY, D. A., WEAVER, R., MELISKO, M. E., SALEH, M. N., ARENA, F. P., FORERO, A., CIGLER, T., STOPECK, A., CITRIN, D., OLIFF, I., BECHHOLD, R., LOUTFI, R., GARCIA, A. A., CRUICKSHANK, S., CROWLEY, E., GREEN, J., HAWTHORNE, T., YELLIN, M. J., DAVIS, T. A. & VAHDAT, L. T. 2015. EMERGE: A Randomized Phase II Study of the Antibody-Drug Conjugate Glembatumumab Vedotin in Advanced Glycoprotein NMB-Expressing Breast Cancer. J Clin Oncol, 33, 1609-19.

YOUNES, A., BARTLETT, N. L., LEONARD, J. P., KENNEDY, D. A., LYNCH, C. M., SIEVERS, E. L. & FORERO-TORRES, A. 2010. Brentuximab vedotin (SGN-35) for relapsed CD30-positive lymphomas. *N Engl J Med,* 363**,** 1812-21.

YOUNG, L. S., YAP, L. F. & MURRAY, P. G. 2016. Epstein–Barr virus: more than 50 years old and still providing surprises. *Nature Reviews Cancer,* 16**,** 789-802.

YU, B., SONDAG, G. R., MALCUIT, C., KIM, M. H. & SAFADI, F. F. 2016. Macrophage-Associated Osteoactivin/GPNMB Mediates Mesenchymal Stem Cell Survival, Proliferation, and Migration Via a CD44-Dependent Mechanism. *J Cell Biochem,* 117**,** 1511-21.

ZHENG, X., WEIGERT, A., REU, S., GUENTHER, S., MANSOURI, S., BASSALY, B., GATTENLOHNER, S., GRIMMINGER, F., PULLAMSETTI, S., SEEGER, W., WINTER, H. & SAVAI, R. 2020. Spatial Density and Distribution of Tumor-Associated Macrophages Predict Survival in Non-Small Cell Lung Carcinoma. Cancer Res, 80, 4414-4425.

ZHOU, L., ZHUO, H., OUYANG, H., LIU, Y., YUAN, F., SUN, L., LIU, F. & LIU, H. 2017. Glycoprotein non-metastatic melanoma protein b (Gpnmb) is highly expressed in macrophages of acute injured kidney and promotes M2 macrophages polarization. Cell Immunol, 316, 53-60.